Alkylidene Installation on Ruthenium: Towards Alternative Routes to Known Metathesis Catalysts and Access to Low-Valent Ruthenium Alkylidenes

Andrew James White

A thesis submitted in partial fulfillment of the requirements for the
Master's Degree in Chemistry

Ottawa-Carleton Chemistry Institute
Faculty of Science
University of Ottawa

Table of Contents

Abstract

Olefin metathesis is a powerful tool for the making and breaking of carbon-carbon double bonds. Among well-defined homogenous catalysts for olefin metathesis, ruthenium-based alkylidenes stand out for their robustness and relative ease-of-use. Synthesis of the most active Ru-based metathesis catalysts remains challenging, however, and there is continued interest in new and improved routes to alkylidene installation as metathesis begins to see wide uptake in industry.

The first part of this thesis focuses on developing new routes to known catalysts. Magnesium carbenoids are investigated as a potential alkylidene source, and in the process a novel route to benzylmagnesium carbenoids is developed. Initially promising results showing ca. 40% conversion to first generation metathesis catalysts failed to lead to a viable high-yield route to Ru-alkylidenes.

A high yield route to $RuCl_2(H_2IMes)(py)_4$ (previously reported in low yields as a decomposition product of the third-generation Grubbs' metathesis catalyst) is developed and this complex is investigated as a precursor to indenylidene-based catalysts. Although $RuCl_2(H_2IMes)(py)_4$ is shown to be substitutionally labile, indenylidene installation could not be achieved.

Finally, zinc aryloxides are investigated as an alternative to thallium and silver reagents for the installation of aryloxide ligands. Initial results indicate that zinc aryloxides are kinetically, though not thermodynamically, competent for the installation of the challenging aryloxide $C_6F_5O^-$ on the second-generation Hoveyda catalyst.

The second part of this thesis concerns progress towards the development of a new low-valent catalyst platform. Initial experiments involving treating the second-generation Hoveyda catalyst with various reducing agents fail to produce low-valent alkylidenes, leading instead to decomposition of alkylidene.

Drawing inspiration from early transition metal systems, the remainder of the second part focuses on alpha-hydride elimination from a Ru^{II} alkyl as a means of accessing low-valent alkylidenes. To this end, a novel benzylruthenium complex as well as bis-benzyl and mono-aryloxide derivatives are developed. While attempts to induce benzyl-to-benzyl hydride abstraction or intramolecular deprotonation of the benzyl ligand failed to produce alkylidenes, ligand-induced benzyl-to-aryloxide hydride abstraction appears to be successful, leading to the observation of a broad ^1H NMR signal in the region characteristic for low-valent Ru-alkylidenes.

Acknowledgements

The work in this thesis could not have been achieved without the expertise and assistance of technical experts at uOttawa. A special thank you to Drs. Glenn Facey and Peter Pallister (uOttawa NMR facility), as well as Roxanne Clément (CCRI).

I owe a debt of gratitude to many past members of the Fogg lab. Dr. Carolyn Higman, it is in many ways your fault that I wound up working with Dr. Fogg, and I cannot thank you enough. Dr. Gwen Bailey, you were a titan in the lab, your wealth of knowledge and experience was an invaluable resource and your presence in the lab is dearly missed by your former colleagues. Dr. Benjamin Ireland, I never actually met you, but your thesis was an invaluable trove of useful information, so I feel I would be remiss to not acknowledge you.

Craig Day and Immanuel Reim, both top-class desk buddies: your interloping on my fortress of solitude is forgiven for the valuable and engaging chemistry discussions you brought with you. Stephanie Ton, my glovebox neighbour and dispositional opposite, you were consistently an excellent sounding board for experimental design. You were also remarkably tolerant of my distinct brand of je-ne-sais-quoi, I hope Denmark treats you well. Daniel Nascimento, you are one weird dude, keep it up. Xinrui Ou and Mason Guy, you two let me indulge in my kinetics nerdery, and I'll always appreciate that.

To the newer members of the Fogg research group, Eliza-Jane, Christian, Nathan and Ryan; I didn't really get to know you guys that closely, but you seem like you'll make decent chemists, best of luck.

Finally, I must thank my supervisor, Deryn Fogg, without whom I would never have written this Masters' thesis.

List of Compounds

Early Transition Metal Complexes

Ta-1	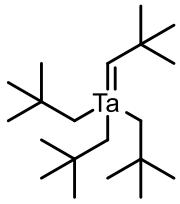	**Ta-2**	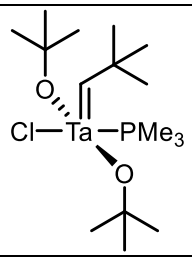
W-1	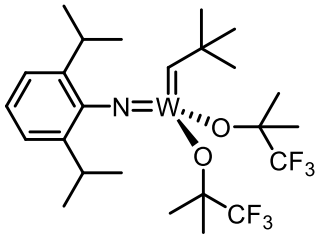	**Mo-1**	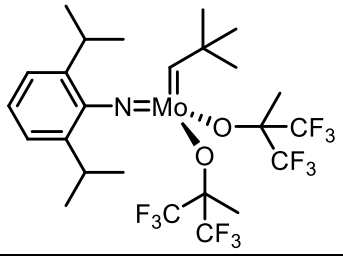
Mo-1	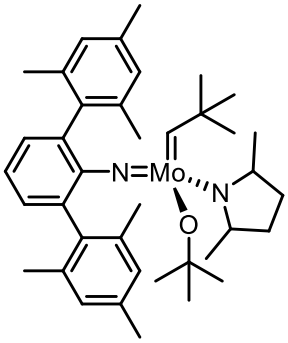	**Ta-3**	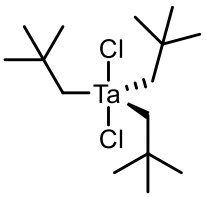
Ta-4	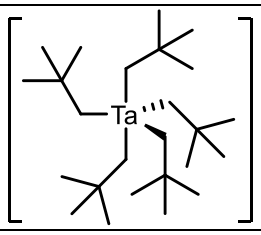	**W-2**	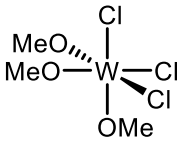
W-3	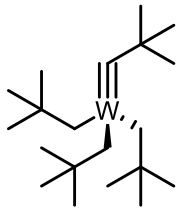	**W-4**	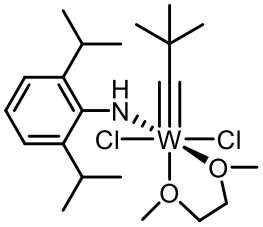
W-5	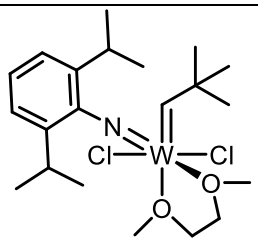	**W-6**	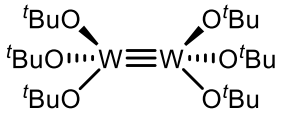

W-7	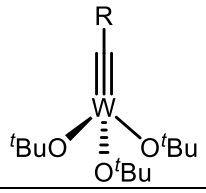		

Ruthenium Complexes

GI	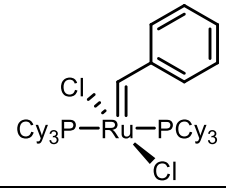	**GII**	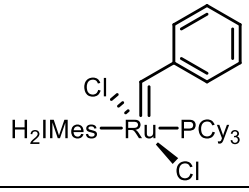
GIII	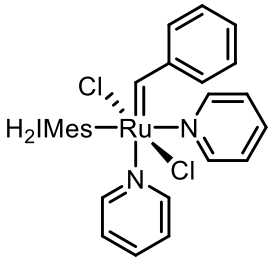	**GI-m**	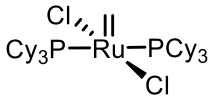
GII-m	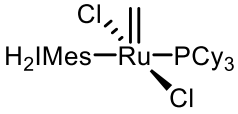	**HII**	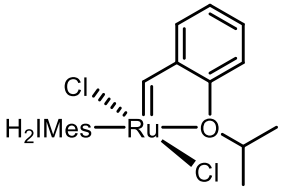
HII-CAAC	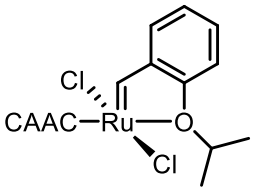	**nG-PPh3**	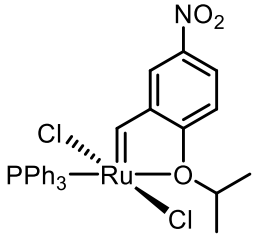
nGII	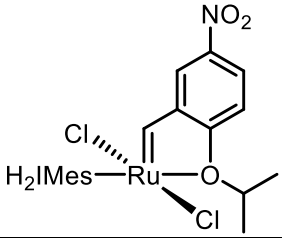	**nG-CAAC**	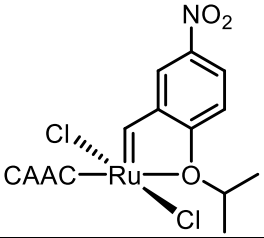
M0	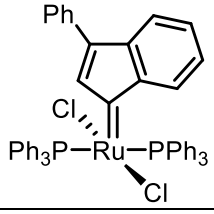	**M1**	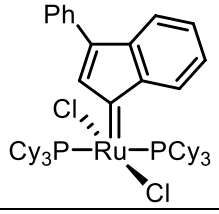

M2	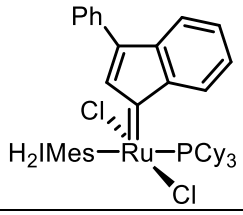	**Ru-1**	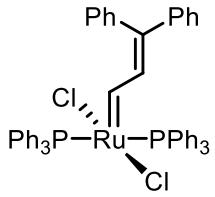
Ru-2	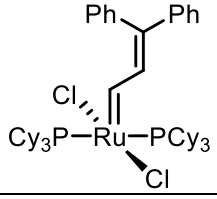	**Ru-3**	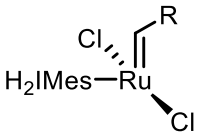
Ru-4	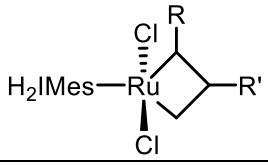	**Ru-5**	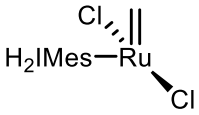
Ru-6	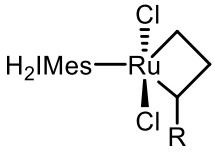	**Ru-7**	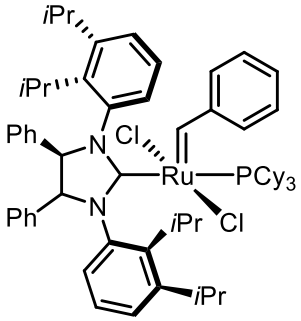
Ru-8	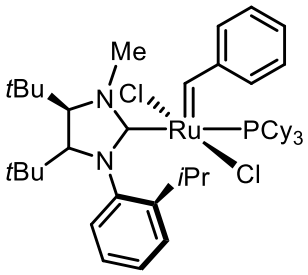	**Ru-9**	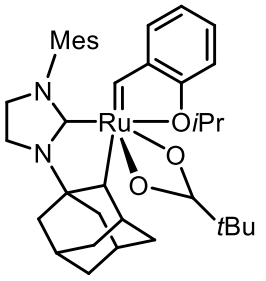
Ru-10	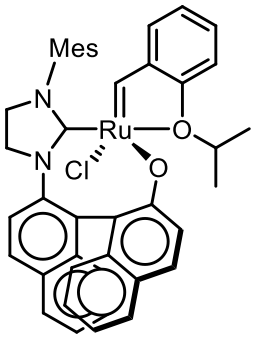	**Ru-11**	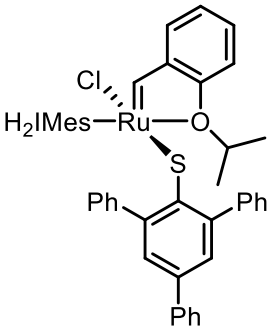

Ru-12	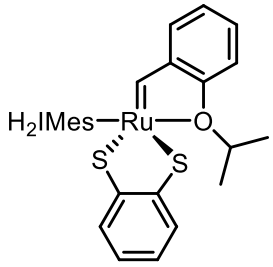	**Ru-13**	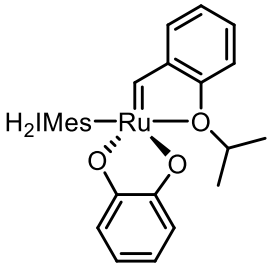
Ru-14	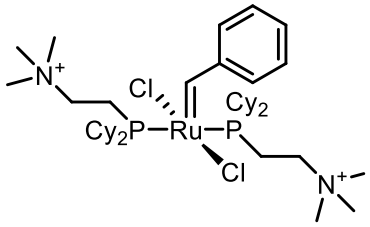	**Ru-15**	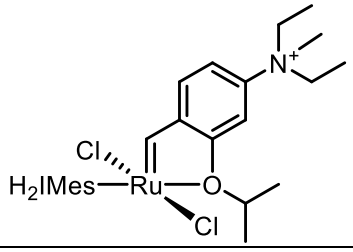
Ru-16	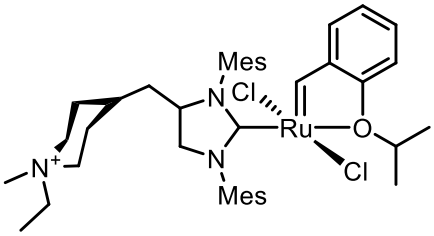	**Ru-17**	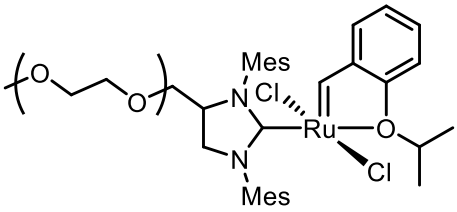
Ru-18	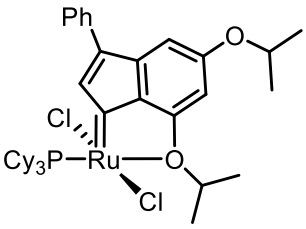	**Ru-19**	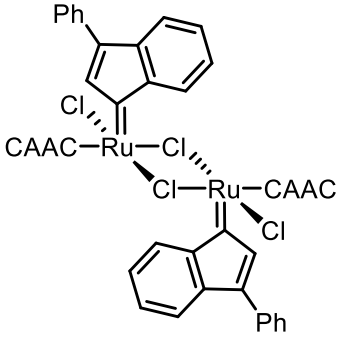
Ru-20	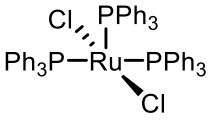	**Ru-21**	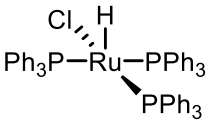
Ru-22	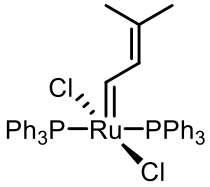	**Ru-23**	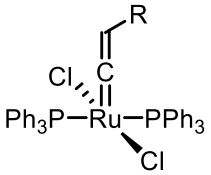
Ru-24	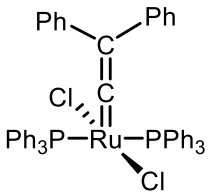	**Ru-25**	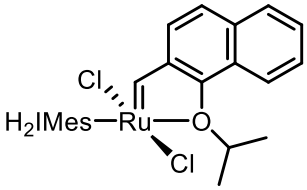

Ru-26	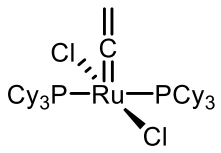	**Ru-27**	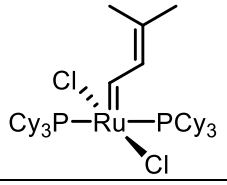
Ru-28	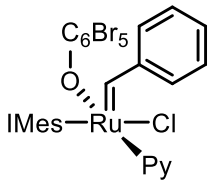	**Ru-29**	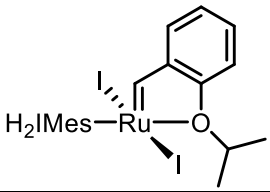
Ru-30	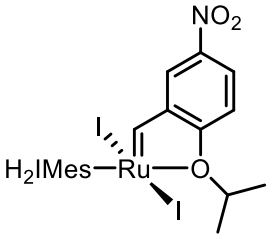	**Ru-31**	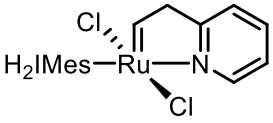
Ru-32	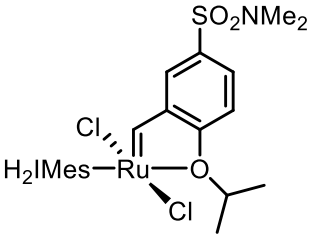	**Ru-33**	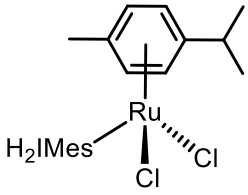
Ru-34	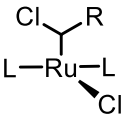	**Ru-35**	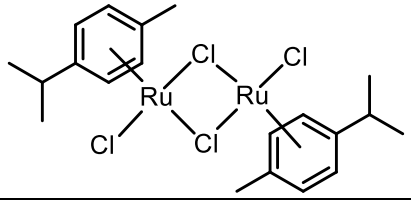
Ru-36	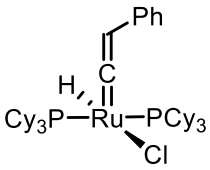	**Ru-37**	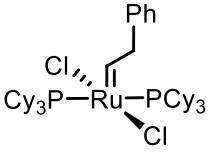
Ru-38	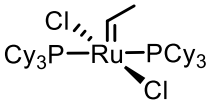	**Ru-39**	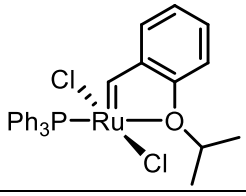
Ru-40	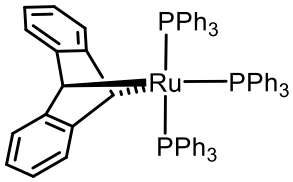	**Ru-41**	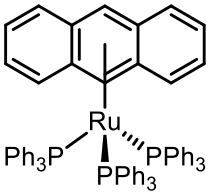

Ru-42	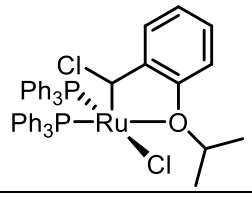	**Ru-43**	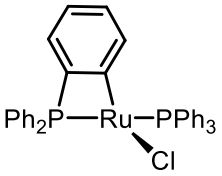
Ru-44	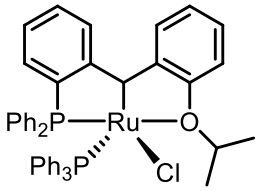	**Ru-45**	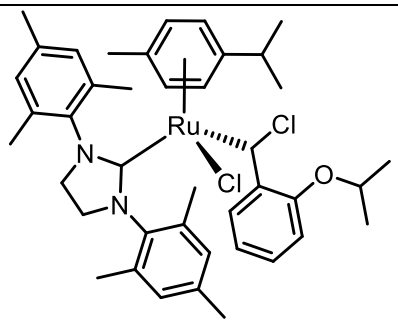
Ru-46	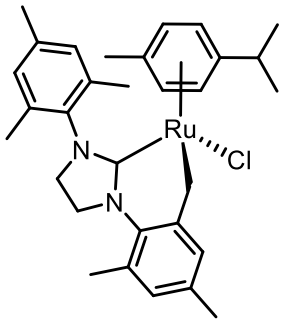	**Ru-47**	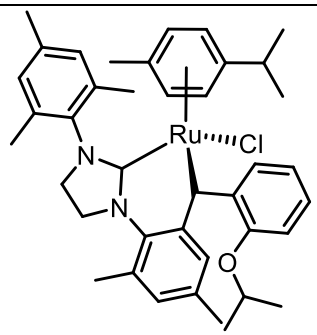
Ru-48	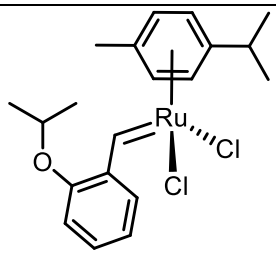	**Ru-49**	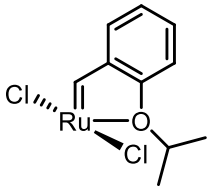
Ru-50	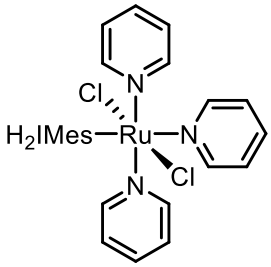	**Ru-51**	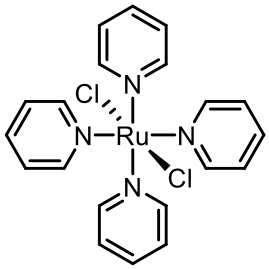
Ru-52a	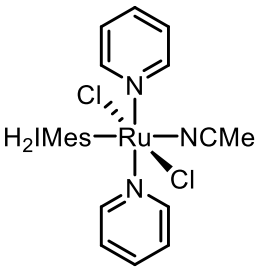	**Ru-52b**	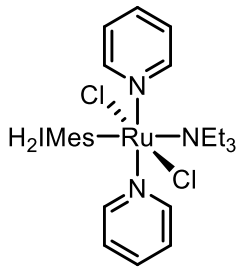

Ru-52c	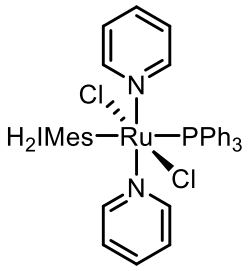	**Ru-52d**	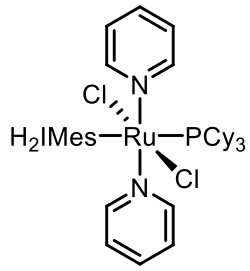
Ru-53a	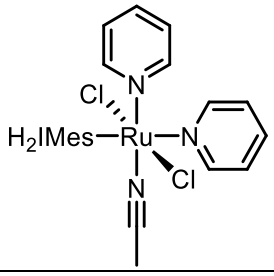	**Ru-53b**	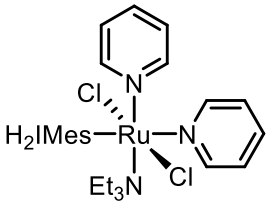
Ru-53c	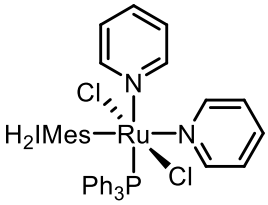	**Ru-53d**	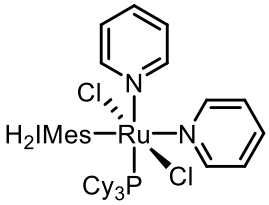
Ru-54	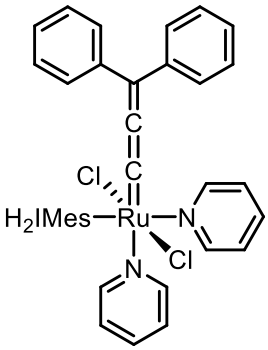	**Ru-55**	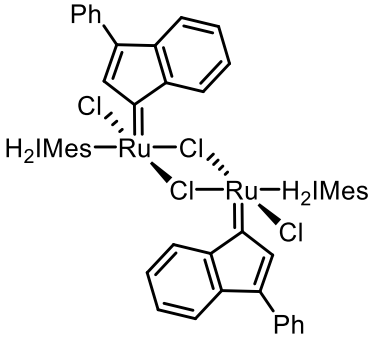
Ru-56a	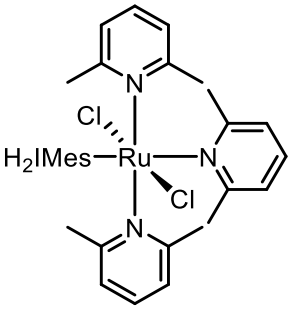	**Ru-56b**	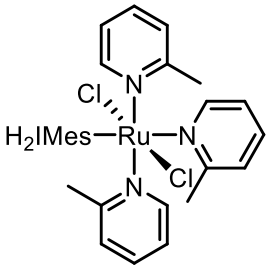

Ru-56c	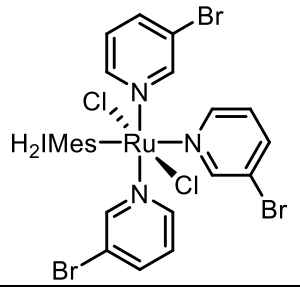	**Ru-57**	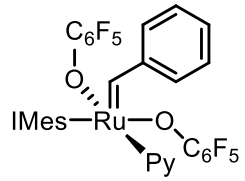
Ru-58	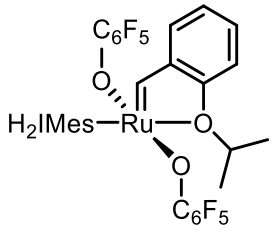	**Ru-59**	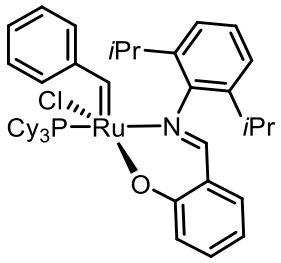
Ru-60	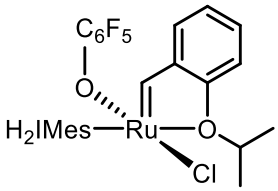	**Ru-61**	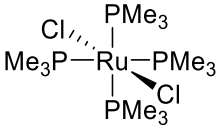
Ru-62	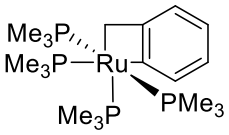	**Ru-63**	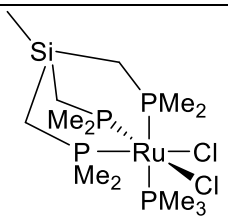
Ru-64	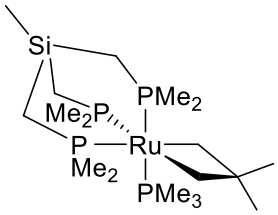	**Ru-65**	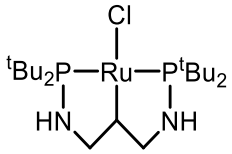
Ru-66	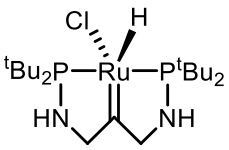	**Ru-67**	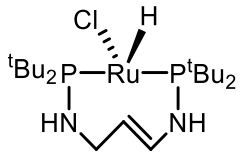
Ru-68	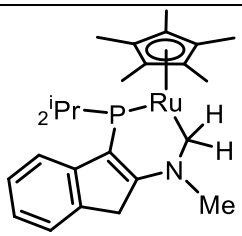	**Ru-69**	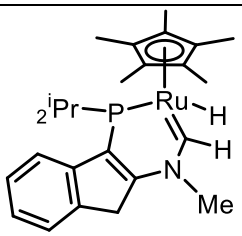

Ru-70	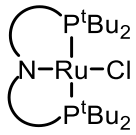	**Ru-71**	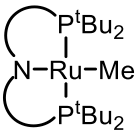
Ru-72	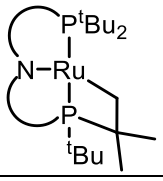	**Ru-73**	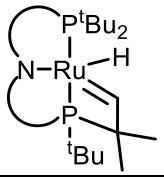
Ru-74	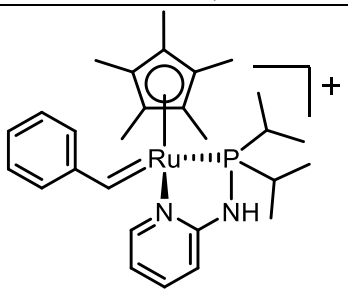	**Ru-75**	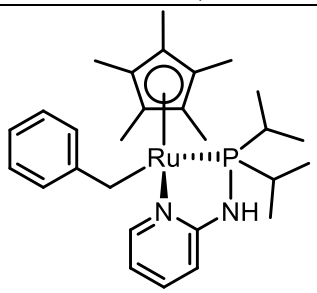
Ru-76	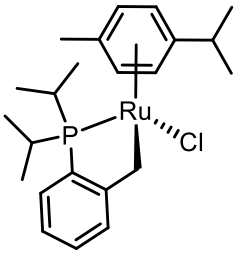	**Ru-77**	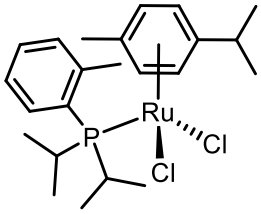
Ru-78	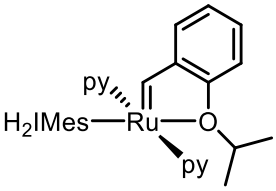	**Ru-79**	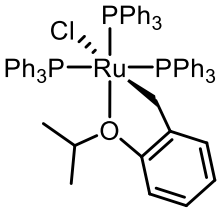
Ru-80	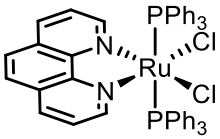	**Ru-81**	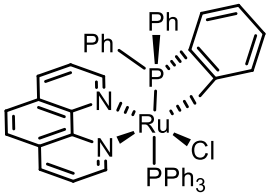
Ru-82	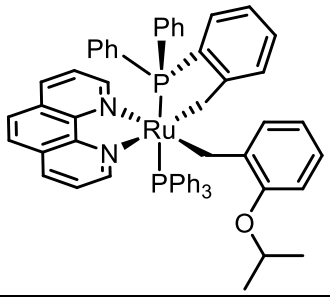	**Ru-83**	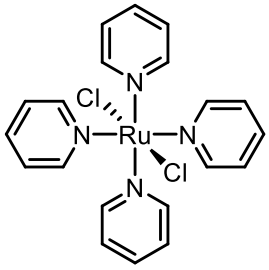

Ru-84	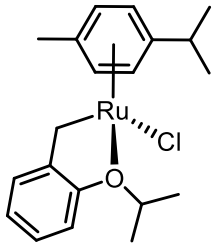	**Ru-84a**	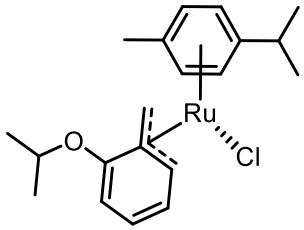
Ru-84b	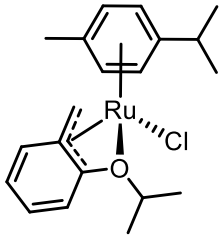	**Ru-85**	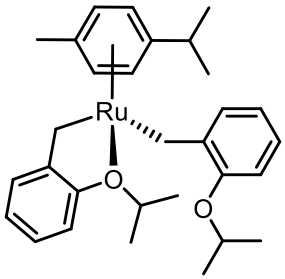
Ru-86	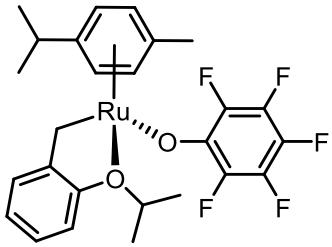	**Ru-87**	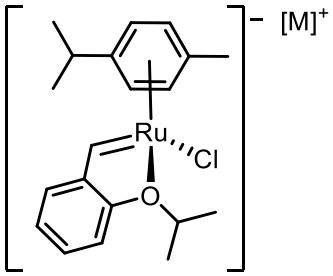 M = Li, K
Ru-88	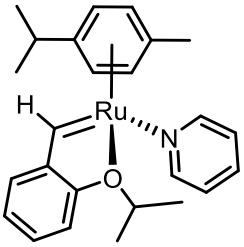	**Ru-89**	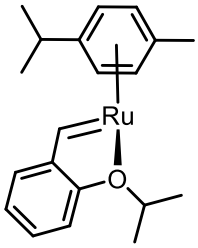
Ru-90	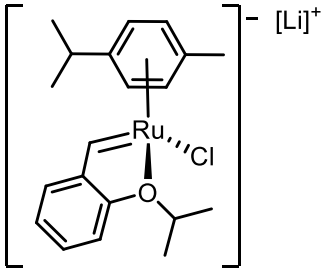	**Ru-91**	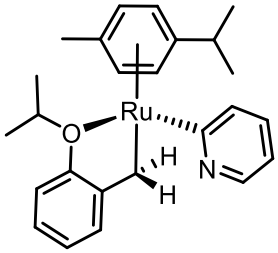

Ru-92	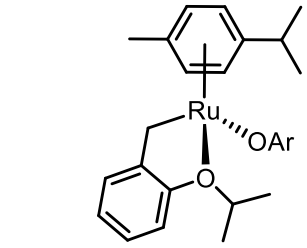 OAr = 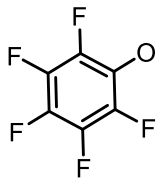 **OAr-1** 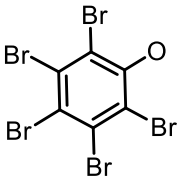 **OAr-2** 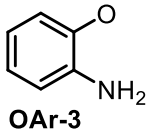 **OAr-3**	**Ru-93**	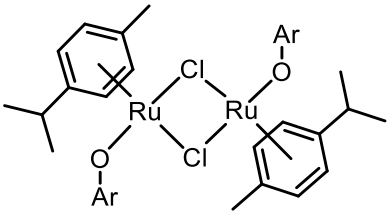
Ru-94	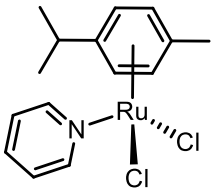	**Ru-95**	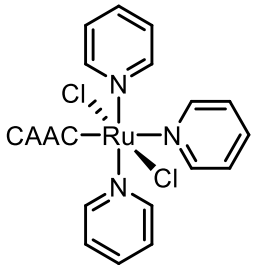
Ru-96	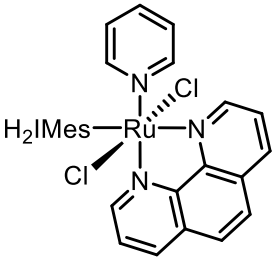	**Ru-97**	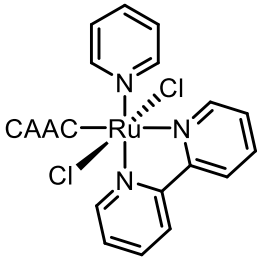
Ru-98	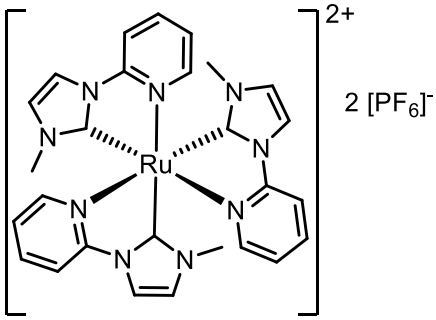 2 $[PF_6]^-$	**Ru-99**	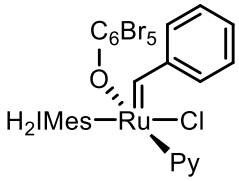

Ru-100	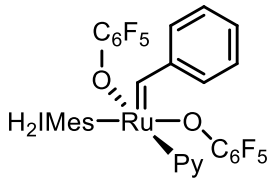	**Ru-101**	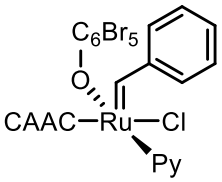
Ru-102	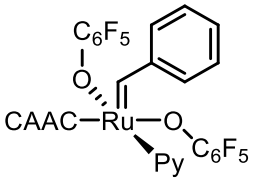	**Ru-103**	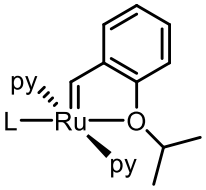
Ru-104	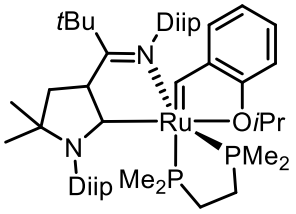	**Ru-105**	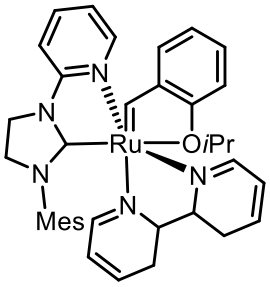
Ru-106	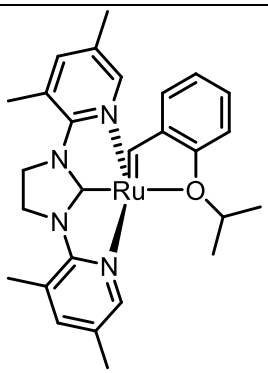	**Ru-107**	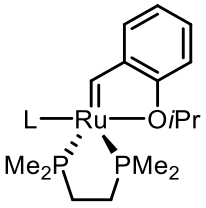
Ru-108	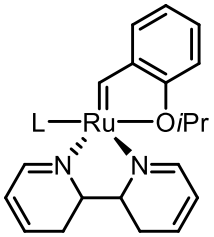	**Ru-109**	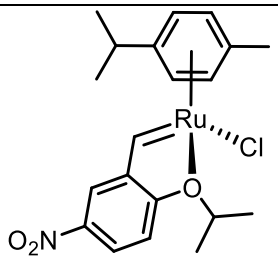
Ru-110	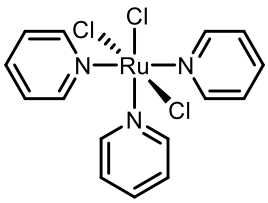	**Ru-111**	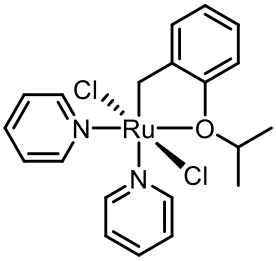

Ru-112	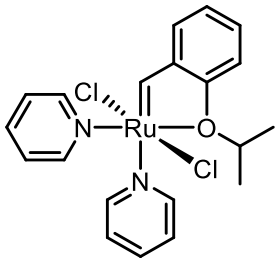	**Ru-113**	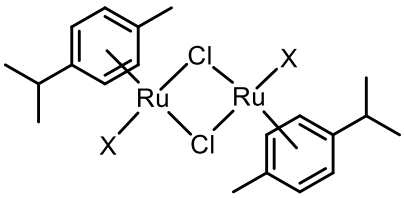 X = Br, I, OR, OAr, NR_2, SR, etc.
Ru-114	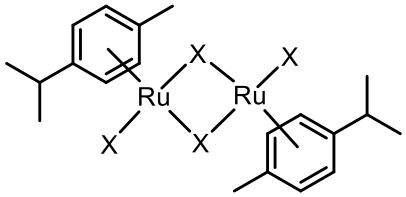 X = Br, I, OR, OAr, NR_2, SR, etc.	**Ru-115**	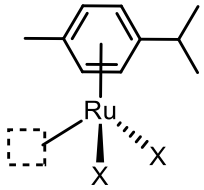 X = Br, I, OR, OAr, NR_2, SR, etc.
Ru-116	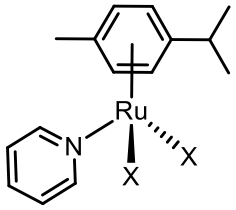 X = Br, I, OR, OAr, NR_2, SR, etc.	**Ru-117**	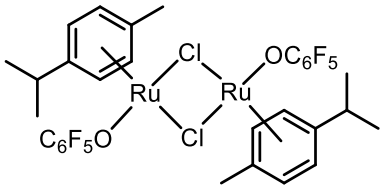
Ru-118	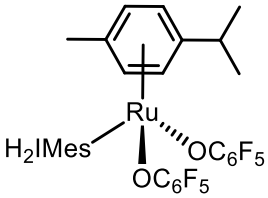	**Ru-119**	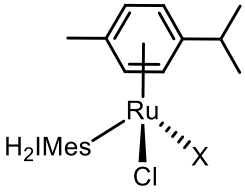 X ≠ Cl
Ru-120	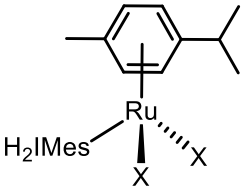 X ≠ Cl	**Ru-121**	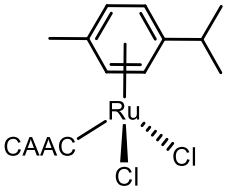 X ≠ Cl

Magnesium Complexes

Mg-1	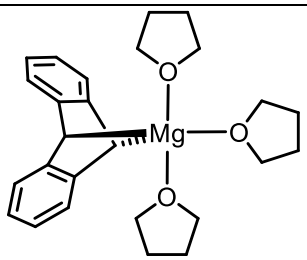	**Mg-2**	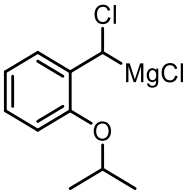

Mg-3	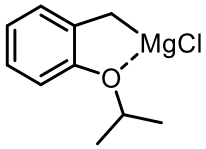	**Mg-3'**	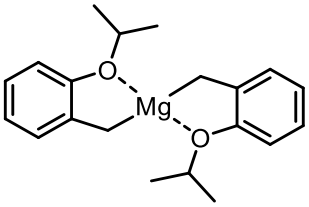
Mg-4	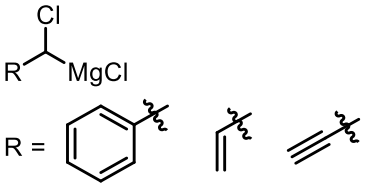	**Mg-5**	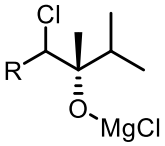
Mg-6	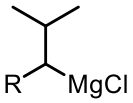	**Mg-7**	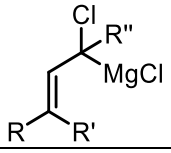
Mg-8	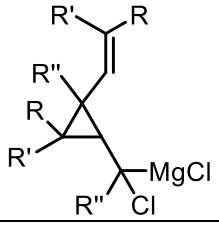	**Mg-9**	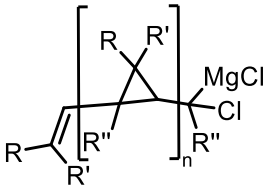
Mg-10	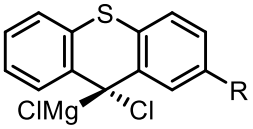	**Mg-11**	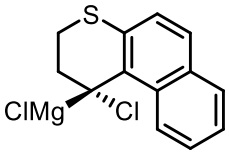
Mg-12	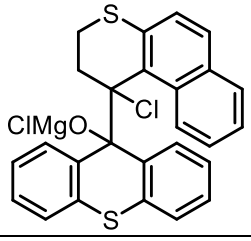		

Organic and Miscellaneous Main Group Compounds

Anthracene	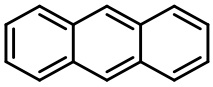	**C-1**	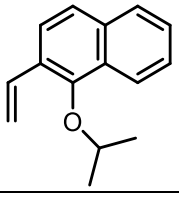

C-2	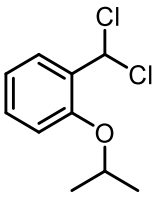	**C-3**	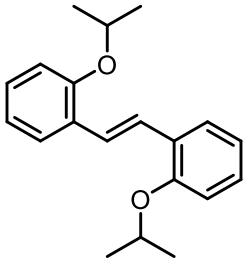
C-4	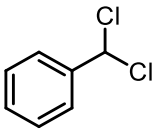	**C-5**	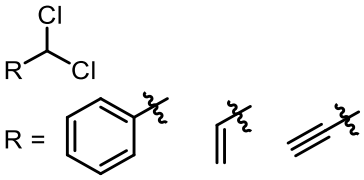
C-6	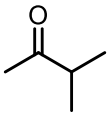	**C-7**	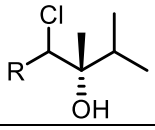
C-8		**C-9**	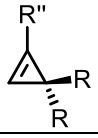
C-10	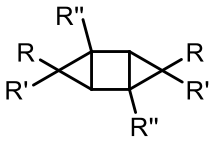	**C-11**	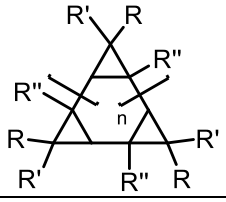
C-12	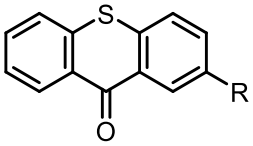	**C-13**	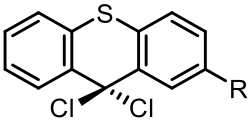
C-14	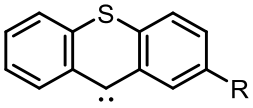	**C-15**	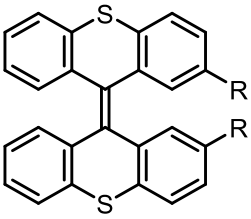
C-16	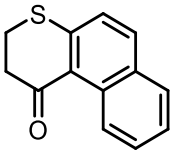	**C-17**	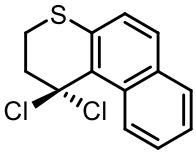

C-18	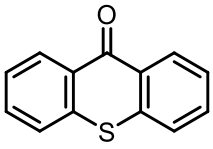	**C-19**	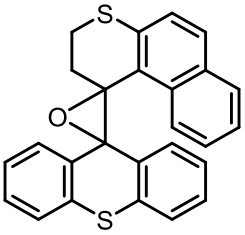
C-20	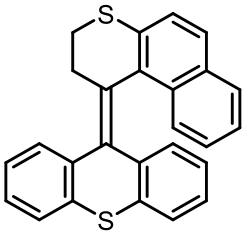	**C-30**	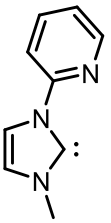
		P-1	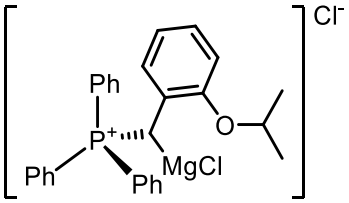

Abbreviations

Ar	aryl
BMC	bimolecular coupling
Bn	benzyl
CM cross metathesis	cross metathesis
CAAC	cyclic alkyl-amino carbene
COSY	correlation spectroscopy
EI	electron impact
GC	gas chromatography
HMBC	heteronuclear multiple bond correlation
HMQC	heteronuclear multiple quantum coherence
Hz	Hertz
IR	infrared
HMDS	Hexamethyldisilane
LDA	Lithium Diisopropylamide
MCB	metallacyclobutane
Mes	mesityl
MAP	monoaryloxide-pyrrolide
MS	mass spectrometry
NHC	*N*-heterocyclic carbene
NMR	nuclear magnetic resonance
NOE(SY)	nuclear Overhauser effect (spectroscopy)
phen	1,10-phenanthroline
ppm	parts per million
py	pyridine
RCM	ring closing metathesis
ROMP	ring opening metathesis polymerization
RT	room temperature
THF	tetrahydrofuran
TOF	turnover frequency
TON	turnover number
XAS	X-ray absorption spectroscopy
XRD	X-ray diffraction

List of Schemes, Figures, and Tables

Chapter 1

Schemes

Figures

Chapter 3

Schemes

Figures

Tables

Chapter 4

Schemes

Figures

Chapter 5

Schemes

Figures

Appendix A

Appendix B

Chapter 1. Introduction

1.1 Olefin Metathesis

First reported by industry in the mid 20th century,[1-5] olefin metathesis involves the exchange of substituents between olefins, leading to a thermodynamic distribution of products (Scheme 1.1), and is perhaps the most atom-economical method for the formation of new carbon-carbon double bonds. In the 1950s, reports by Zeigler of the unexpected formation of 1-butene during the attempted polymerization of ethylene in the presence of nickel[6] were soon followed by the observation of propene undergoing "olefin disproportionation" (an early term for olefin metathesis) and polymerization of cyclic olefins.[5] Throughout the 1960s, researchers continued exploring ring-opening polymerization of cyclic olefins and olefin disproportionation reactions of unfunctionalized alkenes catalyzed by multicomponent systems based on Mo, W, or Ti chlorides or oxides activated with alkylaluminum, but it was not until 1967 that Calderon drew an explicit connection between these two apparently unrelated reactions and coined the modern term "olefin metathesis".[7]

Scheme 1.1: A simplified depiction of the olefin metathesis reaction; substituents are redistributed across the C-C double bond.

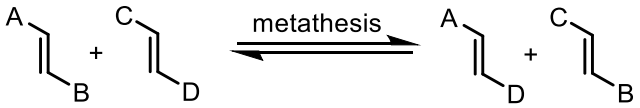

Mechanistic investigations were frustrated by the fact that early catalyst systems were ill-defined multicomponent mixtures which only produced a minute quantity of short-lived active species.[3] It was not until 1974, with Schrock's isolation of a well-defined tantalum alkylidene (**Ta-1**),[8] followed in 1980 by the report of metathesis-active tantalum, niobium, and tungsten alkylidenes[9] that the Chauvin mechanism, which proceeds through metal-alkylidene and metallacyclobutane intermediates (Scheme 1.2), gained experimental evidence and widespread acceptance.[3]

Scheme 1.2: The Chauvin mechanism for olefin metathesis

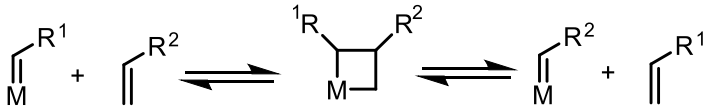

Schrock continued to develop early-metal alkylidenes as metathesis catalysts in the subsequent years,[2, 10] and metal carbenes of this type now commonly bear his name. These "Schrock carbenes" do not bear electron-donating substituents on the carbene carbon, and are best modeled as a triplet carbene engaged in two covalent bonds with the metal centre (and are therefore considered dianionic) (Figure 1.1).[11-13] They are also typically known on high oxidation state early transition metals, which polarizes the metal-carbon double bond towards carbon, giving rise to nucleophilic character on carbon.[11-13] This is in contrast to the earlier known "Fischer carbenes",[14] which bear electron donating substituents on the carbene carbon, exist primarily on electron-rich mid-to-late transition metals, are polarized towards the metal centre, react primarily as electrophiles at the carbene carbon, and are best modelled as singlet carbenes that bind to a metal by σ-donation of

References on page 13

the singlet lone pair and back donation of a pair of electrons from a metal d-orbital (and are therefore neutral ligands).[11-13]

Figure 1.1: Binding mode and characteristics of Schrock and Fisher carbenes

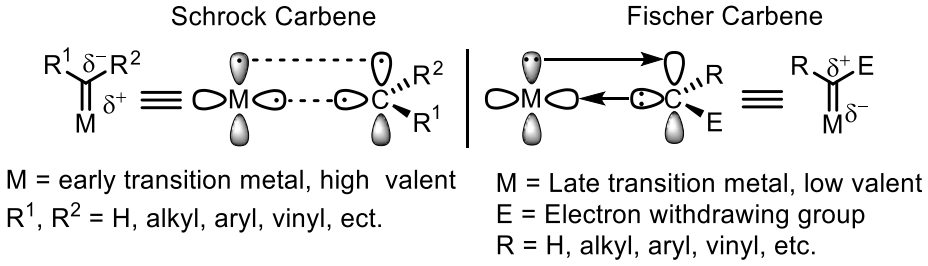

Catalyst productivity was improved by moving from Ta to W[15] and Mo,[16] and replacing the alkyl ligands present in **Ta-1** with bulky alkoxide/aryloxide,[9] imido,[17] and eventually pyrrolide[10] ligands (Figure 1.2). Bulky ligands were targeted to prevent bimolecular coupling and decomposition of the alkylidene, and the highly tunable stereoelectronic properties of these ligands allowed control over activity and selectivity. These developments culminated in the development of the monoaryloxide-pyrrolide ("MAP") catalyst platform (e.g. **Mo-2**), which remains state-of-the-art.[10]

Figure 1.2: Development of early metal metathesis catalysts

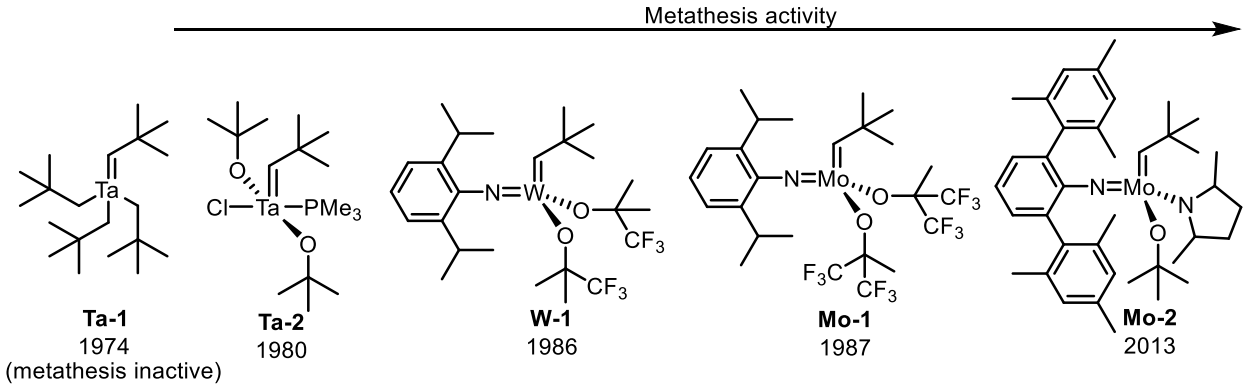

Despite these developments, olefin metathesis would not yet see wide uptake in organic synthesis; the nucleophilic alkylidenes and very oxophilic high oxidation state early metal centres characteristic of the Schrock catalysts led to poor functional group tolerance and high sensitivity to moisture and oxygen.[2] It would not be until the 90s, with Grubbs' synthesis of the less active, but considerably more robust ruthenium metathesis catalysts that organic chemists would embrace olefin metathesis on the bench.[1, 5, 18]

1.1.2 Ruthenium Catalysts

The first ruthenium alkylidene, **Ru-1**, was reported by Grubbs in 1992.[19] Although it was poorly active in metathesis, catalyzing only ROMP of highly strained cyclic olefins, the basic structure of modern ruthenium catalysts remains the same as **Ru-1**;[18] a five-coordinate, square-pyramidal ruthenium complex bearing an apical alkylidene, two anionic ligands (typically, though not

References on page 13

exclusively, chloride), one stabilizing L-ligand that remains coordinated throughout the catalytic cycle, and a second L-ligand which dissociates to permit olefin binding (Figure 1.3).

In contrast to early metal systems, for which more electron-withdrawing ligands improve catalyst activity,[2] activity of ruthenium catalysts is enhanced by stronger electron-donating ligands.[18] This behaviour was noticed early on; replacing PPh_3 in **Ru-1** with stronger-donating PCy_3 produced more active **Ru-2**.[20] Choice of alkylidene also plays a role; benzylidenes are more active than the vinyl alkylidenes in **Ru-1** and **Ru-2**.[21] A benzylidene complex, **GI**,[21] would become known as the "first-generation Grubbs' catalyst"; the attractive combination of moderate activity, high functional group tolerance, and low vulnerability to air and moisture led this catalyst to be widely adopted by organic chemists, and it is still commercially available today.

Figure 1.3: Anatomy of a metathesis catalyst

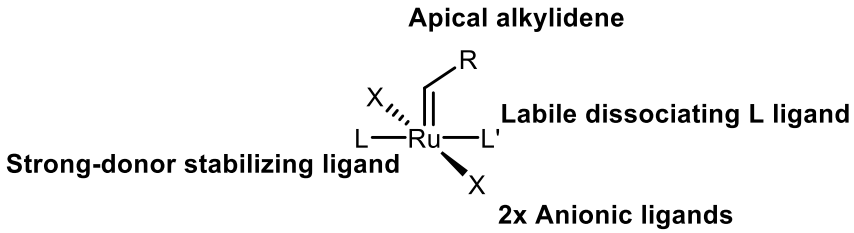

Moving to ever more electron donating stabilizing ligands has led to large increases in catalyst activity; first with the switch from PCy_3 to N-heterocyclic carbenes (NHCs) marking the advent of the "second-generation" catalysts (e.g. **GII**),[22] and more recently with the introduction of cyclic alkyl-amino carbenes (CAACs) (Figure 1.4). It was initially thought that strong donor ligands increased activity by labilizing the dissociating L-ligand and thereby increasing initiation rates,[22] but kinetic studies revealed that the second-generation catalysts actually initiated over two orders of magnitude *more slowly* than the less electron-rich first-generation.[23] Subsequent studies have shown that the improved activity conferred by strong donor ligands comes not from increased initiation efficiency, but by increasing olefin binding affinity and the ease of the cyclometallation step (so-called "high commitment" behaviour).[24-26]

References on page 13

Figure 1.4: Key ruthenium metathesis catalysts, arranged in increasing order of performance

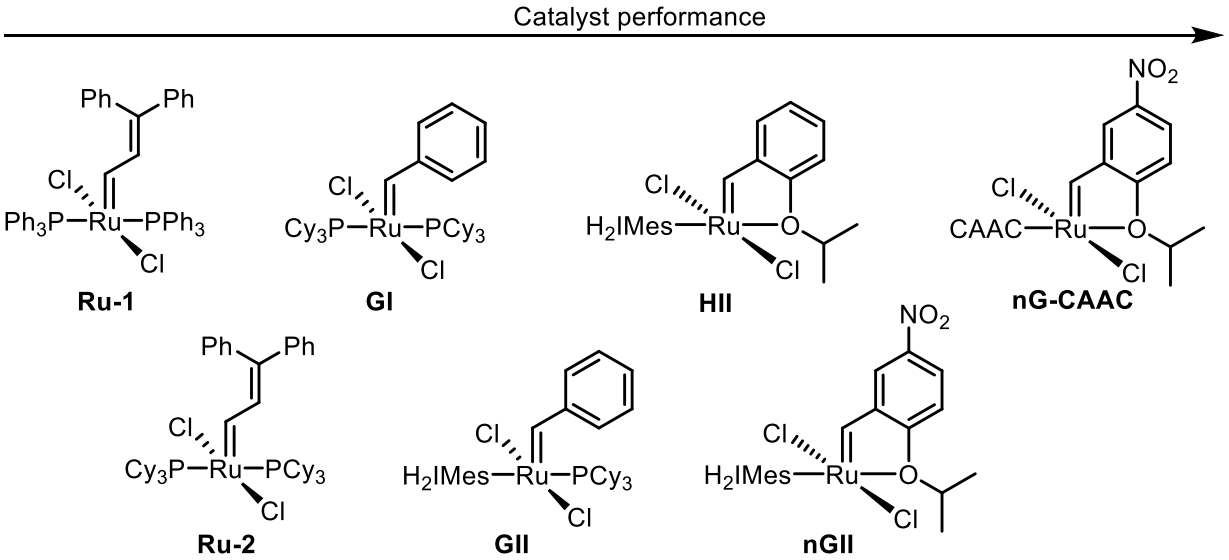

In a separate innovation, Hoveyda introduced a chelating ether functionality on the *ortho* position on benzylidene,[27] eventually leading to the phosphine-free second-generation Hoveyda catalyst, **HII**.[28-29] The chelating benzylidene had the effect of changing the catalytic resting state from the vulnerable 5-coordinate methylidene (Scheme 1.3) to the robust precatalyst by recapture of the chelating benzylidene (the so-called "boomerang mechanism", see Scheme 1.4).[30] Replacement of phosphine by the chelating ether also solved the issue of catalyst death by nucleophilic attack on alkylidene by liberated phosphine, which has been established as a significant decomposition route for phosphine-bearing catalysts.[31] Grela further improved the chelating-benzylidene system with the addition of an electron-withdrawing nitro group *para* to the chelating ether (as in **nGII**), which has the effect of weakening the chelate and boosting the initiation rate.[32]

References on page 13

Scheme 1.3: Catalytic cycle for ruthenium metathesis catalysts with non-chelating alkylidene. Precatalyst and resting state identified

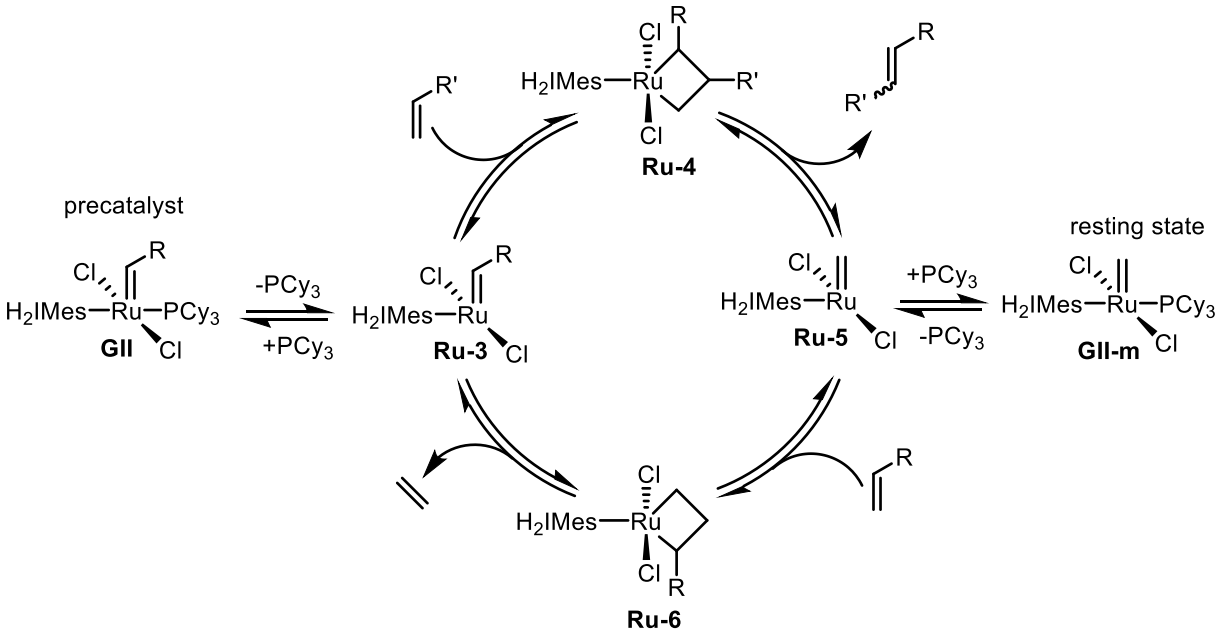

Scheme 1.4: Catalytic cycle for Hoveyda-class ruthenium metathesis catalysts with chelating alkylidene. Precatalyst and resting state are the same species.

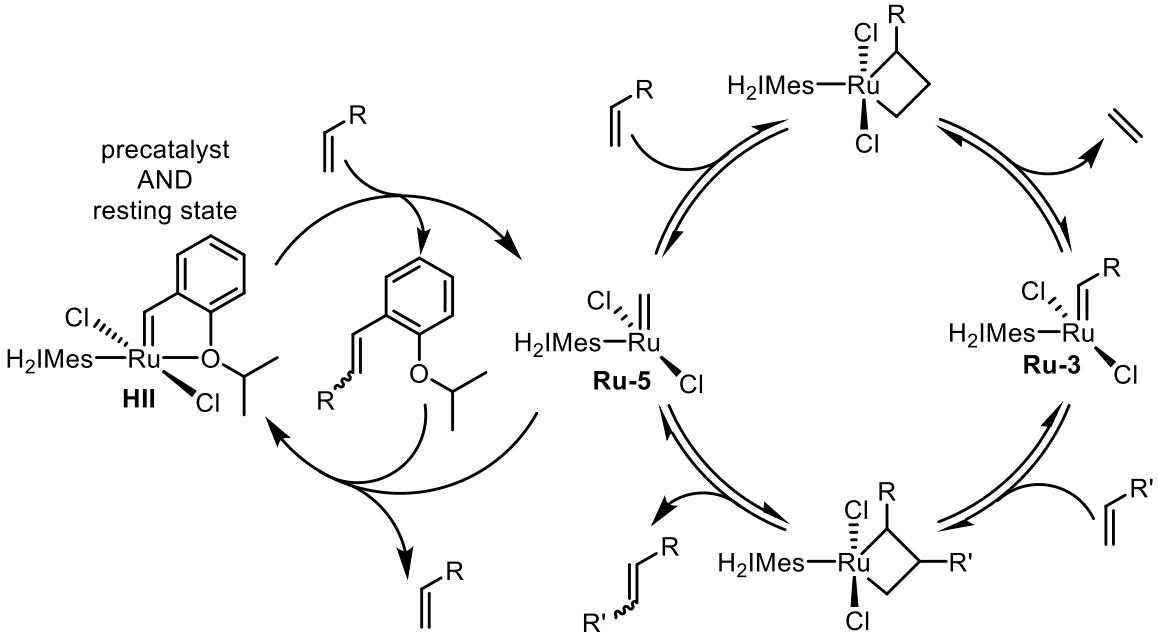

Enantioselective catalysts have also been developed (Figure 1.5).[33] Enantioselective in this context typically means "Z-selective", as kinetically E-selective catalysts remain elusive. However, as the E-isomer is generally the thermodynamically preferred species, this does not generally present an obstacle to accessing E-olefins. Chiral monodentate NHCs of C_2[34-35] and C_1[36] symmetry have both

References on page 13

been deployed in enantioselective variants of the second-generation Grubbs' catalyst. Enantioselective catalysts based on bidentate C-[37] or O-cyclometalated[38-39] NHCs are also known. These highly-tailored NHCs are not trivial to access, replacing a chloride ligand with a bulky thiolate is a comparatively simple and inexpensive method to impart enantioselectivity.[40] Enantioselectivity has also been achieved by replacing both chloride ligands with a bidentate catecholate or catechothiolate ligand. Although some reduction in activity is tolerable if it is accompanied by excellent enantioselectivity, the earliest examples based on C-cyclometalated NHCs were of modest activity *and* enantioselectivity, catalyzing the cross-metathesis of allylbenzene and cis-1,4-diacetoxybutene to 58% conversion and 41% Z-selectivity.[37] By contrast, the activity of modern enantioselective catalysts are generally comparable to their non-selective counterparts, and enantiomeric excesses in the >85% range are not uncommon.[33]

Figure 1.5: Examples of enantioselective catalysts of different types

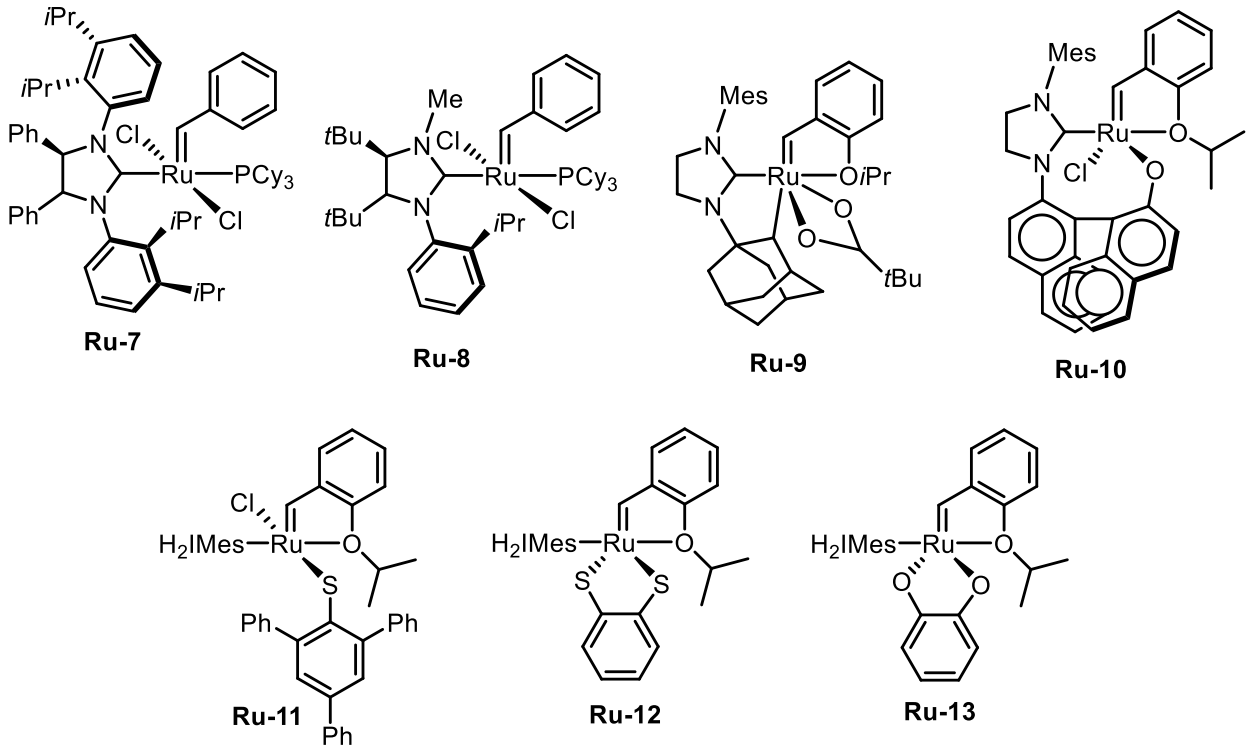

Catalyst solubilization to allow metathesis in aqueous conditions has been pursued by modifying one or more sites with charged or neutral polar groups, or by tethering to water-soluble polymers such as polyethylene-glycol (Figure 1.6).[41-42] Perplexingly, some attempts involved installing charged groups on the alkylidene,[43-46] which, while successful in solubilizing the *precatalyst*, does nothing to keep the active species solvated post-initiation. More fruitful attempts have involved installing charged groups on a non-dissociating NHC[47-48] or modified X-ligand.[49] Yields in aqueous metathesis remain low relative to anhydrous conditions,[41-42] as, despite being marketed as "water-tolerant", ruthenium metathesis catalysts are in fact deactivated/decomposed by water.[31, 50-51] The exact means by which water causes catalyst deactivation is the subject of ongoing research

References on page 13

in the Fogg lab, the fruits of which may lead to a new generation of water-tolerant water-soluble catalysts for aqueous metathesis.

Figure 1.6: Examples of water-soluble metathesis catalysts

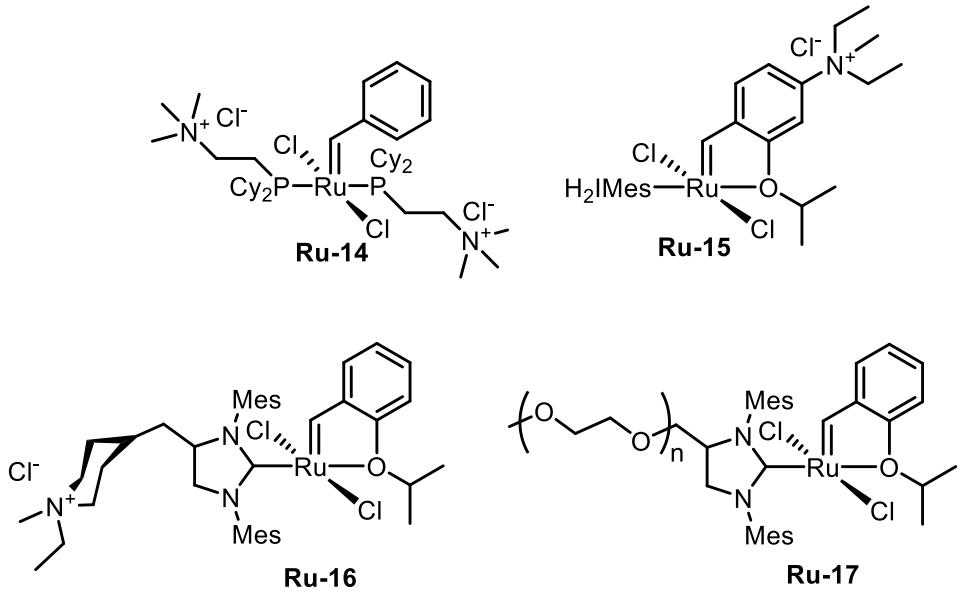

Catalyst immobilization strategies have also been explored. Immobilization has been achieved by tethering to the alkylidene,[52-53] dissociating[54] or non-dissociating[55-56] L-ligands, or modified X-ligands.[57] Catalysts have been tethered to a variety of supports, including polymers,[53, 55-56] silica,[58] and magnetic nanoparticles.[56] Immobilization promises improved catalyst recyclability, ease of separation of ruthenium from the end product, and is amenable to deployment in continuous-flow processes.[59] Disadvantages are reduced activity relative to the free catalysts, presumably due to a combination of steric shielding by the immobilizing support and the impact of catalyst immobilization on diffusion kinetics.[59-60] Tethering at the alkylidene or dissociating L-ligand is of dubious merit. On the one hand, this allows the initiated catalyst to circulate freely in solution, leading to improved performance relative to catalysts tethered at NHC[52] as this mitigates the impact of steric shielding by the support and lack of mobility. On the other hand, this rules out deployment in flow chemistry, and if the catalyst decomposes before it can be recaptured by the solid support, the advantages of immobilization are likewise lost.

In work parallel to the benzylidene catalysts, Dixneuf and other authors have developed the chemistry of indenylidene ruthenium catalysts (Figure 1.7).[61-62] Among reported catalysts, indenylidene analogues to the first and second-generation Grubbs' catalyst (**M1** and **M2**) are known,[63-64] and an isopropoxy-ether functionalized analogue to the Hoveyda-type benzylidene has also been developed (**Ru-18**).[65] With the notable exception of the recently developed chloride-bridged dimeric species **Ru-19**, indenylidene catalysts are significantly less active than their benzylidene counterparts,[66] but have the distinct advantage of not requiring the use of diazo reagents (mutagenic, explosive) in their synthesis.

References on page 13

Figure 1.7: Key indenylidene ruthenium metathesis catalysts.

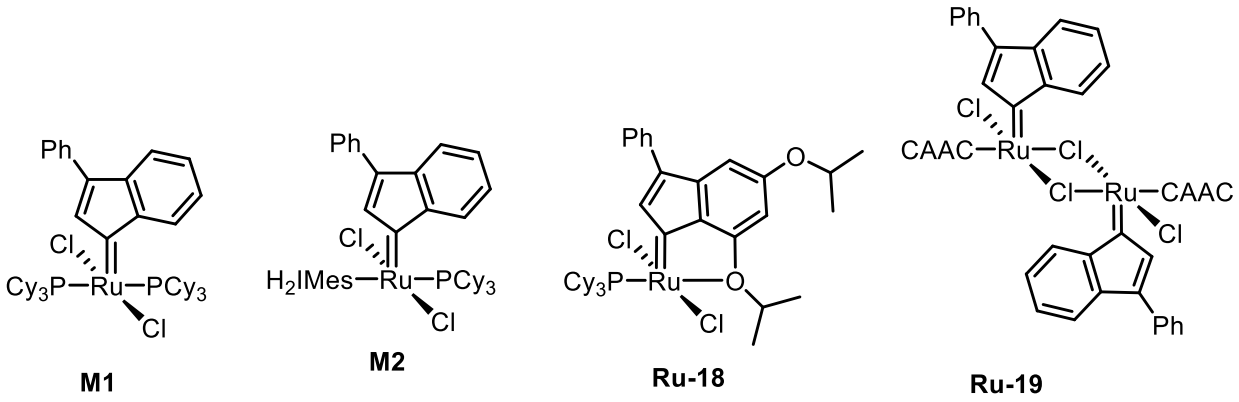

1.2 Catalyst Synthesis

1.2.1 Early Transition Metals

Alkylidene installation is the key step in catalyst synthesis, as the alkylidene functionality is key to the operation of the Chauvin mechanism of olefin metathesis.[3] In early metal systems this is traditionally accomplished by α-hydride abstraction, as typified by Schrock's 1974 synthesis of a tantalum neopentylidene.[8] In this approach, two alkyl ligands (substituted at the beta position to prevent β-hydride elimination) installed cis to one another and subjected to steric pressure will eliminate an alkane, generating the alkylidene (Scheme 1.5). This method is general for the early transition metals, and examples have been reported for W, Zr, Mo, Nb, Ta, Ti, V, Cr, and Re.[67]

Scheme 1.5: Alkylidene installation by α-hydride abstraction, as first reported in the synthesis of **Ta-1**

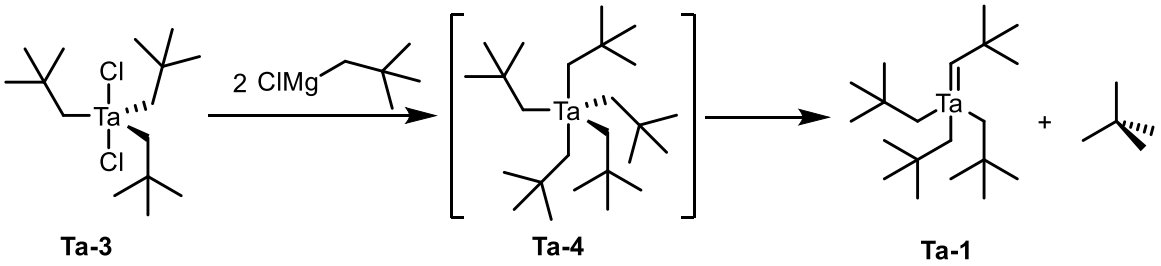

In some instances, such as with tungsten, double α-hydride abstraction can occur, generating instead an alkylidyne species (Scheme 1.6).[68] Alkylidynes are useful in their own right as catalysts for alkyne metathesis, but can also be protonated to alkylidenes. In an elegant example, hydride transfer from a neighbouring amide ligand furnishes both the alkylidene functionality and the bulky protecting imido ligand in a single step (Scheme 1.7).[15]

Scheme 1.6: Double α-hydride elimination to form a tungsten alkylidyne complex

References on page 13

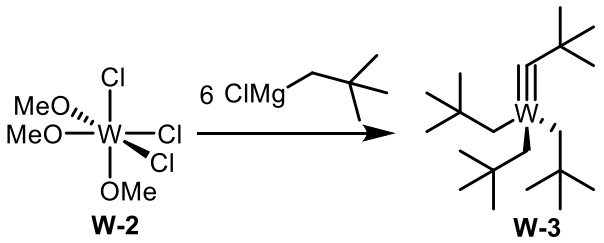

Scheme 1.7: NEt_3-catalyzed intramolecular deprotonation of a neighbouring amide ligand simultaneously converts the alkylidyne ligand to an alkylidene ligand, and the amide ligand to an imido ligand

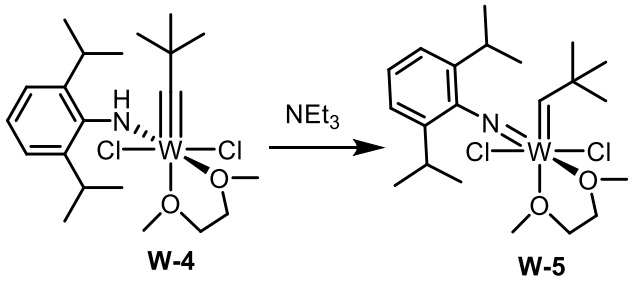

A pathway to early metal alkylidynes (and by protonation, alkylidenes) that does not rely on α-hydride abstraction involves treatment of homobimetallic W or Mo species containing a metal-metal triple bond with alkyne (Scheme 1.8)[69-70]. This is not universal for all W and Mo metal-metal triple bonds, and seems to proceed only for high oxidation-state dimers bearing electron withdrawing aryloxide ligands, which are beneficial for metathesis performance.[2]

Scheme 1.8: Metathesis-like reactivity of triply-bound W dimer and carbynes produces alkylidynes

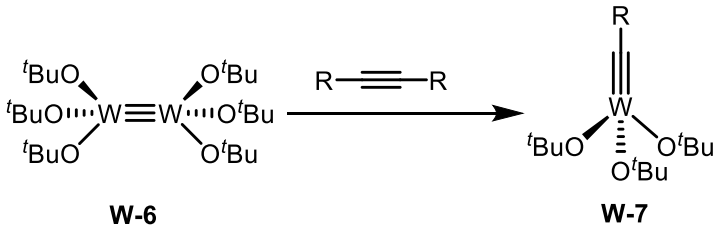

1.2.2 Ruthenium

Alkylidene installation is more challenging on ruthenium than the early metals. α-Hydride abstraction to form metathesis-active alkylidenes is unknown in ruthenium chemistry. The search for a convenient, economical, and safe method for alkylidene installation continues to be a high-value target within the field.

The earliest ruthenium alkylidenes were installed by treating a ruthenium dichloride with diphenylcyclopropene to yield vinyl-alkylidenes (Scheme 1.9).[20] The challenging synthesis and instability of highly strained diphenylcyclopropene served as a significant roadblock to large scale catalyst synthesis, limiting access to Ru alkylidenes for research and industry alike.

Scheme 1.9: Insertion/ring opening of diphenylcyclopropene produced the first known ruthenium metathesis catalyst

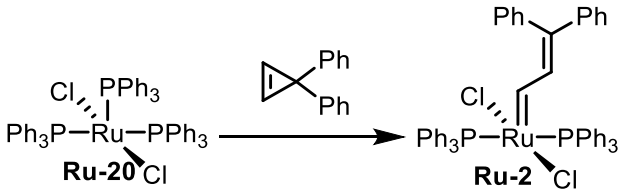

Carbene transfer by aryldiazomethane was the second alkylidene installation method to be developed with the synthesis of the first-generation Grubbs' catalyst (Scheme 1.10).[21, 71] There are well-founded concerns surrounding the explosive and toxic nature of diazo reagents,[72] and this route is operationally intensive on the bench scale. Aryldiazomethane reagents are highly unstable; they must be prepared immediately before use and are notoriously low-yielding. Stoichiometric control is poor, and it is often necessary to use a large (nominal) excess to effect complete conversion of starting material. Although yields in excess of 90% are reported in the literature,[21, 27, 71] in practice challenges in stoichiometric control arising from the volatility and instability of aryldiazomethane reagents mean that yields below 70% are routinely encountered, even in experienced hands. Despite this, carbene transfer by aryldiazomethane has essentially remained the state-of the art method for benzylidene installation. Several alternative routes to benzylidenes have been developed (and will be explored in greater detail in Chapter 3), but none have managed to supplant diazo technology.

Scheme 1.10: Synthesis of the first-generation Grubbs' catalyst by reaction of **Ru-20** with phenyldiazomethane

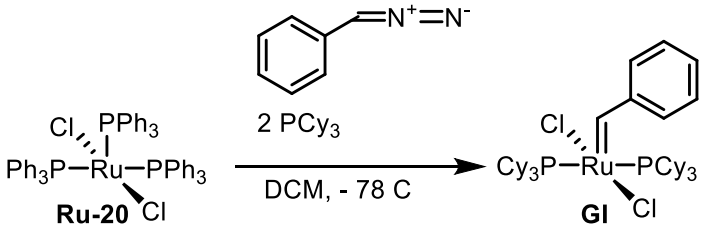

Vinyl-alkylidenes can also be accessed by reaction of a propargylic chloride with a ruthenium hydride (Scheme 1.11).[73-74] These catalysts are less active than the equivalent benzylidenes and little used outside of ROMP.

Scheme 1.11: Cyclopropene-free route to vinyl alkylidenes

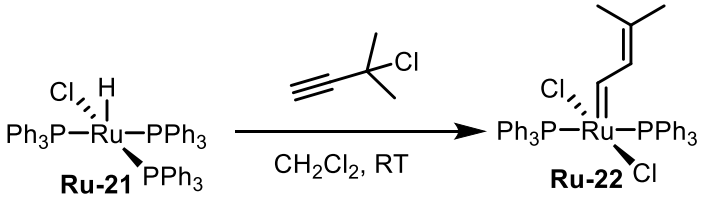

References on page 13

Treating various ruthenium dichloride species with terminal alkynes furnishes ruthenium vinylidenes in a straightforward and typically high yielding procedure (Scheme 1.12), but these complexes are poor metathesis initiators and typically catalyze only ROMP of strained cyclic olefins.[75] Related allenylidene species can be accessed by reaction of ruthenium dichlorides with propargylic alcohols (Scheme 1.13), and share the poor activity of their vinylidene analogues.[76]

Scheme 1.12: Alkyne insertion leads to vinylidenes

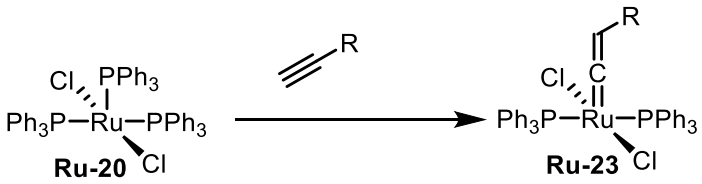

Scheme 1.13: Insertion of propargylic alcohol gives ruthenium allenylidenes, which rearrange in the presence of acid to more active indenylidene species

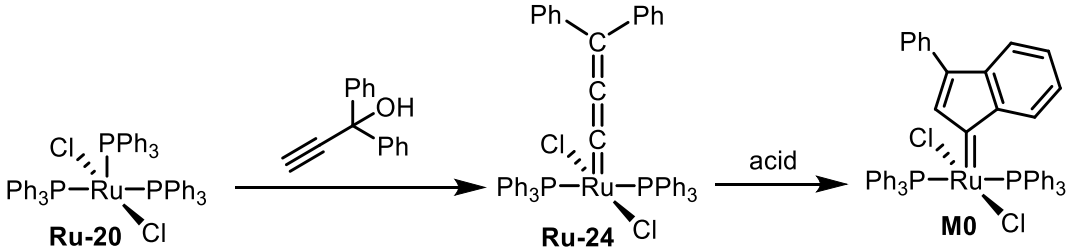

Indenylidene species, arising from acid-catalysed rearrangement of allenylidene, are significantly more active than vinylidene or allenylidene precatalysts, albeit generally less active (with the notable exception of the recently reported dimeric species **Ru-19**) than benzylidenes.[61-62, 77] They are accessed by treating a ruthenium dichloride precursor with 1,1-diphenylpropargyl alcohol in the presence of an acid catalyst, often acyl chloride (Scheme 1.13).[63, 78] The initial product (isolable in the absence of an acid catalyst) is the allenylidene species which rearranges in the presence of acid to form the indenylidene.[78] This is a significantly more reliable and user-friendly procedure than the use of aryldiazomethane reagents, but benzylidenes remain generally more active and therefore more widely used in metathesis.

Access to the most active ruthenium catalysts typically requires modification after alkylidene installation. Metathesis of benzylidene or indenylidene precursors with a tailored olefin can furnish new alkylidenes where there is a thermodynamic driving force in favour of the new alkylidene (Scheme 1.14).[28, 32, 79-81] Many new catalysts were initially reported via this approach, and this remains the only known method to install the nitro-substituted chelating benzylidene that defines the top-performing nitro-Grela family of catalysts.

References on page 13

Scheme 1.14: Metathesis of the second-generation indenylidene catalyst **M2** with a tailored olefin furnishes the highly-active second-generation nitro-Grela catalyst **nGII**

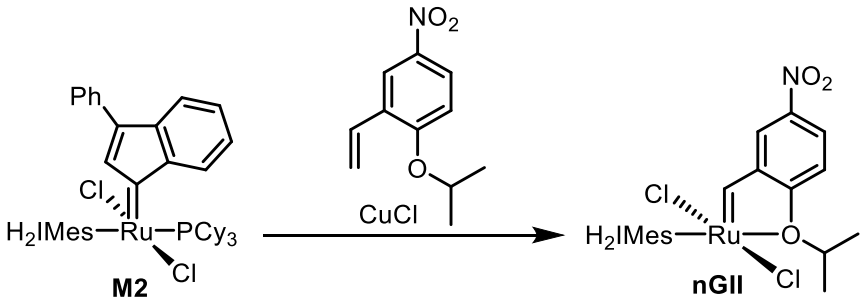

Different stabilizing ligands are installed by simple ligand substitution reactions, typically with first-generation Grubbs or indenylidene catalysts (Scheme 1.15). Historically, this has been the method for installing the H_2IMes ligand that defines the "second-generation" catalysts, though this ligand can now be installed prior to the alkylidene. CAACs, the current bleeding-edge stabilizing ligands, must still be installed after the alkylidene.[82-84]

Scheme 1.15: NHCs such as H_2IMes readily displace a phosphine ligand in the first-generation Grubbs catalyst, granting access to second-generation catalysts

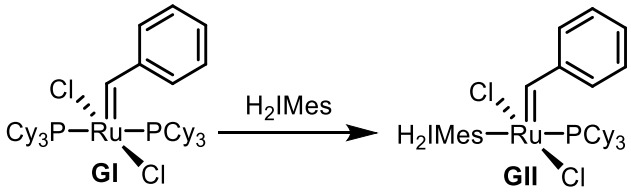

1.3 Scope of This Thesis

The aim of this thesis work is to explore novel methods of catalyst synthesis with particular attention to alkylidene installation. Chapter 2 contains experimental details. Chapter 3 discusses alternative routes to known catalyst species that avoid the use of aryldiazomethanes. α-Chloroalkylruthenium species are identified as a common intermediate arising in several apparently unrelated literature routes to ruthenium alkylidenes, and direct, deliberate installation of the α-chloroalkyl fragment is pursued via α-chloroalkylmagnesium reagents. The first high yield synthesis of $RuCl_2(H_2IMes)(py)_3$ is reported, and this compound is assessed as a potential entry point to metathesis catalysts. Pseudohalide installation by zinc nucleophiles is also explored. In Chapter 4, "low-valent" ruthenium alkylidenes are pursued, both by reduction of known metathesis catalysts and by adapting α-hydride abstraction, ubiquitous in early metal systems, to ruthenium. The latter approach also represents a new method of alkylidene installation for ruthenium metathesis catalysts.

References on page 13

1.4 References

(1) Astruc, D., Olefin Metathesis Reactions: From a Historical Account to Recent Trends. In *Olefin Metathesis*, Grela, K., Ed. John Wiley & Sons, Inc.: 2014; pp 1-36.
(2) Schrock, R. R., Multiple Metal–Carbon Bonds for Catalytic Metathesis Reactions (Nobel Lecture). *Angew. Chem., Int. Ed.* **2006,** *45*, 3748-3759.
(3) Chauvin, Y., Olefin Metathesis: The Early Days (Nobel Lecture). *Angew. Chem., Int. Ed.* **2006,** *45*, 3740-3747.
(4) Mol, J. C., Industrial Applications of Olefin Metathesis. *J. Mol. Catal. A: Chem.* **2004,** *213*, 39-45.
(5) Delaude, L.; Noels, A. F., Metathesis. In *Kirk-Othmer Encyclopedia of Chemical Technology*, John Wiley & Sons, Inc. : 2005.
(6) Ziegler, K.; Holzkamp, E.; Briel, H.; Martin, H., Polymerisation von Äthylen und anderen Olefinen. *Angew. Chem.* **1955**, 426.
(7) Calderon, N.; Chen, H. Y.; Scott, K. W., Olefin Metathesis - A Novel Reaction for Skeletal Transformations of Unsaturated Hydrocarbons. *Tetrahedron Lett.* **1967,** *8*, 3327-3329.
(8) Schrock, R. R., Alkylcarbene Complex of Tantalum by Intramolecular Alpha-Hydrogen Abstraction. *J. Am. Chem. Soc.* **1974,** *96*, 6796-6797.
(9) Schrock, R.; Rocklage, S.; Wengrovius, J.; Rupprecht, G.; Fellmann, J., Preparation and Characterization of Active Niobium, Tantalum and Tungsten Metathesis Catalysts. *J. Mol. Catal.* **1980,** *8*, 73-83.
(10) Schrock, R. R., Recent Advances in High Oxidation State Mo and W Imido Alkylidene Chemistry. *Chem. Rev.* **2009,** *109*, 3211-3226.
(11) Munz, D., Pushing Electrons—Which Carbene Ligand for Which Application? *Organometallics* **2018,** *37*, 275-289.
(12) Montgomery, C. D., Fischer and Schrock Carbene Complexes: A Molecular Modeling Exercise. *J. Chem. Educ.* **2015,** *92*, 1653-1660.
(13) Meissler, G. L.; Tarr, D. A., *Inorganic Chemistry*. 3rd ed.; Pearson Prentice Hall: Upper Saddle River, NJ, 2004.
(14) Fischer, E. O., On the Way to Carbene and Carbyne Complexes**A Nobel lecture translated by P. Legzdins and G.O. Wiedersatz, Technical University, Munich. Copyright © The Nobel Foundation, 1974. In *Adv. Organomet. Chem.*, Stone, F. G. A.; West, R., Eds. Academic Press: 1976; Vol. 14, pp 1-32.
(15) Schaverien, C. J.; Dewan, J. C.; Schrock, R. R., Multiple metal-carbon bonds. 43. Well-Characterized, Highly Active, Lewis Acid Free Olefin Metathesis Catalysts. *J. Am. Chem. Soc.* **1986,** *108*, 2771-2773.
(16) Murdzek, J. S.; Schrock, R. R., Well-Characterized Olefin Metathesis Catalysts that Contain Molybdenum. *Organometallics* **1987,** *6*, 1373-1374.
(17) Schrock, R. R.; Hoveyda, A. H., Molybdenum and Tungsten Imido Alkylidene Complexes as Efficient Olefin-Metathesis Catalysts. *Angew. Chem., Int. Ed.* **2003,** *42*, 4592-4633.
(18) Grubbs, R. H., Olefin-Metathesis Catalysts for the Preparation of Molecules and Materials (Nobel Lecture). *Angew. Chem., Int. Ed.* **2006,** *45*, 3760-3765.
(19) Nguyen, S. T.; Johnson, L. K.; Grubbs, R. H.; Ziller, J. W., Ring-Opening Metathesis Polymerization (ROMP) of Norbornene by a Group VIII Carbene Complex in Protic Media. *J. Am. Chem. Soc.* **1992,** *114*, 3974-3975.

References on page 13

(20) Nguyen, S. T.; Grubbs, R. H.; Ziller, J. W., Syntheses and Activities of New Single-Component, Ruthenium-Based Olefin Metathesis Catalysts. *J. Am. Chem. Soc.* **1993,** *115*, 9858-9859.
(21) Schwab, P.; Grubbs, R. H.; Ziller, J. W., Synthesis and Applications of $RuCl_2(CHR')(PR_3)_2$: The Influence of the Alkylidene Moiety on Metathesis Activity. *J. Am. Chem. Soc.* **1996,** *118*, 100-110.
(22) Scholl, M.; Ding, S.; Lee, C. W.; Grubbs, R. H., Synthesis and Activity of a New Generation of Ruthenium-Based Olefin Metathesis Catalysts Coordinated with 1,3-Dimesityl-4,5-dihydroimidazol-2-ylidene Ligands. *Org. Lett.* **1999,** *1*, 953-956.
(23) Sanford, M. S.; Love, J. A.; Grubbs, R. H., Mechanism and Activity of Ruthenium Olefin Metathesis Catalysts. *J. Am. Chem. Soc.* **2001,** *123*, 6543-6554.
(24) Paredes-Gil, K.; Solans-Monfort, X.; Rodriguez-Santiago, L.; Sodupe, M.; Jaque, P., DFT Study on the Relative Stabilities of Substituted Ruthenacyclobutane Intermediates Involved in Olefin Cross-Metathesis Reactions and Their Interconversion Pathways. *Organometallics* **2014,** *33*, 6065-6075.
(25) Adlhart, C.; Chen, P., Comparing Intrinsic Reactivities of the First- and Second-Generation Ruthenium Metathesis Catalysts in the Gas Phase. *Helv. Chim. Acta* **2003,** *86*, 941-949.
(26) Adlhart, C.; Hinderling, C.; Baumann, H.; Chen, P., Mechanistic Studies of Olefin Metathesis by Ruthenium Carbene Complexes Using Electrospray Ionization Tandem Mass Spectrometry. *J. Am. Chem. Soc.* **2000,** *122*, 8204-8214.
(27) Kingsbury, J. S.; Harrity, J. P. A.; Bonitatebus, P. J.; Hoveyda, A. H., A Recyclable Ru-Based Metathesis Catalyst. *J. Am. Chem. Soc.* **1999,** *121*, 791-799.
(28) Garber, S. B.; Kingsbury, J. S.; Gray, B. L.; Hoveyda, A. H., Efficient and Recyclable Monomeric and Dendritic Ru-Based Metathesis Catalysts. *J. Am. Chem. Soc.* **2000,** *122*, 8168-8179.
(29) Gessler, S.; Randl, S.; Blechert, S., Synthesis and Metathesis Reactions of a Phosphine-Free Dihydroimidazole Carbene Ruthenium Complex. *Tetrahedron Lett.* **2000,** *41*, 9973-9976.
(30) Bates, J. M.; Lummiss, J. A. M.; Bailey, G. A.; Fogg, D. E., Operation of the Boomerang Mechanism in Olefin Metathesis Reactions Promoted by the Second-Generation Hoveyda Catalyst. *ACS Catal.* **2014,** *4*, 2387-2394.
(31) McClennan, W. L.; Rufh, S. A.; Lummiss, J. A. M.; Fogg, D. E., A General Decomposition Pathway for Phosphine-Stabilized Metathesis Catalysts: Lewis Donors Accelerate Methylidene Abstraction. *J. Am. Chem. Soc.* **2016,** *138*, 14668-14677.
(32) Michrowska, A.; Bujok, R.; Harutyunyan, S.; Sashuk, V.; Dolgonos, G.; Grela, K., Nitro-Substituted Hoveyda−Grubbs Ruthenium Carbenes: Enhancement of Catalyst Activity through Electronic Activation. *J. Am. Chem. Soc.* **2004,** *126*, 9318-9325.
(33) Montgomery, P. T.; Johns, A. M.; Grubbs, R. H., Recent Advancements in Stereoselective Olefin Metathesis Using Ruthenium Catalysts. *Catalysts* **2017,** *7*, 87-125.
(34) Funk, T. W.; Berlin, J. M.; Grubbs, R. H., Highly Active Chiral Ruthenium Catalysts for Asymmetric Ring-Closing Olefin Metathesis. *J. Am. Chem. Soc.* **2006,** *128*, 1840-1846.
(35) Berlin, J. M.; Goldberg, S. D.; Grubbs, R. H., Highly Active Chiral Ruthenium Catalysts for Asymmetric Cross- and Ring-Opening Cross-Metathesis. *Angew. Chem., Int. Ed.* **2006,** *45*, 7591-7595.
(36) Fournier, P.-A.; Collins, S. K., A Highly Active Chiral Ruthenium-Based Catalyst for Enantioselective Olefin Metathesis. *Organometallics* **2007,** *26*, 2945-2949.

References on page 13

(37) Endo, K.; Grubbs, R. H., Chelated Ruthenium Catalysts for Z-Selective Olefin Metathesis. *J. Am. Chem. Soc.* **2011,** *133*, 8525-8527.
(38) Van Veldhuizen, J. J.; Campbell, J. E.; Giudici, R. E.; Hoveyda, A. H., A Readily Available Chiral Ag-Based N-Heterocyclic Carbene Complex for Use in Efficient and Highly Enantioselective Ru-Catalyzed Olefin Metathesis and Cu-Catalyzed Allylic Alkylation Reactions. *J. Am. Chem. Soc.* **2005,** *127*, 6877-6882.
(39) Van Veldhuizen, J. J.; Gillingham, D. G.; Garber, S. B.; Kataoka, O.; Hoveyda, A. H., Chiral Ru-Based Complexes for Asymmetric Olefin Metathesis: Enhancement of Catalyst Activity through Steric and Electronic Modifications. *J. Am. Chem. Soc.* **2003,** *125*, 12502-12508.
(40) Occhipinti, G.; Hansen, F. R.; Törnroos, K. W.; Jensen, V. R., Simple and Highly Z-selective Ruthenium-Based Olefin Metathesis Catalyst. *J. Am. Chem. Soc.* **2013,** *135*, 3331-3334.
(41) Sabatino, V.; Ward, T. R., Aqueous Olefin Metathesis: Recent Developments and Applications. *Beilstein J. Org. Chem.* **2019**, 445–468.
(42) Tomasek, J.; Schatz, J., Olefin Metathesis in Aqueous Media. *Green Chem.* **2013,** *15*, 2317-2338.
(43) Roberts, A. N.; Cochran, A. C.; Rankin, D. A.; Lowe, A. B.; Schanz, H.-J., Benzylidene-Functionalized Ruthenium-Based Olefin Metathesis Catalysts for Ring-Opening Metathesis Polymerization in Organic and Aqueous Media. *Organometallics* **2007,** *26*, 6515-6518.
(44) Michrowska, A.; Gułajski, Ł.; Kaczmarska, Z.; Mennecke, K.; Kirschning, A.; Grela, K., A Green Catalyst for Green Chemistry: Synthesis and Application of an Olefin Metathesis Catalyst Bearing a Quaternary Ammonium Group. *Green Chem.* **2006,** *8*, 685-688.
(45) Dunbar, M. A.; Balof, S. L.; Roberts, A. N.; Valente, E. J.; Schanz, H.-J., pH-Responsive Ruthenium-Based Olefin Metathesis Catalysts: Controlled Ring-Opening Metathesis Polymerization in Alcoholic and Aqueous Media upon Acid Addition. *Organometallics* **2011,** *30*, 199-203.
(46) Rix, D.; Clavier, H.; Coutard, Y.; Gulajski, L.; Grela, K.; Mauduit, M., Activated Pyridinium-Tagged Ruthenium Complexes as Efficient Catalysts for Ring-Closing Metathesis. *J. Organomet. Chem.* **2006,** *691*, 5397-5405.
(47) Jordan, J. P.; Grubbs, R. H., Small-Molecule N-Heterocyclic-Carbene-Containing Olefin-Metathesis Catalysts for Use in Water. *Angew. Chem., Int. Ed.* **2007,** *46*, 5152-5155.
(48) Skowerski, K.; Szczepaniak, G.; Wierzbicka, C.; Gułajski, Ł.; Bieniek, M.; Grela, K., Highly Active Catalysts for Olefin Metathesis in Water. *Catal. Sci. Technol.* **2012,** *2*, 2424-2427.
(49) Binder, J. B.; Guzei, I. A.; Raines, R. T., Salicylaldimine Ruthenium Alkylidene Complexes: Metathesis Catalysts Tuned for Protic Solvents. *Adv. Synth. Catal.* **2007,** *349*, 395-404.
(50) Guidone, S.; Songis, O.; Nahra, F.; Cazin, C. S. J., Conducting Olefin Metathesis Reactions in Air: Breaking the Paradigm. *ACS Catal.* **2015,** *5*, 2697-2701.
(51) Jongkind, L. J.; Rahimi, M.; Poole, D.; Ton, S. J.; Fogg, D. E.; Reek, J. N. H., Protection of Ruthenium Olefin Metathesis Catalysts by Encapsulation in a Self-assembled Resorcinarene Capsule. *ChemCatChem* **2020,** *12*, 4019-4023.
(52) Randl, S.; Buschmann, N.; Connon, S. J.; Blechert, S., Highly Efficient and Recyclable Polymer-Bound Catalyst for Olefin Metathesis Reactions. *Synlett* **2001,** *2001*, 1547-1550.

References on page 13

(53) Ahmed, M.; Barrett, A. G. M.; Braddock, D. C.; Cramp, S. M.; Procopiou, P. A., A Recyclable 'Boomerang' Polymer-Supported Ruthenium Catalyst for Olefin Metathesis. *Tetrahedron Lett.* **1999,** *40*, 8657-8662.
(54) Mennecke, K.; Grela, K.; Kunz, U.; Kirschning, A., Immobilisation of the Grubbs III Olefin Metathesis Catalyst with Polyvinyl Pyridine (PVP). *ChemInform* **2006,** *37*.
(55) Nguyen, S. T.; Grubbs, R. H., The Syntheses and Activities of Polystyrene-Supported Olefin Metathesis Catalysts Based on $Cl_2(PR_3)_2Ru = CH{-}CH = CPh_2$. *J. Organomet. Chem.* **1995,** *497*, 195-200.
(56) Skowerski, K.; Bialecki, J.; Czarnocki, S. J.; Zukowska, K.; Grela, K., Effective Immobilization of a Metathesis Catalyst Bearing an Ammonium-Tagged NHC Ligand on Various Solid Supports. *Beilstein J. Org. Chem.* **2016,** *12*, 5-15.
(57) Halbach, T. S.; Mix, S.; Fischer, D.; Maechling, S.; Krause, J. O.; Sievers, C.; Blechert, S.; Nuyken, O.; Buchmeiser, M. R., Novel Ruthenium-Based Metathesis Catalysts Containing Electron- Withdrawing Ligands: Synthesis, Immobilization, and Reactivity. *J. Org. Chem.* **2005,** *70*, 4687-4694.
(58) Nasrallah, H.; Dragoe, D.; Magnier, C.; Crévisy, C.; Mauduit, M.; Schulz, E., Direct Immobilization of Ru-Based Catalysts on Silica: Hydrogen Bonds as Non-Covalent Interactions for Recycling in Metathesis Reactions. *ChemCatChem* **2015,** *7*, 2493-2500.
(59) Suriboot, J.; Bazzi, H. S.; Bergbreiter, D. E. Supported Catalysts Useful in Ring-Closing Metathesis, Cross Metathesis, and Ring-Opening Metathesis Polymerization *Polymers (Basel)* [Online], 2016. PubMed. http://europepmc.org/abstract/MED/30979231

https://doi.org/10.3390/polym8040140

https://europepmc.org/articles/PMC6432279

https://europepmc.org/articles/PMC6432279?pdf=render (accessed 2016/04//).
(60) Hübner, S.; de Vries, J. G.; Farina, V., Why Does Industry Not Use Immobilized Transition Metal Complexes as Catalysts? *Adv. Synth. Catal.* **2016,** *358*, 3-25.
(61) Dixneuf, P. H.; Bruneau, C., Ruthenium Indenylidene Catalysts for Alkene Metathesis. In *Handbook of Metathesis*, Grubbs, R. H.; Wenzel, A. G.; O'Leary, D. J.; Khosravi, E., Eds. 2015; pp 389-416.
(62) Boeda, F.; Clavier, H.; Nolan, S. P., Ruthenium–Indenylidene Complexes: Powerful Tools for Metathesis Transformations. *Chem. Commun.* **2008**, 2726-2740.
(63) Jafarpour, L.; Schanz, H.-J.; Stevens, E. D.; Nolan, S. P., Indenylidene−Imidazolylidene Complexes of Ruthenium as Ring-Closing Metathesis Catalysts. *Organometallics* **1999,** *18*, 5416-5419.
(64) Fürstner, A.; Grabowski, J.; Lehmann, C. W., Total Synthesis and Structural Refinement of the Cyclic Tripyrrole Pigment Nonylprodigiosin. *J. Org. Chem.* **1999,** *64*, 8275-8280.
(65) Tabari, D. S.; Tolentino, D. R.; Schrodi, Y., Reactivation of a Ruthenium-Based Olefin Metathesis Catalyst. *Organometallics* **2013,** *32*, 5-8.
(66) do Nascimento, D. L.; Gawin, A.; Gawin, R.; Guńka, P. A.; Zachara, J.; Skowerski, K.; Fogg, D. E., Integrating Activity with Accessibility in Olefin Metathesis: An Unprecedentedly Reactive Ruthenium-Indenylidene Catalyst. *J. Am. Chem. Soc.* **2019**.
(67) Schrock, R. R., High Oxidation State Multiple Metal-Carbon Bonds. *Chem. Rev.* **2002,** *102*, 145-179.
(68) Schrock, R. R.; Clark, D. N.; Sancho, J.; Wengrovius, J. H.; Rocklage, S. M.; Pedersen, S. F., Tungsten(VI) Neopentylidyne Complexes. *Organometallics* **1982,** *1*, 1645-1651.

(69) Listemann, M. L.; Schrock, R. R., Multiple Metal Carbon Bonds. 35. A General Route to Tri-Tert-Butoxytungsten Alkylidyne Complexes. Scission of Acetylenes by Ditungsten Hexa-Tert-Butoxide. *Organometallics* **1985,** *4*, 74-83.
(70) Schrock, R. R.; Listemann, M. L.; Sturgeoff, L. G., Metathesis of Tungsten-Tungsten Triple Bonds with Acetylenes and Nitriles to Give Alkylidyne and Nitrido Complexes. *J. Am. Chem. Soc.* **1982,** *104*, 4291-4293.
(71) Schwab, P.; France, M. B.; Ziller, J. W.; Grubbs, R. H., A Series of Well-Defined Metathesis Catalysts–Synthesis of $[RuCl_2(=CHR')(PR_3)_2]$ and Its Reactions. *Angew. Chem., Int. Ed. Engl.* **1995,** *34*, 2039-2041.
(72) Bray, P. A.; Sokas, R. K., Delayed Respiratory Fatality From Trimethylsilyldiazomethane: What Do Workers Need to Know About Potentially Hazardous Exposures? *J. Occup. Environ. Med.* **2015,** *57*, e15-e16.
(73) Volland, M. A. O.; Rominger, F.; Eisenträger, F.; Hofmann, P., An 'Old Hydride' in a New Synthesis: a Convenient Approach to Grubbs-type Carbene Complexes $(PPh_3)_2Cl_2Ru(=CH=CH=CR_2)$ and their Hexacoordinate Acetonitrile Adducts. *J. Organomet. Chem.* **2002,** *641*, 220-226.
(74) Amoroso, D.; Snelgrove, J. L.; Conrad, J. C.; Drouin, S. D.; Yap, G. P. A.; Fogg, D. E., An Attractive Route to Olefin Metathesis Catalysts: Facile Synthesis of a Ruthenium Alkylidene Complex Containing Labile Phosphane Donors. *Adv. Synth. Catal.* **2002,** *344*, 757-763.
(75) Dragutan, I.; Verpoort, F.; Dragutan, V.; Drozdzak, R. In *Ruthenium–Vinylidene Complexes: An Efficient Class of Homogeneous Metathesis Catalysts*, Metathesis Chemistry, Dordrecht, 2007//; Imamoglu, Y.; Dragutan, V.; Karabulut, S., Eds. Springer Netherlands: Dordrecht, 2007; pp 137-150.
(76) Bruneau, C., Ruthenium Vinylidenes and Allenylidenes in Catalysis. In *Ruthenium Catalysts and Fine Chemistry: -/-*, Bruneau, C.; Dixneuf, P. H., Eds. Springer Berlin Heidelberg: Berlin, Heidelberg, 2004; pp 125-153.
(77) Nolan, S. P.; Clavier, H.; Urbina-Blanco, C. A., Indenylidene Ruthenium Complex Bearing a Sterically Demanding NHC Ligand: An Efficient Catalyst for Olefin Metathesis at Room Temperature. *Organometallics* **2009,** *28*, 2848-2854.
(78) Shaffer, E. A.; Chen, C.-L.; Beatty, A. M.; Valente, E. J.; Schanz, H.-J., Synthesis of Ruthenium Phenylindenylidene, Carbyne, Allenylidene and Vinylmethylidene Vomplexes from $(PPh_3)_{3-4}RuCl_2$: A Mechanistic and Structural Investigation. *J. Organomet. Chem.* **2007,** *692*, 5221-5233.
(79) Nascimento, D. L.; Davy, E. C.; Fogg, D. E., Merrifield Resin-Assisted Routes to Second-Generation Catalysts for Olefin Metathesis. *Catal. Sci. Technol.* **2018,** *8*, 1535-1544.
(80) van Lierop, B. J.; Reckling, A. M.; Lummiss, J. A. M.; Fogg, D. E., Clean, Convenient, High-yield Access to Second-generation Ru Metathesis Catalysts from Commercially Available Precursors. *ChemCatChem* **2012,** *4*, 2020-2025.
(81) Basak, T.; Grudzień, K.; Barbasiewicz, M., Remarkable Ability of the Benzylidene Ligand To Control Initiation of Hoveyda–Grubbs Metathesis Catalysts. *Eur. J. Inorg. Chem.* **2016,** *2016*, 3513-3523.
(82) Anderson, D. R.; Lavallo, V.; O'Leary, D. J.; Bertrand, G.; Grubbs, R. H., Synthesis and Reactivity of Olefin Metathesis Catalysts Bearing Cyclic (Alkyl)(Amino)Carbenes. *Angew. Chem., Int. Ed.* **2007,** *46*, 7262-7265.

(83) Gawin, R.; Tracz, A.; Chwalba, M.; Kozakiewicz, A.; Trzaskowski, B.; Skowerski, K., Cyclic Alkyl Amino Ruthenium Complexes—Efficient Catalysts for Macrocyclization and Acrylonitrile Cross Metathesis. *ACS Catal.* **2017,** *7*, 5443-5449.
(84) Marx, V. M.; Sullivan, A. H.; Melaimi, M.; Virgil, S. C.; Keitz, B. K.; Weinberger, D. S.; Bertrand, G.; Grubbs, R. H., Cyclic Alkyl Amino Carbene (CAAC) Ruthenium Complexes as Remarkably Active Catalysts for Ethenolysis. *Angew. Chem., Int. Ed.* **2015,** *54*, 1919-1923.

References on page 13

Chapter 2. Experimental Methods

2.1 General Considerations

Unless otherwise specified, reactions were carried out under N_2 using standard glovebox or Schlenk line techniques. Room temperature corresponds to ca. 25 °C in the glovebox, or ca. 23 °C on the Schlenk line. All glassware was oven-dried at 110 °C for minimum 16 h prior to use.

2.1.1 Solvents

Hexanes, toluene, benzene, tetrahydrofuran, dichloromethane, and diethyl ether were degassed and dried with a Glass Contour or Anhydrous Engineering solvent purification system, using dry argon as the protecting gas. Methanol was distilled from magnesium methoxide (prepared by pouring methanol over magnesium activated with I_2); acetone from $CaSO_4$, and pentane from P_2O_5. All distillations were carried out under N_2, after which the solvents were brought into the glovebox. All solvents were stored over 4 Å sieves (except methanol: stored over 3 Å sieves) for at least 12 h before use. Acetone was not stored over sieves, to avoid a self-condensation reaction. Reactions in air were carried out in bench-grade solvents as received.

2.1.2 Deuterated Solvents

Deuterated solvents were purchased from Cambridge Isotope Laboratories. $CDCl_3$ for use with non-air sensitive compounds was stored over 4 Å sieves on the bench. $CDCl_3$ and C_6D_6 for analysis of air or moisture sensitive species were degassed via minimum 4 freeze-pum*p*-thaw cycles and dried over 4 Å molecular sieves for minimum 12 h before use.

2.1.3 Reagents

IMes,[1] H_2IMes,[1] **HII**,[2] Mg-anthracene ·3THF,[3] *o*-(O^{i}Pr)(C_6H_4)CH_2OH,[4] *o*-(O^{i}Pr)(C_6H_4)CHO[5] $RuCl_2$(H_2IMes)(*p*-cymene),[2] $RuCl_2(PPh_3)_3$,[6] $[RuCl_2(p\text{-cymene})]_2$,[7] $RuCl_2$(1,10-phenanthroline)$(PPh_3)_2$,[8] and $RuCl_2(py)_4$[9] were prepared according to published procedures.

$RuCl_3$·xH_2O, n-butyllithium (2.5 M solution in hexanes, AcroSeal®), $MePPh_3$•Br (98%), and 2,4,6-trimethylaniline (97%) were purchased from Acros Organics.

Magnesium turnings (99.998+%), PPh_3 (99%), PCy_3 (97%), and Et_2Zn (95+%) were purchased from Strem Chemicals.

Potassium carbonate (K_2CO_3, 99.0+%), 1,10-phenanthroline (anhydrous, 99%), benzaldehyde (PhCHO, >99%), triethylene glycol (99%), NaH (95%), formic acid (CHOOH, >95%), tetrafluoroboric acid solution (HBF_4; 48 wt % in H_2O), sodium borohydride ($NaBH_4$, ≥96%), glyoxal solution (40 wt % in H_2O), PCl_5 (95%), HC≡CC(C_6H_5)$_2$OH (99%), anthracene (99%), lithium hexamethyldisilane (LiHMDS, 97%), lithium diisopropylamide (LDA, 97%), potassium tri-*sec*-butylborohydride (KBH^{s}Bu$_3$, 1.0 M in THF), sodium (Na, 99.9%), thionyl chloride ($SOCl_2$, 99+%), and α-phellandrene (75+% kosher grade) were purchased from Aldrich.

Pyridine (99.5+%), *p*-toluenesulfonyl hydrazine (98%), triethylorthoformate (98%), 2-picoline (98+%), 2,6-lutidine (98+%), and 3-bromopyridine (98+%) were purchased from Alfa Aesar.

References on page 31

Isopropyl iodide (99.0+%), isopropyl chloride (99.0+%), salicyl alcohol (98+%) and salicylaldehyde (98+%) were purchased from TCI America.

2.2 Instrumentation

2.2.1 NMR Spectroscopy

Room temperature ^{1}H, ^{31}P, ^{1}H-^{1}H COSY, and ^{1}H-^{13}C HMBC spectra were collected on a Bruker Avance 300 spectrometer (chemical shifts reported in ppm). VT NMR was collected on a Bruker Avance II 300 spectrometer. Air-sensitive samples were prepared under N_2 in J-Young or Rotoflow tubes; all other samples were prepared in standard NMR tubes.

2.2.2 Gas Chromatography-Mass Spectrometry

Gas chromatography (GC) coupled to electron ionization mass spectrometry (EI-MS) was performed using an Agilent Technologies 5975B inert XL EI/CL MSD at the CCRI institute laboratory at uOttawa.

2.3 Experimental Data for Chapter 3

2.3.1 Synthesis of Benzal Chloride ($PhCHCl_2$)

26.6 g PCl_5 (127.88 mmol, 1.3 equiv) was dissolved in 30 mL CH_2Cl_2 and cooled to –78 °C. Benzaldehyde (10 mL, 98.58 mmol, 1 equiv) was added dropwise via syringe and the reaction mixture was allowed to warm to 0 °C (ice bath) with stirring over 4 h. After 4 h, the reaction was judged complete by thin-layer chromatography (silica gel plate, Et_2O eluant), and quenched by addition of cold distilled water followed by $CaCO_3$ until evolution of CO_2 ceased. The mixture was then extracted with CH_2Cl_2 (3 x 20 mL) and the combined organic fractions washed with distilled water (3 x 20 mL) and brine (3 x 20 mL). The organic fractions were then dried with $MgSO_4$ and stripped on a rotary evaporator to yield the crude product as a yellow oil. The product was found to decompose on a full-length silica or alumina column, so impurities were removed by quickly passing through a three-finger's width alumina plug with Et_2O as the eluant. Removal of Et_2O under high vacuum afforded the product as a colourless oil. Yield: 10.77 g (68%). The ^{1}H NMR spectrum is consistent with literature values.[10]

^{1}H NMR (300 MHz $CDCl_3$): δ 7.57 (m, 2H, Ph-*H*), 7.39 (m, 3H, Ph-*H*), 6.71 (s, 1H, C*H*Cl_2)

2.3.2 Synthesis of *o*-Isopropoxybenzal Chloride (*o*-$O^iPrC_6H_4CCl_2$)

In a 2-neck round-bottom flask, 16.5 g PCl_5 (79.12 mmol, 1.3 equiv) was dissolved in 30 mL CH_2Cl_2 and cooled to –78 °C in a dry-ice acetone bath. *o*-$O^iPrC_6H_4CHO$ (10 mg, 61 mmol) was added dropwise via syringe and the reaction mixture was allowed to warm to 0 °C (ice bath) with stirring over 4 h, at which point the reaction was judged complete by thin-layer chromatography (silica gel plate, Et_2O eluant), and quenched by addition of cold distilled water. The mixture was then extracted with CH_2Cl_2 (3 x 20 mL) and the combined organic fractions washed with distilled water (3 x 20 mL) and brine (3 x 20 mL). The organic fractions were then dried with $MgSO_4$ and stripped on a rotary evaporator to yield the crude product as a yellow oil, which was subsequently distilled under Schlenk line vacuum at 98 °C to yield the product as a colourless oil. Yield 10.77 g (72%).

References on page 31

Storage and handling note: It was found that storing *o*-O^{i}PrC$_6$H$_4$CCl$_2$ over molecular sieves resulted in an exothermic decomposition to a purple-pink resin within ca. 1 h. When stored at room temperature in the glovebox, the compound turned pink over the course of a week. Thus, it was redistilled and stored in the glovebox freezer (set at –35 °C) as a precaution. Under these conditions, the compound remained stable with no sign of coloration for over six months.

^{1}H NMR (300 MHz, CDCl$_3$): δ 7.83 (ddt, $^5J_{HH}$ = 0.5 Hz, $^4J_{HH}$ = 2.0 Hz, $^3J_{HH}$ = 8.0 Hz, 1H, Ar-*H*), 7.32 (dddd, $^4J_{HH}$ = 2.0 Hz, $^3J_{HH}$ = 7.5 Hz, $^3J_{HH}$ = 8.5 Hz, 1H, Ar-*H*), 7.23 (s, 1H, C*H*Cl$_2$), 7.02 (dddd, $^5J_{HH}$ = 0.5 Hz, $^4J_{HH}$ = 1.0 Hz, $^3J_{HH}$ = 8.0 Hz, 1H, Ar-*H*), 6.89 (dt, $^5J_{HH}$ = 0.5 Hz, $^3J_{HH}$ = 8.5 Hz, 1H, Ar-*H*), 4.62 (m, $^5J_{HH}$ = 0.5 , $^3J_{HH}$ = 6.0 Hz, 1H, C*H*(CH$_3$)$_2$), 1.38 (d, $^3J_{HH}$ = 6.0 Hz, 6H, CH(C*H*$_3$)$_2$).

NOTE: In order to obtain a spectrum with the proper integration, it was necessary to increase the d1 relaxation time to 10 s. Otherwise, the intensity of the signals in the aromatic region was stunted.

2.3.3 Assay of Magnesium-Anthracene Complex (Mg-1)

Mg-1 was prepared according to a reported procedure.[3] As **Mg-1** decomposes in most solvents and is only sparingly soluble in THF (in which it is stable), NMR analysis was not attempted. Reagent purity was determined by titration against MeOH with 1,10-phenanthroline as colorimetric indicator, a method which has not previously been reported for **Mg-1**. 100 mg of **Mg-1** (0.119 mmol) was suspended in ca. 10 mL THF. Addition of 1,10-phenanthroline caused a color change from orange to intense purple-red. A 10% v/v solution of MeOH was added dropwise via a 100 μL gas-tight syringe while the mixture was vigorously stirred until the purple-red colour no longer persisted (96.5 μL, 0.238 mmol, 2 equiv). The endpoint was reached at 99.8% of the expected amount of MeOH, indicating a high degree of purity for **Mg-1** and minimal residual anthracene.

2.3.4 In Situ Preparation and Decomposition of Mg(*o*-O^{i}PrC$_6$H$_4$CHCl)Cl (Mg-2)

115 mg **Mg-1** (0.274 mmol) was suspended in ca. 15 mL THF, and 60.16 mg *o*-(O^{i}Pr)(C$_6$H$_4$)CHCl$_2$ (0.274 mmol, 1 equiv) was added dropwise with vigorous stirring, causing an immediate colour change from bright orange to intense green. Upon complete addition, the colour became light yellow and the reaction was allowed to stir for 3 h. The solvent was removed under vacuum, the off-white residue was taken up in C$_6$H$_6$ and passed through Celite to remove magnesium salts and an aliquot taken for GC-MS analysis. GC-MS analysis indicated 2 major products; anthracene (eluting at ~7.5 min, *m/z* of M$^+$: 178.1 amu) and *o*-(O^{i}Pr)(C$_6$H$_4$)CHCH(C$_6$H$_4$)*o*-O^{i}Pr (eluting at ~9.5 min *m/z* of M$^+$: 296.3 amu). A minor product eluting at ~8.5 min, and with an M$^+$ peak at the same *m/z* value of the species assigned as *o*-(O^{i}Pr)(C$_6$H$_4$)CHCH(C$_6$H$_4$)*o*-O^{i}Pr is presumed to be the minor (E or Z) isomer. An additional minor species eluting at ~5.7 min (M$^+$: 207.1 amu) could not be identified, but is presumed to arise from an impurity in *o*-(O^{i}Pr)(C$_6$H$_4$)CHCl$_2$.

2.3.5 Attempted Trapping of Mg(*o*-O^{i}PrC$_6$H$_4$CHCl)Cl (Mg-2)

In a 20 ml scintillation vial, 126 mg **Mg-1** (0.301 mmol) was suspended in ca. 15 mL THF and 65.91 mg *o*-(O^{i}Pr)(C$_6$H$_4$)CHCl$_2$ (0.301 mmol, 1 equiv) was added rapidly with vigorous stirring. Aliquots were taken and quenched by adding to vials containing ca. 2 mL MeOH at 5 s, 30 s, 1 min, 5 min, 10 min, 15 min, and 30 min. Aliquots were stripped to dryness and analyzed by ^{1}H

References on page 31

NMR spectroscopy to detect and quantify the anticipated hydrolysis product *o*-(O^iPr)(C_6H_4)CH_2Cl. In no case were signals for *o*-(O^iPr)(C_6H_4)CH_2Cl detectable.

2.3.6 Reaction Conditions for Attempted Syntheses of $RuCl_2(=CHPh)(PCy_3)_2$ (GI) and $RuCl_2(=CH\text{-}2\text{-}O^iPrC_6H_4)(PPh_3)$ (Ru-39)

2.3.6.1 Condition 1: Adding Solid Mg-1 to Premixed $RuCl_2(PPh_3)_3$ and o-$O^iPrC_6H_4CHCl_2$ at RT

A 20 mL scintillation vial was charged with 50.0 mg $RuCl_2(PPh_3)_3$ (52.1 μmol), 15 mL THF, 12.7 mg *o*-$O^iPrC_6H_4CHCl_2$ (57.4 μmol, 1.1 equiv), and a stir-bar. With vigorous stirring, 24.0 **Mg-1** (57.4 μmol, 1.1 equiv) was added all at once as a powder, causing an immediate colour change from light brown to dark brown-green. ^1H NMR analysis (C_6D_6) revealed 29% in situ yield of **Ru-39**, as determined by comparison of the integration for the alkylidene signal of **Ru-39** (1H, 16.7 ppm) and anthracene (H9, H10; s, 2H, 8.4 ppm).

2.3.6.2 Condition 2: Adding Solid Mg-1 to Premixed $RuCl_2(PPh_3)_3$ and $PhCHCl_2$ at RT

A 20 mL scintillation vial was charged with 52.0 mg $RuCl_2(PPh_3)_3$ (54.2 μmol), 15 mL THF, 9.6 mg $PhCHCl_2$ (59.6 μmol, 1.1 equiv), and a stir bar. With vigorous stirring, 25.0 mg **Mg-1** (59.6 μmol, 1.1 equiv) and PCy_3 were added all at once as a premixed powder, causing an immediate colour change from light brown to dark brown-red. ^1H NMR revealed 41% in situ yield of **GI**, as determined by comparison of the integration for the alkylidene signal of **GI** (1H, 20.57 ppm) and the signal for the 9 and 10 protons of anthracene (H9, H10; s, 2H, 8.4 ppm).

2.3.6.3 Condition 3: Slowly Adding Mg-1 as a Suspension in THF to Premixed $RuCl_2(PPh_3)_3$ and *o*-$O^iPrC_6H_4CHCl_2$ at RT

A 20 mL scintillation vial was charged with 51.0 mg $RuCl_2(PPh_3)_3$ (53.2 μmol), 15 mL THF, 12.8 mg *o*-$O^iPrC_6H_4CHCl_2$ (58.5 μmol, 1.1 equiv), and a stir bar. With vigorous stirring, 24.5 (58.5 μmol, 1.1 equiv) **Mg-1** was added dropwise as a suspension in THF, causing an immediate colour change from light brown to dark brown-red. ^1H NMR analysis revealed 7% in situ yield of **Ru-39**, as determined by integration of the alkylidene signal for **Ru-39** (1H, ppm) vs anthracene (H9, H10; s, 2H, ppm).

2.3.6.4 Condition 4: Adding Mg-1 to $RuCl_2(PPh_3)_3$ Prior to Addition of *o*-$O^iPrC_6H_4CHCl_2$

A 20 mL scintillation vial was charged with 51.0 mg $RuCl_2(PPh_3)_3$ (53.2 μmol), 15 mL THF, and a stir bar. With vigorous stirring, 24.5 mg **Mg-1** (58.5 μmol, 1.1 equiv) was added dropwise as a suspension in THF, causing a colour change from light brown to dark black-red. 12.8 mg *o*-$O^iPrC_6H_4CHCl_2$ (58.5 μmol, 1.1 equiv) was added dropwise via gas-tight syringe, with no noticeable colour change. ^1H NMR analysis revealed no alkylidene formation.

2.3.6.5 Condition 5: Adding Pre-Generated Mg-2 to $RuCl_2(PPh_3)_3$ at –78 °C

A Schlenk flask was charged with 25.0 **Mg-1** (59.6 μmol, 1.1 equiv), 10 mL THF, and a stir bar and cooled to –78 °C in a dry ice-acetone bath. 13.0 mg *o*-$O^iPrC_6H_4CHCl_2$ (59.6 μmol, 1.1 equiv) was added dropwise via gas-tight syringe, causing a gradual change from a bright orange suspension to an orange suspension with dark green supernatant, to a bright yellow suspension. A

References on page 31

second Schlenk flask was charged with 52.0 mg $RuCl_2(PPh_3)_3$ (54.2 μmol), 10 mL THF, and a stir bar and cooled in a separate dry-ice acetone bath. The magnesium-containing solution was added by cannula, causing a colour change to brown-green. The mixture was allowed to stir for 1 h at –78 °C, then 1 h at 0 °C, and finally 1 h at RT. The solvent was removed. No alkylidene signal was observed in the crude mixture upon ^{1}H NMR analysis.

2.3.6.6 Condition 6: Adding Pre-Generated Mg-2 to $RuCl_2(H_2IMes)$(*p*-cymene) (Ru-33) at –78 °C

A Schlenk flask was charged with 36.1 mg **Mg-1** (86.1 μmol, 1.1 equiv), 10 mL THF, and a stir bar and cooled in a dry ice-acetone bath. 18.9 mg *o*-O^{i}PrC$_6$H$_4$CHCl$_2$ (86.1 μmol, 1.1 equiv) was added dropwise via gas-tight syringe, causing a gradual change from a bright orange suspension to an orange suspension with dark green supernatant, and finally a bright yellow suspension. A second Schlenk flask was charged with 48.0 mg **Ru-33** (78.3 μmol, 1 equiv), 10 mL THF, and a stir bar and cooled in a separate dry-ice acetone bath. The magnesium-containing solution was transferred to the ruthenium-containing flask via cannula, causing a colour change from deep red to brown-black. The mixture was allowed to stir for 1 h at –78 °C, 1 h at 0 °C, and 1h at RT. The solvent was removed. ^{1}H NMR analysis of the crude mixture showed no alkylidene signal.

2.3.6.7 Condition 7: Adding Pre-Generated Mg-2 to $[RuCl_2$(*p*-cymene)$]_2$ (Ru-35) at –78 °C

A Schlenk flask was charged with 34.5 mg **Mg-1** (86.1 μmol, 1.1 equiv), 10 mL THF, and a stir bar and cooled in a dry ice-acetone bath. 18.0 mg *o*-O^{i}PrC$_6$H$_4$CHCl$_2$ (86.1 μmol, 1.1 equiv) was added dropwise via gas-tight syringe, causing a gradual change from a bright orange suspension to an orange suspension with dark green supernatant to a bright yellow suspension. A second Schlenk flask was charged with 24.0 mg **Ru-35** (39.2 μmol), 10 mL THF, and a stir bar and cooled in a separate dry-ice acetone bath. The magnesium-containing solution was transferred to the ruthenium-containing flask via cannula, causing a gradual colour change from light orange to brown-black. The mixture was allowed to stir for 1 h at –78 °C, 1 h at 0 °C, and 1h at RT. The solvent was removed. ^{1}H NMR analysis of the crude mixture showed no alkylidene signal.

2.3.7 Synthesis of $RuCl_2(H_2IMes)(py)_4$ (Ru-50)

In a darkened glovebox, 256 mg (0.418 mmol) **Ru-35** was suspended in 25 mL THF in a round bottom flask equipped with a magnetic stirrer and shielded from external light by aluminum foil. The top of the flask was sealed with a rubber septum and the septum pierced with a 30 mL plastic syringe with the plunger removed. In a separate flask, 262.6 mg (0.857 mmol, 2.05 equiv) H_2IMes was dissolved in 25 mL THF. The H_2IMes solution was then poured into the 30 mL syringe and left to drip through to the round bottom flask containing **Ru-35** over the next 45 min. After the syringe had drained completely, it was quickly rinsed through with ca. 5 mL THF to ensure quantitative transfer. The syringe and septum were thereafter removed and 212 μL pyridine (2.633 mmol, 6.3 equiv) was added via gas-tight syringe. The foil was then removed from the round bottom flask, the glovebox lights turned on, and the reaction mixture left to stir at 60 °C for 4 h, during which time there was a gradual colour change from dark red to dark orange-yellow. ^{1}H NMR analysis of an aliquot taken at this point indicated complete conversion to the target species. The THF was removed under vacuum, and the product was isolated as a bright orange powder by reprecipitation from a minimum volume of CH_2Cl_2 by addition of hexanes followed by cooling in

a freezer set to -40 °C for 12 h. Yield: 263 mg, 88%. ^{1}H NMR chemical shifts are in excellent agreement with those reported.[11]

^{1}H NMR (C_6D_6): δ 9.62 (dt, $^4J_{HH}$ = 1.5 Hz, $^3J_{HH}$ = 5.0 Hz, 4H, *o*-py-*H*), 9.40 (dd, 2H, $^4J_{HH}$ = 1.5 Hz, $^3J_{HH}$ = 5.0 Hz, *o*-py-*H*), 6.52 (dt, 2H, $^4J_{HH}$ = 1.5 Hz, $^3J_{HH}$ = 8.0 Hz, *p*-py-*H*), 6.41 (*m*, $^4J_{HH}$ = 1.5 Hz, $^3J_{HH}$ = 7.5 Hz, 2H, *p*-py-*H*), 6.28 (m, 6H, overlapping H_2IMes-Ar-*H* + *m*-py-*H*), 5.98 (ddd, $^5J_{HH}$ = 1.0 Hz, $^4J_{HH}$ = 5.5 Hz, $^3J_{HH}$ = 7.5 Hz, 4H, *m*-py-*H*), 3.64 (s, 4H, H_2IMes-CH_2), 2.70 (s, 12H, *o*-Mes-CH_3), 1.88, (s, 6H, *p*-Mes-CH_3)

2.3.8 Representative Procedure for Attempted Syntheses of Substituted Pyridine Derivatives of Ru-50

In a darkened glovebox, 50 mg **Ru-33** (81.64 μmol) was dissolved in ca. 15 mL THF. 30 μL 3-Br-py (312 μmol, 3.8 equiv) was added dropwise via gas-tight syringe and the mixture was stirred at 60 °C for 4 h, during which time the colour changed from dark red to orange. The solvent was removed under vacuum. The product $RuCl_2(H_2IMes)(3\text{-Br-py})_3$ (**Ru-56c**) was isolated as a dark orange powder by reprecipitation from a minimum volume of CH_2Cl_2 by addition of hexanes followed by cooling in a freezer set to -35 °C for 12 h. Yield: 55 mg (69%)

^{1}H NMR (C_6D_6): δ 9.70 (m, 2H, *o*-py-*H*), 9.54 (m, 3H, *o*-py-*H*), 9.20 (m, 1H, *o*-py-*H*), 6.68 (s, 1H, Ar-*H*), 6.50 (m, 1H, Ar-*H*), 6.32 (m, 1H, Ar-*H*), 6.00 (m, 1H, Ar-*H*), 5.80 (m, 1H, Ar-*H*), 5.54 (m, 2H, Ar-*H*), 3.50 (s, 4H, H_2IMes-CH_2), 2.79 (s, 3H, *o*-Mes-CH_3) 2.67 (s, 6H, *o*-Mes-CH_3), 2.55 (s, 3H, *o*-Mes-CH_3), 1.87 (s, 6H, *p*-Mes-CH_3).

2.3.9 Representative Procedure for Ligand Substitution Experiments on Ru-50

In a 4 mL scintillation vial, 6.3 mg **Ru-50** (8.80 μmol) and 2.3 mg PPh_3 (8.80 μmol, 1 equiv) were dissolved in ca. 1 mL $CDCl_3$, mixed vigorously for 3 h, and then transferred to a J-Young NMR tube for ^{1}H NMR analysis. Conversion was assessed by comparing the integration ratios of diagnostic signals for the ortho-protons on bound and free pyridine (bound (**Ru-50**): δ 9.03 ppm, 8.72 ppm; free: δ 8.62 ppm), indicating 31% conversion to $RuCl_2(H_2IMes)(py)_2(PPh_3)$ (**Ru-53c**).

2.3.10 Representative Procedure for Attempted Indenylidene Installation on Ru-50/Ru-56c

In a 4 mL scintillation vial, 21.4 mg **Ru-50** (29.9 μmol) was dissolved in 1 mL THF. Added 6.5 mg $HC{\equiv}CC(Ph)_2OH$ (31.4 μmol, 1.05 equiv), rinsing in with an additional 2 mL THF to ensure quantitative transfer. The mixture was brought to 65 °C and let to stir for 4 h, during which time the colour changed from light yellow-orange to dark brown. ^{1}H NMR analysis showed mostly starting material with no signs of allenylidene or indenylidene formation. Workup not pursued.

2.3.11 Representative Procedure for Attempted Synthesis of Ru-58

In a 20 mL vial, 14.3 mg **HII** (22.8 μmol) was dissolved in ca. 5 mL CH_2Cl_2. In a separate vial, $Zn(OC_6F_5)_2$ was prepared by dissolving 8.82 mg C_6F_5OH (47.9 μmol, 2.1 equiv) in CH_2Cl_2 and adding dropwise 2.5 μL of neat Et_2Zn (23.9 μmol, 1.05 equiv). The $Zn(OC_6F_5)_2$ solution was then added dropwise to the solution of **HII**, prompting a steady colour change from green to brown over about 30 min. Reaction progress was monitored by ^{1}H NMR analysis of aliquots taken at 1, 3, and 24 h. Conversion was assessed by comparison of the integration for the alkylidene peaks of

References on page 31

HII (16.59 ppm), **Ru-58** (17.17 ppm), and **Ru-60** (16.9 ppm). Conversion to **Ru-60** reached 50% but no **Ru-58** was observed. Workup was not pursued.

2.4 Experimental Protocols for Chapter 4

2.4.1: Representative Procedure for Attempted Reduction of HII

In a 4 mL vial, 69.0 mg **HII** (0.110 mmol) was dissolved in ca. 2 mL THF and 204 μL tri-*sec*-butylborohydride (1.0 M in THF, 0.110 mmol, 1 equiv) was added dropwise, triggering an immediate colour change from green to black. ^{1}H NMR analysis indicated complete loss of all alkylidene signals and very ill-defined spectrum. Workup not pursued.

2.4.2 Synthesis of *o*-Isopropoxybenzyl Chloride (*o*-(O^{i}Pr)(C$_6$H$_4$)CH$_2$Cl)

o-Isopropoxybenzyl chloride was synthesized according to a modification of a published procedure.[4] On the Schlenk line: a two-neck round bottom flask equipped with condenser and stir bar was loaded with 4.29 g *o*-isopropoxyphenol and 24 mL CH_2Cl_2 as solvent. The flask was cooled to 0 °C in an ice bath, and 3.8 mL $SOCl_2$ (2 equiv) was added dropwise. The mixture was stirred for 30 min at 0 °C, during which time the solution became slightly yellow. The reaction was then stirred at reflux until the yellow colour disappeared, at which point it was deemed complete by TLC (silica gel plate, Et_2O eluant), allowed to cool to room temperature, and excess $SOCl_2$ quenched by slow addition of excess MeOH (added until evolution of gas ceased). The mixture was dried with $MgSO_4$ and solvent removed on the rotovap to give a yellow oil, which was then distilled off of sodium carbonate under Schlenk line vacuum at 95 ° C to give the product as a colourless oil. Yield: 3.64 g, 76%. If sodium carbonate is omitted, product may instead polymerize, forming a dark purple resin. ^{1}H NMR analysis is consistent with reported values.[4]

Storage and handling note: As with the related geminal dichloride, storage over molecular sieves causes decomposition to a purple-pink resin. Decomposition is relatively slow compared to the dichloride (on the order of hours rather than minutes).

^{1}H NMR (300 MHz, $CDCl_3$): δ 7.37 (dd, $^4J_{HH}$ = 1.5 Hz, $^3J_{HH}$ = 7.0 Hz, 1H, Ar-H), 7.28 (td, $^4J_{HH}$ = 2.0 Hz, $^3J_{HH}$ = 8.0 Hz, 1H, Ar-H), 6.92 (t, $^3J_{HH}$ = 8.5 Hz, 2H, Ar-H), 4.66 (s, 2H, Ar-CH_2), 4.62 (sept, $^3J_{HH}$ = 6.0 Hz, 1H O-CH), 1.38 (d, $^3J_{HH}$ = 6.0 Hz, 6H, O^{i}Pr-CH_3).

2.4.3 Preparation of a solution of MgCl(κ^2-*o*-O^{i}PrBn), Mg-1

In the glovebox: added 2g of magnesium turnings (99.998+%, trace metal basis, Aldrich, stored in glovebox upon receipt), 30 mL THF and a stir bar. With vigorous stirring, added dropwise 3g of *o*-isopropoxybenzyl chloride via syringe, monitoring temperature by tactile feedback. The flask began to warm immediately upon addition, indicating initiation without an induction period. The rate of addition was controlled to avoid boiling of THF. The reaction mixture was allowed to stir for 1 h after complete addition, during which time the liquid took on a yellow-grey colour. Excess magnesium and magnesium oxide were removed by filtering through a Celite plug and the Grignard reagent was titrated against dry methanol using 1,10-phenanthroline as an indicator. A stock solution of MeOH in THF was prepared by combining 100 μL MeOH with 9900 μL THF. A 100 μL aliquot of the Grignard reagent was then placed in a 4 mL vial with flea stir bar and

References on page 31

diluted to ca. 1 mL with THF. A single crystal (<1mg) 1,10-phenanthroline was added to the aliquot, producing a deep red-purple colour. The MeOH stock solution was then added dropwise from a 100 μL gas-tight syringe until the deep red-purple vanished. This procedure was repeated 4 times, and the results averaged. Concentration found: 0.54 M. A complementary total base titration was carried out by quenching a 100 μL aliquot of the Grignard reagent with ca. 1 mL MeOH and titrating against a calibrated solution of HCl with phenolphthalein as indicator. Concentration found: 0.54 M. Excellent agreement between titration methods indicates minimal presence of MgOH in Grignard solution.

^{1}H NMR analysis: an aliquot of the Grignard reagent was stripped down under vacuum and the residue taken up in C_6D_6 for analysis. Two sets of signals were detectable, consistent with the Schlenk equilibrium between MgClR and MgR_2. Integration for both species presented as MgClR

^{1}H NMR (300 MHz, C_6D_6): δ 7.30 (d, 1H, Ar-*H*), 6.92 (*td*, $^4J_{HH}$ = 1.5 Hz, $^3J_{HH}$ = 7.0 Hz, 1H, Ar-*H*), 6.5 (m, 2H, Ar-*H*), 4.36 (sept, $^3J_{HH}$ = 6.0 Hz, 1H, OC*H*$(CH_3)_2$), 1.73 (s, 2H, ArCH_2Mg), 1.32 (d, $^3J_{HH}$ = 6.0 Hz, 6H, OCH(CH_3)$_2$)

^{1}H NMR (300 MHz, C_6D_6): δ 7.07 (m, 1H, Ar-*H*), 6.83 (*m*, 1H, Ar-*H*), 6.67 (m, 2H, Ar-*H*), 4.18 (sptd, $^5J_{HH}$ = 0.5 Hz, $^3J_{HH}$ = 6.0 Hz, 1H, OC*H*$(CH_3)_2$), 2.25 (s, 2H, ArCH_2Mg), 1.10 (d, $^3J_{HH}$ = 6.0 Hz, 6H, OCH(CH_3)$_2$)

2.4.4 Representative Procedure for Attempted Installation of *o*-O^{i}PrBn Ligand on Ru^{II} Chlorides

In a 20 mL vial, 112 mg $RuCl_2(PPh_3)_3$ (0.116 mmol) was dissolved in 10 mL THF. 120 μL **Mg-3** (as a 0.97 M solution in THF, 0.116 mmol, 1 equiv) was added dropwise via gas-tight syringe. Over the course of addition of the Grignard reagent, a sequential colour change from brown to amber to black was observed.. ^{1}H NMR analysis at this point showed a very poorly defined mixture consisting of many poorly resolved signals, implying decomposition. Workup not pursued.

2.4.5 Synthesis of RuCl(κ^2-*o*-O^{i}PrBn)(η^6-*p*-cymene) (Ru-84)

In the glovebox: 200 mg (0.327 mmol) of $[RuCl_2(p\text{-cymene})]_2$ was dissolved in ca. 30 mL CH_2Cl_2 in a round bottom flask equipped with a magnetic stir bar. 1239 μL **Mg-3** (as a 0.52 M solution in THF, 0.669 mmol, 2.05 equiv) was added dropwise via gas-tight syringe. Over the course of addition of **Mg-3**, the colour changed from orange-red to a much darker red. Solvent removed under vacuum immediately after complete addition of **Mg-3**. The red residue was extracted with benzene and filtered through Celite until the benzene ran colourless. Benzene was then removed under vacuum and the product was isolated as a crystalline red solid by reprecipitation from a minimum volume of CH_2Cl_2 with hexanes. Yield 213 mg, 82%.

^{1}H NMR (300 MHz, C_6D_6): δ 6.84 (*m*, 2H, benzyl Ar-H), 5.75 (t, $^4J_{HH}$ = 4.0 Hz, 1H, benzyl Ar-H), 5.5 (t, $^4J_{HH}$ = 4.0 Hz, 1H, benzyl Ar-H), 4.92 (s, 1H, benzyl CH_2), 4.56 (s, 1H, *p*-cymene Ar-H), 4.18 (s, 1H, *p*-cymene Ar-H), 3.92 (sept, $^3J_{HH}$ = 6.0 Hz, 1H, O^{i}Pr C-H), 3.65 (s, 1H, *p*-cymene Ar-H), 3.18 (s, 1H, *p*-cymene Ar-H), 2.83 (s, 1H, benzyl CH_2), 2.63 (sept, $^3J_{HH}$ = 7.0 Hz, 1H, Ar-

References on page 31

*i*Pr C*H*), 1.88 (s, 3H, *p*-cymene CH_3), 1.23 (dd, $^5J_{HH}$ = 5.5 Hz, $^3J_{HH}$ = 24.5 Hz, 6H, ^{i}Pr CH_3), 1.02 (br s, 6H, O^{i}Pr CH_3).

2.4.6 General Procedure for Reaction of Ru-84 With Neutral Donors

In the glovebox: 25 mg **Ru-84** (59.5 μmol) was dissolved in ~10 mL THF in a 20 mL vial equipped with a stir bar. 18.24 mg H_2IMes (59.5 μmol, 1 equiv) was then added dropwise as a solution in 5 mL THF. The reaction mixture was allowed to stir for 3 h, during which the colour gradually changed from deep red to dark brown. Removing solvent and taking a crude ^{1}H NMR spectrum showed loss of signals associated with benzyl ligand and bound *p*-cymene, very poorly defined alkyl region, indicative of decomposition. Workup not pursued.

2.4.7 Representative Procedure for Attempted Deprotonation of Ru-84 by Strong Base

In the glovebox: dissolved 32 mg **Ru-84** (76.2 μmol) in ~10 mL benzene in a 20 mL vial equipped with a stir bar. In a separate container, dissolved 12.75 mg LiHMDS (76.2 μmol, 1 equiv) in ~10 mL benzene and this added dropwise to the **Ru-84**-containing vial. Upon complete addition of LiHMDS, observed a colour change from red to very dark brown, nearly black. ^{1}H NMR analysis of an aliquot taken at this point revealed nearly complete loss of all signals outside of a very poorly defined alkyl region. Workup not pursued.

2.4.8 Attempted Deprotonation of Ru-84 by 2-Lithiopyridine

On the Schlenk line: 2-lithiopyridine was generated in-situ according to a literature method.[12] 39.2 μL 2-bromopyridine was diluted with 10 mL THF and cooled to –78 °C (dry-ice acetone bath). 214 μL n-BuLi (0.98 M in hexanes) was then added dropwise against N_2 via gas-tight syringe and left to stir for 30 min during which time the solution became orange-red. In a separate Schlenk flask, dissolved 156.9 mg of **Ru-84** in 10 mL THF and cooled to –78. The 2-lithiopyridine solution was then added by dropwise cannula transfer, maintaining the temperature of both the sending and receiving flasks at –78 C. Reaction left to stir for 1 h, during which time a colour change was observed from light red to dark brown/orange. The reaction was left to stir for an additional 1 h at 0 °C, before warming to room temperature and removing solvent under vacuum. ^{1}H NMR analysis of the crude mixture revealed a very poorly defined spectrum with a large number of broad, ill-defined signals. Workup not pursued.

2.4.9 Synthesis of Ru(κ^2-*o*-O^{i}PrBn)(κ^1-*o*-O^{i}PrBn)(η^6-*p*-cymene) (Ru-85)

In a 4 mL vial, 88.3 mg **Ru-84** (0.210 mmol) was dissolved in ca. 2 mL THF, and 408 μL**Mg-3** (as a 0.58 M solution in THF, 0.221 mmol, 1.05 equiv) was added dropwise via gas-tight syringe. Upon complete addition of **Mg-3**, the colour immediately changed from dark red to light orange. Removed solvent under vacuum, took up the residue in C_6H_6 and passed through Celite to remove magnesium salts. Attempts to isolate product by reprecipitation from minimal CH_2Cl_2 by addition of hexanes unsuccessful. Removal of solvent followed by treatment with hexanes revealed product to be highly soluble in hexanes. Attempted crystallization from neat hexanes in the glovebox freezer (-40 °C, 24 h) was unsuccessful. ^{1}H NMR analysis was carried out on the waxy orange

References on page 31

residue left after removal of solvent under vacuum. For details of spectral analysis, see section **4.2.5** and **Appendix B** Figures B2.11 and B2.12

2.4.10 General Procedure for Reaction of Ru(κ²-*o*-O^{i}PrBn)(κ¹-*o*-isopropoxybenzyl)(η⁶-*p*-cymene) With Neutral Donors

Starting with 56.2 mg **Ru-84** (0.133 mmol), prepared in situ a benzene solution of **Ru-85** according to the method in section **2.4.9**. Added as a solid 25.32 mg 1,10-phenanthroline (0.140 mmol, 1.05 equiv), causing an immediate colour change from light yellow-orange to intense green. The intensely green complex decomposed to a spectroscopically ill-defined black mixture in the time it took to prepare an NMR sample. Workup not pursued.

2.4.11 General Procedure for Attempted Installation of Aryloxides on Ru-84 Via Mg Aryloxides

Dissolved 101.1 mg **Ru-84** (0.240 mmol) in ca. 5 mL THF. In a separate container, prepared in-situ a THF solution of Mg(OC_6F_5)Cl by dissolving 45.42 mg C_6F_5OH (0.247 mmol, 1.025 equiv) in ca. 5 mL THF and adding dropwise 193 μL Mg(*i*Pr)Cl as a 1.28 M solution in THF (0.247 mmol, 1.025 equiv). Added dropwise the generated Mg(OC_6F_5)Cl to the **Ru-84** solution and let stir for 6 h at room temperature. There was no detectable colour change during this time, and ^{1}H NMR analysis of an aliquot taken at this point revealed exclusively starting material. The reaction mixture was heated to 60 °C and let stir an additional 12 h. Again, no colour change was observed and ^{1}H NMR analysis at this point showed exclusively starting material.

2.4.12 General Procedure for Attempted Installation of Aryloxides on Ru-35 Via Mg Aryloxides

Dissolved 23 mg **Ru-35** (375 μmol) in ca. 10 mL THF. In a separate container, prepared in-situ a THF solution of Mg(OC_6F_5)Cl by dissolving 13.82 mg C_6F_5OH (751 μmol, 2 equiv) in ca. 5 mL THF and adding dropwise 58.7 μL Mg(*i*Pr)Cl as a 1.28 M solution in THF (751 μmol, 2 equiv). Added dropwise the generated Mg(OC_6F_5)Cl to the **Ru-84** solution and let stir for 18 h at 68 °C. There was no evidence of colour change after 6 h, and ^{1}H NMR analysis at this point showed exclusively starting material.

2.4.13 Unintentional Synthesis of $RuCl_2$(η⁶-*p*-cymene)(py) (Ru-94)

Dissolved 73 mg **Ru-35** (0.119 mmol) in ca. 10 mL THF, and added 20 μL pyridine (0.244 mmol, 2.05 equiv) via gas-tight syringe. In a separate container, prepared in-situ a THF solution of Mg(OC_6F_5)Cl by dissolving 44.98 mg C_6F_5OH (0.244mmol, 2.05 equiv) in ca. 5 mL THF and adding dropwise 191 μL Mg(*i*Pr)Cl as a 1.28 M solution in THF (0.244 mmol, 2.05 equiv). Added dropwise the generated Mg(OC_6F_5)Cl to the **Ru-84** solution and let stir for 18 h at 68 °C. Observed a gradual colour change from orange-red to yellow-orange during this time. ^{1}H NMR of an aliquot taken at the 6 h mark is a match for known complex **Ru-94**,[13] workup not pursued.

^{1}H NMR (300 MHz, C_6D_6): 9.01 (m, 2H, *o*-py-*H*), 7.73 (m, 1H, *p*-py-*H*), 7.30 (m, 2H, *m*-py-*H*), 5.42 (d, 2H, *p*-cymene-Ar-*H*), 5.22 (d, 2H, *p*-cymene-Ar-*H*), 2.98 (sept, 1H, *p*-cymene-C*H*(CH_3)$_2$), 2.09 (s, 3H, *p*-cymene-Ar-C*H*$_3$), 1.29 (d, 6H, *p*-cymene-CH(C*H*$_3$)$_2$)

2.4.14 Synthesis of Ru(κ^2-*o*-O^{i}PrBn)(OC$_6$F$_5$)(η^6-*p*-cymene) (Ru-86)

Route 1:

In the glovebox, a 20 mL vial was charged with 29.2 mg **Ru-84** (69.5 μmol), 10 mL benzene, and a stir bar. In a separate vial was dissolved 11.6 mg C_6F_5OH (76.5 μmol, 1.1 equiv) in benzene and added dropwise 35.63 μL of 1.0 M $ZnEt_2$ in hexanes (35.6 μmol, 0.5125 equiv) with stirring to generate $Zn(OC_6F_5)_2$ in situ. $Zn(OC_6F_5)_2$ was added dropwise to the vial containing ruthenium and the solution was left to stir 2 h. No noticeable colour change was observed. Solvent was removed under vacuum and the crude mixture analyzed by NMR spectroscopy. ^{1}H NMR analysis revealed complete consumption of starting material and emergence of a new set of signals consistent with the target product. Attempted isolation by extracting the residue with benzene and passing through Celite until benzene ran colourless. Benzene was then removed under vacuum and reprecipitation attempted from a minimum volume of CH_2Cl_2 with hexanes. Only minimal precipitation of a dark brown powder occurred, even after 24 h in a freezer set at -40 C. Precipitate and bright red supernatant were separated via filtration and analyzed by ^{1}H NMR spectroscopy in C_6D_6. The dark brown precipitate showed poorly defined signals not consistent with target product, most signals being of negligible integration compared to residual proton peak. The bright red supernatant showed a new set of signals consistent with the target product plus the reappearance of the signals for starting material. By comparison of integration for the *p*-cymene CH_3 signals for starting material and product, mixture consists of 76% product and 24% starting material.

Route 2:

In the glovebox: 51 mg of **Ru-84** (121 mmol) was dissolved in CH_2Cl_2. 236.1 μL of a 0.54 M THF solution of **Mg-1** (121 mmol 1 equiv) was added dropwise via gas-tight syringe, causing an immediate colour change from dark red to light orange. CH_2Cl_2 was then removed under vacuum and the residue extracted with hexanes and passed through Celite to remove generated $MgCl_2$. In a separate vial, prepared a solution of 22.4 mg C_6F_5OH (121 mmol, 1 equiv) in ca. 5 mL hexanes and added this dropwise to the reaction mixture. Let stir 1 h, during which time a slow colour change from orange to red occurred. Removed solvent and analyzed the intense red residue by ^{1}H NMR (300 MHz, C_6D_6); observed 100% consumption of starting material, liberation of *o*-isopropoxy toluene (confirmed by overlaying a spectrum of deliberately hydrolyzed **Mg-1**), and a new set of signals consistent with target product (and route 1). Product remains highly soluble in hexanes, not yet isolated. ^{1}H NMR values are consistent with product from Route 1 plus 1 equiv of *o*-O^{i}Pr(C_6H_4)CH_3.

^{1}H NMR (300 MHz, C_6D_6): 6.91 (m, 2H, benzyl Ar-*H*), 5.76 (d, $^3J_{HH}$ = 7.5 Hz 1H, benzyl Ar-*H*), 5.11 (d, $^3J_{HH}$ = 6.5 Hz benzyl 1H, Ar-*H*), 5.07 (br s, 1H, benzyl C*H*$_2$), 4.23 ppm (br s, 1H, *p*-cymene Ar-*H*), 3.93 ppm (br s, 1H, *p*-cymene Ar-*H*), 3.89 (sept, $^3J_{HH}$ = 6.0 Hz, 1H, OC*H*) 3.81 (br s, 1H, *p*-cymene Ar-*H*), 3.36 (br s, 1H, *p*-cymene Ar-*H*), 2.58 ppm (sept, $^3J_{HH}$ = 6.9 Hz, 1H, Ar-C*H*), 2.47 (br s, 1H, benzyl C*H*$_2$), 1.19 (br-m, 6H, *p*-cymene Ar-CH(C*H*$_3$)$_2$ NOTE: overlaps with residual hexanes signal), 1.01 (br s, 6H, O^{i}Pr-C*H*$_3$).

References on page 31

2.4.15 Attempted Deprotonation of Ru(κ^2-*o*-O^{i}Pr(C$_6$H$_4$)CH$_2$)(OC$_6$F$_5$)(η^6-*p*-cymene) Ru-86 by LiHMDS

Starting from 103 mg **Ru-84** (0.245 mmol), prepared in situ a benzene solution of **Ru-86** according to **2.4.14** (Route 2). In a separate vial, dissolved 41.4 LiHMDS (0.245 mmol, 1 equiv) in benzene. Added the LiHMDS solution dropwise to **Ru-84**. No noticeable colour change upon addition, so the mixture was left to stir for 8 h. No colour change observed at 8 h, and ^{1}H NMR analysis of an aliquot taken at this point showed mostly starting material with considerable loss of resolution, new broad signals in the alkyl region, and no signal in the alkylidene region. Workup not pursued.

2.4.16 Synthesis of Ru(κ^2-*o*-O^{i}Pr(C$_6$H$_4$)CH$_2$)(py)(η^6-*p*-cymene)

Starting from 25.1 mg **Ru-84** (59.7 μmol), prepared in situ a hexanes solution of **Ru-86** according to **2.4.14** (Route 2). Added dropwise 4.8 μL pyridine (62.7 μmol, 1.05 equiv) via gas-tight syringe and let stir 8 h. No noticeable colour change at this point, but ^{1}H NMR analysis of the crude mixture revealed a broad signal in the alkylidene region at 14.2 ppm, signals for bound pyridine at 8.76 and 8.38 ppm, and no sign of the signals for free pyridine at 8.53, 6.98, and 6.66 ppm, seeming to indicate successful formation of **Ru-88**. Attempts to induce precipitation by cooling in the glovebox freezer (-40 °C) were unsuccessful.

References on page 31

2.5 References

(1) Arduengo, A. J.; Krafczyk, R.; Schmutzler, R.; Craig, H. A.; Goerlich, J. R.; Marshall, W. J.; Unverzagt, M., Imidazolylidenes, Imidazolinylidenes and Imidazolidines. *Tetrahedron* **1999,** *55*, 14523-14534.
(2) Day, C. S.; Fogg, D. E., High-Yield Synthesis of a Long-Sought, Labile Ru-NHC Complex and Its Application to the Concise Synthesis of Second-Generation Olefin Metathesis Catalysts. *Organometallics* **2018,** *37*, 4551-4555.
(3) Bogdanović, B.; Liao, S.-T.; Mynott, R.; Schlichte, K.; Westeppe, U., Rate of Formation and Characterization of Magnesium Anthracene. *Chem. Ber.* **1984,** *117*, 1378-1392.
(4) Sumner, C. R. Treatment of Learning Disabilities and Motor Skills Disorder With Norepinephrine Reuptake Inhibitors. WO2005020975A2, 2005.
(5) Hamlin, T. A.; Kelly, C. B.; Leadbeater, N. E., Dehydrogenation of Perfluoroalkyl Ket-ones by Using a Recyclable Oxoammonium Salt. *Eur. J. Inorg. Chem.* **2013,** *2013*, 3658-3661.
(6) Stephenson, T. A.; Wilkinson, G., New Complexes of Ruthenium(II) and -(III) With Triphenylphosphine, Triphenylarsine, Trichlorostannate, Pyridine, and Other Ligands. *J. Inorg. Nucl. Chem.* **1966,** *28*, 945-956.
(7) Bennett, M. A.; Huang, T. N.; Matheson, T. W.; Smith, A. K.; Ittel, S.; Nickerson, W., (η^6-Hexamethylbenzene)Ruthenium Complexes. In *Inorganic Syntheses*, Fackler, J. P., Ed. John Wiley & Sons, Inc: Hoboken, NJ, USA, 1982; pp 74-78.
(8) Chakravarty, J.; Bhattacharya, S., Synthesis, Characterization, Electron-Transfer Properties and Reactivities of a Group of Ruthenium(II) Complexes with $RuN_2P_2X_2$ (X = Cl, Br) Coordination Spheres. *Polyhedron* **1994,** *13*, 2671-2678.
(9) Bu, Z.; Wang, Z.; Yang, L.; Cao, S., Synthesis of Propylene Carbonate From Carbon Dioxide Using Trans-Dichlorotetrapyridineruthenium(II) as Catalyst. *Appl. Organomet. Chem.* **2010,** *24*, 813-816.
(10) Schaefer, T.; Sebastian, R., Concerning the Internal Rotational Potential in Benzal Chloride. 37Cl/35Cl Isotope Effect on the Methine ^{1}H NMR. *Can. J. Chem.* **1989,** *67*, 2053-2056.
(11) Bailey, G. A.; Foscato, M.; Higman, C. S.; Day, C. S.; Jensen, V. R.; Fogg, D. E., Bimolecular Coupling as a Vector for Decomposition of Fast-Initiating Olefin Metathesis Catalysts. *J. Am. Chem. Soc.* **2018,** *140*, 6931-6944.
(12) Kessar, S.; Zuev, D.; Song, Z.; Wu, Y., 2-Lithiopyridine. In *Encyclopedia of Reagents for Organic Synthesis*, 2011.
(13) Vock, C. A.; Scolaro, C.; Phillips, A. D.; Scopelliti, R.; Sava, G.; Dyson, P. J., Synthesis, Characterization, and in Vitro Evaluation of Novel Ruthenium(II) η^6-Arene Imidazole Complexes. *J. Med. Chem.* **2006,** *49*, 5552-5561.

References on page 31

Chapter 3: Alternative Routes to Important Known Ruthenium Metathesis Catalysts

3.1 Introduction

3.1.1 Background and Motivation

Although great strides in terms of the performance of metathesis catalysts have been made over the last decades (as briefly outlined in Chapter 1), diazo-based methodologies have yet to be supplanted for benzylidene installation. This represents a significant impediment to the development and deployment of metathesis catalysts. For the chemist seeking to leverage or investigate well-known catalysts, the lengthy and challenging synthesis or high price of commercially available catalysts is a high barrier to entry. Development of new catalysts is similarly hindered: most new catalysts are synthesized from the commercially available Grubbs catalysts even where this is not the most atom-economical, cost-effective, or time-efficient route to the desired catalyst.[1] Modified alkylidene catalysts, such as the top-tier nitro-Grela catalyst, are synthesized by cross-metathesis with a commercially available indenylidene or Grubbs-type benzylidene catalyst,[2-4] when it would be more efficient to directly install the desired alkylidene.[1] Pseudohalide catalysts, including most enantioselective catalysts, are accessed by salt metathesis or transmetalation with existing catalysts,[5-12] when it may be easier/more effective to install the pseudohalide on a ruthenium precursor without the sensitive alkylidene functionality and subsequently install the alkylidene.

These synthetic decisions are presumably made to permit use of a commercially-available parent catalyst. This circumvents the challenging and often low-yielding alkylidene installation step (which in the case of benzylidenes requires the use of toxic, mutagenic, and potentially explosive diazo reagents), but may limit scope. For example, attempts by the Barbasiewicz group to synthesize **Ru-25** via metathesis with **M2** produced a polar tar containing only trace amounts of alkylidene,[4] but the Grela group was able to isolate **Ru-25** in 30% yield via metathesis with **GI** (Scheme 3.1).[2] This example demonstrates that catalyst synthesis may fail due to limitations associated with a commercially available precatalyst rather than inherent inaccessibility. **Ru-25** was accessible from another commercial precatalyst, but it is unknown how many potentially useful precatalysts are inaccessible from any commercial precatalyst but could be accessed through other means.

Scheme 3.1: Synthesis of **Ru-25** fails with M2, but proceeds with GI**.**

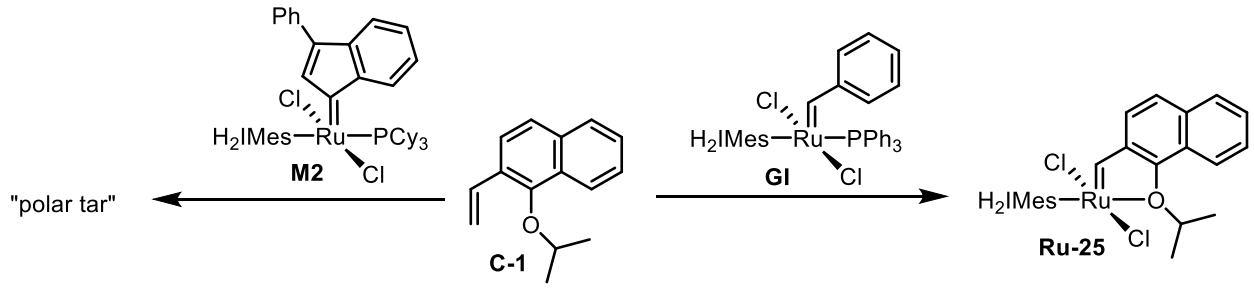

Improved routes to metathesis catalysts are desirable to expand scope and accessibility, and reduce the time required to develop and screen new catalysts. From the perspective of catalyst synthesis,

References on page 60

it is instructive to sort Ru catalysts by ease of synthesis. Accordingly, they are grouped in Figure 3.1 by the number and type of transformations required after the key alkylidene installation step.

Figure 3.1: Categorization of representative metathesis catalysts by synthetic method.

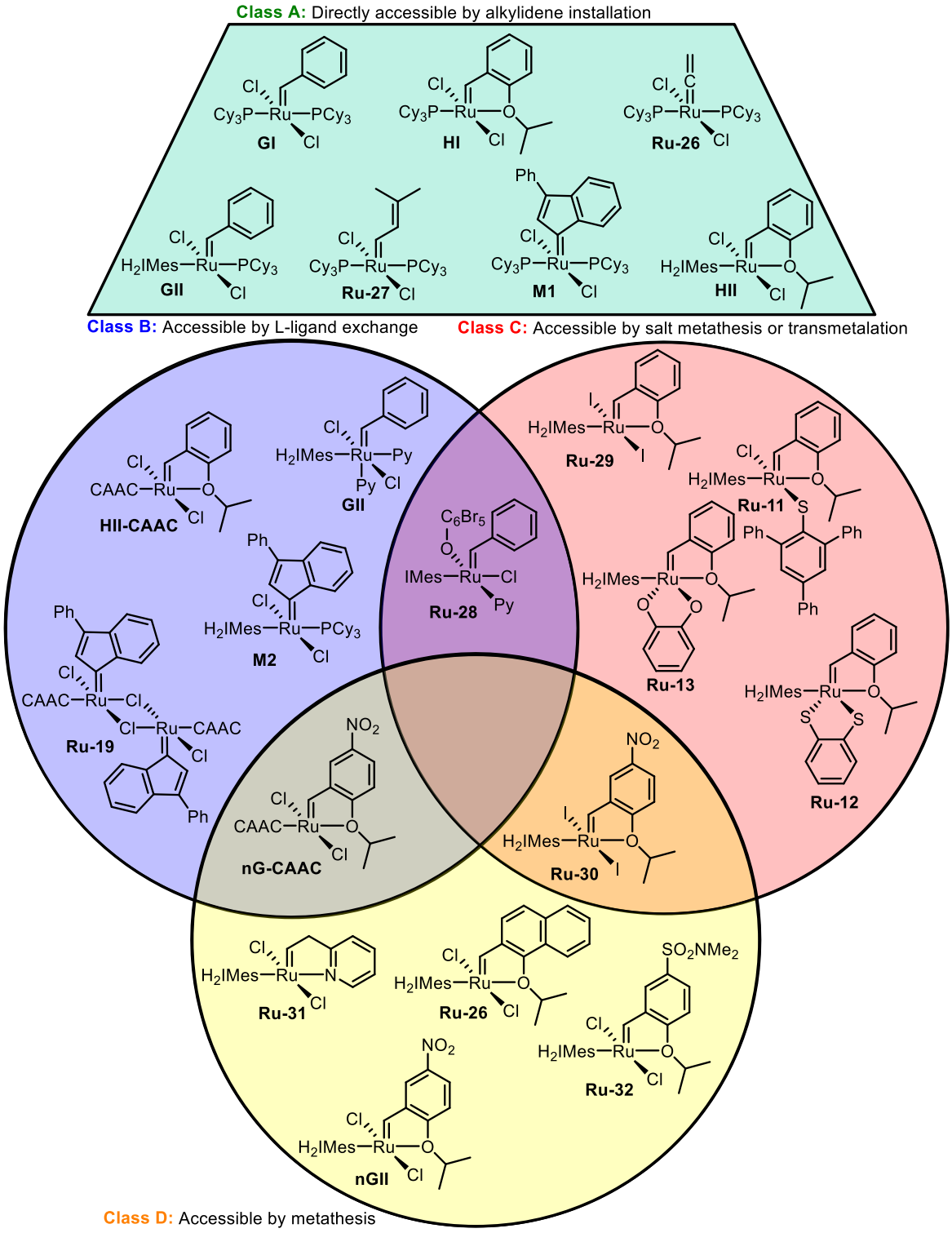

References on page 60

Class A are directly accessible by alkylidene installation on a suitable ruthenium precursor (e.g., by reaction with an aryldiazomethane: Scheme 3.2) and are therefore the most easily accessible catalysts. All other classes of catalyst must be synthesized from a Class A catalyst. This group has traditionally included the first-generation Grubbs[13] and Hoveyda[14] catalysts as well as the first-generation indenylidene[15] catalyst, and has recently expanded to include the second-generation Grubbs and Hoveyda catalysts with the high-yield synthesis of **Ru-33** developed by Craig Day of this research group.[1]

Scheme 3.2: Concise synthesis of the second-generation Hoveyda catalyst, enabled by the high-yield synthesis of **Ru-33**.

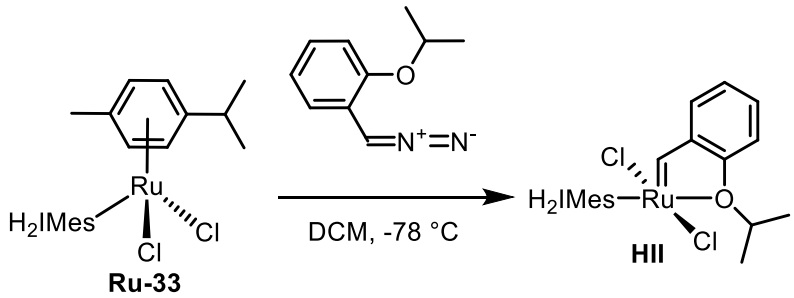

Class B catalysts require neutral ligand exchange after alkylidene installation. These include the recently-developed CAAC catalysts, as well as the second-generation indenylidene species. Although ligand exchange is chemically straightforward, isolated yields are highly variable, particularly in the case of CAAC catalysts (which are currently of high interest), with yields ranging from 15–81% for Hoveyda-type catalysts[16] and 13 to 50% for the more reactive nitro-Grela-CAAC catalysts.[17] As routes to new non-alkylidene ruthenium precursors are developed, more catalysts will move from Class B to Class A: a high yield route to CAAC-functionalized ruthenium dichloride species is a particularly high value target for the field in this context.

Class C catalysts are those with X-ligands modified after alkylidene installation, and this group includes top-performing enantioselective catalysts, as well as most pseudohalide catalysts. Bulky pseudohalide ligands are ubiquitous in early metal systems[18] and are of renewed interest in Ru-based olefin metathesis, with the recent establishment of bimolecular coupling as a critical decomposition pathway for Ru catalysts in general[19] and state-of-the-art CAAC catalysts in particular.[20] Anionic ligand substitution can be challenging[21] and in many cases (particularly for O-based ligands such as carboxylates or aryloxides) the desired transmetalation proceeds only with the use of Ag[5-8, 22-24] (photosensitive, poor stoichiometric control[6]) or Tl[6, 9-11, 25-27] (highly toxic![28-29]) reagents. and in cases where the reaction does proceed with the more user-friendly alkali and alkali earth reagents, it can be slow enough that competing decomposition of alkylidene becomes a concern.[9] Easier access to class C species will require either the development of new and better methods for anionic ligand substitution on Ru-carbene species, or an inversion of the current synthetic paradigm. At present, exchange of anionic ligands is typically carried out *after* alkylidene installation. If this step were instead carried out prior to alkylidene installation on a robust substrate, the sluggish exchange with group 1 and 2 reagents would not be a concern.

References on page 60

Class D catalysts bear modified alkylidene moieties which are not installed directly, but are instead installed post-hoc by metathesis with the appropriate olefin (Scheme 3.3). This method is only effective where there is a thermodynamic preference for the target species. As such, access to non-chelating alkylidenes is not generally possible. Successful installation of chelating alkylidenes typically requires the use of a ligand scavenging agent such as CuCl[30] or various resins,[31-32] increasing operational complexity. As an additional limitation, only alkylidenes for which the parent olefin is accessible may be synthesized, restricting the scope of potential catalysts. Even when synthesis of the olefin is possible, there can be challenges, as with 1-($C{=}CH_2$)-3-(NO_2)-6-(O^iPr)(C_6H_3), the precursor for the nitro-Grela family of catalysts. Synthesis of this modified styrene is typically low-yielding (overall yield of 42% yield from commercially available 2-hydroxy-5-nitrobenzaldehyde is reported),[3] and the styrene itself is highly prone to decomposition and should not be stored for prolonged periods. Attempts by Stephanie Ton of this research group to synthesize the necessary diazo reagent to directly access nitro-Grela catalysts, 1-(N_2CH)-3-(NO_2)-6-(O^iPr)(C_6H_3), were unsuccessful. This provides an additional impetus for the development of a viable alternative to diazo reagents for alkylidene installation beyond the well-established concerns surrounding safety and stoichiometric control; direct installation of 3-nitro-6-isopropoxybenzylidene, and therefore direct access to top-performing catalysts, will remain out of reach until improved methods for alkylidene installation with broader functional group tolerance are developed.

Scheme 3.3: Installation of modified alkylidenes by metathesis with a pre-existing (typically commercially available) metathesis catalyst.

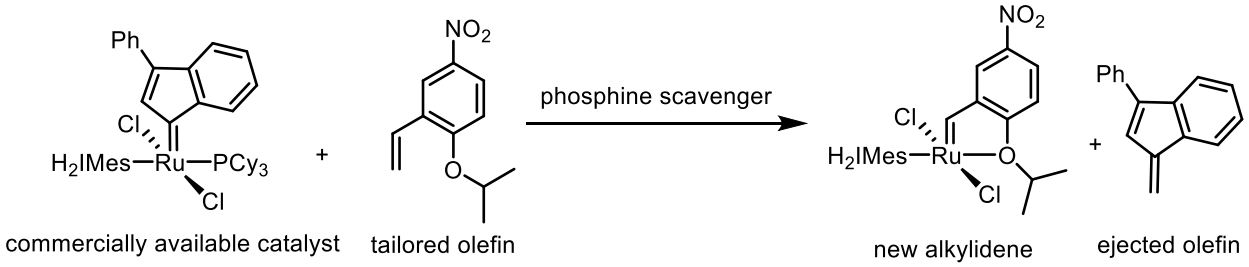

Classes B, C, and D can overlap (e.g. **nG-CAAC** belongs to both class B and D), while class A species act as precursors for the other classes. As the field continues to develop, more catalysts should join class A, while the other categories shrink.

This chapter will discuss efforts to improve access to known metathesis catalysts in three ways: improving access to class A via new methods for alkylidene installation, expanding class A through the development of new ruthenium precursors, and improved access to class C by novel transmetalation techniques.

References on page 60

3.2 Improved Access to Class A Catalysts: α-Chloroalkylruthenium as a Key Intermediate and Synthetic Target

3.2.1 Background: α-Chloroalkylruthenium as a Key Intermediate in Diazo-Free Routes to Alkylidenes

As alluded to in chapter 1, diazo-free routes to ruthenium benzylidenes are of considerable interest, owing to the explosive, toxic, and unstable nature of aryldiazomethane reagents.[33] A survey of the literature reveals a common thread tying together many apparently unrelated approaches. α-Chloroalkylruthenium complex **Ru-34** has been proposed as a key intermediate in multiple routes (Figure 3.2).[34-39] α–Chloride abstraction by intramolecular oxidative addition then generates the alkylidene. Collectively, these routes report moderate to good isolated yield (50-76%), often proceed at room temperature, do not rely on short lived or difficult to handle carbene sources, and allow for direct access to a range of highly active alkylidenes. Routes **D** and **E** give direct access to benzylidenes (the best-studied Ru alkylidenes), and should be adaptable to functionalized benzylidenes such as the ortho-isopropoxy functionalized motif seen in the Hoveyda family of catalysts. In principle, any alkylidene should be accessible, provided that the parent gem-dichloride can be prepared.

Figure 3.2: Routes to ruthenium alkylidenes passing through common intermediate **Ru-34**. Routes accessing **Ru-34** via oxidative addition (blue dot) and olefin insertion (pink dot) are shown.

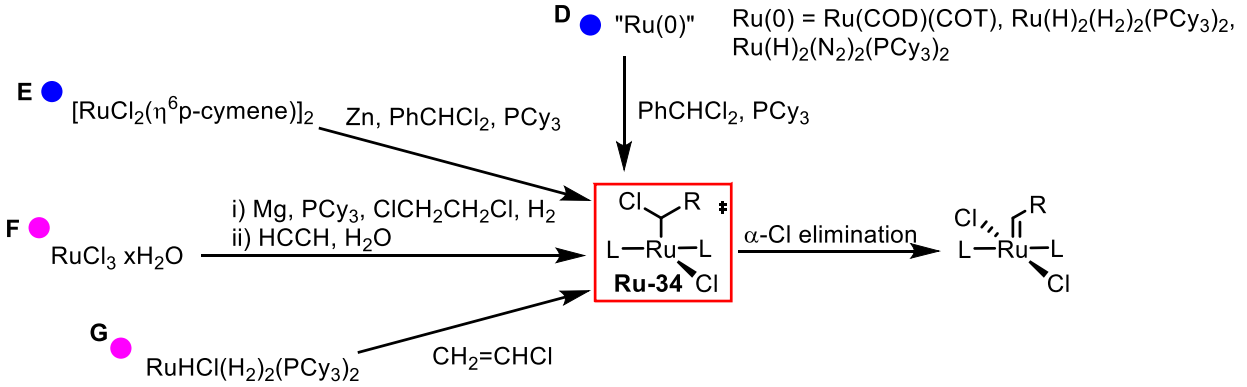

Despite these appealing characteristics, none of these routes has supplanted diazo technology, and each has significant drawbacks. Route **D** proceeds by double oxidation addition of geminal chlorides to Ru(0) precursors (Scheme 3.4). While geminal dichlorides are shelf stable and easily accessible from aldehydes,[40-41] Ru(0) complexes can be challenging to synthesise, often low yielding, and are highly sensitive to heat, atmospheric contamination, and frequently light.[36, 42] Thus, this route effectively shifts the issues of ease of handling, synthesis, and stability from the relatively inexpensive organic fragment to the significantly more expensive ruthenium precursor.

References on page 60

Scheme 3.4: Double oxidative addition of benzal chloride to Ru(COD)(COT) generating **GI**.

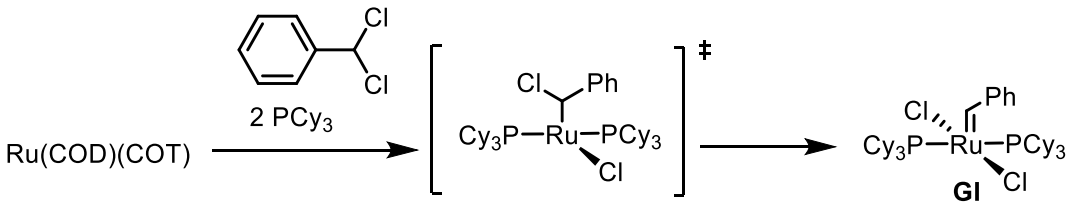

Route **E** avoids the problems associated with Ru(0) precursors, and uses the robust dimeric species $[RuCl_2(p\text{-cymene})]_2$ as the ruthenium source. Its use has only been reported once in the literature, in the supporting information of a 2010 communication describing a route to metal chalcogenocarbonyl complexes,[37] and the reported yield (65%) is lower than what can typically be achieved with aryldiazomethane reagents in skilled hands. While no mechanism was proposed, in-situ reduction of the Ru(II) precursor to Ru(0) which could then undergo oxidative addition to generate **Ru-34** (as in route **D**) and/or zincation of benzal chloride to produce Zn(CHClPh)Cl which can generate **Ru-34** via salt metathesis with $[RuCl_2(\eta^6\text{p-cymene})]_2$ are both possibilities (Scheme 3.5). Given that geminal dichlorides are known to be resistant to metalation,[43-44] and reduction of ruthenium chlorides by zinc is the method for producing Ru(0) species such as Ru(COD)(COT),[42] the Ru(0) route seems more likely.

References on page 60

Scheme 3.5: Alkyl halide zincation (top) and ruthenium reduction (bottom) proposed mechanisms for the generation of **GI**.

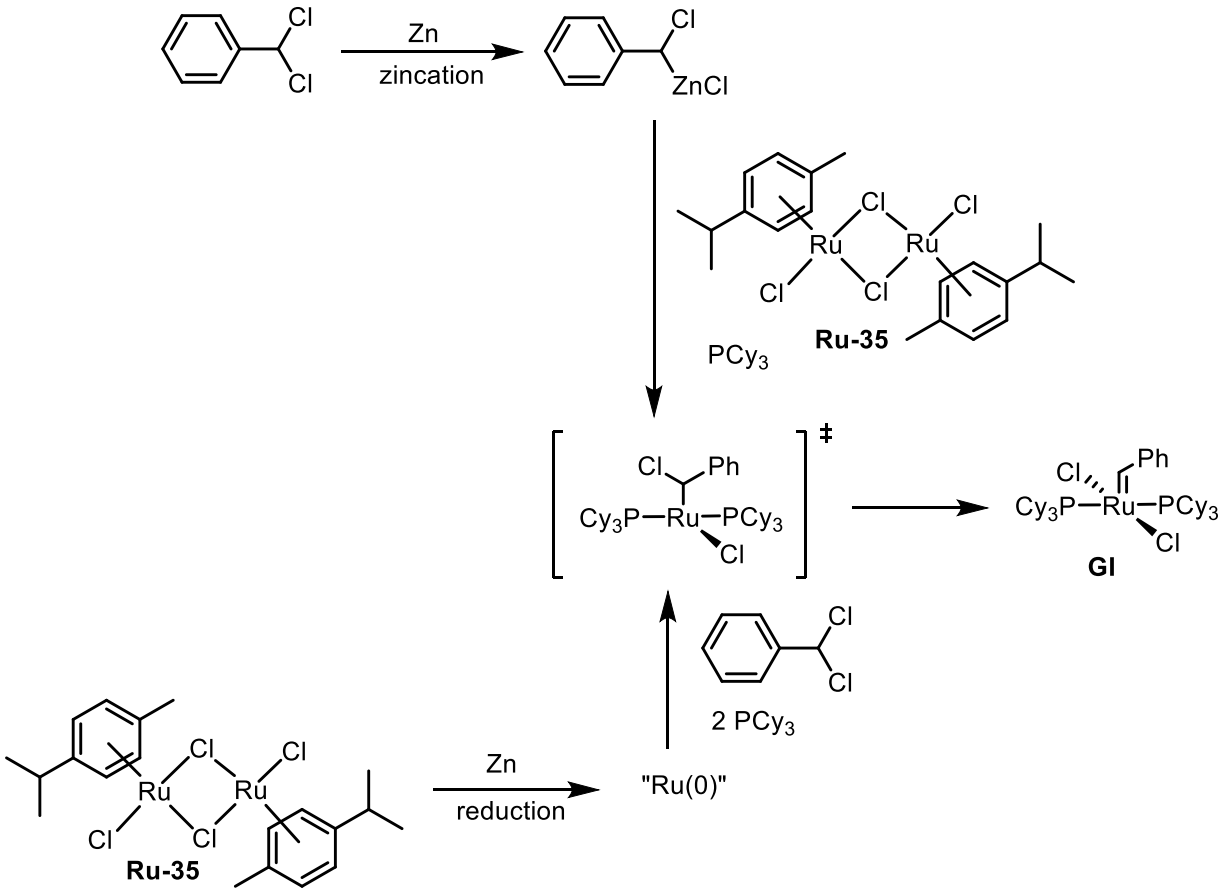

Based on the observation that ruthenium vinylidenes such as $RuHCl(=C=CHR)(PCy_3)_2$ are converted into more active alkylidenes in the presence of $MgCl_2$ and H_2O (proposed to occur via **Ru-1**), Werner reported in 1998 route **F**; a one-pot synthesis of ruthenium alkylidenes from $RuCl_3xH_2O$ (Scheme 3.6).[39] $RuHCl(H_2)(PCy_3)_2$ and $MgCl_2$ are concomitantly generated by mixing $RuCl_3•xH_2O$, PCy_3, and Mg in THF under H_2 at 85 °C. Subsequent addition of a terminal alkylidyne (acetylene or phenylacetylene) generates the vinylidene intermediate **Ru-36** which rapidly converts to alkylidene **Ru-37** on addition of H_2O. Reported isolated yields of alkylidene are 76%, which is excellent considering that this is directly from $RuCl_3$. Most reported routes require the isolation of a Ru^0 or Ru^{II} precursor prior to alkylidene installation and thus will have lower overall yields from $RuCl_3$. However, this route does not allow access to benzylidenes, and is therefore not a viable alternative to diazo reagents.

References on page 60

Scheme 3.6: One pot synthesis of **Ru-37** from $RuCl_3\,xH_2O$

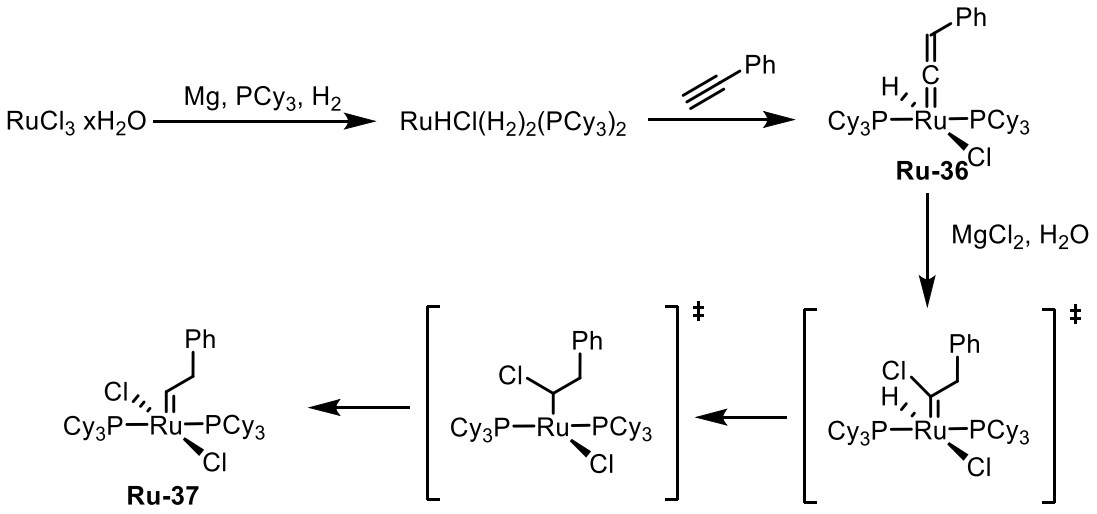

Route **G** has similar issues; access to benzylidenes is not possible, and the reaction does not cleanly produce alkylidenes. A 2002 report by Grubbs shows insertion of vinyl chloride to $RuHCl(H_2)(PCy_3)_2$ to generate an intermediate of the type **Ru-34**, which proceeds to metathesis active ethylidene **Ru-38** (Scheme 3.7), but competing cross metathesis with vinyl chloride generates the less active and unstable **GIm** (Scheme 3.8), and an undetermined competing pathway leads to formation of $Ru(H)_2Cl_2(PCy_3)_2$.[35]

Scheme 3.7: Insertion-elimination of vinyl chloride to produce a ruthenium ethylidene

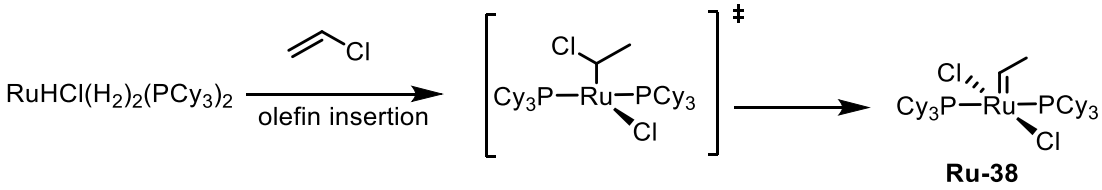

References on page 60

Scheme 3.8: Competing metathesis of vinyl chloride, generating unstable methylidene

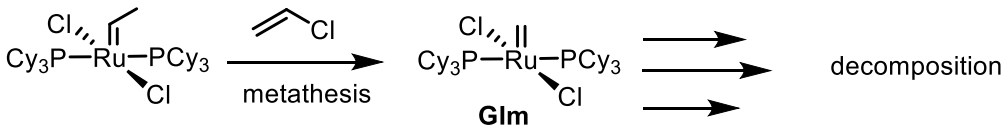

Intrigued by the commonality of **Ru-34** as a proposed intermediate in such a number of routes to alkylidenes, we sought a method to directly install an α-chlorobenzyl functionality on a shelf-stable Ru(II) substrate via salt metathesis with an organomagnesium reagent.

3.2.1 Magnesium Carbenoids: A Potential Source of the α-Chloroalkyl Moiety

α-Haloalkylmagnesium reagents, also known as magnesium carbenoids for their carbene-like reactivity,[45-46] were investigated in this work as a source of the α-chlorobenzyl fragment. Magnesium carbenoids have been deployed in organic synthesis,[47-58] and were instrumental in mechanistic studies of Grignard formation.[43-44] Enantioenriched magnesium carbenoids have additionally been developed[59-61] and used to gain mechanistic insight into the reactivity of organomagnesium reagents both with nucleophiles[62-63] and in transmetalation with transition metal halides[64-65]. Related lithium carbenoids were eschewed, as they are highly unstable and exhibit poor functional group tolerance (the nitro-substituted benzylidene of the top-performing Nitro-Grela type catalysts, for example, would not be accessible). Zinc carbenoids are well-known in literature (most famously as the Simmons-Smith reagent),[66] more stable than magnesium carbenoids, and reported to produce unsubstituted ruthenium benzylidenes and methylidenes in moderate to good yield. However, attempts in this work to extend the reported zinc methodology to Hoveyda-type alkylidenes (see results and discussion, below) failed to produce any detectable alkylidenes.

Magnesium carbenoids can react as either nucleophiles and electrophiles (Scheme 3,9a, 3.9b). They may also liberate highly reactive free carbenes via α-halide elimination (Scheme 3.9c).[45-46, 67] Although a stabilized magnesium carbenoid has been isolated and characterized,[68] α-halide elimination is typically rapid at room temperature, so the carbenoids are typically generated and used without isolation at cryogenic temperatures (e.g., -78 °C, but -40 °C is also reported).[45-46, 67] The carbenoids are not typically directly observed: rather, their formation is inferred from the product distribution.[43-44, 62, 69]

References on page 60

Scheme 3.9: Reactivity of magnesium carbenoids: a) with electrophiles, acting as a source of α-haloalkyl fragment; b) with nucleophiles, generating functionalized Grignard reagents; and c) by intramolecular α-halide elimination, liberating free carbene.

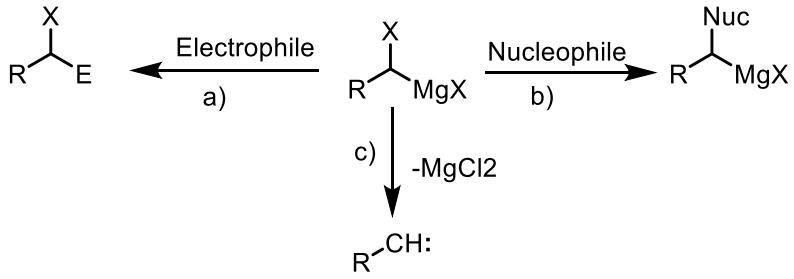

Magnesium carbenoids are more challenging to generate than the related Grignard reagents. Treating geminal dichlorides with magnesium would be a straightforward approach, but geminal dichlorides are surprisingly inert to metalation, even by highly active Reike magnesium at room temperature.[43-44] Heating enables sluggish metalation, but liberation of the free carbene proceeds much more quickly than carbenoid formation at these temperatures. In consequence, the carbenoid cannot be used for reactions with electrophiles or nucleophiles, and only carbene-derived products are observable (Scheme 3.10).

Scheme 3.10: Magnesiation of geminal dichlorides. Magnesiation is slow relative to subsequent liberation of free carbene. In the absence of trapping agent, homocoupling to form olefins is observed.

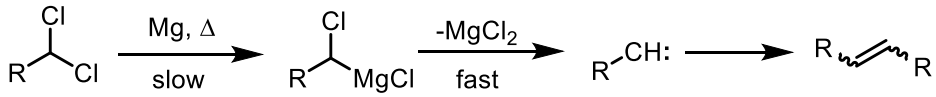

Magnesium-X (X = I, SOAr) exchange with a sacrificial Grignard reagent has been used to generate magnesium carbenoids for organic synthesis (Scheme 3.11).[45-46, 59-61, 67] Magnesium-iodide exchange is little used, as the requisite hetero-geminal dihalides are unstable and challenging to synthesize.[70-71] For this reason, magnesium-iodide exchange is also unsuitable as an alternative to diazo technology for alkylidene installation. α-Chloro sulfoxides are more stable and reliably accessible,[72] but the magnesium-sulfoxide exchange process is an equilibrium procedure that often requires an excess of sacrificial Grignard reagent to drive to completion and will seldom cleanly produce the desired carbenoid but rather a cocktail of organomagnesium species of which the carbenoid is a component.[45-46, 59] This excess sacrificial Grignard would be active in salt metathesis, and likely destroy a portion of any successfully generated ruthenium alkylidene.

Scheme 3.11: Generation of magnesium carbenoids by magnesium-iodide or magnesium-sulfoxide exchange.

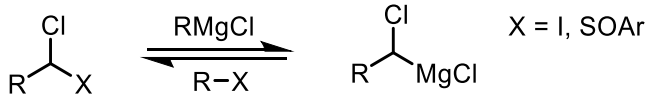

References on page 60

Treatment of α,α-dichlorotoluenes (benzal chlorides) with the magnesium-anthracene complex **Mg-1** was explored as an alternative, stoichiometric route to benzylmagnesium carbenoids based on the known reactivity of **Mg-1** with alkyl halides. The magnesium-anthracene complex is known to react rapidly and stoichiometrically with alkyl halides even at -78 °C.[73-74] Depending on the alkyl halide partner, **Mg-1** may react by one of three pathways (Scheme 3.12).[74] With primary, secondary, and tertiary aliphatic alkyl halides, **Mg-1** behaves like a typical dialkylmagnesium reagent, reacting as a nucleophile to produce a mixture of substituted anthracenes. Carbenoids based on these types of halide are therefore not expected to be accessible. Phenyl chlorides are unreactive at room temperature, while phenyl bromides and iodides react via a single electron transfer (SET) mechanism, wherein one electron is transferred from **Mg-1** to RX. Grignard formation is also observed for these phenyl halides, but only as a minor side reaction, and in any case a phenylmagnesium carbenoid is not possible without invoking supervalent carbon.

When **Mg-1** reacts with β-unsaturated alkyl halides (allyl, propargyl, benzyl, etc.), liberation of anthracene and formation of the corresponding β-unsaturated Grignard reagent is observed as the sole reaction pathway. This reaction proceeds efficiently and with excellent stoichiometric control even at -78 °C, and has been exploited in the synthesis of previously challenging-to-access Grignards including allenylic Grignard[74] and, of particular interest to this thesis, benzylic di-Grignard reagents.[75] If this reactivity can be extended to α,α-dichlorotoluene derivatives, clean, stoichiometric access to benzylic carbenoids at -78 °C will be attainable (Scheme 3.13).

Scheme 3.12: Reaction of **Mg-1** with organic halides may proceed via a) nucleophilic attack by anthracene (primary, secondary, and tertiary aliphatic alkyl halides), b) a single electron transfer mechanism (phenyl bromide/iodide), or c) Grignard formation (β-unsaturated alkyl halides).

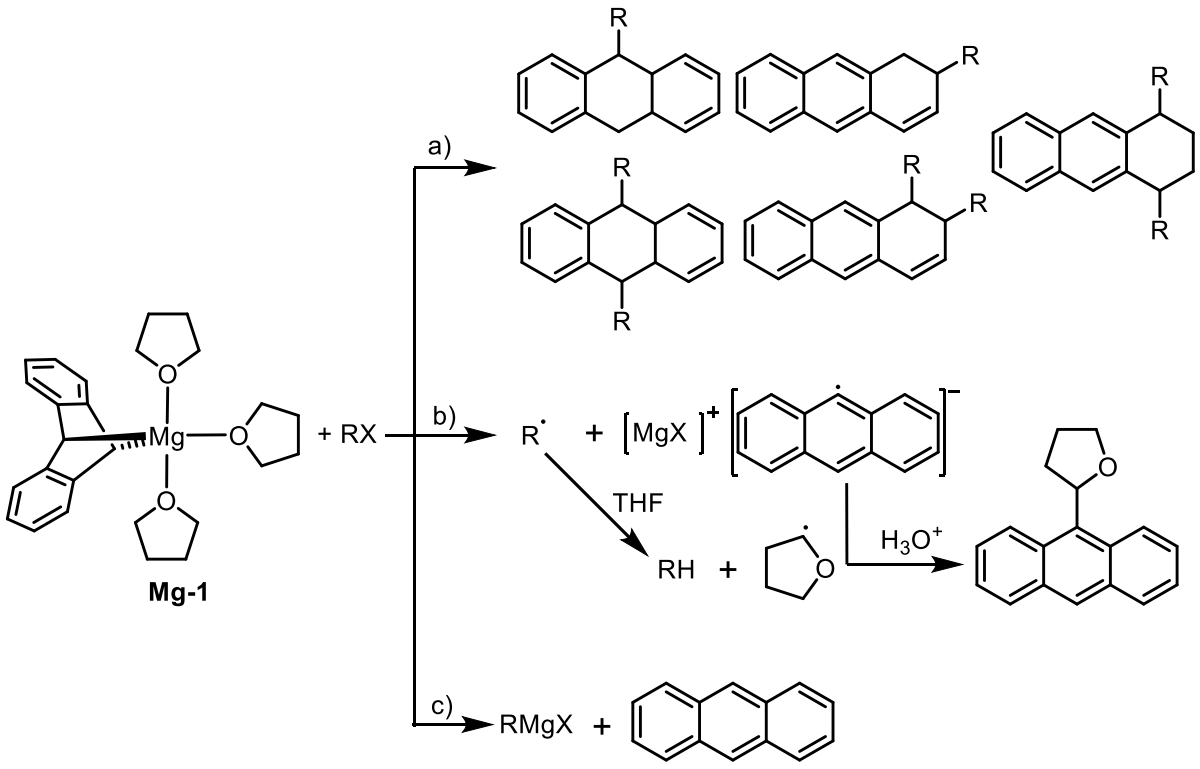

References on page 60

A report of the reaction between 1,1-dichlorocyclopropane and **Mg-1** gives cause for optimism: when combined with **Mg-1** in THF at -78 °C, 14% conversion to carbenoid-derived products was observed, with the mass balance consisting of the products of the nucleophilic attack and SET reaction pathways.[69] 14% is low, but cyclopropanes are not among the alkyl halides known to react primarily by Grignard formation. That any carbenoid was formed under these conditions confirms that **Mg-1** can produce carbenoids at cryogenic temperatures, and gives hope that this will be the preferred reaction pathway when a benzyl 1,1-dihalide is used in place of 1,1-dichlorocyclopropane.

Scheme 3.13: Proposed route to benzylmagnesium carbenoids using the magnesium-anthracene complex as a magnesiating agent.

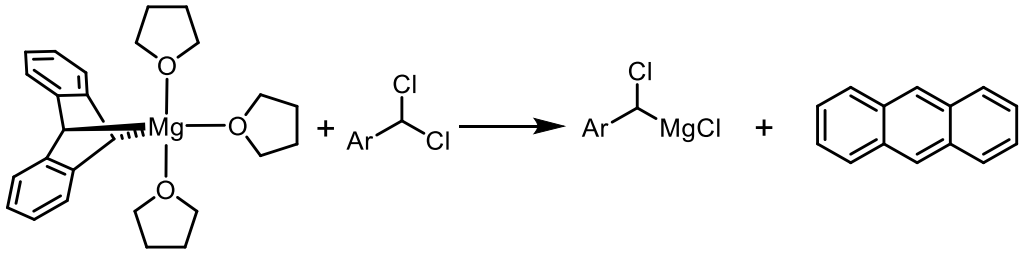

Mg-1

Benzylic carbenoids are of particular interest. Not only do the highest-performing Ru metathesis catalysts tend to bear functionalized benzylidenes,[3, 14, 76-77] but benzylic magnesium carbenoids are currently unknown in the literature. Indeed, the wide range of magnesium carbenoids that have been reported by Mg-sulfoxide exchange[45-46, 67] make the benzylic species conspicuous by their absence. It is unclear whether this is mere coincidence, or a symptom of underlying difficulties in the Mg-sulfoxide exchange or the synthesis of benzylic α-chloro sulfoxides.

3.2.2 Results and Discussion

3.2.2.1 Generation of Benzyl Magnesium Carbenoids Via the Magnesium-Anthracene Complex

Combining a 1:1 molar ratio of **Mg-1** and *o*-isopropoxybenzal chloride at room temperature leads immediately to the formation of anthracene and *o*-isopropoxystilbene, as identified by GC-MS (Scheme 3.14). No substituted anthracene derivatives were detectable, implying that carbenoid formation is the sole reaction pathway. An additional unidentified species is present in small amounts and is presumed to arise from an impurity in either **Mg-1** or **C-2**. The formation of *o*-isopropoxystilbene is presumed to be evidence of carbenoid formation and subsequent liberation and homocoupling of the free carbene. It was hoped that potential chelation of the O^{i}Pr functionality might stabilize the carbenoid enough that it might be transiently observed at room temperature, but this turned out not to be the case. Attempts to trap out the carbenoid with MeOH were likewise unsuccessful (Scheme 3.15), the *o*-isopropoxybenzyl chloride that would be the expected product of carbenoid protonation was never observed no matter how quickly the MeOH was added. Interestingly, the outcome was spectroscopically identical even if the MeOH was

References on page 60

present prior to the addition of the magnesium-anthracene complex, indicating a preference for formation of the carbenoid over $Mg(OMe)_2$, and for carbene homocoupling over protonation.

Scheme 3.14: Addition of **Mg-1** to 1-($CHCl_2$)-2-(O^iPr)(C_6H_4) (**C-2**) leads to formation of anthracene and stilbenoid, indirect evidence of formation of carbenoid **Mg-2**.

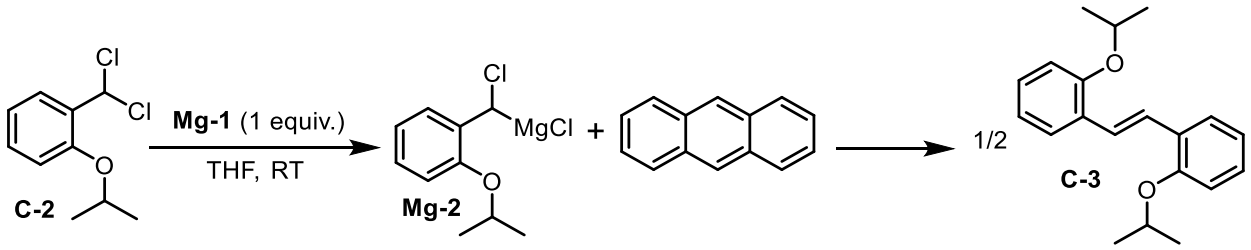

Scheme 3.15: Room temperature trapping experiments failed to show trapping of carbenoid **Mg-2**.

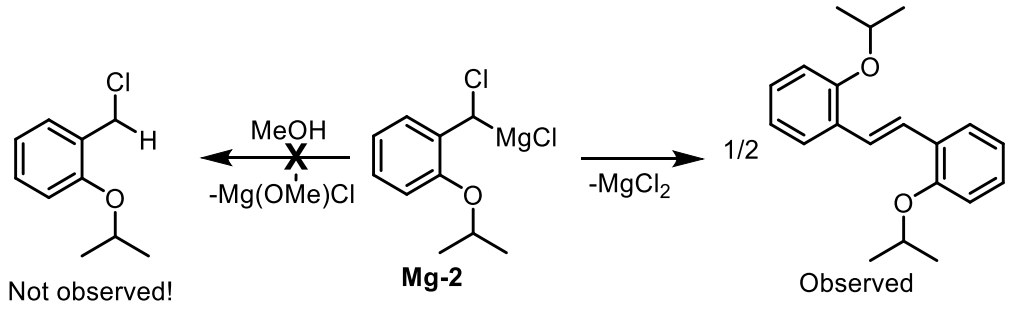

3.2.2.2 Attempted Alkylidene Installation Via Magnesium Carbenoids

Adding as a solid the magnesium-anthracene complex to a stirred solution of $RuCl_2(PPh_3)_3$ and *o*-isopropoxybenzal chloride in THF at room temperature (Scheme 3.16) led to an immediate colour change from brown to brown-red. ^1H NMR analysis reveals approximately 29% conversion to the known species **Ru-39** as judged by comparison of the integrals for the alkylidene proton against those for the protons in the 9 and 10 positions on anthracene. If the same procedure is repeated instead in the presence of two equivalents PCy_3 and using benzal chloride in place of isopropoxybenzal-chloride, a similar in-situ yield (41%) of the first-generation Grubbs' catalyst is instead observed, again determined on the basis of the diagnostic alkylidene signal (Scheme 3.17). In both cases the reaction is rapid and appears to have reached an end point within five min of adding the magnesium-anthracene complex.

References on page 60

Scheme 3.16: Adding 1 equiv of **Mg-1** to a room temperature solution of **Ru-20** and **C-2** in THF produces known alkylidene **Ru-39** in 29% in-situ yield.

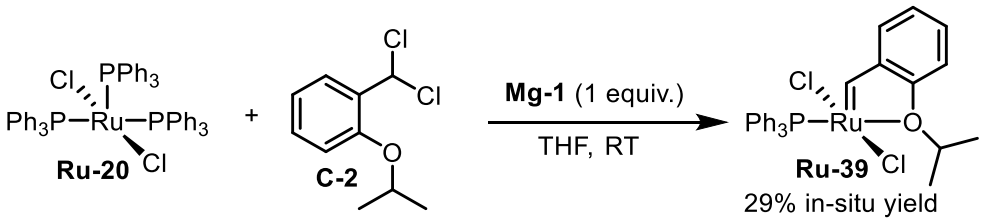

Scheme 3.17: Adding 1 equiv **Mg-1** and two equiv PCy3 to a room temperature solution of **Ru-20** and **C-4** in THF produces known alkylidene species **GI** in 41% in-situ yield.

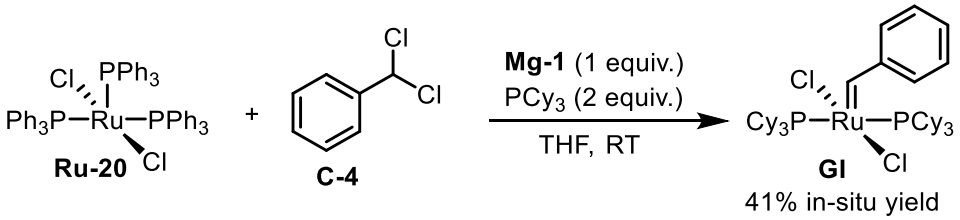

Though these early results are promising, subsequent attempts to improve the in-situ yield were unsuccessful. Adding the magnesium-anthracene complex slowly as a suspension in THF made no discernable difference to reaction outcome. Given the rapidity of carbenoid homocoupling previously observed (vide supra), alternative mechanisms of alkylidene formation not involving a magnesium carbenoid were considered (Scheme 3.18): in these alternative mechanisms, the magnesium-anthracene complex reacts with **Ru-20**, generating either a Ru(II) η^2-Ru-anthracene complex by transmetalation (**Ru-40**) or a Ru(0) η^6-Ru-anthracene complex (**Ru-41)** by reduction. Subsequent insertion into a C-Cl bond on isopropoxybenzal chloride would then furnish **Ru-39**. In order to probe this mechanism, the reaction conditions were changed such that $RuCl_2(PPh_3)_3$ was treated first with **Mg-1** and then *o*-isopropoxybenzal chloride, but this method yielded no spectroscopically detectable products, providing evidence against these non-carbenoid mechanisms.

References on page 60

Scheme 3.18: Proposed non-carbenoid mechanisms for the formation of HII from the reaction of **Mg-1** and **Ru-20**.

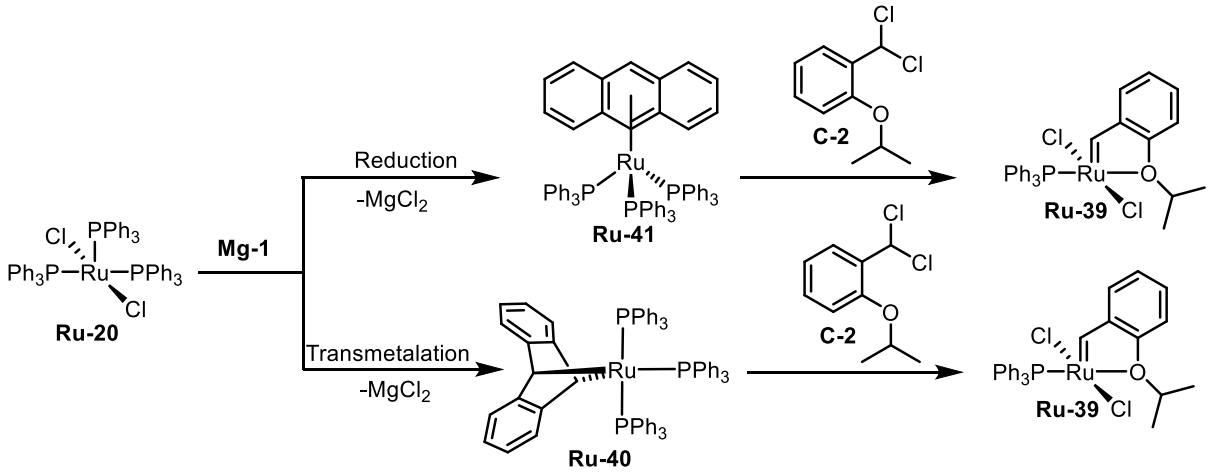

Attempting to address the known thermal instability of magnesium carbenoids[46, 78] by first generating **Mg-2** at -78 °C and adding this to a solution of $RuCl_2(PPh_3)_3$ also at -78 °C similarly showed no evidence of alkylidene formation. Instead decomposition of $RuCl_2(PPh_3)_3$ is observed. Carbenoids are known to react with phosphines, including triphenylphosphine, to form phosphonium salts.[79] It is possible that while low temperatures are successful in stabilizing **Mg-2**, the desired transmetalation step does not proceed at these temperatures and exclusively reaction with phosphine to produce **P-1** occurs (Scheme 3.19). This would also account for the low yields of alkylidene at room temperature if reaction with phosphine is kinetically favoured.

Scheme 3.19: Proposed competing reaction of **Mg-2** with $RuCl_2(PPh_3)_3$ and free PPh_3.

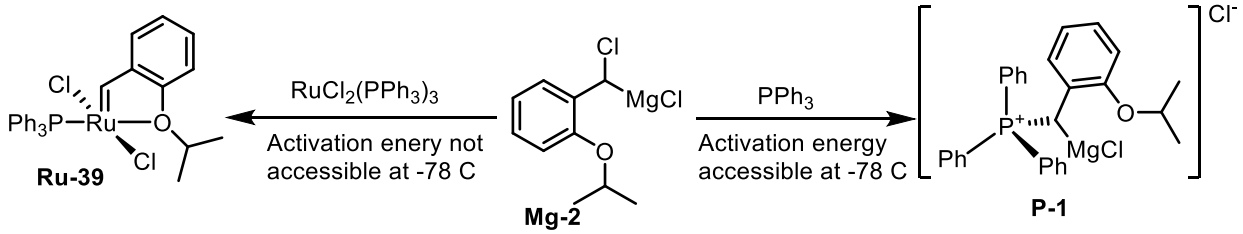

Alternatively, if transmetalation does proceed, ortho metalation of bound PPh_3 could also account for the low yield of alkylidenes at room temperature and total decomposition at -78 °C (Scheme 3.20). Bulky alkyl- and arylphosphines, particularly triphenylphosphine, are prone to cyclometallation on ruthenium when in the presence of strong bases or when sharing the coordination sphere with carbanions.[80-83] However, the α-Cl-*o*-O^{i}Pr-toluene that would be liberated by such a cyclometallation reaction could not be detected. In a slight variation of this mechanism, if the α-chlorobenzyl fragment in **Ru-42** retains its carbenoid character, C-H insertion onto the benzyl carbon rather than the ruthenium centre would account for the absence of free α-chloro-*o*-isopropoxytoluene and simultaneously liberate an equivalent of HCl, which would lead to further reaction and decomposition of ruthenium species.

References on page 60

Scheme 3.20: Cyclometalation of PPh_3, known to occur on Ru centres, could contribute to low yield of desired alkylidene.

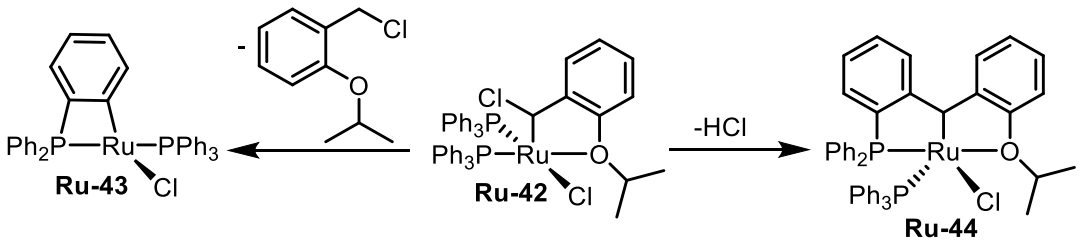

In order to remove competing reaction with free phosphine and ortho-metalation of bound phosphine as potential complications, alkylidene installation was attempted on a phosphine-free ruthenium precursor. **Ru-33**, the high yield synthesis of which had at the time recently been developed in this group by Craig Day,[1] was chosen as a phosphine-free precursor that also offered potential direct access to second-generation catalysts, as it is already functionalized with the N-heterocyclic carbene H_2IMes. Unfortunately, replacing $RuCl_2(PPh_3)_3$ with **Ru-33** led to an intractable black mixture with no spectroscopically detectable products (Scheme 3.21). The mode by which **Ru-33** decomposes in this instance is unclear, but C-H activation of an H_2IMes mesityl proton is known for benzylruthenium species[84] and is a potential primary decomposition event here (Scheme 3.22).

Scheme 3.21: Reaction of **Ru-33** with 1 equiv **Mg-2** (generated in-situ) does not produce alkylidenes.

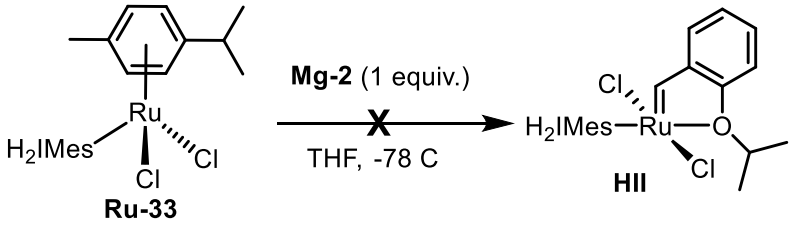

References on page 60

Scheme 3.22: Potential decomposition routes for **Ru-33** on exposure to **Mg-2**.

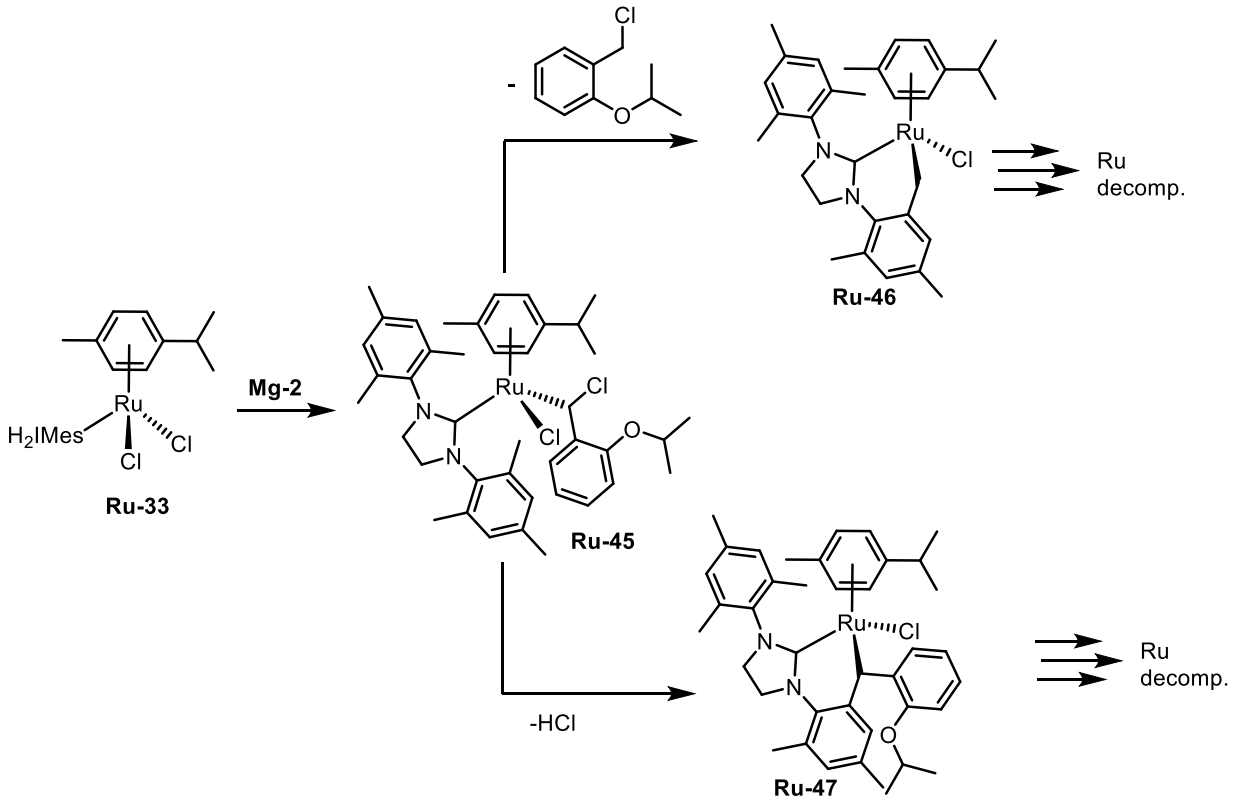

Dimeric $[RuCl_2(p\text{-cymene})]_2$ (**Ru-35**), although free of both phosphine and NHC, similarly did not produce alkylidenes when treated with **Mg-1** (Scheme 3.23). Once again, decomposition to a spectroscopically ill-defined mixture was observed. Presumably, dissociation of p-cymene to produce coordinatively unsaturated **Ru-49** is followed by rapid decomposition.

Scheme 3.23: Reaction of $[RuCl_2(p\text{-cymene})]_2$ with **Mg-2** and proposed decomposition route.

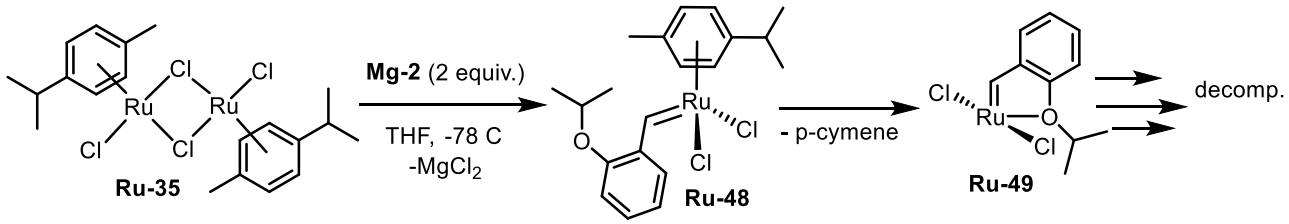

The initial result of 35-47% in-situ yield of first-generation metathesis catalysts is promising, but lack of success in improving upon these yields led eventually to the abandonment of this route as a viable alternative to diazo reagents for carbene installation.

3.3 Expanding Class A: Investigation of New Catalyst Precursors

3.3.1 Introduction: Ru(II) Pyridine Complexes as Potential Catalyst Precursors

Equally important to developing new methodologies for alkylidene and pseudohalide installation, another key avenue for expanding access to ruthenium metathesis catalysts is exploring new

References on page 60

catalyst precursor species. The recent development of a high-yield route to **Ru-33** by Craig Day of this group is an example of the benefits that can be reaped by this approach; this previously difficult to access compound is the basis of what is now the most succinct and atom economical route to second-generation catalysts.[1]

A drawback to the use of **Ru-33** is its thermal and photolytic instability.[1] Experience in the Fogg group indicates that, even when stored in the freezer (set at – 40 °C) in an inert atmosphere glovebox, the compound slowly decomposes in the solid state, to the point of requiring recrystallization after two to three weeks of storage. For the research chemist, catalyst precursors should ideally be shelf stable, allowing for mass production and storage before being shipped to the end user to be converted into the desired catalyst.

$RuCl_2(H_2IMes)(py)_3$ (**Ru-50**) similarly has potential to grant direct access to NHC-functionalized catalysts (Scheme 3.24), and is anticipated to exhibit greater thermal and photolytic stability than **Ru-33**, making it a better candidate for storage and transport. **Ru-50** has previously been reported as a decomposition product of the third-generation Grubbs catalyst, and was isolated in 29% yield by the deliberate decomposition of **GII**.[85] The fact that this species was accessible only by the decomposition of a metathesis-active benzylidene (and even then only in low yields) rendered it unattractive for further study, and there are no subsequent literature reports of its isolation. A convenient route to **Ru-50** would therefore be of interest.

Scheme 3.24: Predicted synthesis of the third-generation Grubbs catalyst from **Ru-50.**

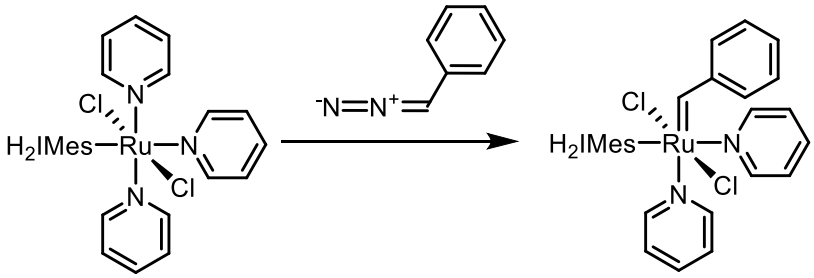

Ru-50 **GIII**

One can imagine substitution of one pyridine of the tetrakis-pyridine complex $RuCl_2(py)_4$ (**Ru-51**) as a concise route to **Ru-50** (Scheme 3.25), but despite the reputation of pyridine as a labile ligand elsewhere in the ruthenium metathesis literature,[86] this compound has been found by past experience in the Fogg group (unpublished results) to be remarkably inert to ligand substitution. Compounding the matter is the near complete insolubility of **Ru-51** in most organic solvents. It is very slightly soluble in CH_2Cl_2, but this solvent is incompatible with free H_2IMes.[1]. Routes to **Ru-50** that do not proceed through **Ru-51** were therefore investigated.

References on page 60

Scheme 3.25: Hypothetical route to **Ru-50**, not pursued due to surprising inertness of **Ru-51** to ligand substitution.

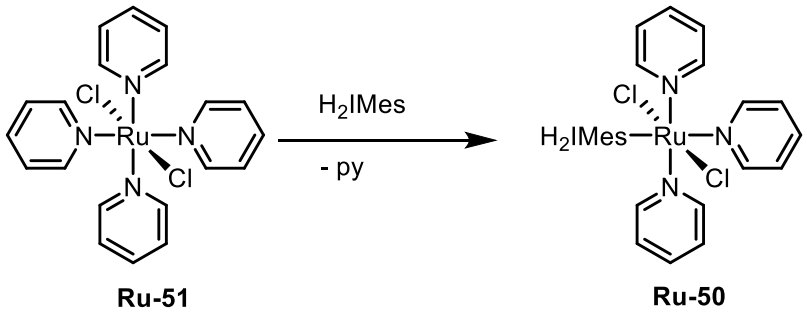

Ru-51 **Ru-50**

3.3.2 Results and Discussion: High Yield Synthesis of $RuCl_2(H_2IMes)(Py)_3$ and $RuCl_2H_2IMes(3\text{-}Br\text{-}Py)_3$ and Investigation as Catalyst Precursors

A route to **Ru-50** was realized by leveraging the thermal and photolytic lability of the p-cymene ligand in **Ru-33**. In a one pot procedure starting from **Ru-35**, adding 3.3 equivalents of pyridine to an in-situ generated THF solution of **Ru-33** and stirring for three h at 60 °C in a well-lit glovebox, yielded after workup **Ru-50** in 88% yield as a bright orange powder (Scheme 3.26). ^{1}H NMR analysis was consistent with the values reported by Grubbs.[85] Unlike the tetrakis pyridine complex **Ru-51**, **Ru-50** is readily soluble in THF and Benzene, presumably by virtue of the large organic framework of the H_2IMes ligand.

Scheme 3.26: Synthesis of **Ru-50** from dimeric **Ru-35**.

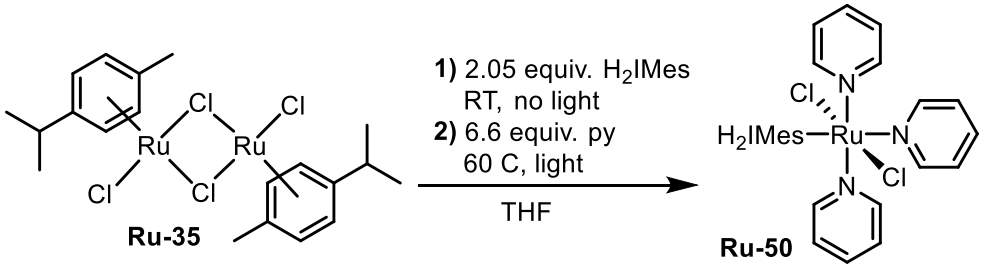

Ru-35 **Ru-50**

The lability of pyridine in **Ru-50** was interrogated by a series of ligand exchange experiments, tracked by monitoring the easily distinguishable signals for the ortho protons in bound and free pyridine by ^{1}H NMR spectroscopy. Donors selected to cover a range of donicity and steric bulk were added to a sample of **Ru-50** in $CDCl_3$, the results are summarized in Table 3.1, below. NEt_3 and PCy_3 both fail to substitute pyridine. MeCN and PPh_3 both partially substitute pyridine, effecting 67% conversion to **Ru-53a** and 25% conversion to **Ru-53c**, respectively This confirms **Ru-50** to be more active in ligand substitution than tetrakis pyridine complex **Ru-51**, though the site of ligand substitution is surprising. Both steric and electronic arguments would lead one to assume that substitution of the pyridine trans to H_2IMes should be preferred, as this site is the most sterically accessible, and strong sigma donation from the NHC should labilize the trans pyridine. However, substitution is observed exclusively cis to NHC, as determined by examining the ^{1}H NMR signals for the pyridine ortho protons. The parent compound displays two sets of bound pyridine signals in a 2:1 ratio, corresponding to the two pyridines cis to NHC and one pyridine

References on page 60

trans to NHC. Substitution of the pyridine trans to NHC will preserve the symmetry of the cis pyridines, and the substituted species should show only one signal for bound pyridine in a 2:1 ratio to the signal for liberated pyridine. Instead, where substitution is observed, two new signals for bound pyridine are observed in addition to free pyridine are observed in a 1:1:1 ratio, consistent with substitution of a pyridine cis to NHC. Steric bulk appears more important than the electronics of the incoming ligand. PCy_3 is the strongest donor examined, but does not coordinate at all. PPh_3 is a weaker donor than PCy_3, yet does partially coordinate. Likewise, MeCN is considered a weak donor, but as the least sterically demanding ligand caused the highest conversion of any ligand examined. Steric clash between bulkier ligands and the mesityl arms of H_2IMes accounts for better binding of sterically undemanding ligands cis to the NHC. The preference for substitution in this position is likely due to a combination of steric repulsion between the H_2IMes mesityl arms acting to labilize the cis-pyridines and strong donation from H_2IMes increasing back-donation to and stabilizing the trans pyridine (Figure 3.3). A similar electronically driven stabilizing "inverse trans-effect" has been established for PCy_3 in the second-generation Grubbs catalyst,[87] and back-donation to the π* antibonding orbital of pyridine is known[88-93], although any impact of pyridine backbonding has not been discussed in the ruthenium metathesis literature.

Table 3.1: Results of ligand exchange experiments with **Ru-50**. Pyridine substitution is observed exclusively cis to NHC.

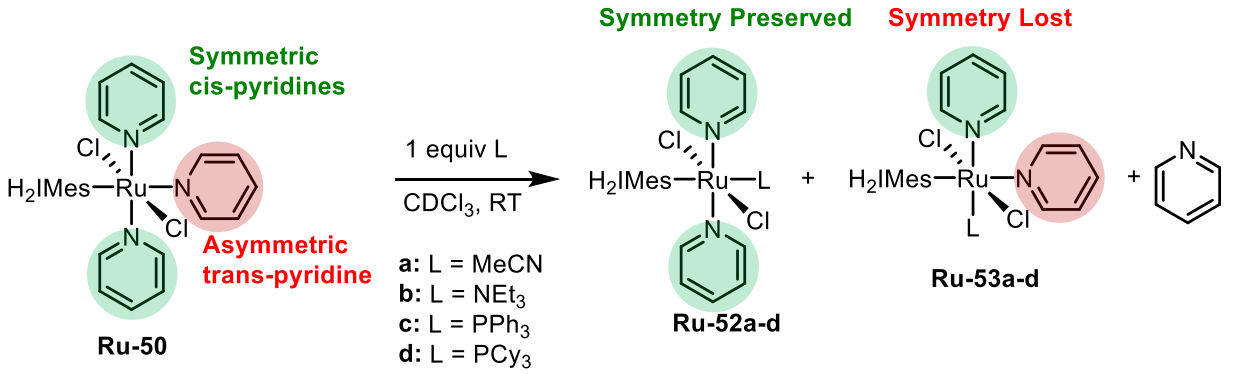

L	% Ru-50	% Ru-52	% Ru-53	Conversion
MeCN	35	0	65	65 %
NEt_3	100	0	0	0 %
PPh_3	69	0	31	31 %
PCy_3	100	0	0	0 %

References on page 60

Figure 3.3: Factors that may contribute to substitution of pyridine cis rather than trans to NHC in **Ru-50**. Steric repulsion from NHC mesityl arms labilizes cis-pyridines, while strong sigma donation from NHC increases back-bonding to trans-pyridine.

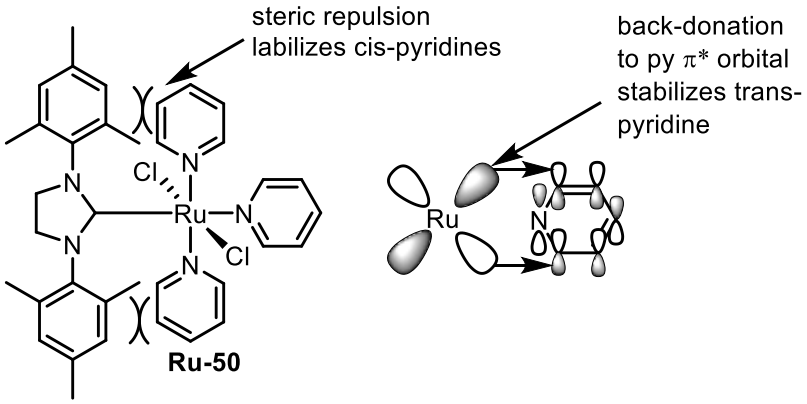

Treatment of **Ru-50** with phenyldiazomethane is expected to yield the third-generation Grubbs' catalyst, **GIII** (Scheme 3.24). However, as the field is seeking to transition away from diazo reagents, vinylidene installation was instead attempted, with the goal being to isolate **Ru-54** and subsequently treat with an acid source to both trigger vinylidene-to-indenylidene rearrangement and sequester pyridine (Scheme 3.27). If successful, this would provide a succinct route to **Ru-55**, which is an NHC-functionalized analogue to the highly active chloride bridged species **Ru-19**. Unfortunately, treatment of **Ru-50** with 1.1 equivalents of $CHC{\equiv}C(Ph)_2OH$ in THF or DCM at room temperature failed to induce conversion to the target allenylidene. ^1H NMR analysis revealed mostly starting material, indicating that $CHC{\equiv}C(Ph)_2OH$ is unable to successfully displace pyridine in **Ru-50**. Heating the reaction to 60 °C and letting it stir overnight did not solve this issue.

Scheme 3.27: Attempted synthesis of **Ru-54** and predicted conversion to **Ru-55**. Unfortunately, **Ru-50** was unreactive to $CHC{\equiv}C(Ph)_2OH$.

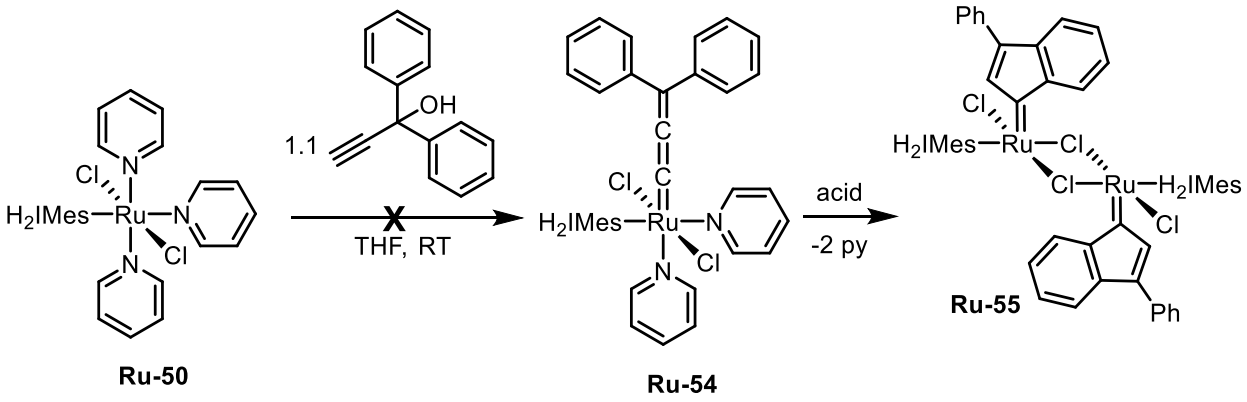

On the assumption that insufficient lability of pyridine is the main obstacle to vinylidene installation, variants of **Ru-50** functionalized with more labile pyridine derivatives were sought. Labilization by both steric pressure (2-Me-py, 2,6-Me-py) and electronic withdrawal (3-Br-py) were pursued (Scheme 3.28). 2-Me-py and 2,6-Me-py both failed to install, and only

References on page 60

decomposition of **Ru-50** was observed. 3-bromopyridine did bind successfully, and **Ru-56c** was isolated as a vibrant orange powder in 68 % yield, confirmed by diagnostic ^{1}H NMR signals for the ortho-protons of bound 3-Br-py. The lower isolated yield may reflect the increased lability of 3-bromopyridine, or the increased solubility of **Ru-56c** over **Ru-50**. The Mes-*o*-C*H*$_3$ signals, which appear as a single singlet at 2.78 ppm integrating for 12 protons in **Ru-50** appear in **Ru-56c** as three singlets at 2.78 ppm (3H), 2.67 ppm (6H), and 2.56 ppm (3H), indicating restriction of rotation of the mesityl arms about the C-N bond, presumably due to steric clash with the 3-Br functionality on pyridine. Rotation of the whole NHC about the Ru-C bond is unrestricted, as indicated by the signal for the NHC backbone C*H*$_2$ protons, which appears as a single singlet integrating for 4 protons. Although 3-bromopyridine should be more labile than pyridine, **Ru-56c** also failed to produce vinylidenes when treated to 1.1 equivalents of CHC≡C(Ph)$_2$OH.

Scheme 3.28: Synthesis of substituted pyridine derivatives of **Ru-50**. Only 3-Br-py derivative **Ru-56c** could be successfully isolated.

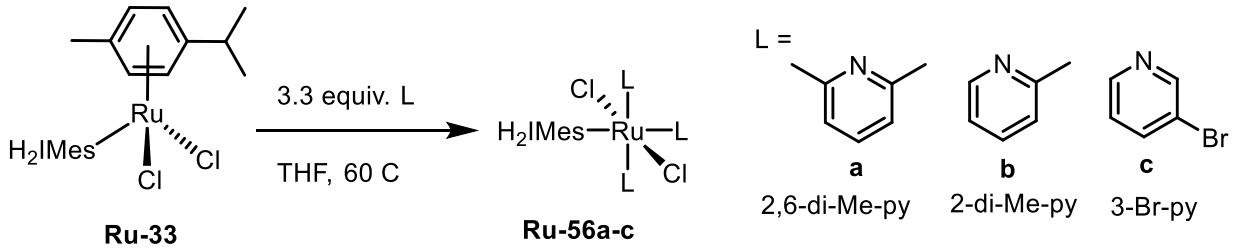

Ru-33 **Ru-56a-c**

Attempting to promote the reaction of **Ru-50** with CHC≡C(Ph)$_2$OH by adding 0.1 equiv acetyl chloride as an acid source in order to force the dissociation of pyridine led to rapid decomposition to an ill-defined black mixture (Scheme 3.29). The persistent failure to observe formation of an allenylidene or vinylidene complex, even when pyridine is forcibly sequestered suggests that the problem with this reaction lies not with the dissociation of pyridine, but with the association of 1,1-diphenylpropargyl alcohol (Scheme 3.30). Based on the ligand exchange experiments above, dissociation of pyridine occurs cis- to H$_2$IMes, and successful association of incoming ligand is heavily dependant on steric bulk. Steric repulsion could therefore be preventing the initial side on approach and binding of CHC≡C(Ph)$_2$OH. This idea could be probed by replacing the symmetrically bulky H$_2$IMes with an unsymmetrical NHC or, more interestingly, one of the unsymmetrically bulky CAAC ligands that have recently been deployed in record-breaking catalysts (Scheme 3.30).[16-17, 20, 94-96]

References on page 60

Scheme 3.29: Addition of acetyl chloride to Ru-50 and CHC≡C(Ph)$_2$OH causes rapid decomposition to an ill-defined black mixture.

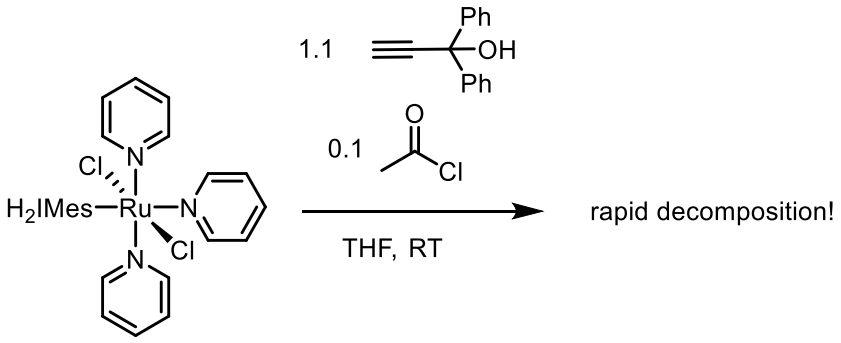

Ru-50

Scheme 3.30: Steric clash may be preventing coordination of CHC≡C(Ph)$_2$OH. This may be alleviated by switching to asymmetrically bulky NHC or CAAC ligands.

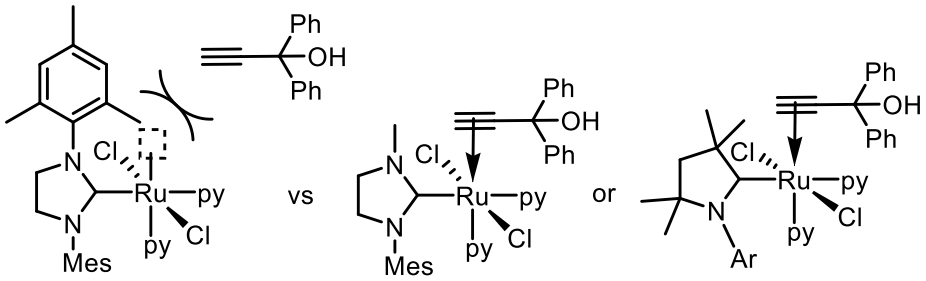

3.4 Improved Access to Class C: Zinc Aryloxides as an Alternative Transmetalating Agent

3.4.1 Introduction: Pseudohalide Ligands, Challenges and Opportunities

Alkoxide and Aryloxide ligands, with their highly tunable stereoelectronic properties, are ubiquitous in group 6 metathesis catalysts, where they are readily installed by salt metathesis with group 1 alkyl/aryloxides.

Various pseudohalides have been installed on ruthenium metathesis catalysts (Figure 3.4), but despite early reports of impressive activity from pseudohalide-bearing catalysts such as **Ru-28** and **Ru-57**, which achieved turnover numbers in the RCM of diethyl-diallylmalonate of > 40 000 (ground-breaking at the time, and comparable to modern state-of-the-art catalysts), they have not seen wide uptake within the field. This may soon change, as the recent establishment of bimolecular coupling as a key decomposition route for ruthenium metathesis catalysts and the revelation that top-performing CAAC-functionalized Ru-carbene complexes[17, 77, 94-95, 97-99] decompose primarily via bimolecular pathways,[100] and the mechanistic confirmation of the role of chloride ligands in bimolecular coupling.[100-101] have sparked renewed interest in bulky pseudohalide ligands as a means of preventing or retarding coupling. Convenient methods for pseudohalide installation are therefore of interest.

References on page 60

Figure 3.4: Selected examples of pseudohalide-bearing Ru-based metathesis catalysts

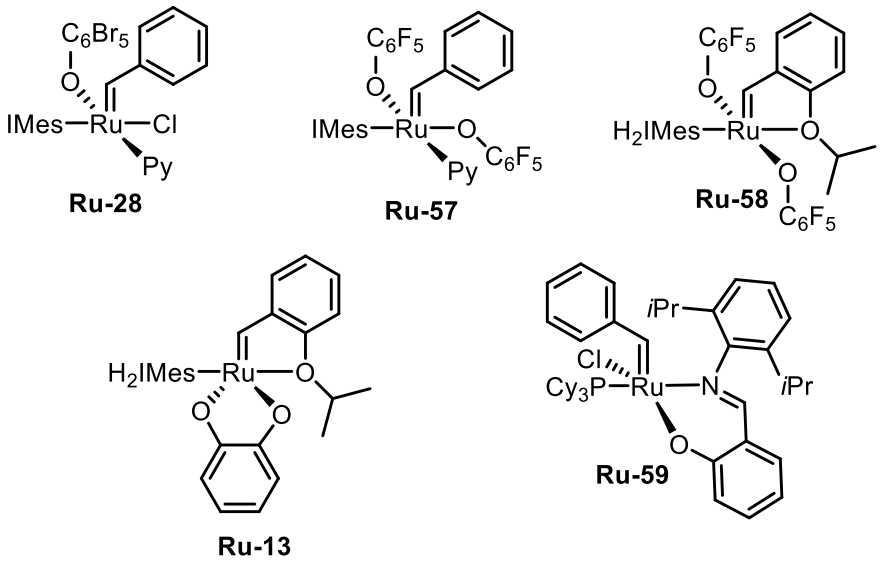

Pseudohalide installation by salt metathesis with group 1 nucleophiles is inconsistently successful on ruthenium metathesis catalysts: thiolate,[102] catecholate,[103] catechothiolate,[103] PhO^-,[104] $tBuO^-$[105] have all been installed well from alkali metal nucleophiles, while electron-deficient aryloxide ($C_6X_5O^-$, X = F, Cl, Br), perfluoronated carboxylate,[7, 22] sulfoxide,[7] nitro,[5] isocyanate,[8] isothiocyanate,[8] *o*-Schiff-base-aryloxide,[25-27, 106] and bidentate NHC-Aryloxide[24, 107-109] ligands have only been installed via the use of silver or thallium nucleophiles. In general, it seems that softer and more electron rich pseudohalides tend to install well from alkali metal nucleophiles, while harder and electron deficient pseudohalides tend to require the use of Ag or Tl. This presents a challenge, as thallium and its compounds are highly toxic,[28-29] requiring great care in use and in the disposal of the resultant waste. Silver nucleophiles, while not nearly as toxic as thallium, are highly photosensitive and stoichiometric control is therefore challenging. Silver waste also requires special handling and disposal in many jurisdictions. As well, both metals are relatively pricey, especially compared to sodium.

The surprising inertness to substitution of chloride shown by ruthenium metathesis catalysts is not unique. $W(NtBu)Cl_2[P_2(NtBu)_3]$, $Mo(NtBu)Cl_2[P_2(NtBu)_3]$, and $MnCl(NtBu)_3$ are all inert to substitution of chloride by carbon, oxygen, and nitrogen nucleophiles as the lithium or magnesium reagents, but will react with Ag or Tl nucleophiles.[110-112] Pyrrolide-based PNP ligands failed to install on Ir or Ru substrates from the Li nucleophile and could only be successfully installed from Ag or Tl.[113] β-Ketoiminate and related β-Ketoiminato ligands were successfully installed on Pd and Ni with Tl nucleophiles while Li and K failed.[114-115] There are numerous other examples of pseudohalide installation on various metal centres using Ag or Tl nucleophiles without comment on the performance of group 1 or 2 nucleophiles.[116-124] A safer and more convenient alternative method for pseudohalide installation would therefore be highly desirable and broadly applicable in the field of transition metal chemistry.

References on page 60

The superior transmetalating ability of Ag and Tl nucleophiles is likely a kinetic rather than thermodynamic phenomenon, and has been attributed to the higher electrophilicity of Ag^+ and Tl^+ cations facilitating access to the four-membered transition state **TS-1** (Scheme 3.31).[112] Wilkinson has suggested the involvement of electrophilic attack on chloride by Ag^+ or Tl^+.[112] Analogy has also been drawn to the accelerating effect of Ag^+ and Tl^+ cations in nucleophilic substitutions of organic halides, where it is discussed in terms of "electrophilic pull" of heavy metal cations.[125] A similar effect is known in halide substitution of metal complexes in aqueous media.[126] We therefore considered whether other, less toxic and photosensitive late metal nucleophiles might exhibit a similar electrophilically-driven accelerating effect.

Scheme 3.31: Electrophilicity of heavy/late metal cations (Tl^I pictured) is believed to be responsible for improved activity in transmetalation relative to alkali/alkali earth cations.

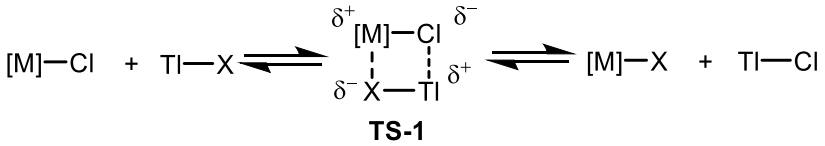

Zinc nucleophiles stand out as a promising candidate transmetalating agent. They are thermally and photolytically stable, easily accessible either by deprotonation of the appropriate acid with diethyl zinc or salt metathesis between a group 1 or 2 nucleophile and $ZnCl_2$, and zinc is effectively non-toxic. Zinc nucleophiles also have an excellent pedigree as the transmetalating agent of choice in palladium-catalyzed cross-coupling,[127-129] where it has been commented that reactions in the absence of zinc are often "agonizingly slow".[129] The utility of zinc in this context has been attributed to the ease of transmetalation both to and from zinc nucleophiles;[127] exactly the property sought in the present context.

Installation of $C_6F_5O^-$, among both the hardest and most electron deficient pseudohalides that have been installed on Ru metathesis catalysts,, represents a highly challenging test-scenario for an alternative transmetalating agent. While other electron deficient pseudohalides have been installed with Ag nucleophiles, Buchmeiser specifically states that it was necessary to use Tl to successfully install $C_6F_5O^-$ on the second-generation Hoveyda catalyst.[22] We therefore decided to test $Zn(OC_6F_5)_2$ as an alternative to $TlOC_6F_5$ in the installation of $C_6F_5O^-$ on the second-generation Hoveyda catalyst.

3.4.2 Results and Discussion: Aryloxide Installation by $Zn(OC_6F_5)_2$

Treating the second-generation Hoveyda catalyst, **HII,** to 1 equiv of in-situ generated $Zn(OC_6F_5)_2$ did not proceed cleanly to the expected bis-aryloxide species **Ru-58** (Scheme 3.32). Instead, three alkylidene signals at 16.63, 16.90, and 17.17 ppm were detectable by ^1H NMR spectroscopy. The signal at 16.63 ppm corresponds to unreacted **HII**, the signal at 17.17 ppm is consistent with the target bis-aryloxide **Ru-58**, and the signal at ppm is presumed to arise from mono-aryloxide species **Ru-60**. The distribution of these three species depends on the solvent used (Table 3.2), suggesting a solvent-dependent equilibrium.

References on page 60

Scheme 3.32: Reaction of 1 equiv. $Zn(OC_6F_5)_2$ with **HII**. $Zn(OC_6F_5)_2$ generated in-situ by adding dropwise 1.0M $ZnEt_2$ in hexanes to a solution of C_6F_5OH in the appropriate solvent. The $Zn(OC_6F_5)_2$ is then added dropwise to a stirred solution of **HII**.

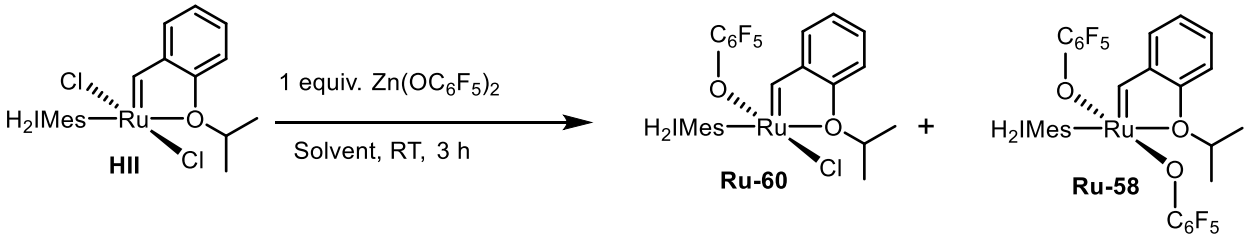

Table 3.2: Product distribution observed for reaction of **HII** with 1 equiv. $Zn(OC_6F_5)_2$ in different solvents, as determined by relative integration of alkylidene signals for each species in the ^1H NMR spectrum of an aliquot taken from the reaction mixture.

Solvent	**HII**	**Ru-60**	**Ru-58**	**% "Zn-OAr" consumed**
CH_2Cl_2	50%	50%	0%	25%
C_6H_6	26%	65%	9%	41%
THF	24%	70%	6%	41%

The fact that in no case even 50% of the available "Zn-OAr" fragment is consumed suggests that only the bis aryloxide species $Zn(OC_6F_5)_2$ is competent to install aryloxide, while concomitantly generated monoaryloxide $Zn(OC_6F_5)Cl$ acts as a source of chloride rather than aryloxide (Scheme 3.33), This should be confirmed by repeating the attempted transmetalation with 2 equiv $Zn(OC_6F_5)Cl$ in place of 1 equiv $Zn(OC_6F_5)_2$, in which case little to no aryloxide transfer would confirm that $Zn(OC_6F_5)Cl$ is not competent as a source of aryloxide (Scheme 3.34), and a follow-up reaction where a genuine sample of bis-aryloxide **Ru-58** is treated with 2 equivalents of $Zn(OC_6F_5)Cl$, in which case formation of **Ru-60** and/or **HII** would indicate that $Zn(OC_6F_5)Cl$ can act as a source of chloride (Scheme 3.35).

Scheme 3.33: Proposed equilibrium between **HII**, **Ru-58**, and **Ru-60**, with $Zn(OC_6F_5)Cl$ acting as a source of chloride rather than aryloxide.

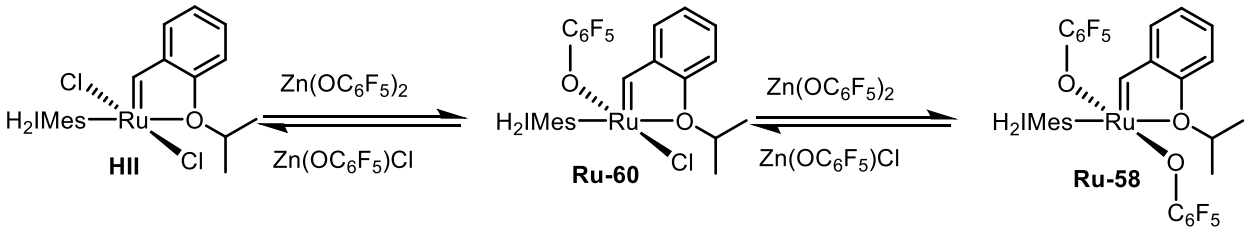

Equilibrium is reached rapidly (≤ 1 h) when CH_2Cl_2 or C_6H_6 are used as the solvent. Rechlorination of **Ru-58**/**Ru-60** or decomposition of $Zn(OC_6F_5)_2$ by CH_2Cl_2 was not considered as a concern, as

References on page 60

Ru-58 has been previously synthesized in CH_2Cl_2 and characterized in $CDCl_3$,[22] and zinc nucleophiles are routinely prepared and used in CH_2Cl_2 without incident (e.g. in the Simmons-Smith reaction).[130] Aryloxide installation proceeds more slowly (equilibrium reached after 24 h) in THF, presumably due to coordination of THF to $Zn(OC_6F_5)_2$. It appears that $Zn(OC_6F_5)$ is kinetically but not thermodynamically competent in transmetalation. Ag and Tl nucleophiles have precipitation of highly insoluble AgCl and TlCl as a strong thermodynamic driving force, but $ZnCl_2$ and especially $Zn(OC_6F_5)Cl$ are considerably more soluble and cannot therefore act as a good thermodynamic sink. Attempting to stabilize/sequester $ZnCl_2$ by performing the reaction in the presence of 1 equivalent 18-crown-6 did not lead to greater conversion, but did cause the reactions in C_6H_6 and CH_2Cl_2 to behave like the reaction in THF; equilibrium was reached more slowly and conversions matched those observed for THF.

Scheme 3.34: Proposed experiment to probe whether $Zn(OC_6F_5)Cl$ is competent as a source of aryloxide

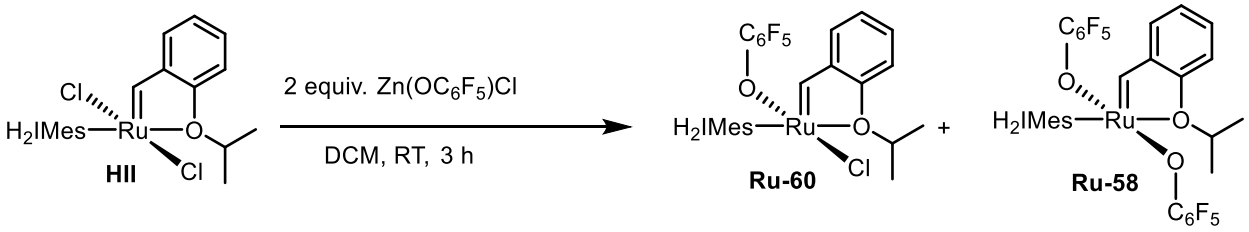

Scheme 3.35: Proposed experiment to probe whether $Zn(OC_6F_5)Cl$ can act as a source of chloride.

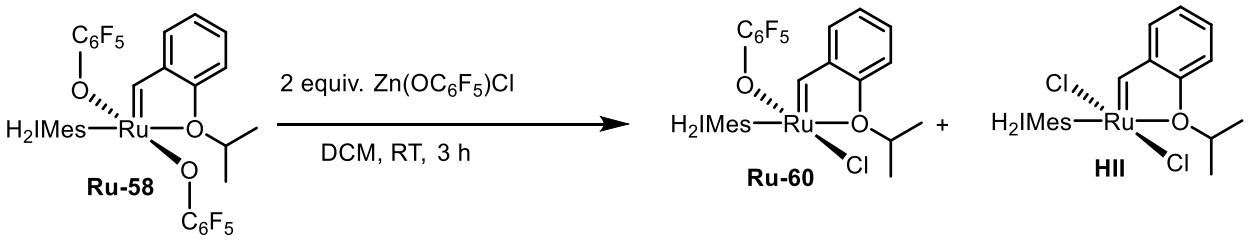

One solution to access **Ru-58** would be to simply use an excess of $Zn(OC_6F_5)_2$. However, this is wasteful, precludes the possibility of stoichiometric control and access to the mono-aryloxide species **Ru-60**, and the presence of a large excess of zinc reagent would significantly complicate workup. A better solution would be to combine the favourable thermodynamics of alkali metal reagents with the superior kinetics of zinc nucleophiles by generating $Zn(OC_6F_5)_2$ catalytically from a stoichiometric amount of $Na(OC_6F_5)$ and a catalytic (1-5 mol%) amount of $ZnCl_2$, thereby minimizing the presence and impact of $Zn(OC_6F_5)Cl$ and $ZnCl_2$ (Scheme 3.36). A conceptually similar approach has been deployed in the cross-coupling of organosodium reagents enhanced by a catalytic amount (10 mol%) of $ZnCl_2$.[131]

References on page 60

Scheme 3.36: Proposed use of $ZnCl_2$ as a catalytic aryloxide transfer agent

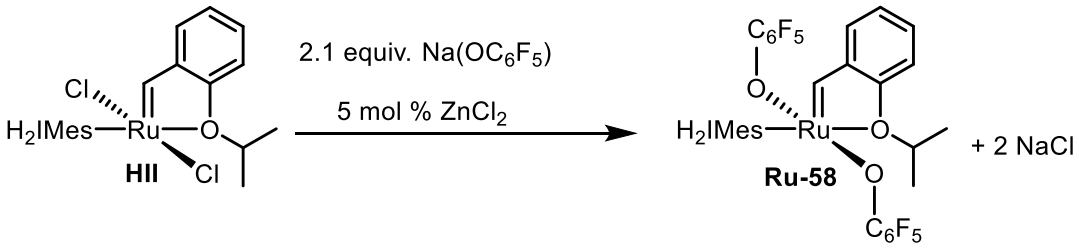

If successful, $ZnCl_2$ would be acting as a catalytic anionic ligand transfer agent. This approach may be broadly applicable, not just to pseudohalide installation. For example, exchanging Cl^- for I^- on metathesis catalysts via salt metathesis with NaI is often sluggish, requiring 8 h in the case of the first-generation Grubbs catalyst. [132] A catalytic amount of $ZnCl_2$ could significantly accelerate this exchange.

3.5 Conclusions

A new route to magnesium carbenoids from geminal dichlorides has been achieved utilizing the magnesium-anthracene complex **Mg-1**. However, and in spite of early promising results, an effective route to ruthenium alkylidenes utilizing magnesium carbenoids could not be realized. Ancillary ligand incompatibilities are suspected as a key issue to overcome.

The first high-yield synthesis of $RuCl_2(H_2IMes)(py)_3$ (**Ru-50)** is reported. Ligand exchange experiments indicate that **Ru-50** is both more soluble and substitutionally labile than tetrakis pyridine species $RuCl_2(py)_4$ (**Ru-51**), although ligand exchange unexpectedly occurs primarily cis to H_2IMes. Despite the increased lability, indenylidene installation was unsuccessful both on **Ru-50** and the more labile still $RuCl_2(H_2IMes)(3\text{-Br-py})_3$ (**Ru-56c**). Steric clash with the bulky H_2IMes ligand is believed to be responsible both for the unexpected preference for substitution cis to H_2IMes and the failure of indenylidene to install. Derivatives of **Ru-50** bearing unsymmetrically bulky NHC or CAAC ligands are proposed as a solution to this steric crowding.

Zinc aryloxides have been invested as an attractive alternative to thallium and silver for the installation of pseudohalides on metathesis catalysts. Initial results suggest that zinc aryloxides are kinetically but not thermodynamically competent as an aryloxide source; reaction proceeds rapidly, but in no case was even 50% of available Zn-OAr bond consumed. Utilizing a catalytic amount of $ZnCl_2$ in the presence of sodium aryloxides (which are themselves thermodynamically but not kinetically competent) is proposed as a solution that leverages both the kinetic advantages of electrophilic Zn^{2+} and the thermodynamic sink of NaCl.

References on page 60

3.6 References

(1) Day, C. S.; Fogg, D. E., High-Yield Synthesis of a Long-Sought, Labile Ru-NHC Complex and Its Application to the Concise Synthesis of Second-Generation Olefin Metathesis Catalysts. *Organometallics* **2018,** *37*, 4551-4555.
(2) Barbasiewicz, M.; Szadkowska, A.; Makal, A.; Jarzembska, K.; Woźniak, K.; Grela, K., Is the Hoveyda–Grubbs Complex a Vinylogous Fischer-Type Carbene? Aromaticity-Controlled Activity of Ruthenium Metathesis Catalysts. *Chem. Eur. J.* **2008,** *14*, 9330-9337.
(3) Michrowska, A.; Bujok, R.; Harutyunyan, S.; Sashuk, V.; Dolgonos, G.; Grela, K., Nitro-Substituted Hoveyda−Grubbs Ruthenium Carbenes: Enhancement of Catalyst Activity through Electronic Activation. *J. Am. Chem. Soc.* **2004,** *126*, 9318-9325.
(4) Basak, T.; Grudzień, K.; Barbasiewicz, M., Remarkable Ability of the Benzylidene Ligand To Control Initiation of Hoveyda–Grubbs Metathesis Catalysts. *Eur. J. Inorg. Chem.* **2016,** *2016*, 3513-3523.
(5) Buchmeiser, M. R.; Ahmad, I.; Gurram, V.; Kumar, P. S., Pseudo-Halide and Nitrate Derivatives of Grubbs and Grubbs–Hoveyda Initiators: Some Structural Features Related to the Alternating Ring-Opening Metathesis Copolymerization of Norborn-2-ene with Cyclic Olefins. *Macromolecules* **2011,** *44*, 4098-4106.
(6) Halbach, T. S.; Mix, S.; Fischer, D.; Maechling, S.; Krause, J. O.; Sievers, C.; Blechert, S.; Nuyken, O.; Buchmeiser, M. R., Novel Ruthenium-Based Metathesis Catalysts Containing Electron- Withdrawing Ligands: Synthesis, Immobilization, and Reactivity. *J. Org. Chem.* **2005,** *70*, 4687-4694.
(7) Krause, J. O.; Nuyken, O.; Wurst, K.; Buchmeiser, M. R., Synthesis and Reactivity of Homogeneous and Heterogeneous Ruthenium-Based Metathesis Catalysts Containing Electron-Withdrawing Ligands. *Chem. Eur. J.* **2004,** *10*, 777-784.
(8) Kumar, P. S.; Wurst, K.; Buchmeiser, M. R., Isocyanate- and Isothiocyanate-Derived RuIV-Based Alkylidenes: Synthesis, Structure, and Activity. *Chem. Asian J.* **2009,** *4*, 1275-1283.
(9) Conrad, J. C.; Amoroso, D.; Czechura, P.; Yap, G. P. A.; Fogg, D. E., The First Highly Active, Halide-Free Ruthenium Catalyst for Olefin Metathesis. *Organometallics* **2003,** *22*, 3634-3636.
(10) Conrad, J. C.; Parnas, H. H.; Snelgrove, J. L.; Fogg, D. E., Highly Efficient Ru-Pseudohalide Catalysts for Olefin Metathesis. *J. Am. Chem. Soc.* **2005,** *127*, 11882–11883.
(11) Conrad, J. C.; Snelgrove, J. L.; Eeelman, M. D.; Hall, S.; Fogg, D. E., Ruthenium Aryloxide Catalysts: Synthesis and Applications in Ring-Closing Metathesis. *J. Mol. Catal. A: Chem.* **2006,** *254*, 105-110.
(12) Monfette, S.; Marleau-Gillette, S.; Conrad, J. C.; McDonald, R.; Fogg, D. E., A Ru-isocyanate initiator for fast, living, precisely controlled ring-opening metathesis polymerization at ambient temperatures. *Dalton Trans.* **2012,** *41*, 14476-14479.
(13) Schwab, P.; Grubbs, R. H.; Ziller, J. W., Synthesis and Applications of $RuCl_2(CHR')(PR_3)_2$: The Influence of the Alkylidene Moiety on Metathesis Activity. *J. Am. Chem. Soc.* **1996,** *118*, 100-110.
(14) Kingsbury, J. S.; Harrity, J. P. A.; Bonitatebus, P. J.; Hoveyda, A. H., A Recyclable Ru-Based Metathesis Catalyst. *J. Am. Chem. Soc.* **1999,** *121*, 791-799.
(15) Dorta, R.; Kelly III, R. A.; Nolan, S. P., Cross Metathesis Allowing the Conversion of a Ruthenium Indenylidene Complex into Grubbs' Catalyst. *Adv. Synth. Catal.* **2004,** *346*, 917-920.

(16) Marx, V. M.; Sullivan, A. H.; Melaimi, M.; Virgil, S. C.; Keitz, B. K.; Weinberger, D. S.; Bertrand, G.; Grubbs, R. H., Cyclic Alkyl Amino Carbene (CAAC) Ruthenium Complexes as Remarkably Active Catalysts for Ethenolysis. *Angew. Chem., Int. Ed.* **2015,** *54*, 1919-1923.
(17) Gawin, R.; Tracz, A.; Chwalba, M.; Kozakiewicz, A.; Trzaskowski, B.; Skowerski, K., Cyclic Alkyl Amino Ruthenium Complexes—Efficient Catalysts for Macrocyclization and Acrylonitrile Cross Metathesis. *ACS Catal.* **2017,** *7*, 5443-5449.
(18) Schrock, R. R., Multiple Metal–Carbon Bonds for Catalytic Metathesis Reactions (Nobel Lecture). *Angew. Chem., Int. Ed.* **2006,** *45*, 3748-3759.
(19) Bailey, G. A.; Foscato, M.; Higman, C. S.; Day, C. S.; Jensen, V. R.; Fogg, D. E., Bimolecular Coupling as a Vector for Decomposition of Fast-Initiating Olefin Metathesis Catalysts. *J. Am. Chem. Soc.* **2018,** *140*, 6931-6944.
(20) Nascimento, D. L.; Fogg, D. E., Origin of the Breakthrough Productivity of Ruthenium–Cyclic Alkyl Amino Carbene Catalysts in Olefin Metathesis. *J. Am. Chem. Soc.* **2019,** *141*, 19236-19240.
(21) Fulton, J. R.; Holland, A. W.; Fox, D. J.; Bergman, R. G., Formation, Reactivity, and Properties of Nondative Late Transition Metal−Oxygen and −Nitrogen Bonds. *Acc. Chem. Res.* **2002,** *35*, 44-56.
(22) Halbach, T. S.; Mix, S.; Fischer, D.; Maechling, S.; Krause, J. O.; Sievers, C.; Blechert, S.; Nuyken, O.; Buchmeiser, M. R., Novel Ruthenium-Based Metathesis Catalysts Containing Electron-Withdrawing Ligands: Synthesis, Immobilization, and Reactivity. *J. Org. Chem.* **2005,** *70*, 4687–4694.
(23) Krause, J. O.; Nuyken, O.; Buchmeiser, M. R., Factors Relevant for the Ruthenium–Benzylidene-Catalyzed Cyclopolymerization of 1,6-Heptadyines. *Chem. Eur. J.* **2004,** *10*, 2029-2035.
(24) Van Veldhuizen, J. J.; Campbell, J. E.; Giudici, R. E.; Hoveyda, A. H., A Readily Available Chiral Ag-Based N-Heterocyclic Carbene Complex for Use in Efficient and Highly Enantioselective Ru-Catalyzed Olefin Metathesis and Cu-Catalyzed Allylic Alkylation Reactions. *J. Am. Chem. Soc.* **2005,** *127*, 6877-6882.
(25) Chang, S.; Jones, L.; Wang, C.; Henling, L. M.; Grubbs, R. H., Synthesis and Characterization of New Ruthenium-Based Olefin Metathesis Catalysts Coordinated with Bidentate Schiff-Base Ligands. *Organometallics* **1998,** *17*, 3460-3465.
(26) Vila, A. M. L.; Monsaert, S.; Drozdzak, R.; Wolowiec, S.; Verpoort, F., New Indenylidene-Schiff Base-Ruthenium Complexes for Cross-Metathesis and Ring-Closing Metathesis. *Adv. Synth. Catal.* **2009,** *351*, 2689-2701.
(27) Drozdzak, R.; Ledoux, N.; Allaert, B.; Dragutan, I.; Dragutan, V.; Verpoort, F., Rational Design and Convenient Synthesis of a Novel Family of Ruthenium Complexes with O,N-Bidentate Ligands. *Cent. Eur. J. Chem.* **2005,** *3*, 404-416.
(28) Pike, R. D., Thallium: Organometallic Chemistry Based in part on the article Thallium: Organometallic Chemistry by William S. Rees, Jr. & Gertrud Kräuter which appeared in the Encyclopedia of Inorganic Chemistry, First Edition. In *Encyclopedia of Inorganic and Bioinorganic Chemistry*, Scott, R. A., Ed. 2011.
(29) Galvan-Arzate, S.; Santamaria, A., Thallium toxicity. *Toxicol. Lett.* **1998,** *99*, 1–13.
(30) Garber, S. B.; Kingsbury, J. S.; Gray, B. L.; Hoveyda, A. H., Efficient and Recyclable Monomeric and Dendritic Ru-Based Metathesis Catalysts. *J. Am. Chem. Soc.* **2000,** *122*, 8168-8179.

References on page 60

(31) Nascimento, D. L.; Davy, E. C.; Fogg, D. E., Merrifield Resin-Assisted Routes to Second-Generation Catalysts for Olefin Metathesis. *Catal. Sci. Technol.* **2018,** *8*, 1535-1544.
(32) van Lierop, B. J.; Reckling, A. M.; Lummiss, J. A. M.; Fogg, D. E., Clean, Convenient, High-yield Access to Second-generation Ru Metathesis Catalysts from Commercially Available Precursors. *ChemCatChem* **2012,** *4*, 2020-2025.
(33) Bray, P. A.; Sokas, R. K., Delayed Respiratory Fatality From Trimethylsilyldiazomethane: What Do Workers Need to Know About Potentially Hazardous Exposures? *J. Occup. Environ. Med.* **2015,** *57*, e15-e16.
(34) Belderrain, T. R.; Grubbs, R. H., Reaction Between Ruthenium(0) Complexes and Dihalo Compounds. A New Method for the Synthesis of Ruthenium Olefin Metathesis Catalysts. *Organometallics* **1997,** *16*, 4001-4003.
(35) Wilhelm, T. E.; Belderrain, T. R.; Brown, S. N.; Grubbs, R. H., Reactivity of $Ru(H)(H_2)Cl(PCy_3)_2$ with Propargyl and Vinyl Chlorides: New Methodology To Give Metathesis-Active Ruthenium Carbenes. *Organometallics* **2002,** *16*, 3867-3869.
(36) Oliván, M.; Caulton, K. G., C−(Halide) Oxidative Addition Routes to Ruthenium Carbenes. *Inorg. Chem.* **2002,** *38*, 566-570.
(37) Mutoh, Y.; Kozono, N.; Araki, M.; Tsuchida, N.; Takano, K.; Ishii, Y., Ruthenium Seleno- and Tellurocarbonyl Complexes: Selenium and Tellurium Atom Transfer to a Terminal Carbido Ligand. *Organometallics* **2010,** *29*, 519-522.
(38) Iwatani, K.; Hori, Y.; Hagiwara, T. Jpn. Kokai Tokkyo Koho. 2000.
(39) Wolf, J.; Stuer, W.; Grunwald, C.; Schwab, P.; Schulz, M.; Werner, H., Ruthenium Trichloride, Tricyclohexylphosphane, 1-Alkynesm Magnesium, Hydrogen, and Water--Ingredients of an Efficient One-Pot Synthesis of Ruthenium Catalysts for Olefin Metathesis. *Angew. Chem., Int. Ed.* **1998,** *37*, 1124-1126.
(40) Rowlands, G. J., 29.2.1.1.2 Method 2: Chlorination of the Carbonyl Group. In *Science of Synthesis*, Thieme Chemistry: 2007; Vol. 29, p 67.
(41) Aghapour, G.; Afzali, A., Facile Conversion of Aldehydes and Ketones to gem-Dichlorides Using Chlorodiphenylphosphine/N-Chlorosuccinimide as a New and Neutral System. *Synth. Commun.* **2008,** *38*, 4023-4035.
(42) Pertici, P.; Vitulli, G., A New Synthetic Method for the Preparation of Cyclo-olefin Ruthenium Complexes. *Dalton Trans.* **1980,** *3*, 1961-1964.
(43) Ashby, E. C.; Deshpande, A. K.; Doctorovich, F., Mechanism of Reaction of Geminal Dihalides with Magnesium. Evidence for the Formation of Carbenes from Radical Precursors. The Similarity in Reactions of Geminal Dihalides with Magnesium and $LiAlH_4$. *J. Org. Chem.* **1994,** *59*, 6223-6232.
(44) Doctorovich, F.; Deshpande, A. K.; Ashby, E. C., Concerning the Preparation of Geminal Digrignard Reagents.: The Mechanism of Reaction of Geminal Dihalides with Magnesium and Sodium. *Tetrahedron* **1994,** *50*, 5945-5956.
(45) Kimura, T., Recent Advances in Magnesium Carbenoid Chemistry. *Synthesis* **2017,** *49*, 5105-5119.
(46) Satoh, T., Recent Advances in the Chemistry of Magnesium Carbenoids. *Chem. Soc. Rev.* **2007,** *36*, 1561-1572.
(47) Ishida, N.; Saitoh, H.; Sugiyama, S.; Satoh, T., Synthesis of Conjugated Enynes from Ketones and Aldehydes by 1,2-CC Insertion and 1,2-CH Insertion of Carbenoids as the Key Reactions. *Tetrahedron* **2011,** *67*, 3081-3090.

References on page 60

(48) Kimura, T.; Nishida, J.; Kashiwamura, G.; Kobayashi, G.; Satoh, T., Synthesis of Cyclopropane-Fused α-Chlorolactones Utilizing the Nucleophilicity of Cyclopropylmagnesium Carbenoids. *Tetrahedron Lett.* **2014,** *55*, 1428-1430.
(49) Momochi, H.; Noguchi, T.; Miyagawa, T.; Ogawa, N.; Tadokoro, M.; Satoh, T., The First Example for the Asymmetric Aynthesis of Allenes by the Doering–LaFlamme Allene Synthesis with Enantiopure Cyclopropylmagnesium Carbenoids. *Tetrahedron Lett.* **2011,** *52*, 3016-3019.
(50) Nakaya, N.; Sugiyama, S.; Satoh, T., A New Synthesis, Including Asymmetric Synthesis, of Alkylidenecyclopropanes by 1,2-CC Insertion of Cyclobutylmagnesium Carbenoides as the Key Reaction. *Tetrahedron Lett.* **2009,** *50*, 4212-4216.
(51) Ogata, S.; Masaoka, S.; Sakai, K.; Satoh, T., The First Example of Regiospecific Magnesium Carbenoid 1,3-CH Insertion: its Mechanism and Stereochemistry. *Tetrahedron Lett.* **2007,** *48*, 5017-5021.
(52) Saitoh, H.; Watanabe, T.; Kimura, T.; Kato, Y.; Satoh, T., New Synthesis of Multisubstituted Cyanocyclopropanes by the Intramolecular SN2 Alkylation and 1,3-CC Insertion Reaction of Magnesium Carbenoids as the Key Reactions. *Tetrahedron* **2012,** *68*, 2481-2495.
(53) Satoh, T.; Awata, Y.; Kato, Y.; Ogata, S.; Ishigaki, M.; Sugiyama, S.; Saitoh, H., Synthesis, Including Asymmetric Synthesis, of 1-Substituted Cyclopentenes From Cyclobutanones with One-Carbon Ring-Expansion by 1,2-Carbon-Carbon Insertion of Magnesium Carbenoids. *Tetrahedron* **2011,** *67*, 1102-1113.
(54) Satoh, T.; Awata, Y.; Ogata, S.; Sugiyama, S.; Tanaka, M.; Tori, M., A Synthesis of Esters, Amides, and Sulfones Bearing a 1-Cyclopentenyl Group at the α-Position from Cyclobutanones with One-Carbon Ring-Expansion. *Tetrahedron Lett.* **2009,** *50*, 1961-1964.
(55) Satoh, T.; Kashiwamura, G.; Nagamoto, S.; Sasaki, Y.; Sugiyama, S., Insertion of Cyclopropanes Between a Carbonyl Carbon and an α-Carbon of Carbonyl Compounds with Cyclopropylmagnesium Carbenoids. *Tetrahedron Lett.* **2011,** *52*, 4468-4472.
(56) Satoh, T.; Kuramoto, T.; Ogata, S.; Watanabe, H.; Saitou, T.; Tadokoro, M., Asymmetric Synthesis of Bicyclo[n.1.0]Alkanes by the Enantioselective 1,3-CH Insertion Reaction of Chiral Magnesium Carbenoids. *Tetrahedron: Asymmetry* **2010,** *21*, 1-5.
(57) Satoh, T.; Yamashita, H.; Musashi, J., A New Synthesis of β,γ-Unsaturated Esters from Three Components, Aldehydes, Chloromethyl p-Tolyl Sulfoxide, and tert-Butyl Acetate, via Magnesium Carbenoid 1,2-CH and 1,2-CC Insertion as the Key Reaction. *Tetrahedron Lett.* **2007,** *48*, 7295-7300.
(58) Watanabe, H.; Ogata, S.; Satoh, T., A Method for the Synthesis of Cyclopropanes by Regiospecific and Regioselective Magnesium Carbenoid 1,3-CH Insertion as the Key Reactions. *Tetrahedron* **2010,** *66*, 5675-5686.
(59) Hoffmann, R. W., The Quest for Chiral Grignard reagents. *Chem. Soc. Rev.* **2003,** *32*, 225-230.
(60) Hoffmann, R. W.; Nell, P. G.; Leo, Roland; Harms, K., Highly Enantiomerically Enriched α-Haloalkyl Grignard Reagents. *Chem. Eur. J.* **2000,** *6*, 3359-3365.
(61) Hoffmann, R. W.; Hölzer, B.; Knopff, O.; Harms, K., Asymmetric Synthesis of a Chiral Secondary Grignard Reagent. *Angew. Chem., Int. Ed.* **2000,** *39*, 3072-3074.
(62) Hoffmann, R. W.; Hölzer, B., Concerted and Stepwise Grignard Additions, Probed with a Chiral Grignard Reagent. *Chem. Commun.* **2001**, 491-492.
(63) Hoffmann, R. W.; Hölzer, B.; Knopff, O., Amination of Grignard Reagents with Retention of Configuration. *Org. Lett.* **2001,** *3*, 1945-1948.

References on page 60

(64) Hoffmann, R. W.; Hölzer, B., Stereochemistry of the Transmetalation of Grignard Reagents to Copper (I) and Manganese (II). *J. Am. Chem. Soc.* **2002,** *124*, 4204-4205.
(65) Hölzer, B.; Hoffmann, R. W., Kumada–Corriu Coupling of Grignard Reagents, Probed with a Chiral Grignard Reagent. *Chem. Commun.* **2003**, 732-733.
(66) Simmons, H. E.; Smith, R. D., A New Synthesis of Cyclopropanes From Olefins. *J. Am. Chem. Soc.* **1958,** *80*, 5323-5324.
(67) Gessner, V. H., Stability and reactivity control of carbenoids: recent advances and perspectives. *Chem. Commun.* **2016,** *52*, 12011-12023.
(68) Boche, G.; Harms, K.; Marsch, M.; Müller, A., 9-Bromo-9-[(Bromomagnesium)Methylene]Fluorene–Tetrahydrofuran (1/4) Structure of a MgBr/Br Carbenoid. *J. Chem. Soc., Chem. Commun.* **1994**, 1393-1394.
(69) Bogdanović, B.; Schlichte, K.; Westeppe, U., Dehalogenierungen von geminalen Dihalogencyclopropanen, α,α-Dichlorcyclobutanonen und Halogenketonen mit Hilfe von Magnesiumanthracen·3THF. *Chem. Ber.* **1988,** *121*, 27-32.
(70) Rowlands, G. J., 29.2.3 Product Subclass 3: Cl/I Acetals. In *Science of Synthesis*, Thieme Chemistry: 2007; Vol. 29, p 87.
(71) Rowlands, G. J., 29.2.4.2 Applications of Product Subclass 4 in Organic Synthesis. In *Science of Synthesis*, Thieme Chemistry: 2007; Vol. 29, p 101.
(72) Diaper, C. M., 29.4 Product Class 4: Hal/S, Hal/Se, and Hal/Te Acetals. In *Science of Synthesis*, Thieme Chemistry: 2007; Vol. 29, p 193.
(73) Bogdanovic, B., Magnesium Anthracene Systems and Their Application in Synthesis and Catalysis. *Acc. Chem. Res.* **1988,** *21*, 261-267.
(74) Bogdanovič, B.; Janke, N.; Kinzelmann, H.-G., Use of Magnesium Anthracene·3THF in Synthesis: Generation of Grignard Compounds and Other Reactions with Organic Halides. *Chem. Ber.* **1990,** *123*, 1507-1516.
(75) Raston, C. L.; Salem, G., Magnesium Anthracene: an Alternative to Magnesium in the High Yield Synthesis of Grignard Reagents. *J. Chem. Soc., Chem. Commun.* **1984**, 1702-1703.
(76) Gawin, R.; Tracz, A.; Chwalba, M.; Kozakiewicz, A.; Trzaskowski, B.; Skowerski, K., Cyclic Alkyl Amino Ruthenium Complexes - Efficient Catalysts for Macrocyclization and Acrylonitrile Cross Metathesis. *ACS Catal.* **2017,** *7*, 5443-5449.
(77) Kajetanowicz, A.; Chwalba, M.; Gawin, A.; Tracz, A.; Grela, K., Non-Glovebox Ethenolysis of Ethyl Oleate and FAME at Larger Scale Utilizing a Cyclic (Alkyl)(Amino)Carbene Ruthenium Catalyst. *Eur. J. Lipid Sci. Technol.* **2019**, 1900263.
(78) Kimura, T., Recent Advances in Magnesium Carbenoid Chemistry. *Synthesis* **2017**, 5105-5119.
(79) Ramazanov, I. R.; Yaroslavova, A. V.; Dzhemilev, U. M., Reactions of Phosphines with Aluminum Carbenoids. *Russ. J. Appl. Chem.* **2011,** *47*, 295-297.
(80) Cole-Hamilton, D. J.; Wilkinson, G., Ortho-Metallated Triphenylphosphine(2-Diphenylphosphinophenyl) and Related Complexes of Ruthenium(II): Interaction of Chlorohydridotris(Triphenylphosphine)Ruthenium(II) with Methyl and Trimethylsilylmethyl Alkylating Agents (Li, Mg, Zn); Hydrido Methyl and Trimethylsilylmethyl Complexes. *J. Chem. Soc., Dalton Trans.* **1977**, 797-804.
(81) Czerwinska, I.; Far, J.; Kune, C.; Larriba-Andaluz, C.; Delaude, L.; De Pauw, E., Structural Analysis of Ruthenium–Arene Complexes using Ion Mobility Mass Spectrometry, Collision-Induced Dissociation, and DFT. *Dalton Trans.* **2016,** *45*, 6361-6370.

References on page 60

(82) Onitsuka, K.; Nishii, M.; Matsushima, Y.; Takahashi, S., Unexpected Formation of the Vinyl−Phosphonio Complex [CpRu(PPh$_3$)(C$_6$H$_4$PPh$_2$CHCH$_2$)][PF$_6$] from a Vinylidene Complex via Nucleophilic Addition and Ortho Metalation of Triphenylphosphine. *Organometallics* **2004,** *23*, 5630-5632.
(83) Stolzenberg, A. M.; Muetterties, E. L., Rapid, Reversible Ortho Metalation in Chlorohydridotris(Triphenylphosphine)Ruthenium(III) and its Role in the Catalytic Hydrogenation of Alkynes. *Organometallics* **1985,** *4*, 1739-1742.
(84) Crabtree, R. H., Deactivation in Homogeneous Transition Metal Catalysis: Causes, Avoidance, and Cure. *Chem. Rev.* **2015,** *115*, 127-150.
(85) Hong, S. H.; Wenzel, A. G.; Salguero, T. T.; Day, M. W.; Grubbs, R. H., Decomposition of Ruthenium Olefin Metathesis Catalysts. *J. Am. Chem. Soc.* **2007,** *129*, 7961-7968.
(86) Sanford, M. S.; Love, J. A.; Grubbs, R. H., A Versatile Precursor for the Synthesis of New Ruthenium Olefin Metathesis Catalysts. *Organometallics* **2001,** *20*, 5314-5318.
(87) Lummiss, J. A. M.; Higman, C. S.; Fyson, D. L.; McDonald, R.; Fogg, D. E., The Divergent Effects of Strong NHC Donation in Catalysis. *Chem. Sci.* **2015,** *6*, 6739-6746.
(88) Rodriguez, J., The Bonding of Acetate, Methoxy, Thiomethoxy and Pyridine to Cu Surfaces: a Molecular Orbital Study. *Surf. Sci.* **1992,** *273*, 385-404.
(89) Boldt, N. J.; Goodwill, K. E.; Bocian, D. F., Comparison of Back-Bonding in Osmium(II) Versus Iron(II) Octaethylporphyrins via Resonance Raman Spectroscopy. *Inorg. Chem.* **1988,** *27*, 1188-1191.
(90) Kim, D.; Su, Y. O.; Spiro, T. G., Back-Bonding in Ruthenium Porphyrins as Monitored by Resonance Raman Spectroscopy. *Inorg. Chem.* **1986,** *25*, 3993-3997.
(91) House, D. A.; Browning, J.; Zipper, L.; Marty, W., Anionopentaaminecobalt(III) Complexes with Polyamine Ligands: Part 30. The Base Hydrolysis Kinetics and Structure Determination of some [CoCl(N)$_5$]$^{2+}$ Complexes Containing Pyridine Ligands. *Inorg. Chim. Acta* **1999,** *288*, 181-188.
(92) Fielder, S. S.; Osborne, M. C.; Lever, A. B. P.; Pietro, W. J., First-Principles Interpretation of Ligand Electrochemical (EL(L)) Parameters. Factorization of the .sigma. and .pi. Donor and .pi. Acceptor Capabilities of Ligands. *J. Am. Chem. Soc.* **1995,** *117*, 6990-6993.
(93) Kadono, K.; Hori, H.; Fukuda, K.; Inoue, H.; Shirai, T.; Fluck, E., Spectroscopic Characterization of Iron Complexes of Methyl Pheophorbide With Pyridine and its Derivatives. *Inorg. Chim. Acta* **1992,** *201*, 213-218.
(94) Nascimento, D. L.; Gawin, A.; Gawin, R.; Guńka, P. A.; Zachara, J.; Skowerski, K.; Fogg, D. E., Integrating Activity with Accessibility in Olefin Metathesis: An Unprecedentedly Reactive Ruthenium-Indenylidene Catalyst Bearing a Cyclic Alkyl Amino Carbene. *J. Am. Chem. Soc.* **2019,** *141*, 10626–10631.
(95) Gawin, R.; Kozakiewicz, A.; Guńka, P. A.; Dąbrowski, P.; Skowerski, K., Bis(Cyclic Alkyl Amino Carbene) Ruthenium Complexes: A Versatile, Highly Efficient Tool for Olefin Metathesis. *Angew. Chem., Int. Ed.* **2017,** *56*, 981–986.
(96) Anderson, D. R.; Lavallo, V.; O'Leary, D. J.; Bertrand, G.; Grubbs, R. H., Synthesis and Reactivity of Olefin Metathesis Catalysts Bearing Cyclic (Alkyl)(Amino)Carbenes. *Angew. Chem., Int. Ed.* **2007,** *46*, 7262-7265.
(97) Marx, V. M.; Sullivan, A. H.; Melaimi, M.; Virgil, S. C.; Keitz, B. K.; Weinberger, D. S.; Bertrand, G.; Grubbs, R. H., Cyclic Alkyl Amino Carbene (CAAC) Ruthenium Complexes as Remarkably Active Catalysts for Ethenolysis. *Angew. Chem., Int. Ed.* **2015,** *54*, 1919–1923.

References on page 60

(98) Zhang, J.; Song, S.; Wang, X.; Jiao, J.; Shi, M., Ruthenium-Catalyzed Olefin Metathesis Accelerated by the Steric Effect of the Backbone Substituent in Cyclic (Alkyl)(Amino) Carbenes. *Chem. Commun.* **2013,** *49*, 9491–9493.
(99) Butilkov, D.; Frenklah, A.; Rozenberg, I.; Kozuch, S.; Lemcoff, N. G., Highly Selective Olefin Metathesis with CAAC-Containing Ruthenium Benzylidenes. *ACS Catal.* **2017,** *7*, 7634–7637.
(100) Nascimento, D. L.; Fogg, D. E., Origin of the Breakthrough Productivity of Ruthenium-CAAC Catalysts in Olefin Metathesis (CAAC = Cyclic Alkyl Amino Carbene). *J. Am. Chem. Soc.* **2019,** *141*, 19236–19240.
(101) Bailey, G. A.; Foscato, M.; Higman, C. S.; Day, C. S.; Jensen, V. R.; Fogg, D. E., Bimolecular Coupling as a Vector for Decomposition of Fast-Initiating Olefin Metathesis Catalysts. *J. Am. Chem. Soc.* **2018,** *140*, 6931–6944.
(102) Occhipinti, G.; Hansen, F. R.; Törnroos, K. W.; Jensen, V. R., Simple and Highly Z-selective Ruthenium-Based Olefin Metathesis Catalyst. *J. Am. Chem. Soc.* **2013,** *135*, 3331-3334.
(103) Khan, R. K. M.; Torker, S.; Hoveyda, A. H., Readily Accessible and Easily Modifiable Ru-Based Catalysts for Efficient and Z-Selective Ring-Opening Metathesis Polymerization and Ring-Opening/Cross-Metathesis. *J. Am. Chem. Soc.* **2013,** *135*, 10258-10261.
(104) Coalter, I. I. I. J. N.; Bollinger, J. C.; Eisenstein, O.; Caulton, K. G., R-Group Reversal of Isomer Stability for $RuH(X)L_2(CCHR)$ vs. $Ru(X)L_2(CCH_2R)$: Access to Four-Coordinate Ruthenium Carbenes and Carbynes. *New J. Chem.* **2000,** *24*, 925-927.
(105) Sanford, M. S.; Henling, L. M.; Day, M. W.; Grubbs, R. H., Ruthenium-Based Four-Coordinate Olefin Metathesis Catalysts. *Angew. Chem., Int. Ed.* **2000,** *39*, 3451-3453.
(106) Binder, J. B.; Guzei, I. A.; Raines, R. T., Salicylaldimine Ruthenium Alkylidene Complexes: Metathesis Catalysts Tuned for Protic Solvents. *Adv. Synth. Catal.* **2007,** *349*, 395-404.
(107) Van Veldhuizen, J. J.; Garber, S. B.; Kingsbury, J. S.; Hoveyda, A. H., A Recyclable Chiral Ru Catalyst for Enantioselective Olefin Metathesis. Efficient Catalytic Asymmetric Ring-Opening/Cross Metathesis in Air. *J. Am. Chem. Soc.* **2002,** *124*, 4954-4955.
(108) Opstal, T.; Couchez, K.; Verpoort, F., Easily Accessible Ring Opening Metathesis and Atom Transfer Radical Polymerization Catalysts based on Arene, Norbornadiene and Cyclooctadiene Ruthenium Complexes Bearing Schiff Base Ligands. *Adv. Synth. Catal.* **2003,** *345*, 393-401.
(109) Occhipinti, G.; Jensen, V. R.; Bjørsvik, H.-R., Green and Efficient Synthesis of Bidentate Schiff Base Ru Catalysts for Olefin Metathesis. *J. Org. Chem.* **2007,** *72*, 3561-3564.
(110) Danopoulos, A. A.; Wilkinson, G.; Sweet, T.; Hursthouse, M. B., Synthesis and X-ray Crystal Structure of Chloro Tris(Tert-Butylimido)Manganese. *J. Chem. Soc., Chem. Commun.* **1993**, 495-496.
(111) Danopoulos, A. A.; Wilkinson, G.; Sweet, T. K. N.; Hursthouse, M. B., Non-Oxo Chemistry of Manganese in High Oxidation States. Part 1. Mononuclear Tert-Butylimido Compounds of Manganese-(VII) and -(VI). *J. Chem. Soc., Dalton Trans.* **1994**, 1037-1049.
(112) Danopoulos, A. A.; Wilkinson, G.; Sweet, T. K. N.; Hursthouse, M. B., A New Type of Iminophosphine Ligand from Interaction of $Li_2M(NBu^t)_4$, M = W, Mo and PX_3, X = Cl, Br. Crystal Structures of $W(NBu^t)Br_2[P_2(NBu^t)_3]$ and $W(NBu^t)Cl(SC_6F_5)[P_2(NBut)_3]$. *Polyhedron* **1994,** *13*, 2899-2905.

References on page 60

(113) Kessler, J. A.; Iluc, V. M., Ag(I) and Tl(I) Precursors as Transfer Agents of a Pyrrole-Based Pincer Ligand to Late Transition Metals. *Inorg. Chem.* **2014,** *53*, 12360-12371.
(114) Lee, D.-H.; Hwang, Y.-J.; 윤진산; Choi, M.-K.; 이익모, Novel and Efficient Palladium Complexes with β-Ketoiminate Ligands for the Polymerization of Norbornene. *Bull. Korean Chem. Soc.* **2009,** *30*, 636-646.
(115) Wiencko, H. L.; Kogut, E.; Warren, T. H., Neutral β-Diketiminato Nickel(II) Monoalkyl Complexes. *Inorg. Chim. Acta* **2003,** *345*, 199-208.
(116) Arsenov, M. A.; Kharitonov, V. B.; Sovdagarova, E. R.; Smol'yakov, A. F.; Loginov, D. A., (Indenyl)Rhodacarboranes. Electronic Versus Steric Effects on the Conformation of Cyclic Ligands. *J. Organomet. Chem.* **2018,** *865*, 45-50.
(117) Rödl, C.; Wolf, R., Cobalt(I) and Nickel(II) Complexes of Bis(1,3-diphosphacyclobutadiene) Sandwich Anions. *Eur. J. Inorg. Chem.* **2016,** *2016*, 736-742.
(118) Tice, N. C.; Snyder, C. A.; Preston, A. Z.; Wieliczko, M. B.; Young, J. O. E.; Hinson, D. F., Synthesis and Structure of Some Group VII 1,2-Diacyl Cyclopentadiene Complexes and Their Pyridazine Derivatives. *Transition Met. Chem.* **2012,** *37*, 141-147.
(119) Albéniz, A. C.; Espinet, P.; Pérez-Mateo, A., Palladium(II) Allylic Complexes by Carbene Transmetalation and Migratory Insertion Reactions: Synthesis and Side Reactions. *J. Org. Chem.* **2010,** *695*, 441-445.
(120) Vicente, J.; Gil-Rubio, J.; Guerrero-Leal, J.; Bautista, D., Synthesis of Rhodium(I) and Rhodium(III) Perfluoroalkyl Complexes from $[Rh(\mu\text{-}OH)(COD)]_2$. *Dalton Trans.* **2009**, 3854-3866.
(121) DeMott, J. C.; Basuli, F.; Kilgore, U. J.; Foxman, B. M.; Huffman, J. C.; Ozerov, O. V.; Mindiola, D. J., Silver(I) and Thallium(I) Complexes of a PNP Ligand and Their Utility as PNP Transfer Reagents. *Inorg. Chem.* **2007,** *46*, 6271-6276.
(122) Fernandes, A. C.; Romão, C. C.; Royo, B., Novel Carbohydrate-Substituted Cyclopentadienyls of Titanium, Molybdenum, Manganese and Iron. *J. Organomet. Chem.* **2003,** *682*, 14-19.
(123) Zanella, P.; Mascellani, N.; Cason, A.; Garon, S.; Rossetto, G.; Carta, G., Synthesis and Characterization of Bis(indenyl) zirconium Aryloxide Derivatives and Their use in α-Olefin Polymerization. *Appl. Organomet. Chem.* **2001,** *15*, 717-724.
(124) Baron, M.; Dall'Anese, A.; Miolato, A.; Cairoli, M. L. C.; Di Marco, V.; Graiff, C.; Pöthig, A.; Tubaro, C., New Homoleptic Gold Carbene Complexes via Ag–Au Transmetalation: Synthesis and Application of $[Au(diNHC)_2]^{3+}$ Cations as 1H-NMR and UV-vis Halide Sensors. *New J. Chem.* **2020,** *44*, 5343-5353.
(125) Gould, E. S., *Mechanism and Structure in Organic Chemistry*. Holt, Rhinehart, and Winston: New York, 1959.
(126) Wilkins, R. G., The Study of Kinetics and Mechanism of Reactions of Transition Metal Complexes. Allyn & Bacon: Boston, MA, 1974.
(127) Negishi, E.-i., Magical Power of Transition Metals: Past, Present, and Future (Nobel Lecture). *Angew. Chem., Int. Ed.* **2011,** *50*, 6738-6764.
(128) Jana, R.; Pathak, T. P.; Sigman, M. S., Advances in transition metal (Pd,Ni,Fe)-catalyzed cross-coupling reactions using alkyl-organometallics as reaction partners. *Chem. Rev.* **2011,** *111*, 1417-1492.
(129) Nicolaou, K. C.; Bulger, P. G.; Sarlah, D., Palladium-Catalyzed Cross-Coupling Reactions in Total Synthesis. *Angew. Chem., Int. Ed.* **2005,** *44*, 4442-4489.

References on page 60

(130) Lévesque, É.; Goudreau, S. R.; Charette, A. B., Improved Zinc-Catalyzed Simmons–Smith Reaction: Access to Various 1,2,3-Trisubstituted Cyclopropanes. *Org. Lett.* **2014,** *16*, 1490-1493.
(131) Asako, S.; Nakajima, H.; Takai, K., Organosodium Compounds for Catalytic Cross-Coupling. *Nature Catal.* **2019,** *2*, 297-303.
(132) Sanford, M. S.; Love, J. A.; Grubbs, R. H., Mechanism and Activity of Ruthenium Olefin Metathesis Catalysts. *J. Am. Chem. Soc.* **2001,** *123*, 6543-6554.

References on page 60

Chapter 4. Toward Low-Valent Ruthenium Alkylidenes

4.1 Introduction

4.1.1 Setting the Stage: What is a "Low-Valent" Ruthenium Alkylidene?

The oxidation state of Ru metathesis catalysts is a controversial subject in the literature, owing to debate as to how the alkylidene moiety contributes to the oxidation state.[1-8] If the alkylidene is considered a neutral "L-donor" ligand (like Fischer carbenes), then the metathesis precatalysts are Ru(II). They are then oxidized to Ru(IV) upon cycloaddition of incoming olefin to form the metallacyclobutane intermediate. If instead the alkylidene is considered a dianionic ligand (like Schrock carbenes in group 6 metathesis catalysts), then both the precatalyst and MCB intermediate are Ru(IV), and the oxidation state is unchanged throughout the catalytic cycle.

The Ru(II)/Ru(IV) debate is beyond the scope of this thesis, and we will not weigh in on the contribution of the alkylidene moiety to the oxidation state. Whether the precatalyst is considered Ru(II) or Ru(IV), omitting the 2 anionic ligands present on all known neutral precatalysts will reduce the oxidation state by 2. Thus, in the present context, a "low-valent ruthenium alkylidene" is defined as a ruthenium centre 2 oxidation states lower than the well-known metathesis catalysts of type $RuX_2L_2(=CHR)$.

4.1.2 Motivation: Why are Low-Valent Alkylidenes Desirable?

Major advances in catalyst productivity have been achieved by increasing electron density on ruthenium by moving to more strongly donating stabilizing ligands; first with the switch from phosphines to NHC (marking the dawn of the "second-generation" catalysts),[9] and more recently with the introduction of CAAC ligands.[10] This has been a highly successful strategy; increasing electron density on ruthenium has increased substrate scope relative to the earliest catalysts (which were active only in ROMP of strained cyclic olefins) and vastly improved turnover numbers achievable in metathesis, allowing for the use of reduced catalyst loading.[9, 11-15] Spurred by the success of the NHC catalysts, catalyst development has been driven by the search for ever more strongly-donating stabilizing ligands which remain compatible with metathesis catalysts. Enhanced electron density at Ru is believed to increase olefin affinity and promote the cycloaddition step in metathesis by increasing the degree of backbonding into the olefin π^* antibonding orbitals.[16-19]

An alternative approach to increasing electron density on Ru that does not appear to have been widely investigated is reducing the oxidation state of the catalyst. Omitting the 2 anionic ligands present in all known neutral catalysts would decrease the oxidation state by 2 and formally increase electron density on ruthenium by 2 electrons. Such low-valent alkylidenes could potentially be the most electron-rich Ru metathesis catalysts to date.

Current "high-valent" Ru alkylidenes are "mildly to moderately" electrophilic[7] and therefore susceptible to attack by nucleophiles.[20-26] Indeed, nucleophilic abstraction of alkylidene by phosphine has been established as a major decomposition pathway for Grubbs-type catalysts,[25, 27] and helps account for the declining use of phosphines as labile ligands in Ru-catalyzed olefin metathesis. The sole published example of a low-valent Ru alkylidene, by contrast, reacts primarily

References on page 92

as a nucleophile at carbon, although this low-valent (and therefore nucleophilic) character is not maintained on exposure to olefin, owing to an oxidatively non-innocent nitrosyl ligand (vide infra).[28] A low-valent Ru alkylidene that remains low-valent (i.e. without oxidatively non-innocent ligands) is therefore expected to maintain its nucleophilic character. This would be a boon both in terms of improving catalyst lifetimes in the presence of nucleophilic contaminants, and in allowing the very well-developed toolbox of highly-tailored phosphine ligands to be once again deployed in Ru catalysts for olefin metathesis.

Moving to low-valent systems may also help address the issue of bimolecular coupling (BMC). BMC of the methylidene intermediate has recently been established as one of the major inherent decomposition pathways for Ru metathesis catalysts,[29] and is especially relevant to the ground-breaking CAAC catalysts, which have recently been shown to decompose almost exclusively by BMC.[30] Natural bond orbital (NBO) analysis of proposed BMC intermediate species has suggested that the interaction leading to coupling is enhanced by polarization of the Ru=C π-orbital towards Ru and resultant polarization of the corresponding Ru=C π*-antibonding orbital towards carbon. A lower-valent methylidene Ru=C is expected to be significantly less polarized towards Ru. In fact, reports of a nucleophilic low-valent Ru methylidene suggest that the Ru=C π-orbital may be polarized in the opposite direction, towards carbon. This has the potential to disrupt the orbital overlap that in high-valent methylidene species enables BMC.

4.1.3 Background: Precedent for Low-Valent Ru Alkylidenes

Current Ru metathesis catalysts are, compared to their early metal predecessors, already examples of "low-valent" alkylidenes. Group 6 metathesis catalysts, the state of the art before the advent of Ru metathesis catalysts, tend to be in the highest possible oxidation state,[31] while all known Ru metathesis catalysts are at most in the +4 oxidation state, far below the maximum oxidation state of +8.[32] Given that ruthenium catalysts have already shown that high oxidation states are not a requirement for high metathesis performance, it is not unreasonable to pursue even lower states.

Alluded to above is the sole example of a formally low-valent Ru alkylidene, the Roper compound **Ru-61** (Scheme 4.1), bearing an anionic chloride and cationic linear nitrosyl ligand.[28] This species was isolated in excellent yield (88%) by reaction of the 16-electron, coordinatively unsaturated $RuCl(NO)(PPh_3)_2$ with diazomethane. In contrast to high-valent Ru alkylidenes which exhibit electrophilic character, **Ru-61** reacts primarily as a nucleophile at carbon. However, when treated with olefin (ethylene or C_2F_4) or diphenylacetylene, formation of methylphosphonium ylide by nucleophilic attack of phosphine is observed. This switching of carbene reactivity from nucleophilic to electrophilic was attributed to the oxidative non-innocence of the nitrosyl ligand. The nitrosyl ligand was proposed to produce electronic unsaturation at Ru by switching from the linear 3-electron donor configuration to the bent one-electron donor configuration, enabling coordination of olefin. Additionally, back-donation from Ru to olefin is believed to further diminish the nucleophilic character and increase electrophilic character at methylidene.

References on page 92

Scheme 4.1: Oxidative non-innocence of NO ligand allows nucleophilic attack on methylidene.

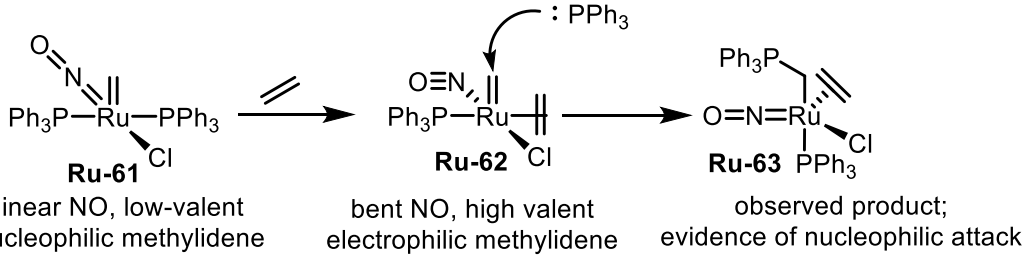

Thus although the methylidene species in the absence of olefin is low-valent, when exposed to olefin it shares the same oxidation state and electrophilic character at methylidene as conventional metathesis catalysts. To evaluate the feasibility of low-valent metathesis catalysts, oxidatively non-innocent ligands must therefore be avoided.

Two approaches to low-valent Ru alkylidenes are examined in this thesis: reduction of known high-valent metathesis catalysts, and removal of an α-proton from a Ru(II) alkyl species..

4.1.4 α-Hydride Elimination From Ru(II) Alkyl Species

Although common in early metal systems, the method of α-elimination to form alkylidenes developed by Schrock[31] is rare in ruthenium chemistry. There are as yet no reports in the literature of this approach being used to generate metathesis-active Ru species, although examples have been reported of the unintended, sterically-induced transformation of alkylidene species into alkyidynes.[33-34] Adapting the Schrock methodology to Ru(II) systems could plausibly yield low-valent Ru alkylidenes

4.1.5 α-Elimination: Early Transition Metals vs. Ruthenium

In complexes of the early transition metals, the alkylidene functionality is commonly generated via α-elimination from an alkyl ligand, as immortalized by Schrock's famous synthesis of a tantalum neopentylidene in 1974.[35] The approach is simple: 2 alkyl ligands (substituted at the β position to prevent β-hydride elimination) installed cis to one another and subjected to steric pressure will eliminate an alkane, generating the alkylidene. This method is general for the early transition metals, and examples have been reported for W, Zr, Mo, Nb, Ta, Ti, V, Cr, and Re.[31] However, setting up similar conditions on ruthenium does not produce alkylidenes, but rather leads to cyclometallation of the alkyl ligands. (Scheme 4.2). Installing a benzyl ligand on ruthenium leads to *o*-metalation,[36-37] and neopentyl ligands undergo γ-elimination to form a metallacyclobutane [38-39] ω-Elimination of a terminal proton to form metallacycles seems to be general for late metal systems[40] —indeed, a study by Whitesides found that late metals exhibit a preference for ω-elimination from alkyl ligands up to 5 carbons long.[41] The divergent elimination behaviour of early- vs. late-metal systems does not appear to have been commented on in the literature.

References on page 92

Scheme 4.2: Cyclometalation of benzyl and neopentyl ligands on ruthenium.

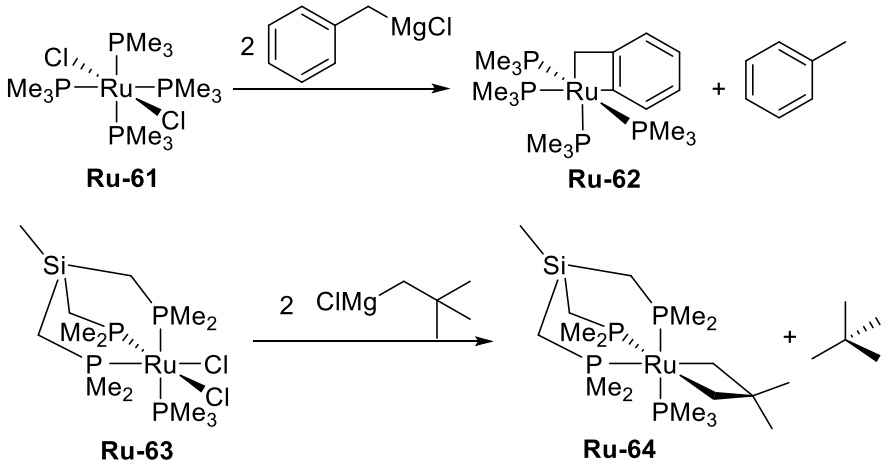

When ω-elimination is suppressed by chelation, fixing all protons more distant than the α-position away from the metal centre, α-elimination to form alkylidenes on ruthenium can proceed. Three such examples leading to high-valent alkylidenes are known in the literature (**Figure 4.1**).

In example **A**, reported by Gusev in 2006, the pincer ligand on **Ru-65** bearing both α and β protons undergoes reversible elimination from both positions, generating an equilibrium mixture of alkylidene **Ru-66** and olefinic **Ru-67** species.[42]

First reported in 2005 by Stradiotto, in example **B**, **Ru-68** bears no β protons and all other potentially available protons are held away by chelation, leading to reversible α-elimination favouring the alkylidene species **Ru-69**.[43] The σ-alkyl species **Ru-68** can be trapped by adding an L-donor.[44]

Example **C** arises from the attempted installation of a methyl group on **Ru-70** by Caulton in 2005**:** rather than expected methyl species **Ru-71**, alkylidene formation is observed via an initial ω-elimination from a *tert*-butyl group on the bulky pincer ligand to produce a coordinatively unsaturated tricyclic **Ru-72** followed by α-elimination to generate alkylidene species **Ru-73**, relieving coordinative unsaturation..[45]

References on page 92

Figure 4.1: Known examples of α-elimination to form alkylidenes on ruthenium.

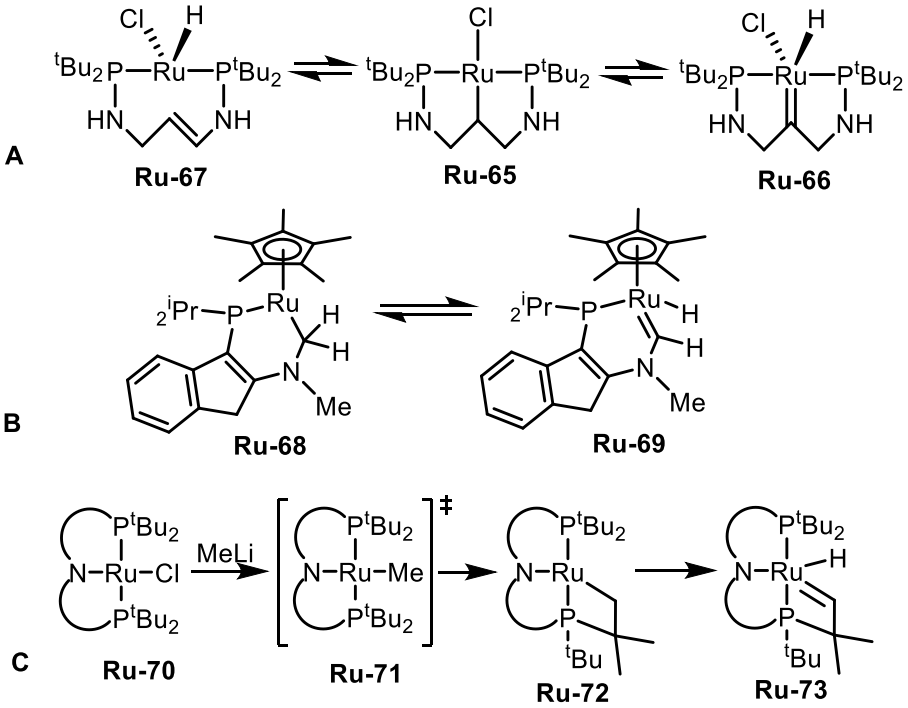

The alkylidenes produced by routes **A-C** are high-valent, and ill-suited as metathesis catalysts, but demonstrate that alkylidene formation via α-elimination on ruthenium is possible, and, combined with the above examples of cyclometallation from benzyl and neopentyl ligands, provide clear design criteria for promoting the desired α-elimination chemistry:

1. The alkyl ligand must not bear β-hydrogens
2. The alkyl ligand must either lack more distant hydrogens, or must hold them away from the metal centre by chelation

4.1.6 First Synthetic Target: A Stable Benzylruthenium Complex.

The first step towards low-valent alkylidenes by α-elimination or deprotonation is the synthesis of a Ru(II) alkyl complex. A benzylruthenium complex was chosen as a specific target, as this ligand class bears no β-protons (necessary to avoid decomposition by β-hydride elimination), and are readily installed on transition metals by salt metathesis of a metal chloride with a benzyl Grignard (Scheme 4.3). As an additional advantage, benzyl Grignards are among the easiest organomagnesium species to synthesize, a clear advantage over neopentyl Grignards, which, while also lacking β-protons, are notoriously difficult to make.[46]

References on page 92

Scheme 4.3: Installation of the benzyl ligand by salt metathesis with benzyl Grignard.

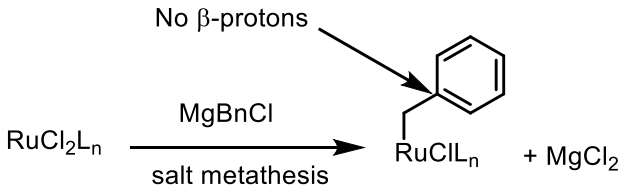

Benzylruthenium complexes are rare in the literature, likely owing to the vulnerability of the benzyl ligand to *o*-metalation.[28] **Ru-74**, the sole literature example of an isolable benzylruthenium with an unfunctionalized benzyl ligand, was reportedly isolated in 20% yield by treating parent benzylidene complex **Ru-75** with $NaBH_4$ (Scheme 4.4).[47] The low yield, the highly robust cyclopentadienyl ligand that would have to be removed, and the fact that one must first synthesize a benzylidene complex by use of phenyldiazomethane, make this an unappealing means of installing a benzyl ligand for the purpose of accessing low-valent alkylidenes.

Scheme 4.4: Synthesis of benzylruthenium complex **Ru-74** by reduction/protonation of **Ru-75**.

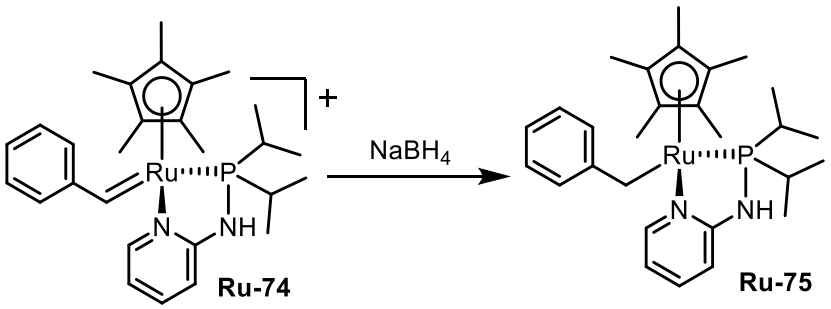

Typically, if cyclometallation is to be avoided, a chelating group must be present, as in **Ru-76**, where the benzyl ligand is stabilized against *o*-metalation by a chelating P(*i*Pr)$_2$ substituent. Complex **Ru-76** was reportedly isolated in 36% yield by treating **Ru-77** with NaOAc in methanol (Scheme 4.5).[48]

Scheme 4.5: Synthesis of benzylruthenium complex **Ru-76** by deprotonation of modified phosphine ligand P(*i*Pr)$_2$(*o*-Tol).

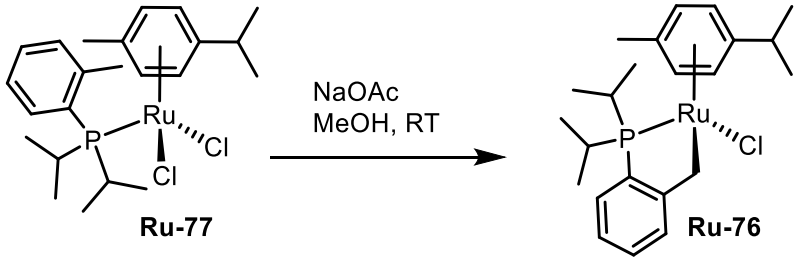

References on page 92

4.2 Results and Discussion

4.2.1 Reduction of High-Valent Metathesis Catalysts

The second-generation Hoveyda catalyst was treated with a variety of reducing agents (Na, $NaBH_4$, $KBH(s\text{-}Bu)_3$, and Mg-anthracene · 3THF) in the presence of pyridine, targeting **Ru-78** (Scheme 4.6). In all cases, decomposition to a spectroscopically ill-defined black mixture was observed. It is likely that the alkylidene functionality is incompatible with strong reducing agents. Consistent with this hypothesis, Valerga and co-workers reported that reaction of **Ru-74** with $NaBH_4$ in methanol proceeds via reduction of the benzylidene moiety (Scheme 4.4, vide supra).[47] In the literature reaction, **Ru-75** could be isolated in low yield (20%). However, the corresponding reduced-alkylidene species for **HII** was not observed in the present work, likely due to subsequent decomposition.

Scheme 4.6: Attempted reduction of the second-generation Hoveyda catalyst by various reducing agents. Pyridine added to occupy open coordination sites that would be generated by successful reduction of chloride ligands.

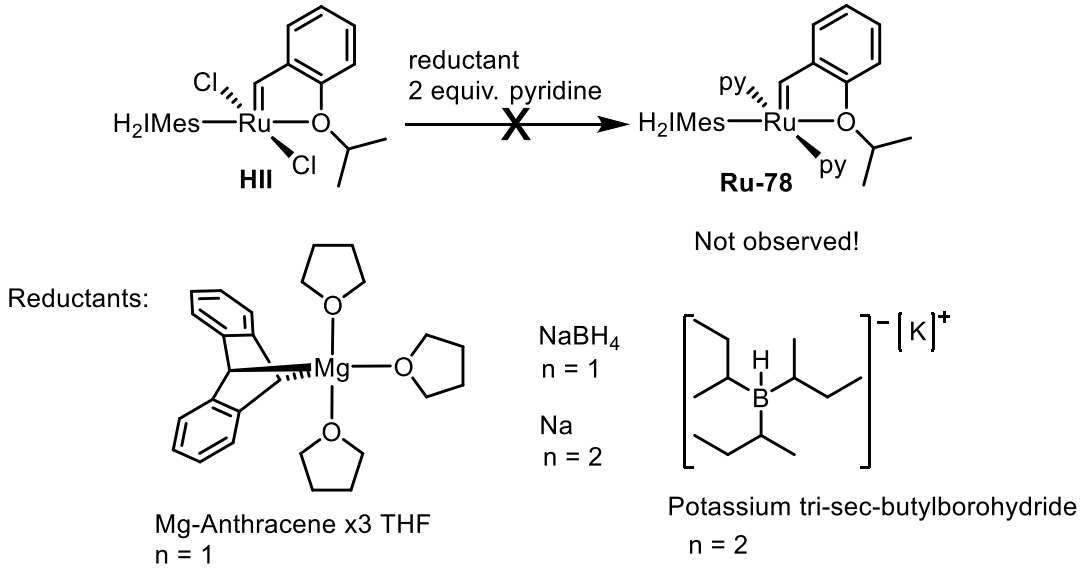

4.2.2 Benzyl Ligand Redesign and Synthesis

To prevent *o*-metalation, a chelating *o*-isopropoxybenzyl ligand was targeted. In this structure, one vulnerable *o*-hydrogen is removed entirely, while the other is held away from the metal centre by chelation. The *o*-O^{i}Pr group was chosen as the chelating group by analogy to the *o*-O^{i}Pr functionality in the Hoveyda-class catalysts. This group is already known to stabilize ruthenium effectively without introducing unwanted side-reactions, and is also known to dissociate relatively readily to allow metathesis[49]—this second point is why the diisopropylphosphine motif seen in **Ru-76** was eschewed; the superior binding ability of phosphine is expected to severely retard initiation relative to the more labile ether functionality.

o-Isopropoxybenzyl chloride was converted to the corresponding Grignard reagent (**Mg-3**) by dropwise addition to magnesium turnings in THF (Scheme 4.7), as confirmed by ^{1}H NMR and

References on page 92

colorimetric analysis. Grignard reactions can be slow to initiate, but in this case an exotherm occurred immediately on adding the benzyl halide. Benzyl halides are known to magnesiate readily,[50] and the ease with which this *o*-isopropoxybenzyl chloride initiates may be due to stabilization by intramolecular chelation.

Scheme 4.7: Synthesis of **Mg-3** and simplified representation of the Schlenk equilibrium (solvent and chloride-bridged species omitted).

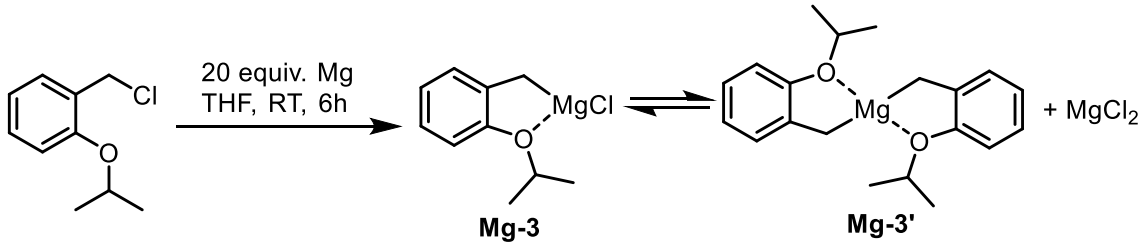

^{1}H NMR analysis of **Mg-3** in C_6D_6 showed complete loss of the signals for the benzyl halide precursor, confirming complete conversion. Two new sets of signals were present in a 1:4 ratio, both having the same number of peaks and multiplicity as the parent benzyl halide, as is consistent with **Mg-3**. The signal doubling is presumed to arise from the Schlenk equilibrium, well established for organomagnesium halides.[51] Whether the **Mg-3** or **Mg-3'** side of the equilibrium is favoured was not examined.

Prior to use, it was necessary to determine the purity and concentration of the Grignard reagent. Non-Grignard bases (e.g. $Mg(OH)_2$) can arise from contaminants in the solvent or the alkyl halide, or atmospheric contamination. Any such base would be highly deleterious in the present work, given the risk of competing salt metathesis. **Mg-3** was titrated against dry isopropanol in THF, with 1,10-phenanthroline as indicator. This method is sensitive *only* to the Mg-C bond, and does not report on the total amount of base present in solution.[52] A second titration was therefore performed to measure total base content. Accordingly, an aliquot of **Mg-3** was deliberately hydrolyzed with excess methanol, and titrated against a standardized solution of HCl using phenolphthalein as indicator. As the Mg-C and total base titrations agreed within 1%, confirming the absence of non-Grignard base, the solution of **Mg-3** was deemed suitable for use.

4.2.3 The Search for a Suitable Ruthenium Substrate: Failed Candidates

Initial attempts to install the *o*-O^{i}Pr modified benzyl ligand on ruthenium were frustrated by ancillary ligand incompatibilities. Reaction with $RuCl_2(PPh_3)$ (**Ru-20**) (Scheme 4.8), a classic and easily accessible ruthenium precursor, did not produce the expected benzylation product **Ru-79**. Instead, a black, spectroscopically ill-defined mixture was observed. *o*-Metalation of the PPh_3 ligand may account for the observed decomposition, which would suggest a fundamental incompatibility between the PPh_3 and benzyl ligands. The septet at 4.2 ppm expected for the liberated *o*-isopropoxytoluene was not detected in the ^{1}H NMR spectrum, however, calling this mechanism into question.

Scheme 4.8: Reaction of **Ru-20** with **Mg-3** did not yield spectroscopically observable products. Reaction attempted in THF, Et_2O, C_6H_6, and hexanes.

References on page 92

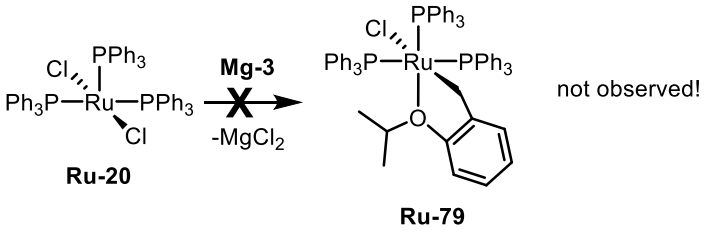

Reaction of **Mg-3** with $RuCl_2(\kappa^2$-1,10-phenanthroline)$(PPh_3)_2$ (**Ru-80**) (Scheme 4.9) proceeded more smoothly than with **Ru-20**, inasmuch as it did not lead to immediate decomposition. Instead slow conversion of poorly soluble brown **Ru-80** to a highly soluble purple mixture was observed. In this case, the poor solubility and slow reactivity of **Ru-80** prevented stoichiometric control, so 2 equiv **Mg-3** were used. Although **Ru-80** is more soluble in benzene than THF, the reaction was found to proceed more quickly in THF, reaching a visual endpoint (complete solubilization of the mixture) in 6 h at RT in THF, but requiring 24 h in benzene. The ^{1}H NMR spectrum of this mixture is difficult to interpret, with many overlapping signals in the aromatic and alkyl regions. The absence of a signal in the alkylidene region rules out successful α-elimination. ^{31}P NMR analysis indicates the presence of multiple minor species and a single major species (accounting for about 56% of total integration) characterized by 2 doublets of equal intensity at 32.2 and -11.8 ppm, indicating loss of symmetry of the phosphorus ligands. The mixture is thermally stable; heating to 75 °C for 8 h did not change the product distribution. The upfield signal suggests *o*-metalation of one PPh_3 ligand,[53] while the relatively small P-P coupling constant (10 Hz) is indicative of mutually cis phosphines. Together, this implies formation of either **Ru-81** or **Ru-82**, depending on whether one or 2 equiv **Mg-3** react. **Ru-81** seems most likely, as it is difficult to rationalize addition of a second equivalent of **Mg-3** without triggering cyclometallation of the second PPh_3. A multiplet at 4.15, a singlet at 2.22, and a doublet at 1.06 ppm in the ^{1}H NMR spectrum are a close match for the spectrum of **Mg-3** (obtained above), which further suggests mono-addition. In either case, this reaction confirmed the incompatibility of PPh_3 and benzyl ligands on ruthenium, and directed our attention toward phosphine-free ruthenium substrates.

Scheme 4.9: Proposed major product of reaction between **Ru-80** and **Mg-3** based on available spectroscopic data.

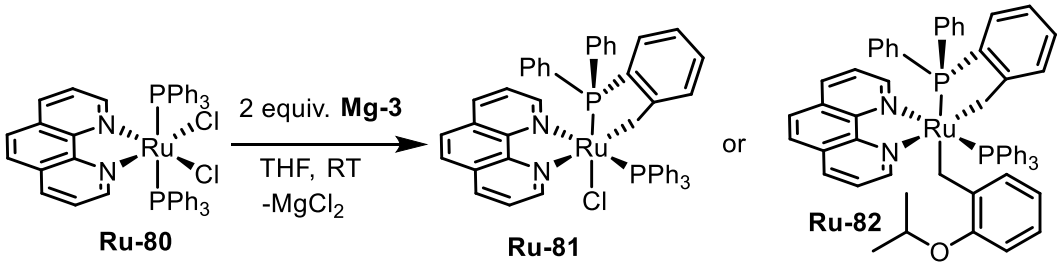

Despite the common lability of pyridine ligands, $RuCl_2(py)_4$ (**Ru-51**) is known from previous experience in the Fogg group to be surprisingly resistant to ligand substitution reactions. It was hoped, however, that salt metathesis would proceed (Scheme 4.10). Unfortunately, **Ru-51** was completely inert to **Mg-3**. No reaction was evident after stirring for 48 h in either THF or benzene at RT or reflux: no colour change or solubilization of **Ru-51** was observed, and the persistence of

Mg-3 was confirmed by addition of 1,10-phenanthroline as a colorimetric indicator. Poor solubility cannot alone account for the lack of reactivity, as **Mg-3** reacts readily even with a suspension of **Ru-20** in hexanes (in which **Ru-20** is insoluble). The complete inactivity of **Ru-51** suggests that the required salt metathesis with **Mg-3** is dissociative in pyridine, as expected if it were to proceed via 6-coordinate transition state **TS-2**. The non-lability of pyridine in **Ru-51** therefore precludes salt metathesis. Successful installation of a benzyl ligand on ruthenium will require a substrate which either has or can readily produce an open coordination site.

Scheme 4.10: Proposed dissociative (in pyridine) mechanism for salt metathesis. Non-lability of pyridine prevents access to transition state **TS-2**. **Ru-83** never observed.

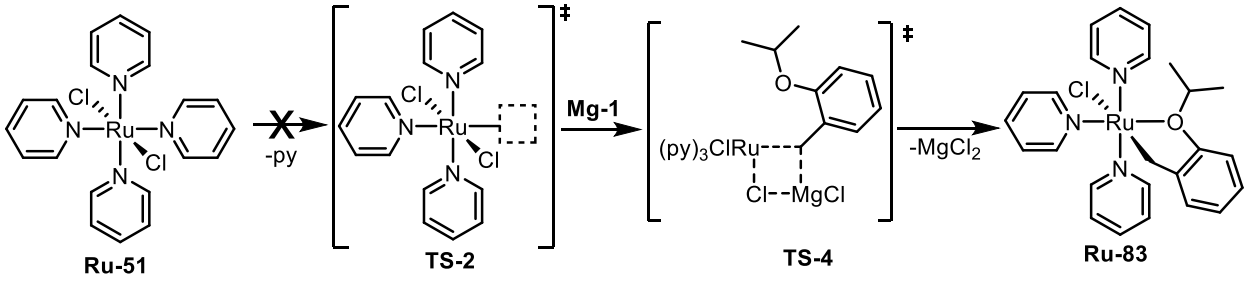

4.2.4 Successful Installation of Modified Benzyl Ligand on $[RuCl_2(p\text{-cymene})]_2$. Synthesis, Isolation, and Characterization of RuCl(*o*-isopropoxybenzyl)(*p*-cymene)

In contrast to the difficulties outlined above, **Mg-3** reacts rapidly and cleanly with dimeric $[RuCl_2(p\text{-cymene})]_2$ (**Ru-35**) to afford the novel benzylruthenium species **Ru-84** (Scheme 4.11), as confirmed by ^{1}H NMR analysis. The reaction proceeds readily at RT by adding a solution of **Mg-3** in THF to **Ru-35** in THF, CH_2Cl_2, or C_6H_6. CH_2Cl_2 is the preferred solvent, however, as **Ru-35** is only sparingly soluble in THF or C_6H_6. The reaction can be worked up immediately after completing the addition of **Mg-3**. As the $MgCl_2$ coproduct is fairly soluble in the CH_2Cl_2-THF solvent mixture, it was removed by switching solvent systems to C_6H_6 before filtering through Celite. **Ru-84** can then be isolated as a microcrystalline red solid in 72-82% yield by reprecipitation from CH_2Cl_2. **Ru-84** itself is effectively insoluble in hexanes. However, the bis-benzylruthenium species (**Ru-85**, vide infra), formed in small amounts if the Grignard reagent is present in slight stoichiometric excess or added too rapidly, is highly soluble in hexanes, so washings are frequently orange to orange-red.

References on page 92

Scheme 4.11: High-yield synthesis of **Ru-84**.

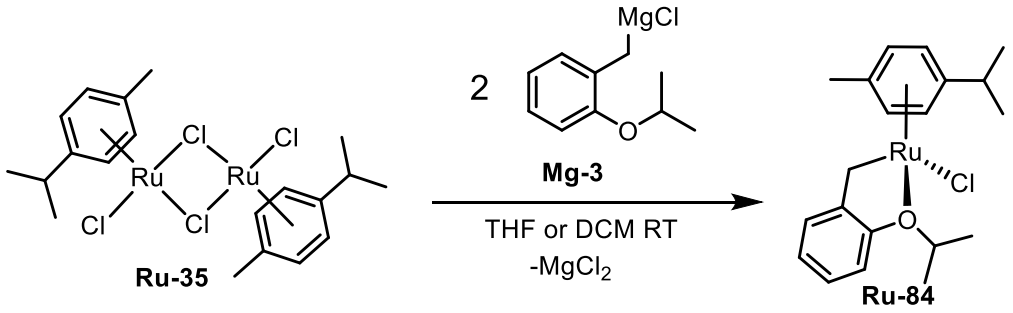

The dark red benzylruthenium complex **Ru-84** is readily soluble in CH_2Cl_2 and THF, moderately soluble in C_6H_6 and effectively insoluble in hexanes. The complex is stable in solution and shows no thermal degradation by ^1H NMR analysis after 72 h at 60 °C in C_6D_6.

Structure assignment is confirmed by ^1H, ^{13}C, ^1H-^1H COSY, and ^1H-^{13}C HMBC NMR experiments. Several unusual spectral features warrant comment. The signals corresponding to the benzylic protons, which would be expected as two closely spaced or overlapping doublets, appear as singlets with a ca. 2 ppm difference in chemical shift (4.92 and 2.83 ppm). The signals for the *p*-cymene aryl protons, which in an η^6-aryl-ruthenium complex of C1 symmetry are typically observed as four doublets, likewise lack fine structure and appear as broad singlets at 4.56, 4.18, 3.65, and 3.17 ppm. Taken together, this suggests that the geometry of the benzyl chelate forces one benzyl proton into the deshielding region generated by the π-aryl system of the *p*-cymene ligand, accounting for the unusually deshielded benzylic signal at 4.92 ppm. This could also cause steric interaction with the *p*-cymene substituents. Rotation of the *p*-cymene ligand on the NMR timescale would explain the absence of splitting in the signals for both the benzyl and the *p*-cymene aryl protons. This is confirmed by adding pyridine to cause dechelation of the benzyl ligand. The *p*-cymene aryl protons resolve from broad singlets to doublets as expected, and the 2 benzyl protons converge to an AB pair of doublets ($\Delta\nu/J = 3$) centred at a chemical shift of 3.5 ppm. That the benzyl protons remain magnetically inequivalent even after dechelation suggests restricted rotation for the benzyl ligand, not unreasonable given the sterically congested nature of the pyridine adduct.

Also notable is the unusually upfield shift of two aromatic proton signals for the benzyl group, at 5.5 and 5.7 ppm, while the remaining benzyl aromatic protons appear in the typical aryl region (6.8 ppm). This is reminiscent of the upfield shift observed for ortho-protons in η^3-coordinated benzyl ligands, and the η^3 binding mode would also account for the large difference in chemical shift between the benzylic protons.[54] However, the benzyl ligand **Ru-84** bears only one *o*-proton, and therefore the unusual shielding observed for *2* Ar-H signals cannot be accounted for by η^3 coordination. Chelation may enforce η^1-binding of the benzyl ligand in **Ru-84**. The η^3-isomers **Ru-84a** and **Ru-84b** require either dechelation or high ring strain combined with unusually high electron count and coordination number (Scheme 4.12). Outer sphere chloride isomers were not considered, as **Ru-84** is fairly soluble in C_6H_6.

References on page 92

Scheme 4.12: Possible binding modes of the *o*-O^{i}Pr benzyl ligand in **Ru-84**.

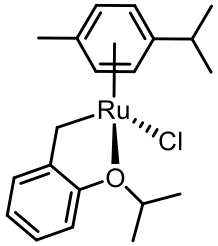

Ru-84
η^1-Benzyl
5-membered chelate, low strain
18-Electron, 6-coordinate

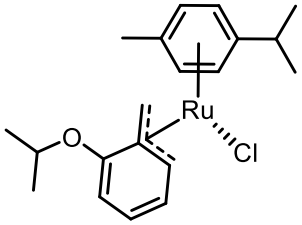

Ru-84a
η^3-Benzyl
No chelation
18-Electron, 6-coordinate

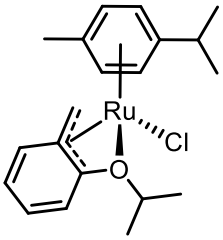

Ru-84b
η^3-Benzyl
3-membered chelate, high strain
20-Electron, 8-coordinate

The chemical shift, peak width, and resolution are all noticeably solvent-dependent. The signals which appear broad in C_6D_6 are noticeably sharper in $CDCl_3$, with the p-cymene Ar-*H* appear as doublets as expected. The two unusually upfield benzyl Ar-*H* signals remain abnormal, with one signal now appearing closer to the normal aromatic region at 6.22 ppm, and the other even further upfield than in C_6D_6 at 4.90 ppm.

4.2.5 Installation of Second Equivalent of Modified Benzyl Ligand

Treating **Ru-84** with a second equivalent of *o*-isopropoxybenzyl Grignard proceeds smoothly to afford a bright orange solution. The ^{1}H NMR spectrum is consistent with the expected bis-benzyl species **Ru-85** (Scheme 4.13) based on observed 2:3 integration ratio between a multiplet at 4.57 ppm (assigned as 2x OC*H*Me$_2$) and a singlet at 2 ppm (assigned as Ar-C*H*$_3$), as well as temperature-dependant spectral features detailed below. A yield has yet to be determined, as isolation was frustrated by the high solubility of the product in hexanes. However, this facilitates separation from the $MgCl_2$ by-product, by simply removing solvent, resuspending the residue in hexanes and filtering through Celite.

Scheme 4.13: Addition of a second equivalent of *o*-O^{i}Pr benzyl ligand to **Ru-84**.

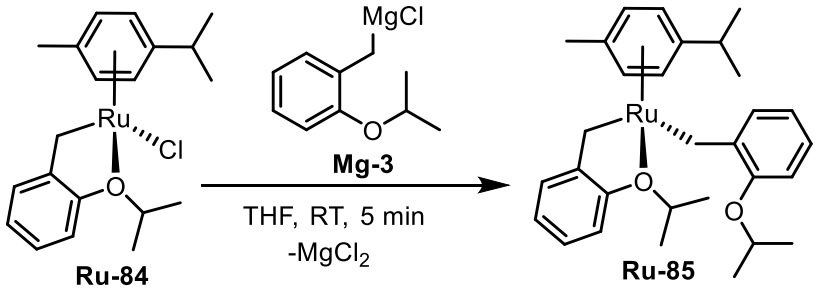

Ru-84 **Ru-85**

The room-temperature ^{1}H NMR spectrum of this complex is ill-defined. The expected well-defined peaks for the upfield aryl protons of the benzyl ligands at ~6.5 ppm and of the *p*-cymene group at ~3-5ppm were not observed. Instead, very broad signals are seen that are difficult to distinguish from the baseline. The non-aromatic *p*-cymene signals, by contrast, appear well-defined. A septet at 2.43 ppm (C*H*Me$_2$), a singlet at 2.00 ppm (Ar-C*H*$_3$), and doublet at 1.26 ppm (CH(C*H*$_3$)$_2$) are

References on page 92

all present in the expected 1:3:6 integration ratio. In a typical region for a chelating ArOC*H*Me$_2$ signal on ruthenium (4.5ppm),[49, 55-63] there is an ill-defined multiplet, which integrates to 2 protons relative to the well-defined *p*-cymene Ar-C*H*$_3$ singlet (3 H), consistent with the presence of 2 equiv *o*-O^{i}Pr benzyl ligand. Also consistent with bis-addition of the chelating benzyl ligand, a doublet at 1.46 ppm integrates to 12 protons (2x OCH(C*H*$_3$)$_2$). When the sample is cooled to -40 °C, the extremely broad signals at ~6.5 and ~3.8ppm resolve to well defined signals, and the poorly resolved multiplet at 4.5ppm now appears as 2 overlapping septets. These observations are consistent with successful synthesis of **Ru-85**, with the temperature-dependent spectral features best explained by competition for chelation between the 2 isopropoxybenzyl ligands on NMR timescale at RT (Scheme 4.14). On cooling there is no longer sufficient thermal flux to allow dechelation and rechelation of the O^{i}Pr groups and the associated signals become well-resolved.

Scheme 4.14: Fluxional exchange between two chelating benzyl groups at room temperature.

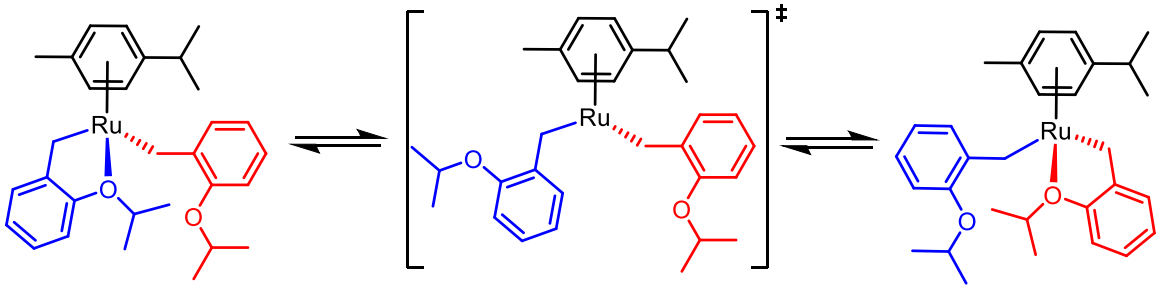

As additional evidence for successful addition of a second *o*-isopropoxybenzyl ligand, protonolysis of **Ru-85** with 1 equiv pentafluorophenoxide liberates *o*-isopropoxytoluene and **Ru-86** (Scheme 4.23, vide infra).

4.2.6 Attempts to Induce α-Elimination from Bis-Benzylruthenium Species

Although the bis-benzylruthenium species was not successfully isolated, α-elimination from in situ-generated **Ru-85** was attempted, on the assumption that the alkylidene product, having eliminated one benzyl ligand, would be less soluble in hexanes and easier to isolate. Thus, **Ru-85** was treated with neutral donor ligands in an attempt to induce α-hydride elimination by increasing steric pressure (Scheme 4.15). Arylphosphine ligands were avoided in light of the risk of cyclometallation described above.

Scheme 4.15: Attempted sterically-induced α-hydride abstraction from **Ru-85**.

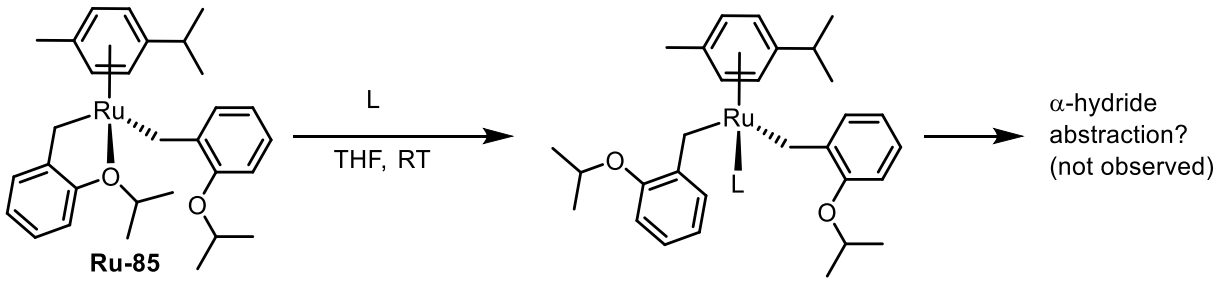

References on page 92

Ru-85 was unreactive to pyridine, even in large excess (20 equiv). Pyridine does not compete well for coordination with the chelating O^{i}Pr functionality in the parent mono-benzyl species **Ru-84**, so it is not entirely surprising that it has difficulty coordinating when it must also compete with a second equivalent of chelating benzyl ligand.

When much more strongly donating and sterically demanding NHC ligands, i.e. IMes or H_2IMes, were added (in the presence of 3 equiv pyridine, added to stabilize potential coordinative unsaturation that would arise from displacement of *p*-cymene), the solution darkened from light yellow-orange to dark brown over 6 h. ^{1}H NMR analysis showed complete disappearance of the free carbene, but overlaying the spectrum of this reaction mixture with that of **Ru-85** showed that **Ru-85** remained, and no new septets (diagnostic for the *o*-O^{i}Pr benzyl and *p*-cymene ligands) were detectable, indicating a lack of reaction with **Ru-85**. Steric pressure may prevent coordination of NHC, leading eventually to decomposition of the free carbene in solution.

1,10-Phenanthroline rapidly forms an intensely coloured green solution when added to **Ru-85** in THF. However, the product(s) decomposes to a spectroscopically ill-defined black mixture in the time it takes to prepare an NMR sample. Thus, although **Ru-85** appears primed for α-hydride abstraction, efforts thus far have led to decomposition or no reaction at all.

4.2.7 Attempted Deprotonation of Modified Benzyl Ligand

The extreme deshielding of the benzyl proton at 4.9 ppm for **Ru-84** suggests potential for deprotonation by base (Scheme 4.16). In principle, deprotonation should produce an anionic low-valent alkylidene **Ru-87** which, if the reaction is carried out in a non-polar solvent such as benzene, should precipitate, allowing easy isolation. Addition of a donor ligand should then allow elimination of chloride along with cationic counterion, giving the neutral Ru alkylidene **Ru-88**.

Scheme 4.16: Attempted synthesis of **Ru-88** by deprotonation of **Ru-84**.

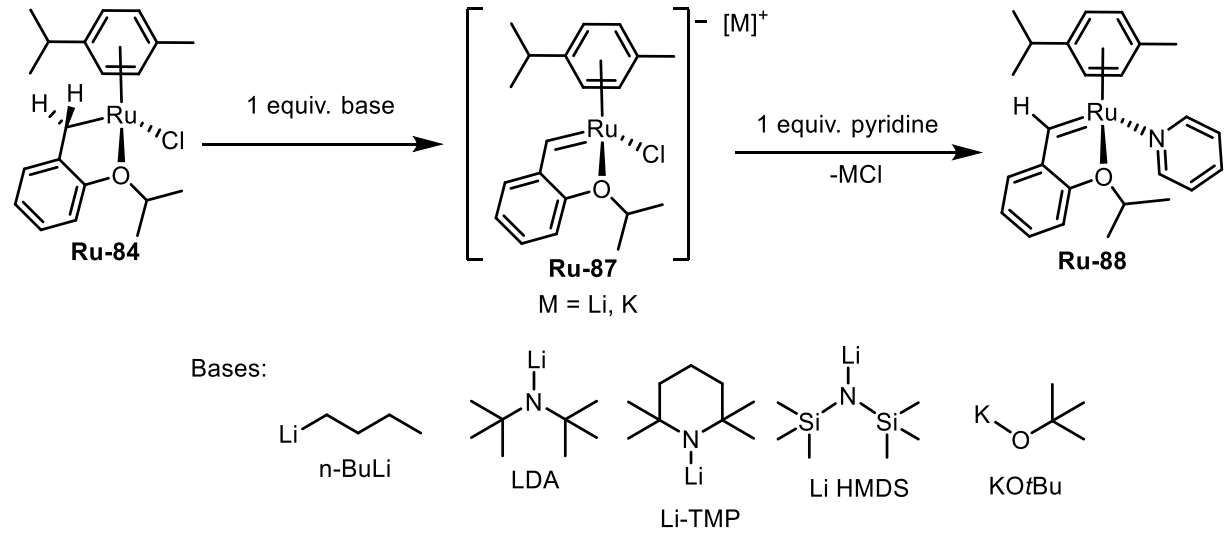

A variety of strong bases was deployed in this reaction; n-BuLi, LiHMDS, LiTMP, LDA, and KOtBu. In all cases, when **Ru-84** was treated with 1 equiv base in benzene at RT, an intractable black mixture formed. The rate of reaction varied with the benzene-solubility of the base, but in

References on page 92

no case was anything other than a spectroscopically ill-defined black mixture observed. The reaction with n-BuLi was carried out at -78 °C in THF, but the result was the same.

It is possible that the target anionic alkylidene **Ru-87** is too unstable to be observed, and that it forms but rapidly eliminates XCl (X = Li, K), subsequently decomposing due to coordinative unsaturation (Scheme 4.17). With this in mind, the deprotonation reaction was repeated in the presence of pyridine, with the hope that pyridine could trap out the low-coordinate alkylidene. The ^{1}H NMR spectrum of the crude reaction mixture again showed multiple species, with no signals in the alkylidene region, or for the stilbene (**C-3**) that could arise from BMC of the alkylidene were it to be generated.

Scheme 4.17: Proposed decomposition of **Ru-87** by elimination of MCl and subsequent decomposition of coordinatively unsaturated **Ru-89**.

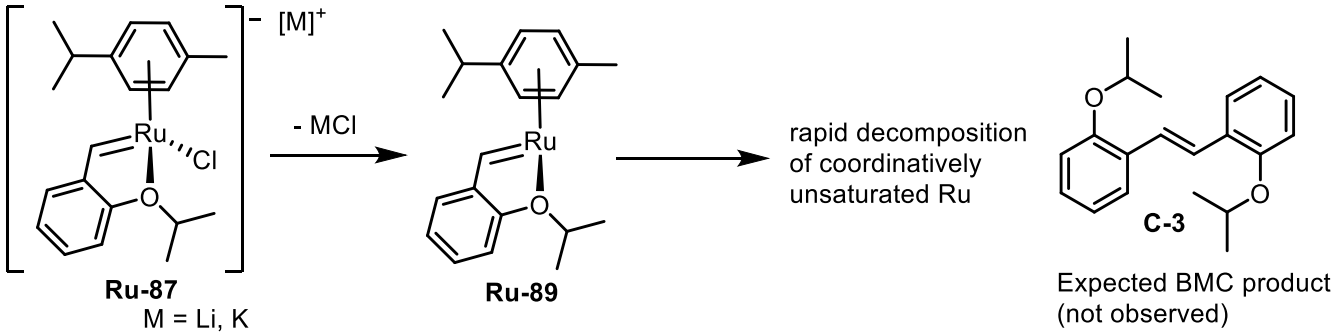

An additional issue with deprotonation by base is competing salt metathesis of the chloride ligand. 2-Pyridylithium was investigated as a potential solution (Scheme 4.18). If deprotonation occurs, concomitant-generation of pyridine could stabilize the alkylidene by displacing chloride to generate a neutral species. If salt metathesis occurs, the resultant 2-pyridyl ligand may itself abstract an α-proton from the neighbouring benzyl ligand.

References on page 92

Scheme 4.18: Rationale for the use of 2-pyridyllithium. Deprotonation or salt metathesis can both reasonably lead to **Ru-88**.

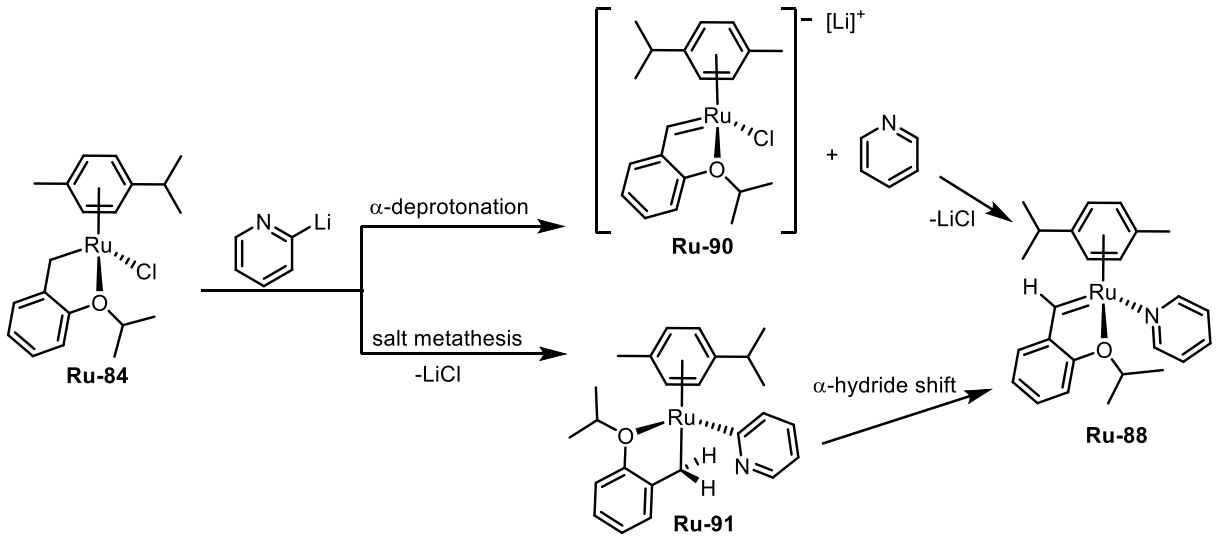

Unfortunately, as with the other bases examined, when **Ru-84** was treated with 2-pyridylithium in THF at -78 °C, immediate decomposition to a spectroscopically ill-defined black mixture was observed. Attack on chloride and subsequent decomposition (in this case likely beginning with *o*-hydride elimination from the 2-pyridyl ligand) is consistent with observations, and suggests that if deprotonation at the benzyl position is to be successful, the chloride ligand must either be sterically protected or replaced by another ligand that will be less vulnerable to attack. Replacement of chloride with sterically bulky pseudohalide ligands was investigated to this end.

4.2.8 Second Synthetic Target: Replacement of Chloride with Aryloxide

Aryloxide ligands are anticipated to be less vulnerable to attack by strong bases than chloride: the steric bulk of the aryl group should protect the alkoxide from attack (especially by bulkier bases such as LDA or NaHMDS), and the elimination of XOAr (X = alkali metal) is far less favourable than XCl. As noted above, prior work from the Fogg and Caulton groups demonstrated that aryloxide ligands can abstract the α-proton from an adjacent alkylidene ligand where steric pressure permits, eliminating the phenol and generating an alkylidyne.[33, 64] If H-abstraction from an alkyl ligand can be induced likewise, to give an alkylidene functionality, this obviates the need for base. Aryloxides in particular promote this intramolecular α-elimination; *tert*-butoxide ligands do not,[65] presumably for steric reasons.

Salt metathesis of the chloride ligand on **Ru-84** was undertaken using magnesium aryloxides, prepared in situ by deprotonation of the parent phenol by isopropylmagnesium chloride in THF or benzene. Pentafluoroaryloxide, pentabromoaryloxide, and 2-aminophenoxide were chosen to represent a range of steric and electronic properties. No electron-rich aryloxides were used, nor was simple phenoxide, as previous investigations of ruthenium aryloxides have shown that unless the aryloxide is electron-deficient,[66] or bears an *o*-chelating group,[67] it may rearrange to a piano-stool structure (Figure 4.2).[66]

References on page 92

Figure 4.2: Aryloxide σ to π rearrangement on ruthenium.

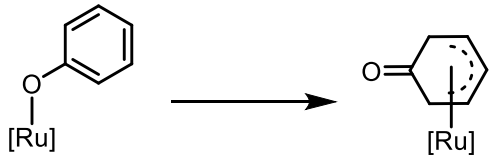

Ru-84 was surprisingly inert to salt metathesis with magnesium aryloxides (Scheme 4.19). When the reactions were carried out at RT in benzene, THF, or CH_2Cl_2, no reaction was observed after 24 h; ^{1}H NMR analysis showed only starting material and solvent. At 60 °C, $MgOC_6F_5$ (**OAr-1**) and $MgOC_6Br_5$ (**OAr-2**) similarly showed no reaction. In contrast, reaction with Mg(*o*-NH_2)OC_6H_4 (**OAr-3**) at 60 °C caused a colour change from red to purple. However, ^{1}H NMR analysis of the crude mixture showed only starting material, suggesting that if salt metathesis does proceed, the product is not thermally stable.

Scheme 4.19: Attempted installation of aryloxides on **Ru-84**. Only starting material observed whether reaction is carried out at room temperature or 60 °C.

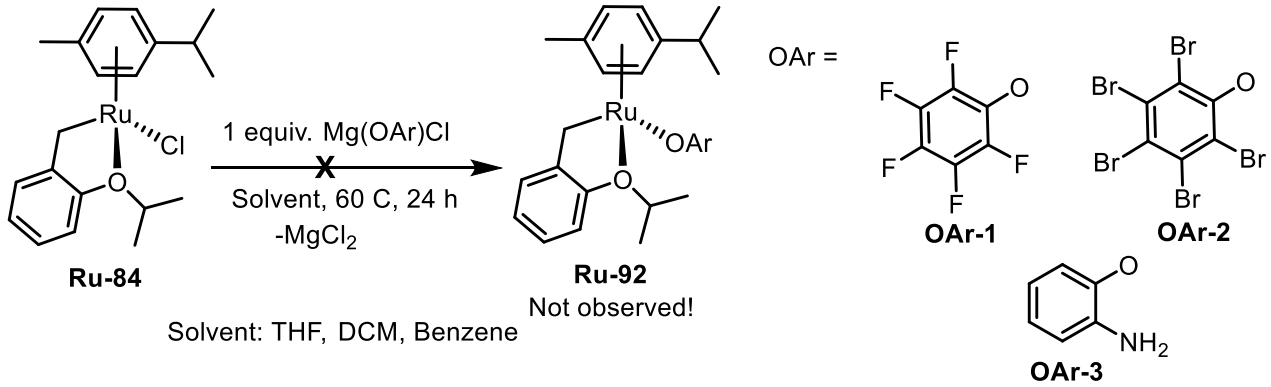

As an alternative route to complexes of type **Ru-92**, reaction with $[RuCl_2(p\text{-cymene})]_2$ was explored, with the idea being to isolate aryloxide dimer **Ru-93** and then benzylate to access **Ru-92** (Scheme 4.20). As with **Ru-84**, $[RuCl_2(p\text{-cymene})]_2$ was completely inert to salt metathesis with magnesium aryloxides at RT, nor could products be detected at 60 °C. Addition of pyridine to help break up the chloride-bridged dimer, in the hope that this would facilitate aryloxide salt metathesis, resulted only in clean conversion to known[68] pyridine adduct $RuCl_2$(py)(*p*-cymene) (**Ru-94**) (Scheme 4.21).

References on page 92

Scheme 4.20: Potential alternative route to **Ru-92**. Unfortunately, **Ru-93** could not be isolated.

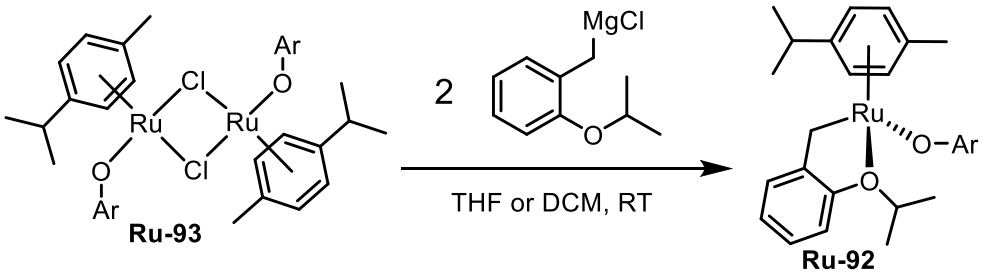

Scheme 4.21: Attempted aryloxide installation leads instead to formation of **Ru-94**.

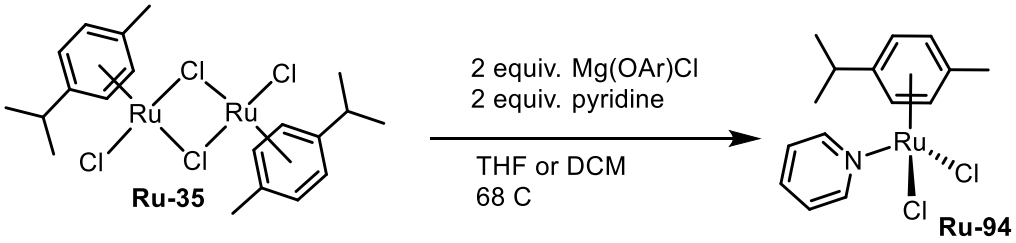

Difficulties in aryloxide installation from group 1 and 2 nucleophiles are not unheard of,[69-72] including in Ru chemistry. In such cases Ag[63, 73] or Tl[67, 74-75] aryloxides are instead deployed. The superior transmetalating ability of these late metal aryloxides has been attributed to the high electrophilicity of Tl^+ and Ag^+ cations, and the reaction has been proposed to initiate by electrophilic attack on chloride.[71] However, in light of the high toxicity of thallium reagents[76] and high photosensitivity of Ag[77], alternative means of aryloxide installation were sought. Zn^{2+} is known as a moderate Lewis acid, and may thus exhibit a similar electrophilic accelerating effect to Ag^+ and Tl^+. Also noteworthy is the excellent pedigree of zinc nucleophiles as transmetalating agents in palladium chemistry, where Negishi states that zinc nucleophiles are the transmetalating agent of choice,[78] and it has elsewhere been stated that cross-couplings in the absence of zinc tend to be "agonizingly lethargic".[79]

When a CH_2Cl_2 solution of **Ru-84** was treated with 0.5 equiv $Zn(OC_6F_5)_2$ (generated in situ by dissolving the parent phenol in CH_2Cl_2 and adding dropwise a 1.0M solution of $ZnEt_2$ in hexanes), a slight colour change from red to orange-red was observed (Scheme 4.22). ^{1}H NMR analysis of the crude reaction mixture showed complete consumption of **Ru-84**, and emergence of a new set of signals consistent with the target **Ru-86**. Specifically, a septet at 3.89 ppm (OC*H*Me_2), two upfield doublets at 5.76 and 5.17 ppm (Ar-*H*), and a broad singlet at 1 ppm, are characteristic of the chelating *o*-O^{i}PrBn ligand, as seen in **Ru-84**. The septet at 2.57 ppm (C*H*Me_2), singlet at 1.95 ppm (Ar-CH_3), and broad doublet at 1.17 ppm (CH(CH_3)$_2$) are typical of η^{-6} *p*-cymene on ruthenium.[80-82] Complete spectral assignment will require ^{1}H-^{1}H COSY experiments, as it is otherwise impossible to distinguish between the 4 *p*-cymene Ar-*H* and 2 benzylic CH_2 signals, each of which appear as broad singlets ranging from ~2-5 ppm and some of which overlap.

References on page 92

Although the electron-deficient OC_6F_5 should make **Ru-86** less electron rich than the parent chloride species (**Ru-84**), the ^{1}H NMR signals for **Ru-86** are not generally more deshielded than those in **Ru-84**. Most signals appear within +/- 0.1 ppm of their counterpart signal in **Ru-84**, with no bias towards shielding/deshielding relative to **Ru-84**. The most shielded of the benzylic Ar-*H* signals, which appears at 5.55 ppm in **Ru-84** has shifted 0.38 ppm upfield to 5.17 ppm in **Ru-86**, the largest change in shift for any signal relative to **Ru-84**. This large change in chemical shift is in contrast to the other unusually shielded Ar-*H* signal, which appears at 5.76 ppm in both **Ru-84** and **Ru-86**. The relatively large increase in shielding observed for the signal at 5.17 ppm and lack of change for the signal at 5.76 ppm may indicate a degree of coplanarity between the benzyl and aryloxide ring systems. Being oriented towards the in-plane shielding region of C_6F_5O would account for the increase in shielding for the signal observed at 5.17 ppm, and coplanarity between the rings would orient the remaining benzylic Ar-*H*s away from the influence of the anisotropic C_6F_5O, accounting for the lack of impact observed for the signal at 5.76 ppm. ^{1}H-^{19}F HOESY will indicate whether the Ar-*H* signal at 5.17 ppm is indeed oriented towards the C_6F_5O ring.

Scheme 4.22: Successful aryloxide installation via transmetalation with zinc pentafluorophenoxide.

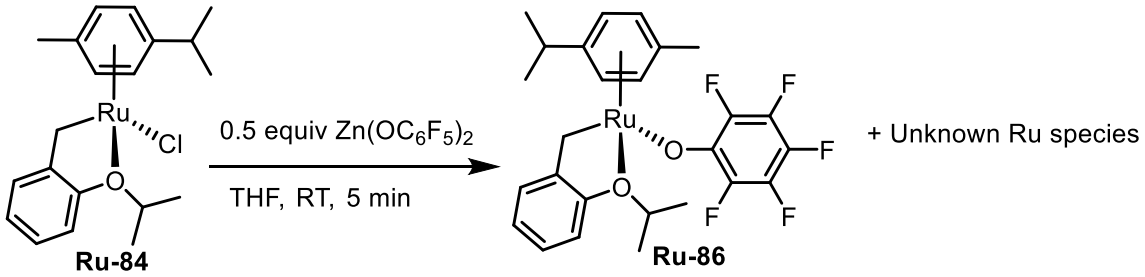

Upon workup it was revealed that two products were present, one insoluble in hexanes and inconsistent with the target species by ^{1}H NMR analysis, and a second major product, soluble in hexanes and consistent with the target species. These were separated by filtration, and the filtrate (mostly hexanes with residual CH_2Cl_2 from the attempted reprecipitation) was left in the glovebox freezer (set at -40 °C) overnight in hopes of precipitating the target species. After 24 h in the freezer, there was no evidence of precipitation and ^{1}H NMR analysis now showed trace amounts of **Ru-84**, which had not been present in the crude reaction mixture. This is presumably the result of slow rechlorination of **Ru-86** in CH_2Cl_2. The difficulty in isolating **Ru-86**, combined with the fact that it is not the sole ruthenium product make it difficult to carry forward to attempt generation of the alkylidene, as it is effectively impossible to gauge stoichiometry.

A solution was found in an alternative approach to aryloxide installation. Adding C_6F_5OH to bis-benzyl complex **Ru-85** (generated in situ) effected deprotonation of the phenol, installing the aryloxide and liberating 1 equiv. *o*-isopropoxytoluene (Scheme 4.23), as judged by comparing the integration of the doublet at 5.76 ppm (1H, Ar-*H*) associated with **Ru-86** to signals associated with *o*-O^{i}PrTol at 6.66 ppm (*d*, 1H, Ar-*H*), 2.27 ppm (*s*, 3H, C*H*$_3$), and 1.11ppm (*d*, 6H, OCH(C*H*$_3$)$_2$. The **Ru-86** product remains highly soluble in hexanes, and did not precipitate from hexanes overnight in the freezer at – 40 °C, but appears to be the sole ruthenium product; other signals present in the ^{1}H NMR spectrum are accounted for by contaminants in the Grignard reagent and

References on page 92

the liberated *o*-isopropoxytoluene, as confirmed by overlaying the spectrum containing **Ru-86** with that of deliberately hydrolyzed **Mg-3**. The ^{1}H NMR spectrum is also in concordance with **Ru-86** generated via the zinc aryloxide route, with the exception of signals at ~1.28 ppm and ~2.44 ppm. When **Ru-86** is prepared via salt metathesis with $Zn(OC_6F_5)_2$, these signals are very broad and ill-defined. In the spectrum for **Ru-86** obtained by deprotonation of C_6F_5OH, the broad signal at ~2.44 ppm appears as a septet centred at 2.47 ppm and the signal at ~1.28 ppm resolves to a broad doublet at 1.22 ppm. The difference in appearance of these peaks is likely due to differences in the solvent system between routes. The spectrum of **Ru-86** produced by deprotonation of C_6F_5OH also contains one equiv *o*-isopropoxytoluene, which can act as a coordinating solvent. Given the apparent lack of Ru side-products, **Ru-86** generated via deprotonation of C_6F_5OH by **Ru-85** was carried forward to attempt alkylidene installation.

Scheme 4.23: Alternative route to **Ru-86** via **Ru-85**.

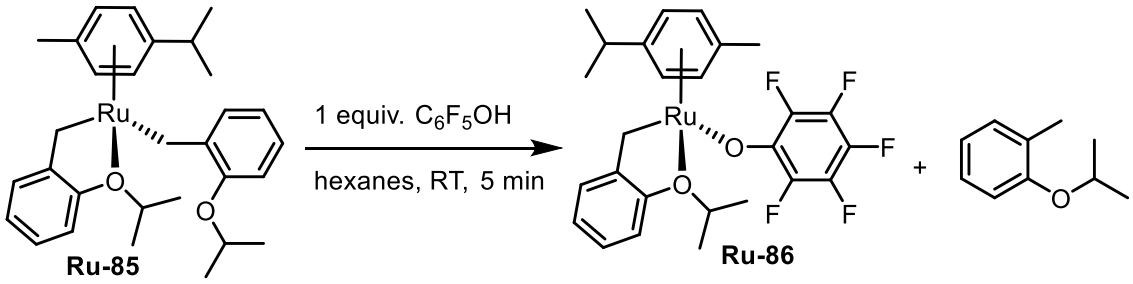

4.2.9 Attempted Deprotonation of Aryloxide-Benzylruthenium

An in situ generated solution of **Ru-86** in benzene was treated with one equiv LiHMDS, targeting **Ru-88** (Scheme 4.24). In contrast to the corresponding reaction with the parent chloride species **Ru-84**, which under the same conditions decomposed rapidly to an intractable black mixture, no colour change occurred over 24 h. ^{1}H NMR spectrum of the crude reaction mixture at this point revealed mostly starting material signals with significant loss of resolution and some new broad signals present in the alkyl region. It seems that replacing chloride with pentafluorophenoxide was successful in supressing undesired salt-metathesis, but the desired α-deprotonation of the benzyl ligand remains elusive. It is possible that LiHMDS is too sterically bulky to access the benzyl protons, in which case a less bulky base such as MeLi or n-BuLi may be successful.

Scheme 4.24: Attempted deprotonation of **Ru-86**.

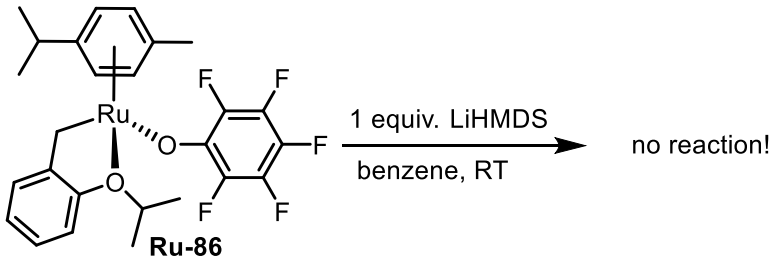

References on page 92

4.2.10 Intramolecular α-Hydride Abstraction by Pentafluorophenoxide: Apparent Success

Adding an equivalent of pyridine to a hexanes solution of **Ru-86** prepared in situ resulted in no colour change after 8 h (Scheme 4.25). However, ^{1}H NMR analysis of the crude reaction mixture revealed a new species, no sign of free pyridine, and a very broad signal ($\omega_{0.5}$= 58.6Hz) in the alkylidene region (14.2 ppm), suggesting successful generation of the target benzylidene species **Ru-88**. The alkylidene signal is highly shielded relative to high-valent Hoveyda-type alkylidenes (for which the [Ru]=C*H*Ar signal is found in the 16-18 ppm range),[49, 56] but is near the chemical shift of the only known low-valent ruthenium methylidene, the Roper complex **Ru-58** (13.3 ppm).[28] The solubility of the product in hexanes poses challenges for isolation but suggests opportunities for carrying out metathesis in non-traditional solvents in which known high-valent catalysts are insoluble.

Scheme 4.25: Synthesis of putative product **Ru-88**. Difficulty in the isolation of intermediates **Ru-85** and **Ru-86** mean that they are most conveniently generated in situ and carried forward.

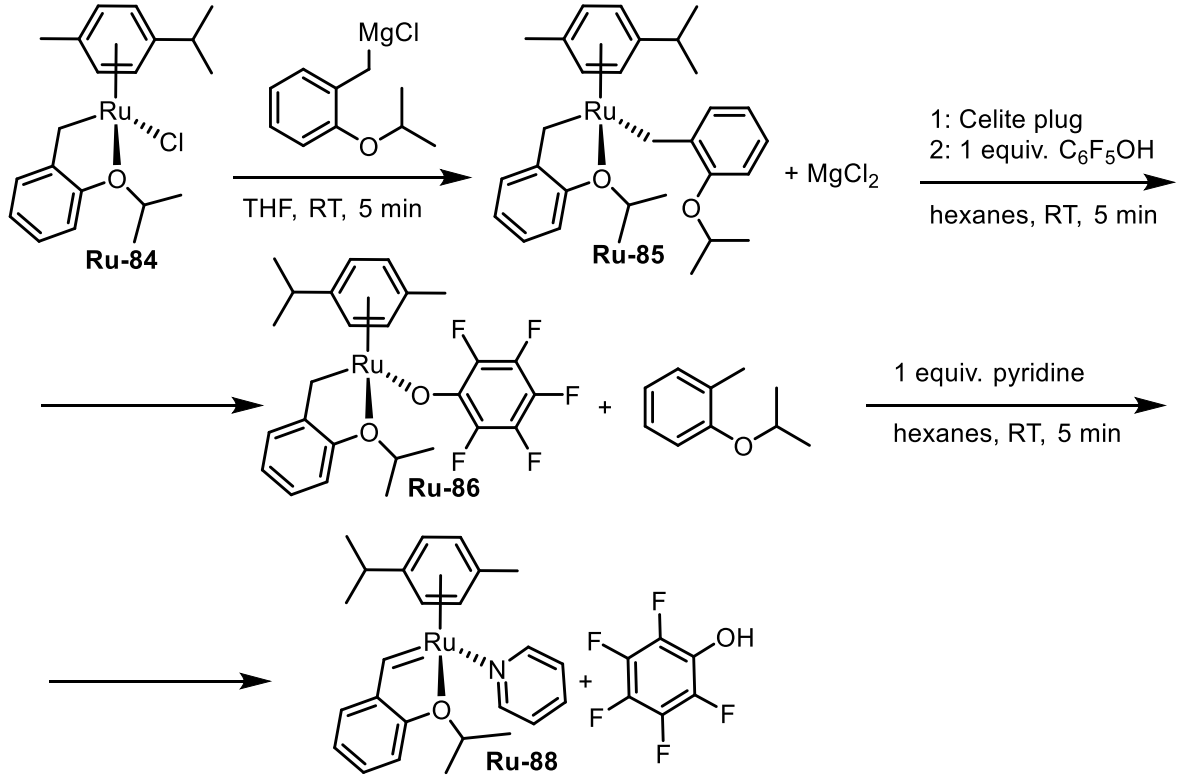

Pyridine could effect proton abstraction (Scheme 4.26) via an associative pathway, by which coordination of pyridine causes dechelation of the benzyl ligand, permitting it to adopt a conformation suitable for α-elimination. Alternatively, a dissociative mechanism could be operative, in which α-hydride elimination from **Ru-86** is spontaneous and reversible, with pyridine acting only to trap out the benzylidene species. The inertness of **Ru-86** towards LiHMDS is evidence against the dissociative mechanism. If C_6F_5OH were being spontaneously eliminated, it should be rapidly deprotonated by LiHMDS, leaving behind coordinatively unsaturated **Ru-89**.

References on page 92

Scheme 4.26: Plausible mechanisms for alkylidene formation from **Ru-86**.

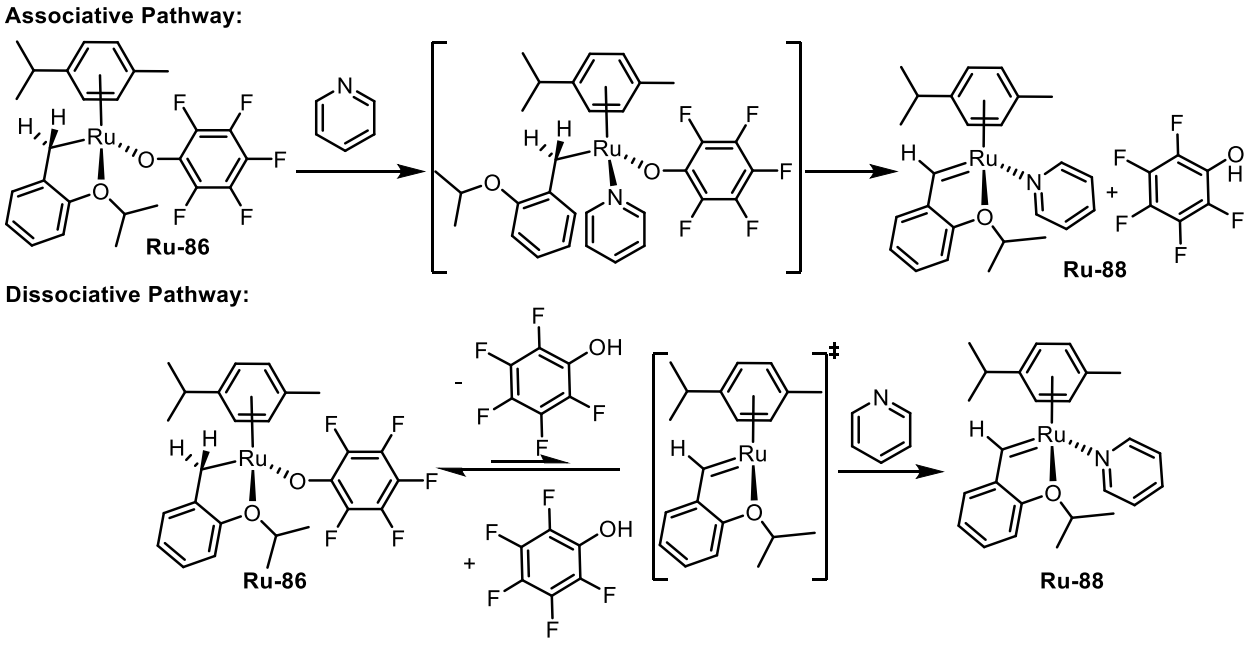

The breadth of the benzylidene signal in the crude reaction mixture is surprising, as alkylidene signals are typically sharp and well-resolved. If liberation of C_6F_5OH is reversible (e.g. via nucleophilic attack on C_6F_5OH by benzylidene, regenerating the benzyl and pentafluorophenoxide ligands (Scheme 4.27)), this could account for the broadness of the alkylidene signal, but in that case all signals should be broadened. Instead, many are well defined, with clearly visible fine structure, particularly the O^{i}Pr and *p*-cymene Ar^{i}Pr methine septets.

Scheme 4.27: Reversible alkylidene formation could account for the broadness of the alkylidene signal.

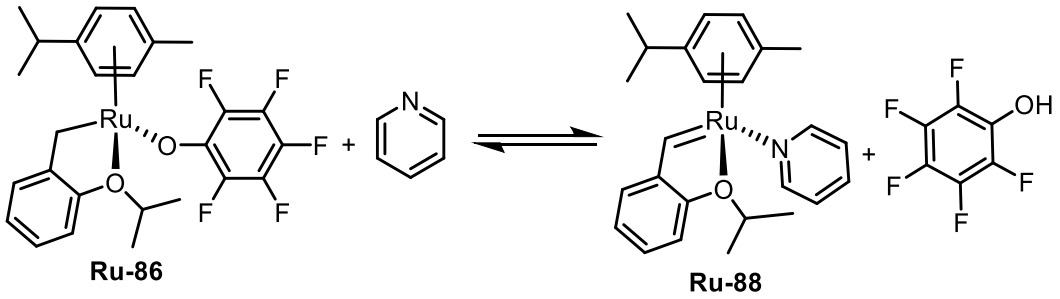

If the benzylidene proton is in communication with the *p*-cymene aryl system, rotation of *p*-cymene could also account for the broadness of the benzylidene signal, similar to the effect observed on the benzylic protons in the parent species, **Ru-84**. However, one would then expect to see broadened signals for the *p*-cymene protons, indicative of rotation on the NMR timescale. While the signals associated with the *p*-cymene aryl protons are indeed broadened, as in parent complexes **Ru-86** and **Ru-84**, 2 sets of well-defined *p*-cymene signals are seen for the *p*-cymene

References on page 92

C*H*$_3$ and methine C*H* signals, which suggests restricted rotation giving rise to 2 rotamers rather than rapid rotation to account for signal broadening.

A third possibility is an exchange process between the benzylidene and phenolic protons (Scheme 4.28). This would account for the broadness of the benzylidene signal without implying other spectroscopic features which cannot be accounted for. Nucleophilicity of the benzylidene carbon, rather than acidity of the benzylidene proton, is suspected to be the driving force for proton exchange, as the low-valent alkylidene is expected to be highly electron rich, and therefore not particularly acidic. This could be probed by spiking the mixture with deuterated pentafluorophenol, which should diminish the benzylidene signal. Alternatively, removing C_6F_5OH by adding an equivalent of a non-coordinating base such as NEt_3 and removing the resultant salt by filtration may cause the alkylidene signal to sharpen and resolve.

Scheme 4.28: Proposed exchange process between benzylidene and phenolic protons.

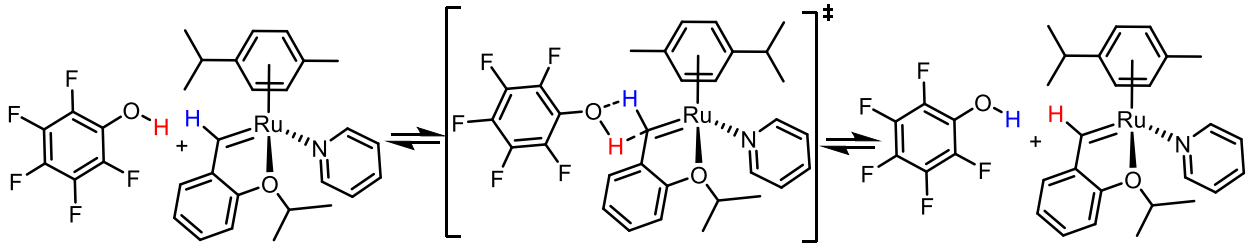

4.3 Conclusions

While reduction of existing high-valent metathesis catalyst **HII** was found to be ineffective as a route to low-valent alkylidenes (in all cases leading to decomposition and complete loss of alkylidene), significant progress towards an α-hydride-elimination-based route to low-valent alkylidenes has been achieved. A high-yield route to novel chelating benzylruthenium complex **Ru-84** has been developed. A second equivalent of the benzyl ligand was successfully installed in **Ru-85**, but attempts to induce Schrock-style alkyl-to-alkyl hydride abstraction by adding steric pressure were unsuccessful. Deprotonation of the benzyl ligand on both chloride species **Ru-84** and aryloxide complex **Ru-86** were likewise unsuccessful in generating the desired alkylidene. Of note, however, is the emergence of an NMR signal at 14.2 ppm when aryloxide species **Ru-86** was treated with pyridine, which may indicate successful formation of an alkylidene species.

References on page 92

4.4 References

(1) Frenking, G.; Solà, M.; Vyboishchikov, S. F., Chemical Bonding in Transition Metal Carbene Complexes. *J. Organomet. Chem.* **2005,** *690*, 6178-6204.
(2) Vyboishchikov, S. F.; Frenking, G., Structure and Bonding of Low-Valent (Fischer-Type) and High-Valent (Schrock-Type) Transition Metal Carbene Complexes. *Chem. Eur. J.* **1998,** *4*, 1428-1438.
(3) du Toit, J. I.; van Sittert, C. G. C. E.; Vosloo, H. C. M., Towards a Better Understanding of Alkene Metathesis: Elucidating the Properties of the Major Metal Carbene Catalyst Types. *Monatsh. Chem.* **2015,** *146*, 1115-1129.
(4) Santamaría, J.; Aguilar, E., Beyond Fischer and Schrock Carbenes: Non-Heteroatom-Stabilized Group 6 Metal Carbene Complexes – a General Overview. *Org. Chem. Front.* **2016,** *3*, 1561-1588.
(5) Esteruelas, M. A.; González, A. I.; López, A. M.; Oñate, E., An Osmium-Carbene Complex with Fischer−Schrock Ambivalent Behavior. *Organometallics* **2003,** *22*, 414-425.
(6) Whited, M. T.; Grubbs, R. H., Late Metal Carbene Complexes Generated by Multiple C−H Activations: Examining the Continuum of M═C Bond Reactivity. *Acc. Chem. Res.* **2009,** *42*, 1607-1616.
(7) Occhipinti, G.; Jensen, V. R., Nature of the Transition Metal–Carbene Bond in Grubbs Olefin Metathesis Catalysts. *Organometallics* **2011,** *30*, 3522-3529.
(8) Occhipinti, G.; Bjørsvik, H.-R.; Jensen, V. R., Quantitative Structure−Activity Relationships of Ruthenium Catalysts for Olefin Metathesis. *J. Am. Chem. Soc.* **2006,** *128*, 6952-6964.
(9) Scholl, M.; Ding, S.; Lee, C. W.; Grubbs, R. H., Synthesis and Activity of a New Generation of Ruthenium-Based Olefin Metathesis Catalysts Coordinated with 1,3-Dimesityl-4,5-dihydroimidazol-2-ylidene Ligands. *Org. Lett.* **1999,** *1*, 953-956.
(10) Anderson, D. R.; Lavallo, V.; O'Leary, D. J.; Bertrand, G.; Grubbs, R. H., Synthesis and Reactivity of Olefin Metathesis Catalysts Bearing Cyclic (Alkyl)(Amino)Carbenes. *Angew. Chem., Int. Ed.* **2007,** *46*, 7262-7265.
(11) Marx, V. M.; Sullivan, A. H.; Melaimi, M.; Virgil, S. C.; Keitz, B. K.; Weinberger, D. S.; Bertrand, G.; Grubbs, R. H., Cyclic Alkyl Amino Carbene (CAAC) Ruthenium Complexes as Remarkably Active Catalysts for Ethenolysis. *Angew. Chem., Int. Ed.* **2015,** *54*, 1919-1923.
(12) Vougioukalakis, G. C.; Grubbs, R. H., Ruthenium-Based Heterocyclic Carbene-Coordinated Olefin Metathesis Catalysts. *Chem. Rev.* **2010,** *110*, 1746-1787.
(13) Scholl, M.; Trnka, T. M.; Morgan, J. P.; Grubbs, R. H., Increased Ring Closing Metathesis Activity of Ruthenium-Based Olefin Metathesis Catalysts Coordinated with Imidazolin-2-Ylidene Ligands. *Tetrahedron Lett.* **1999,** *40*, 2247-2250.
(14) Weskamp, T.; Kohl, F. J.; Hieringer, W.; Gleich, D.; Herrmann, W. A., Highly Active Ruthenium Catalysts for Olefin Metathesis: The Synergy of N-Heterocyclic Carbenes and Coordinatively Labile Ligands. *Angew. Chem., Int. Ed.* **1999,** *38*, 2416-2419.
(15) Nguyen, S. T.; Johnson, L. K.; Grubbs, R. H.; Ziller, J. W., Ring-Opening Metathesis Polymerization (ROMP) of Norbornene by a Group VIII Carbene Complex in Protic Media. *J. Am. Chem. Soc.* **1992,** *114*, 3974-3975.
(16) Adlhart, C.; Chen, P., Comparing Intrinsic Reactivities of the First- and Second-Generation Ruthenium Metathesis Catalysts in the Gas Phase. *Helv. Chim. Acta* **2003,** *86*, 941-949.
(17) Adlhart, C.; Hinderling, C.; Baumann, H.; Chen, P., Mechanistic Studies of Olefin Metathesis by Ruthenium Carbene Complexes Using Electrospray Ionization Tandem Mass Spectrometry. *J. Am. Chem. Soc.* **2000,** *122*, 8204-8214.

References on page 92

(18) Paredes-Gil, K.; Solans-Monfort, X.; Rodriguez-Santiago, L.; Sodupe, M.; Jaque, P., DFT Study on the Relative Stabilities of Substituted Ruthenacyclobutane Intermediates Involved in Olefin Cross-Metathesis Reactions and Their Interconversion Pathways. *Organometallics* **2014,** *33*, 6065-6075.
(19) Sanford, M. S.; Love, J. A.; Grubbs, R. H., Mechanism and Activity of Ruthenium Olefin Metathesis Catalysts. *J. Am. Chem. Soc.* **2001,** *123*, 6543-6554.
(20) Harlow, K. J.; Hill, A. F.; Welton, T.; White, A. J. P.; Williams, D. J., Regioselective Nucleophilic Addition to Vinyl Carbenes (Metallabutadienes): Crystal Structure of [Ru{CH(CHCPh$_2$)SC(NMe$_2$)S}(S$_2$CNMe$_2$)(CO)(PPh$_3$)]. *Organometallics* **1998,** *17*, 1916-1918.
(21) Hansen, S. M.; Rominger, F.; Metz, M.; Hofmann, P., The First Grubbs-Type Metathesis Catalyst with Cis Stereochemistry: Synthesis of [(η_2-dtbpm)Cl$_2$Ru=CH−CH=CMe$_2$] from a Novel, Coordinatively Unsaturated Dinuclear Ruthenium Dihydride. *Chem. Eur. J.* **1999,** *5*, 557-566.
(22) Galan, B. R.; Pitak, M.; Keister, J. B.; Diver, S. T., Isocyanide-Promoted Ylidene Transfer to Phosphorus: Rearrangement in the First-Generation Grubbs Complex. *Organometallics* **2008,** *27*, 3630-3632.
(23) Ireland, B. J.; Dobigny, B. T.; Fogg, D. E., Decomposition of a Phosphine-Free Metathesis Catalyst by Amines and Other Bronsted Bases: Metallacyclobutane Deprotonation as a Major Deactivation Pathway. *ACS Catal.* **2015,** *5*, 4690-4698.
(24) Diesendruck, C. E.; Tzur, E.; Lemcoff, N. G., The Versatile Alkylidene Moiety in Ruthenium Olefin Metathesis Catalysts. *Eur. J. Inorg. Chem.* **2009,** *2009*, 4185-4203.
(25) McClennan, W. L.; Rufh, S. A.; Lummiss, J. A. M.; Fogg, D. E., A General Decomposition Pathway for Phosphine-Stabilized Metathesis Catalysts: Lewis Donors Accelerate Methylidene Abstraction. *J. Am. Chem. Soc.* **2016,** *138*, 14668-14677.
(26) Gallop, M. A.; Roper, W. R., Carbene and Carbyne Complexes of Ruthenium, Osmium, and Iridium. In *Adv. Organomet. Chem.*, Stone, F. G. A.; West, R., Eds. Academic Press: 1986; Vol. 25, pp 121-198.
(27) Hong, S. H.; Wenzel, A. G.; Salguero, T. T.; Day, M. W.; Grubbs, R. H., Decomposition of Ruthenium Olefin Metathesis Catalysts. *J. Am. Chem. Soc.* **2007,** *129*, 7961-7968.
(28) Burrell, A. K.; Clark, G. R.; Rickard, C. E. F.; Roper, W. R.; Wright, A. H., Synthesis and Reactions of Ru(=CH2)Cl(NO)(PPh$_3$)$_2$, a Stable Terminal Methylene Complex and the Crystal Structure of Ru(CH$_2$PPh$_3$)(η^2-C2F$_4$)Cl(NO)(PPh$_3$). *J. Chem. Soc., Dalton Trans.* **1991**, 609-614.
(29) Bailey, G. A.; Foscato, M.; Higman, C. S.; Day, C. S.; Jensen, V. R.; Fogg, D. E., Bimolecular Coupling as a Vector for Decomposition of Fast-Initiating Olefin Metathesis Catalysts. *J. Am. Chem. Soc.* **2018,** *140*, 6931-6944.
(30) Nascimento, D. L.; Fogg, D. E., Origin of the Breakthrough Productivity of Ruthenium–Cyclic Alkyl Amino Carbene Catalysts in Olefin Metathesis. *J. Am. Chem. Soc.* **2019,** *141*, 19236-19240.
(31) Schrock, R. R., High Oxidation State Multiple Metal-Carbon Bonds. *Chem. Rev.* **2002,** *102*, 145-179.
(32) Cotton, S. A., Ruthenium and Osmium. In *Chemistry of Precious Metals*, Springer Netherlands: Dordrecht, 1997; pp 1-77.
(33) Coalter, I. I. I. J. N.; Bollinger, J. C.; Eisenstein, O.; Caulton, K. G., R-Group Reversal of Isomer Stability for RuH(X)L$_2$(CCHR) vs. Ru(X)L$_2$(CCH$_2$R): Access to Four-Coordinate Ruthenium Carbenes and Carbynes. *New J. Chem.* **2000,** *24*, 925-927.

References on page 92

(34) Conrad, J. C.; Amoroso, D.; Czechura, P.; Yap, G. P. A.; Fogg, D. E., The First Highly Active, Halide-Free Ruthenium Catalyst for Olefin Metathesis. *Organometallics* **2003,** *22*, 3634-3636.
(35) Schrock, R. R., Alkylcarbene Complex of Tantalum by Intramolecular Alpha-Hydrogen Abstraction. *J. Am. Chem. Soc.* **1974,** *96*, 6796-6797.
(36) Calabrese, J. C.; Colton, M. C.; Hersovitz, T.; Klabunde, U.; Parshall, G. W.; Thorn, D. L.; Tulip, T. H., Transition Metal Hydride Complexes Via Distal C-H Activation. *Ann. N. Y. Acad. Sci.* **1983**, 302-312.
(37) Statler, J. A.; Wilkinson, G., Alkyl, Hydrido-, and Related Compounds of Ruthenium(II) with Trimethylphosphine. X-Ray Cystal Structures of Hydrido(tetrahydroborato-HH')trist(trimethylphosphine)ruthenium(II), Tri-u-chloro-bis[tris(trimethylphosphine)ruthenium(II)] Tetrafluoroborate, and Bis[cis-methyltetrakis(trimethylphosphine)ruthenio]mercury(II)–tetrahydrofuran(1/1). *Dalton Trans.* **1984**, 1731-1984.
(38) McNeill, K.; Andenen, R. A.; Bergman, R. G., Interconversion of a 3,3-Dimethylruthenacyclobutane and a Methyl(2-methallyl)ruthenium Complex: The First Direct Observation of Reversible β-Methyl Elimination/Migratory Insertion. *J. Am. Chem. Soc.* **1995,** *117*, 3625-3626.
(39) McNeill, K.; Andersen, R. A.; Bergman, R. G., C-C and C-H Bond Activation at Ruthenium(II): The Stepwise Degradation of a Neopentyl Ligand to a Trimethylenemethane Ligand. *J. Am. Chem. Soc.* **1997,** *119*, 11244-11254.
(40) Jennings, P. W.; Johnson, L. L., Metallacyclobutane Complexes of the Group Eight Transition Metals: Synthesis, Characterizations, and Chemistry. *Chem. Rev.* **2005,** *94*, 2241-2290.
(41) DiCosimo, R.; Moore, S. S.; Sowinski, A. F.; Whitesides, G. M., Cyclometalation of Dialkylbis(triethylphosphine)platinum(II) Complexes: Formation of Pt,Pt-Bis(triethylphosphine)platinacycloalkanes. *J. Am. Chem. Soc.* **1982,** *104*, 124-133.
(42) Kuznetsov, V. F.; Abdur-Rashid, K.; Lough, A. J.; Gusev, D. G., Carbene vs olefin products of C-H activation on ruthenium via competing α- and β-H elimination. *J. Am. Chem. Soc.* **2006,** *128*, 14388-14396.
(43) Rankin, M. A.; McDonald, R.; Ferguson, M. J.; Stradiotto, M., Coordinatively unsaturated cationic and zwitterionic [Cp *Ru(κ^2-P,N)] complexes: Ligand-assisted double-geminal C-H bond activation and reversible α-H elimination at ruthenium. *Angew. Chem., Int. Ed.* **2005,** *44*, 3603-3606.
(44) Rankin, M. A.; Maclean, D. F.; McDonald, R.; Ferguson, M. J.; Lumsden, M. D.; Stradiotto, M., Probing the dynamics and reactivity of a stereochemically nonrigid Cp*Ru(H)(κ^2-P,carbene) complex. *Organometallics* **2009,** *28*, 74-83.
(45) Ingleson, M. J.; Yang, X.; Pink, M.; Caulton, K. G., [(^{t}Bu$_2$PCH$_2$SiMe$_2$)$_2$N]RuCH$_3$: The Origin of Extremely Facile, Double H-C(sp^3) Activation Generating a "Hydrido-Carbene" Complex. *J. Am. Chem. Soc.* **2005,** *127*, 10846-10847.
(46) Grandner, J. M.; Shao, H.; Grubbs, R. H.; Liu, P.; Houk, K. N., Origins of the Stereoretentive Mechanism of Olefin Metathesis With Ru-Dithiolate Catalysts. *J. Org. Chem.* **2017,** *82*, 10595-10600.
(47) Macías-Arce, I.; Puerta, M. C.; Valerga, P., Half-Sandwich Benzylidene Ruthenium Complexes Bearing Phosphanyl-Pyridine Ligands: Reactivity towards Nucleophiles and Electrophiles. *Eur. J. Inorg. Chem.* **2010,** *2010*, 1767-1776.

References on page 92

(48) Sun, R.; Chu, X.; Zhang, S.; Li, T.; Wang, Z.; Zhu, B., Synthesis, Structure, Reactivity, and Catalytic Activity of Cyclometalated (Phosphine)- and (Phosphinite)ruthenium Complexes. *Eur. J. Inorg. Chem.* **2017,** *2017*, 3174-3183.
(49) Kingsbury, J. S.; Harrity, J. P. A.; Bonitatebus, P. J.; Hoveyda, A. H., A Recyclable Ru-Based Metathesis Catalyst. *J. Am. Chem. Soc.* **1999,** *121*, 791-799.
(50) Yanagisawa, A., Product Subclass 8: Benzylic Grignard Reagents. In *Category 1, Organometallics*, 2004 ed.; Yamamoto, H., Ed. Georg Thieme Verlag: Stuttgart, 2004; Vol. 7.
(51) Schlenk, W.; Schlenk jun., W., Über die Konstitution der Grignardschen Magnesiumverbindungen. *Ber. Dtsch. Chem. Ges.* **1929,** *62*, 920-924.
(52) Lin, H.-S.; Paquette, L. A., A Convenient Method for Determining the Concentration of Grignard Reagents. *Synth. Commun.* **1994,** *24*, 2503-2506.
(53) Cole-Hamilton, D. J.; Wilkinson, G., Ortho-Metallated Triphenylphosphine(2-Diphenylphosphinophenyl) and Related Complexes of Ruthenium(II): Interaction of Chlorohydridotris(Triphenylphosphine)Ruthenium(II) with Methyl and Trimethylsilylmethyl Alkylating Agents (Li, Mg, Zn); Hydrido Methyl and Trimethylsilylmethyl Complexes. *J. Chem. Soc., Dalton Trans.* **1977**, 797-804.
(54) Trost, B. M.; Czabaniuk, L. C., Structure and Reactivity of Late Transition Metal η^3-Benzyl Complexes. *Angew. Chem., Int. Ed.* **2014,** *53*, 2826-2851.
(55) Buchmeiser, M. R.; Ahmad, I.; Gurram, V.; Kumar, P. S., Pseudo-Halide and Nitrate Derivatives of Grubbs and Grubbs–Hoveyda Initiators: Some Structural Features Related to the Alternating Ring-Opening Metathesis Copolymerization of Norborn-2-ene with Cyclic Olefins. *Macromolecules* **2011,** *44*, 4098-4106.
(56) Garber, S. B.; Kingsbury, J. S.; Gray, B. L.; Hoveyda, A. H., Efficient and Recyclable Monomeric and Dendritic Ru-Based Metathesis Catalysts. *J. Am. Chem. Soc.* **2000,** *122*, 8168-8179.
(57) Krause, J. O.; Nuyken, O.; Buchmeiser, M. R., Factors Relevant for the Ruthenium–Benzylidene-Catalyzed Cyclopolymerization of 1,6-Heptadyines. *Chem. Eur. J.* **2004,** *10*, 2029-2035.
(58) Krause, J. O.; Nuyken, O.; Wurst, K.; Buchmeiser, M. R., Synthesis and Reactivity of Homogeneous and Heterogeneous Ruthenium-Based Metathesis Catalysts Containing Electron-Withdrawing Ligands. *Chem. Eur. J.* **2004,** *10*, 777-784.
(59) Kumar, P. S.; Wurst, K.; Buchmeiser, M. R., Isocyanate- and Isothiocyanate-Derived RuIV-Based Alkylidenes: Synthesis, Structure, and Activity. *Chem. Asian J.* **2009,** *4*, 1275-1283.
(60) Michrowska, A.; Bujok, R.; Harutyunyan, S.; Sashuk, V.; Dolgonos, G.; Grela, K., Nitro-Substituted Hoveyda−Grubbs Ruthenium Carbenes: Enhancement of Catalyst Activity through Electronic Activation. *J. Am. Chem. Soc.* **2004,** *126*, 9318-9325.
(61) Tanaka, K.; Böhm, V. P. W.; Chadwick, D.; Roeper, M.; Braddock, D. C., Anionic Ligand Exchange in Hoveyda−Grubbs Ruthenium(II) Benzylidenes. *Organometallics* **2006,** *25*, 5696-5698.
(62) Wappel, J.; Urbina-Blanco, C. A.; Abbas, M.; Albering, J. H.; Saf, R.; Nolan, S. P.; Slugovc, C., Halide Exchanged Hoveyda-Type Complexes in Olefin Metathesis. *Beilstein J. Org. Chem.* **2010,** *6*, 1091-1098.
(63) Van Veldhuizen, J. J.; Campbell, J. E.; Giudici, R. E.; Hoveyda, A. H., A Readily Available Chiral Ag-Based N-Heterocyclic Carbene Complex for Use in Efficient and Highly Enantioselective Ru-Catalyzed Olefin Metathesis and Cu-Catalyzed Allylic Alkylation Reactions. *J. Am. Chem. Soc.* **2005,** *127*, 6877-6882.

References on page 92

(64) Conrad, J. C.; Snelgrove, J. L.; Eeelman, M. D.; Hall, S.; Fogg, D. E., Ruthenium Aryloxide Catalysts: Synthesis and Applications in Ring-Closing Metathesis. *J. Mol. Catal. A: Chem.* **2006,** *254*, 105-110.
(65) Sanford, M. S.; Love, J. A.; Grubbs, R. H., A Versatile Precursor for the Synthesis of New Ruthenium Olefin Metathesis Catalysts. *Organometallics* **2001,** *20*, 5314-5318.
(66) Snelgrove, J. L.; Conrad, J. C.; Eelman, M. D.; Moriarty, M. M.; Yap, G. P. A.; Fogg, D. E., Inhibiting $\sigma \rightarrow \pi$ Isomerization of Aryloxide Ligands in Late Transition-Metal Complexes. *Organometallics* **2005,** *24*, 103-109.
(67) Monfette, S.; Fogg, D. E., Ruthenium Metathesis Catalysts Containing Chelating Aryloxide Ligands. *Organometallics* **2006,** *25*, 1940-1944.
(68) Bennett, M. A.; Smith, A. K., Arene Ruthenium(II) Complexes Formed by Dehydrogenation of Cyclohexadienes with Ruthenium(III) Trichloride. *J. Chem. Soc., Chem. Commun.* **1974**, 233-241.
(69) Danopoulos, A. A.; Wilkinson, G.; Sweet, T. K. N.; Hursthouse, M. B., Non-Oxo Chemistry of Manganese in High Oxidation States. Part 1. Mononuclear Tert-Butylimido Compounds of Manganese-(VII) and -(VI). *J. Chem. Soc., Dalton Trans.* **1994**, 1037-1049.
(70) Danopoulos, A. A.; Wilkinson, G.; Sweet, T.; Hursthouse, M. B., Synthesis and X-ray Crystal Structure of Chloro Tris(Tert-Butylimido)Manganese. *J. Chem. Soc., Chem. Commun.* **1993**, 495-496.
(71) Danopoulos, A. A.; Wilkinson, G.; Sweet, T. K. N.; Hursthouse, M. B., A New Type of Iminophosphine Ligand from Interaction of $Li_2M(NBu^t)_4$, M = W, Mo and PX_3, X = Cl, Br. Crystal Structures of $W(NBu^t)Br_2[P_2(NBu^t)_3]$ and $W(NBu^t)Cl(SC_6F_5)[P_2(NBu^t)_3]$. *Polyhedron* **1994,** *13*, 2899-2905.
(72) Fulton, J. R.; Holland, A. W.; Fox, D. J.; Bergman, R. G., Formation, Reactivity, and Properties of Nondative Late Transition Metal−Oxygen and −Nitrogen Bonds. *Acc. Chem. Res.* **2002,** *35*, 44-56.
(73) Yang, D.; Tang, Y.; Song, H.; Wang, B., o-Aryloxide-N-heterocyclic Carbenes: Efficient Synthesis of the Proligands and Their *p*-cymene Ruthenium Complexes. *Organometallics* **2015,** *34*, 2012-2017.
(74) Halbach, T. S.; Mix, S.; Fischer, D.; Maechling, S.; Krause, J. O.; Sievers, C.; Blechert, S.; Nuyken, O.; Buchmeiser, M. R., Novel Ruthenium-Based Metathesis Catalysts Containing Electron- Withdrawing Ligands: Synthesis, Immobilization, and Reactivity. *J. Org. Chem.* **2005,** *70*, 4687-4694.
(75) Chang, S.; Jones, L.; Wang, C.; Henling, L. M.; Grubbs, R. H., Synthesis and Characterization of New Ruthenium-Based Olefin Metathesis Catalysts Coordinated with Bidentate Schiff-Base Ligands. *Organometallics* **1998,** *17*, 3460-3465.
(76) Nolan, S. P.; Clavier, H.; Urbina-Blanco, C. A., Indenylidene Ruthenium Complex Bearing a Sterically Demanding NHC Ligand: An Efficient Catalyst for Olefin Metathesis at Room Temperature. *Organometallics* **2009,** *28*, 2848-2854.
(77) Reisinger, A.; Himmel, D.; Krossing, I., $AgOC(CF_3)_3$ and $AgOSi^iPr_3$—Synthesis and Characterization of a Donor-Free Silver(I) Alkoxide and Silyl Oxide. *Angew. Chem., Int. Ed.* **2006,** *45*, 6997-7000.
(78) Negishi, E., Magical Power of Transition Metals: Past, Present, and Future (Nobel Lecture). *Angew. Chem., Int. Ed.* **2011,** *50*, 6738-6764.
(79) Nicolaou, K. C.; Bulger, P. G.; Sarlah, D., Palladium-Catalyzed Cross-Coupling Reactions in Total Synthesis. *Angew. Chem., Int. Ed.* **2005,** *44*, 4442-4489.

(80) Day, C. S.; Fogg, D. E., High-Yield Synthesis of a Long-Sought, Labile Ru-NHC Complex and Its Application to the Concise Synthesis of Second-Generation Olefin Metathesis Catalysts. *Organometallics* **2018,** *37*, 4551-4555.
(81) Jafarpour, L.; Huang, J.; Stevens, E. D.; Nolan, S. P., (*p*-cymene)RuLCl$_2$ (L = 1,3-Bis(2,4,6-trimethylphenyl)imidazol-2-ylidene and 1,3-Bis(2,6-diisopropylphenyl)imidazol-2-ylidene) and Related Complexes as Ring Closing Metathesis Catalysts. *Organometallics* **1999,** *18*, 3760-3763.
(82) Serron, S. A.; Nolan, S. P., Enthalpies of Reaction of ((*p*-cymene)RuCl$_2$)$_2$ with Monodentate Tertiary Phosphine Ligands. Importance of Both Steric and Electronic Ligand Factors in a Ruthenium(II) System. *Organometallics* **1995,** *14*, 4611-4616.

References on page 92

Chapter 5. Conclusions and Future Work

5.1 Benzyl Magnesium Carbenoids

Although treatment of benzal dichlorides with 1 equiv. of the magnesium-anthracene complex **Mg-1** appears to be successful in generating α-chlorobenzylmagnesium reagents (Scheme 5.1), a high yield route to ruthenium alkylidenes based on salt metathesis of **Mg-2** with ruthenium dichloride precursors could not be realized. Although a straightforward, rapid procedure at room temperature did produce first generation precatalysts **Ru-39** and **GI** with in situ yields of up to 41%, this is inferior to isolated yields obtainable with current diazo-based approaches, and workup was not pursued. Attempts to improve the in-situ yield of metathesis catalysts by switching ruthenium substrates and/or moving to reduced temperatures to help stabilize the magnesium carbenoid were unsuccessful, and may indicate a fundamental incompatibility between the magnesium carbenoid and the ligand sets used in this work. Further attempts with different ruthenium substrates may yet lead to a viable alternative route to metathesis catalysts.

Scheme 5.1: Synthesis of magnesium carbenoid **Mg-2** via reaction of **Mg-1** with a substituted benzal dichloride.

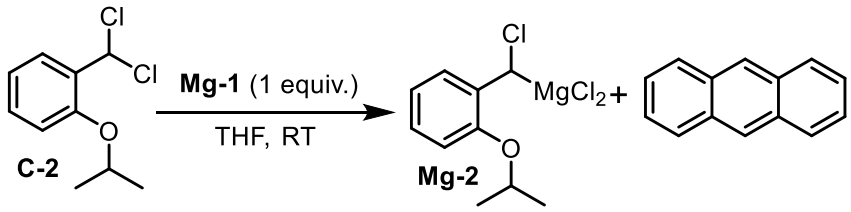

Aspects of this work may have intriguing implications beyond olefin metathesis or indeed ruthenium chemistry. Treatment of β-unsaturated geminal dihalides with **Mg-1** represents a novel approach to magnesium carbenoid synthesis with advantages over existing approaches based on Mg-X exchange (X = I or sulfoxide). The reaction appears to be stoichiometric, obviating the need for excess sacrificial Grignard reagent and greatly improving the atom economy of downstream steps. It is also novel: no prior examples of benzyl nor any other β-unsaturated magnesium carbenoids have yet been reported.

To expand on the initial findings in this thesis, the generality of carbenoid formation for β-unsaturated geminal dihalides should be examined. To that end, allyl and propargyl as well as benzyl carbenoids should be targeted. The utility of these carbenoids in organic applications typical for other carbenoids should be examined, e.g. in reactions with electrophiles and nucleophiles. Methyl isopropyl ketone ($CH_3COCH(CH_3)_2$) is a good candidate electrophile for these reactions, as the C*H*$(CH_3)_2$ proton provides a convenient spectroscopic handle (Scheme 5.2). Mg(*i*Pr)Cl, for the same reason, is a good candidate nucleophile (Scheme 5.2). Electrophilic and nucleophilic trapping reactions would provide additional confirmation of carbenoid formation to reinforce the detection of carbene homocoupling products via GC-MS in this thesis work.

Scheme 5.2: Proposed nucleophilic (i) and electrophilic (ii) trapping experiments to confirm the synthesis of magnesium carbenoids via **Mg-1** and demonstrate their use in organic synthesis.

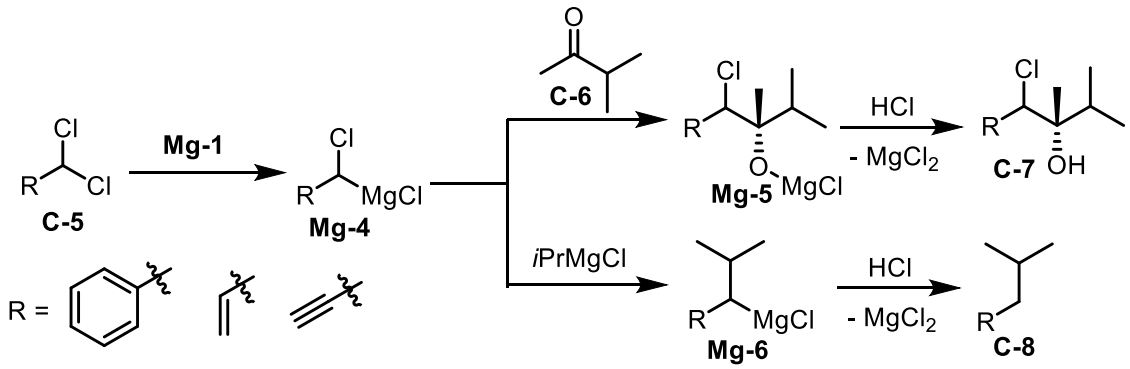

Carbenoids are known to react with alkenes and alkynes (as in the Simmons-Smith reaction[1]), and as such inter- or intramolecular reaction of allyl/propargyl carbenoids with the inbuilt alkene/alkyne may outcompete reaction with external nucleophiles or electrophiles. In this case, only the resultant cyclopropanation products will be detectable (Scheme 5.3).

Scheme 5.3: Postulated cyclopropanation chemistry of allyl magnesium carbenoids: i) intramolecular cyclopropenation, ii) homocoupling to form a new carbenoid, iii) intramolecular cyclopropanation, iv) propagation by addition of further equivalents of **Mg-7**, v) termination by intramolecular cyclopropanation.

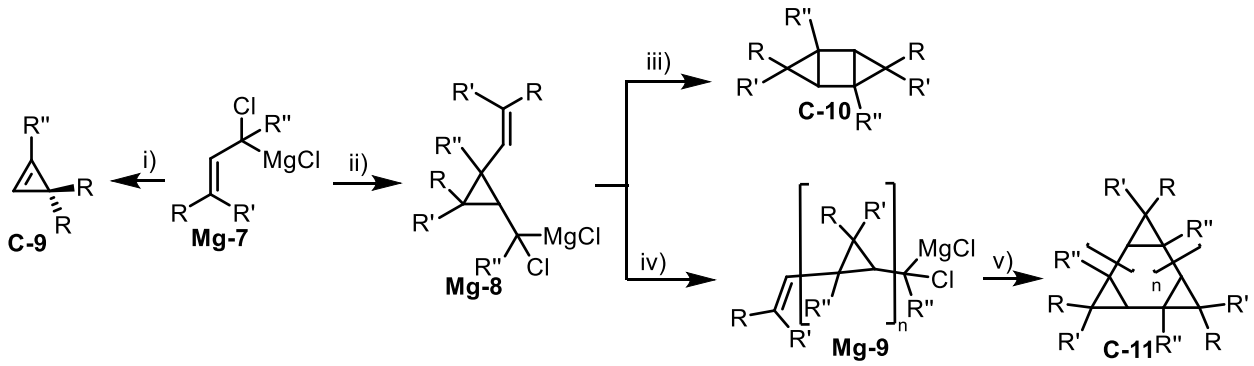

Intramolecular reaction of allyl carbenoids should be disfavoured by the high ring strain inherent to cyclopropenes. Intermolecular cyclization with a second equivalent of carbenoid is therefore expected to be the preferred pathway, generating a new β-cyclopropyl magnesium-carbenoid. From here, either termination by intramolecular cyclization or propagation by addition to another equivalent of allyl carbenoid are both reasonable propositions. Strained polycyclic hydrocarbons of the type **C-10** have been investigated as potential rocket propellants, and were found to be among the highest performing candidates.[2] Unfortunately, there are currently no convenient routes to such species; new and potentially scalable methods of accessing such polycycles are therefore of interest.

The potential reaction pathways of propargyl magnesium carbenoids mirror those of the allyl carbenoids, but addition of the carbenoid across an alkyne rather than alkene will produce extremely strained cyclopropenes rather than cyclopropanes.

This new approach to carbenoid formation may enable a convenient and diazo-free route to tetrasubstituted olefins, particularly sterically-crowded Feringa-type molecular motors, all known examples of which bear an element of unsaturation β to the central "axle" olefin.[3] Symmetric olefins can be targeted by carbenoid homocoupling (Scheme 5.4), and asymmetric olefins by reaction with an appropriate carbonyl and olefination of the resultant epoxide[4-6] (Scheme 5.5). If successful, this should allow access to a broad range of tetrasubstituted olefins, provided that the parent ketones are accessible. Mono-, di-, and trisubstituted olefins should also be accessible from aldehydes, but convenient and effective routes to such species are already known (e.g. the Wittig reaction).

Scheme 5.4: Proposed synthesis of symmetric sterically crowded olefins via a β-unsaturated magnesium carbenoid intermediate (**Mg-10**). In-situ liberation of free carbene and subsequent homocoupling produces the olefin. Any symmetric olefin should be targetable provided that a) there is an element of unsaturation β to the olefin and b) there are no functional groups present that would not be tolerated by an organomagnesium reagent.

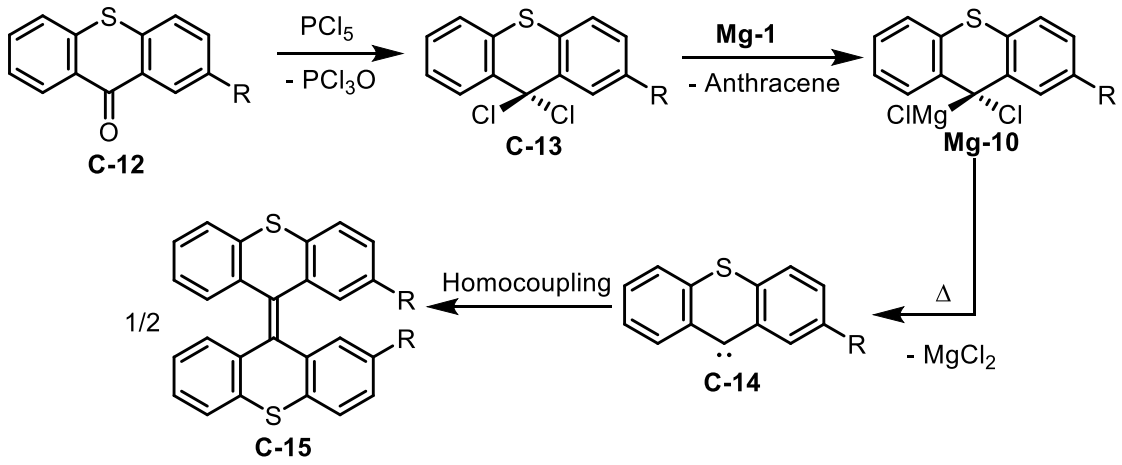

Scheme 5.5: Proposed synthesis of unsymmetrical sterically crowded olefins via a β-unsaturated magnesium carbenoid intermediate. Nucleophilic addition of carbenoid **Mg-11** to carbonyl **C-15** furnishes an α-chloro magnesium alkoxide (**Mg-12**) which should readily undergo an intramolecular S_N2, liberating $MgCl_2$ and a tetrasubstituted epoxide (**C-16**). Finally, olefination of the epoxide is expected to generate an unsymmetrical tetrasubstituted olefin. Via this approach it is not critical that both sides of the sterically crowded olefin have β-unsaturation; only the carbonyl that acts as a precursor to the magnesium carbenoid need be β-unsaturated. The carbonyl that reacts as an electrophile with the carbenoid may be fully saturated if desired.

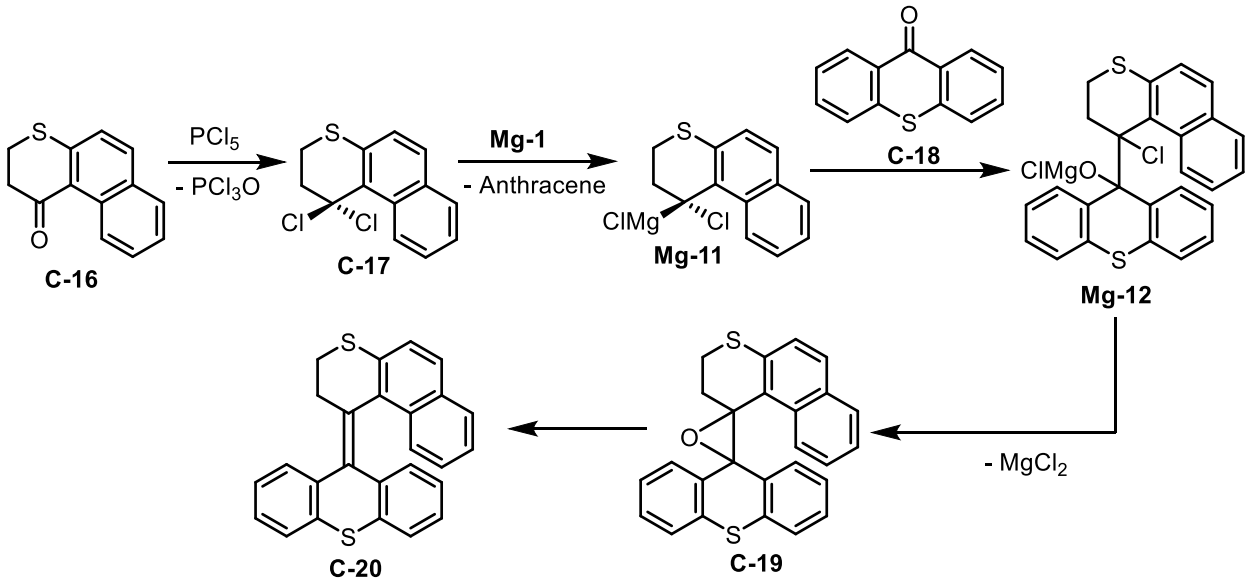

5.2 Indenylidene Installation on Ru-50 Derivatives

Although a high yield route to **Ru-50** (and 3-bromopyridine derivative **Ru-56c**) was realized, and **Ru-50** was found to be significantly more soluble and substitutionally labile than tetrakis pyridine complex **Ru-51**, attempts to install the allenylidene and indenylidene functionality were not successful. The unexpected finding that ligand substitution occurs cis rather than trans to H_2IMes on **Ru-50**, and that steric bulk is a better predictor of substitution success than denticity, may indicate that allenylidene/indenylidene installation is prevented by steric shielding from the bulky mesityl arms of H_2IMes. To alleviate this, **Ru-95**, functionalized with an asymmetric CAAC ligand should be targeted (Scheme 5.6). Given the challenges associated with both CAAC liberation and the instability of p-cymene piano stool complexes of ruthenium, this should be attempted as a one pot reaction from **Ru-35**.

Scheme 5.6: Proposed synthesis of **Ru-95** based on high-yield synthesis of **Ru-50** developed in this work.

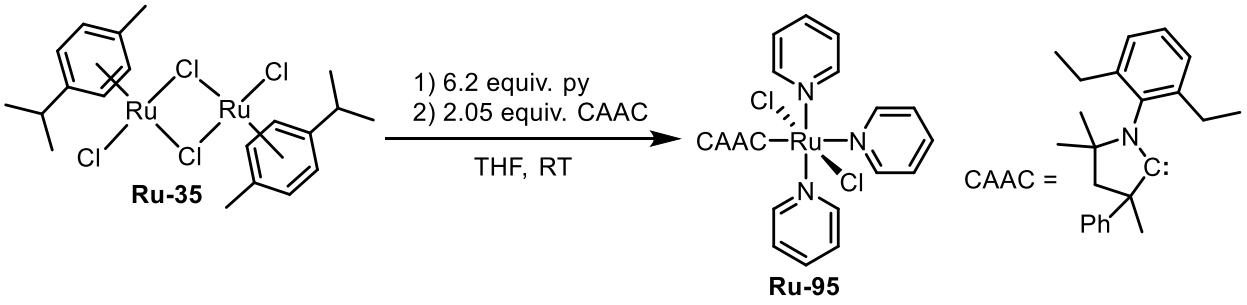

Even if allenylidene/indenylidene installation fails on **Ru-95**, it may be possible to directly access CAAC-functionalized Hoveyda-type catalysts via a diazo reagent (Scheme 5.7). Although the field is seeking to move away from diazo-based alkylidene installation, direct and atom-economical access to CAAC-functionalized catalysts would be a significant advance.

Scheme 5.7: Proposed diazo-based synthesis of CAAC-functionalized Hoveyda catalyst **HII-CAAC**

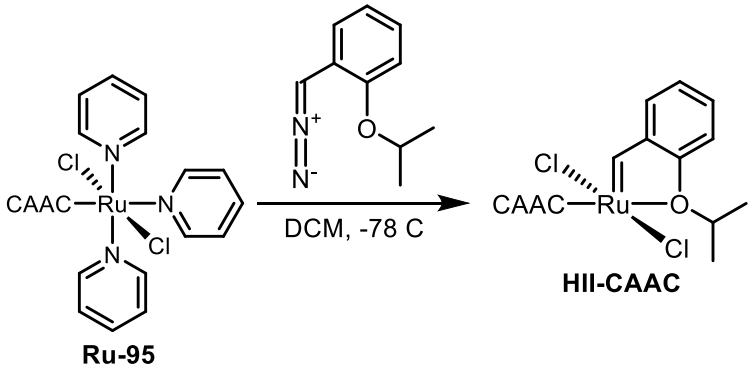

5.3 Alternative Uses for Ru-50; a Potent Photocatalyst Precursor?

NHC-functionalized pyridyl and polypyridyl complexes of ruthenium have recently been investigated as photosensitizers in photocatalytic water splitting and hydrogen transfer.[7-8] **Ru-50**, or derivatives obtained by replacing two or more pyridine ligands with a polypyridyl (e.g. 2,2'-bipyridine) (Figure 5.1), may likewise be photochemically useful.

Figure 5.1: Known Ru-pyridine (**Ru-50**) and proposed Ru-polypyridyl (**Ru-96-97**) species may be efficient photosensitizers.

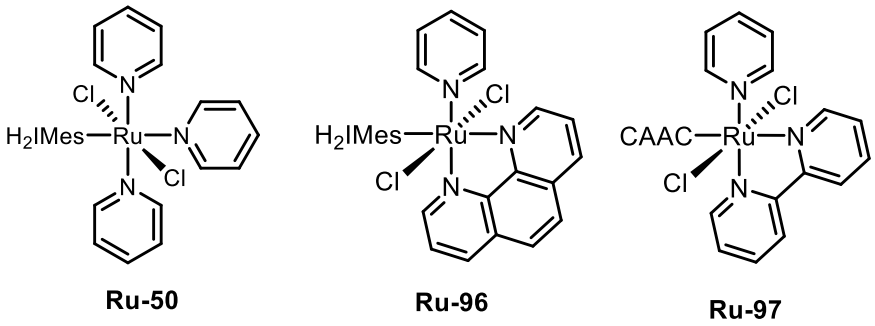

Ru-50 **Ru-96** **Ru-97**

Along the same lines, the synthetic route to **Ru-50** developed in this work, which is operationally straightforward and high-yielding, may be adaptable to existing NHC-functionalized Ru-based photosensitizers. Currently, such complexes are synthesized in a one-pot procedure from $RuCl_3 \cdot (_xH_2O)$ and the NHC precursor salt (Scheme 5.9), requiring extended reaction times at elevated temperatures (12h at 190 °C in the example shown) and yields are moderate-to-low (15-69%). By contrast, the synthetic route to **Ru-50** presented in this work proceeds at room temperature, can be carried out from start to isolation of purified product in under 4 h, and yields of over 80% are typical. Adaptation of this synthetic route should allow faster, more convenient access to photochemically active Ru-NHC complexes (Scheme 5.10), accelerating developments in the field.

Scheme 5.9: Current synthetic route to NHC-pyridyl ruthenium complexes.

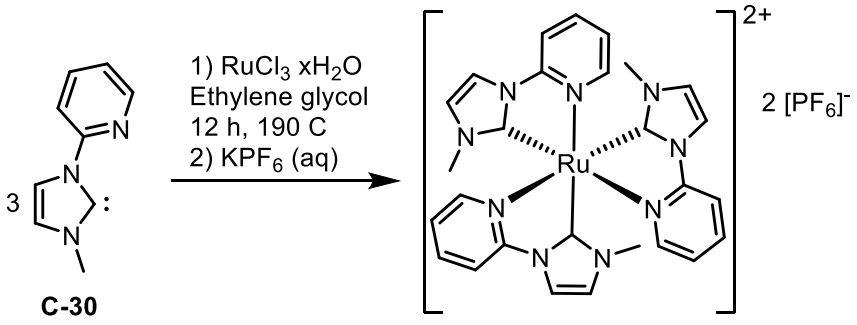

C-30 **Ru-98**

Scheme 5.10: Proposed alternative synthesis of known photosensitizer **Ru-98** based on route to **Ru-57** developed in this work.

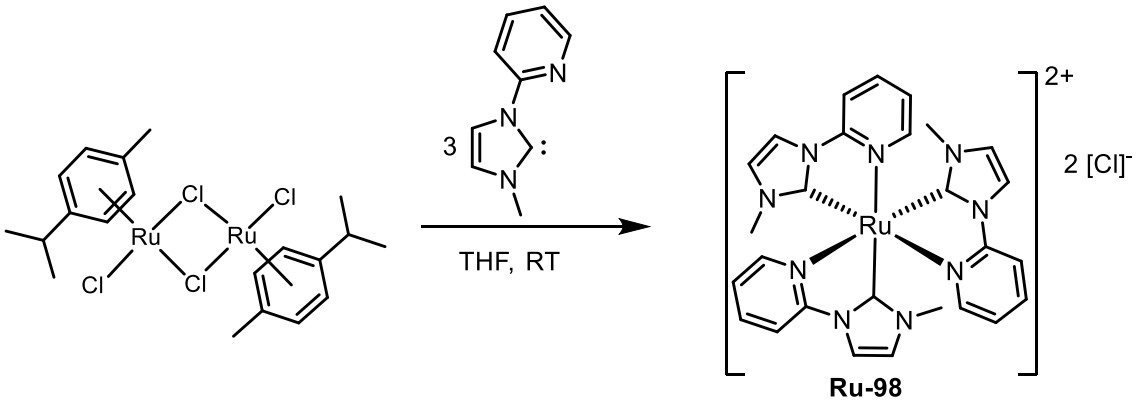

5.4 Zinc Nucleophiles as an Alternative to Silver and Thallium for Transmetalation

Preliminary results indicate that zinc nucleophiles are kinetically but not thermodynamically competent for the installation of $C_6F_5O^-$ on **HII**. The thermodynamic outcome appears partially dependent on the ruthenium substrate, as installation of $C_6F_5O^-$ on **Ru-84** seems to proceed to completion. Given that under no tested conditions did the reaction with **HII** consume more than 50% of available zinc-aryloxide bond, it seems that $Zn(OC_6F_5)_2$ is more thermodynamically competent as an aryloxide source than $Zn(OC_6F_5)Cl$, and that the latter may in fact be acting as a source of chloride in this reaction. It may be possible to force the reaction to completion by using a stoichiometric amount of (thermodynamically competent, kinetically incompetent) $NaOC_6F_5$ and a catalytic amount of $ZnCl_2$, thus allowing zinc to act as an anionic ligand transfer agent. Alternatively, using a large excess of $Zn(OC_6F_5)_2$ should allow complete conversion of **HII**, although at the expense of a more laborious workup.

If this zinc-based approach to aryloxide installation is successful, H_2IMes and CAAC derivatives of the unusually high-performing IMes catalysts **Ru-28** and **Ru-57** should immediately be targeted (Figure 5.2). The CAAC derivatives **Ru-101** and **Ru-102** are of particular interest, as catalysts bearing this CAAC ligand have been shown to decompose almost exclusively by BMC, and bulky pseudohalide ligands are anticipated to prevent this decomposition route. **Ru-101** and **Ru-102** may therefore offer unprecedented catalyst longevity.

Figure 5.2: Structures of known high-performance pseudohalide-functionalized Ru metathesis catalysts bearing the generally low-performance NHC IMes and proposed variants bearing higher performance H_2IMes or CAAC ligands. To be accessed using Zn as a transmetalating agent rather than Tl.

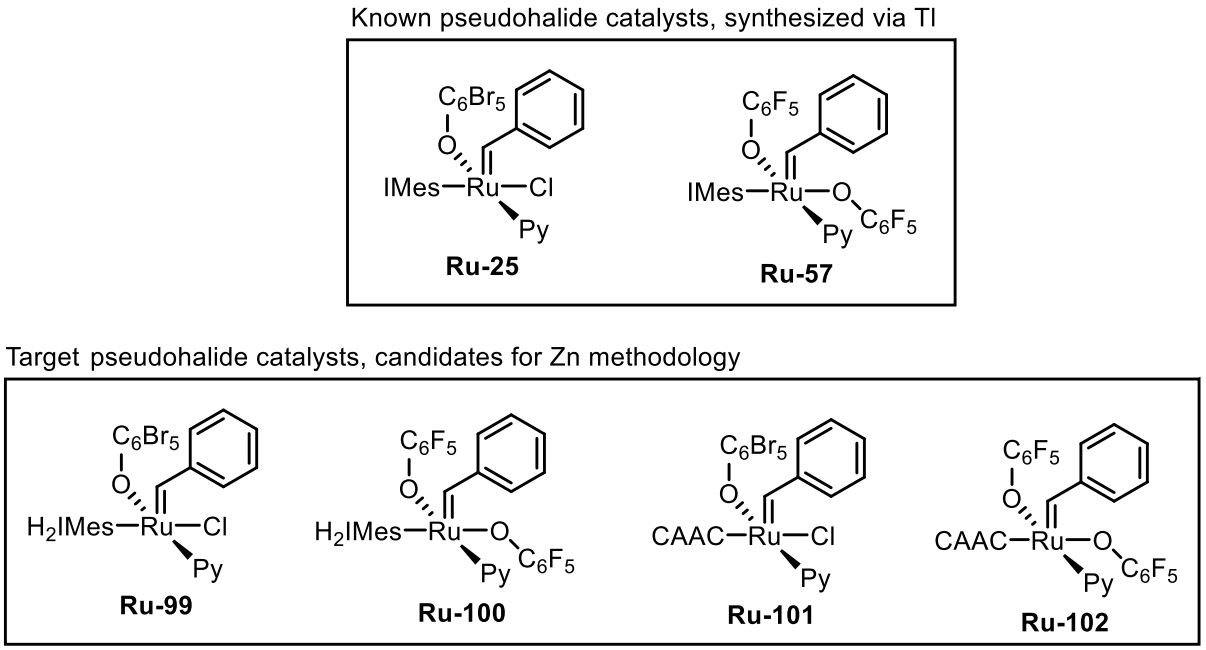

Additionally, the generality of the use of Zn nucleophiles for otherwise challenging transmetalations should be investigated. As outlined in Chapter 3, there are examples across the d-block of complexes that do not transmetalate with group 1 or 2 nucleophiles but will with Ag or Tl nucleophiles. Aryloxide installation on $MnCl(NtBu)_3$ and β-diketoiminate installation on $[Pd(PPh_3)MeCl]_2$ would be excellent test reactions to probe the effectiveness of zinc nucleophiles for transmetalation with both early and late transition metals.

5.5 Confirmation of Low-Valent Alkylidene and Evaluation as Metathesis Catalyst

The observation of a broad signal at ~14.2 ppm is an exciting early indicator for the successful synthesis of low-valent alkylidene **Ru-88**, but synthesis of the tentatively assigned **Ru-88** must be replicated and the identity of the product confirmed. Isolation should be achieved by first removing C_6F_5OH by addition of NEt_3 and passing through Celite to remove the resultant salt. Precipitation from a concentrated pentane solution, potentially under cooling in a dry-ice ethanol bath should then yield the isolated product. Alternatively, given the apparent high solubility of **Ru-88** in hexanes, precipitation from water or methanol may be possible. This would not be an option with parent complexes **Ru-85** or **Ru-86** (which are similarly highly soluble in hexanes), as the Ru-alkyl and Ru-alkoxide functionalities are basic enough to be sensitive to protic media. Ru-alkylidenes, however, are generally tolerant of protic solvents, and **Ru-88** is already known to tolerate the presence of C_6F_5OH, which is significantly more acidic than H_2O or MeOH. Recrystallization from minimum THF via addition of H_2O or MeOH may kill two birds with one stone; furnishing crystals

of **Ru-88** and washing away C_6F_5OH with the aqueous supernatant. X-ray quality crystals will allow unambiguous structural assignment.

Once **Ru-88** has been confirmed, it should be evaluated as a metathesis catalyst. Ring-closing metathesis of DDM is a benchmark reaction commonly used for this purpose by the Fogg group (Scheme 5.12). As this is the first generation low-valent metathesis catalyst, poor performance relative to current state-of-the-art high-valent catalysts should not be entirely unexpected.

Scheme 5.12: RCM of DDM

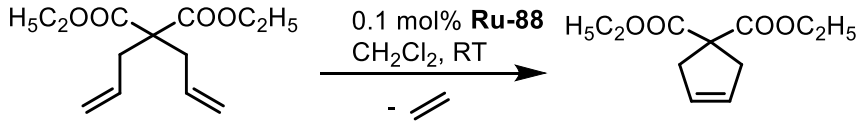

Regardless of the outcome of metathesis screening (high metathesis activity, poor metathesis activity, or metathesis inactive), a second-generation of low-valent alkylidene should be targeted by replacing the p-cymene ligand to bring the system more in line with the geometric properties of known high-valent metathesis catalysts (Figure 5.3). As a result of the higher electron density on ruthenium, higher lability of stabilizing ligands relative to known high-valent catalysts is anticipated. While facile dissociation of one ligand is desirable for catalyst initiation, further loss of labile ligands may lead to catalyst death and therefore poor metathesis performance. It may therefore be desirable to replace the labile monodentate pyridine ligands in structures like **Ru-88** or **Ru-103** with chelating ligands. This could be achieved with known tridentate variants of H_2IMes (as in **Ru-106**), which would offer maximum stability. Alternatively, combining a monodentate carbene with a bidentate stabilizing ligand (such as 2,2'-bipyridine (bipy) as in **Ru-108**, or 1,2-bis(dimethylphosphino)ethane (dmpe) as in **Ru-107**) should offer both improved stability and stereoselectivity by the same principal as known high-valent dithiolate catalysts. Combining a bidentate carbene (both NHC[9] and CAAC[10] variants of which are known) and a bidentate stabilizing ligand (as in **Ru-104** and **Ru-105**) may provide the best combination of stability and stereoselectivity. While this does require exceeding the typical coordination number of 5 for known metathesis catalysts, high-performing catalysts with coordination number 6 are known.[11] So long as ligands are carefully selected to prevent steric clash with incoming olefin, catalyst performance need not be negatively impacted.

Figure 5.3: Proposed second-generation low-valent Ru metathesis catalysts, grouped according to ligand denticity

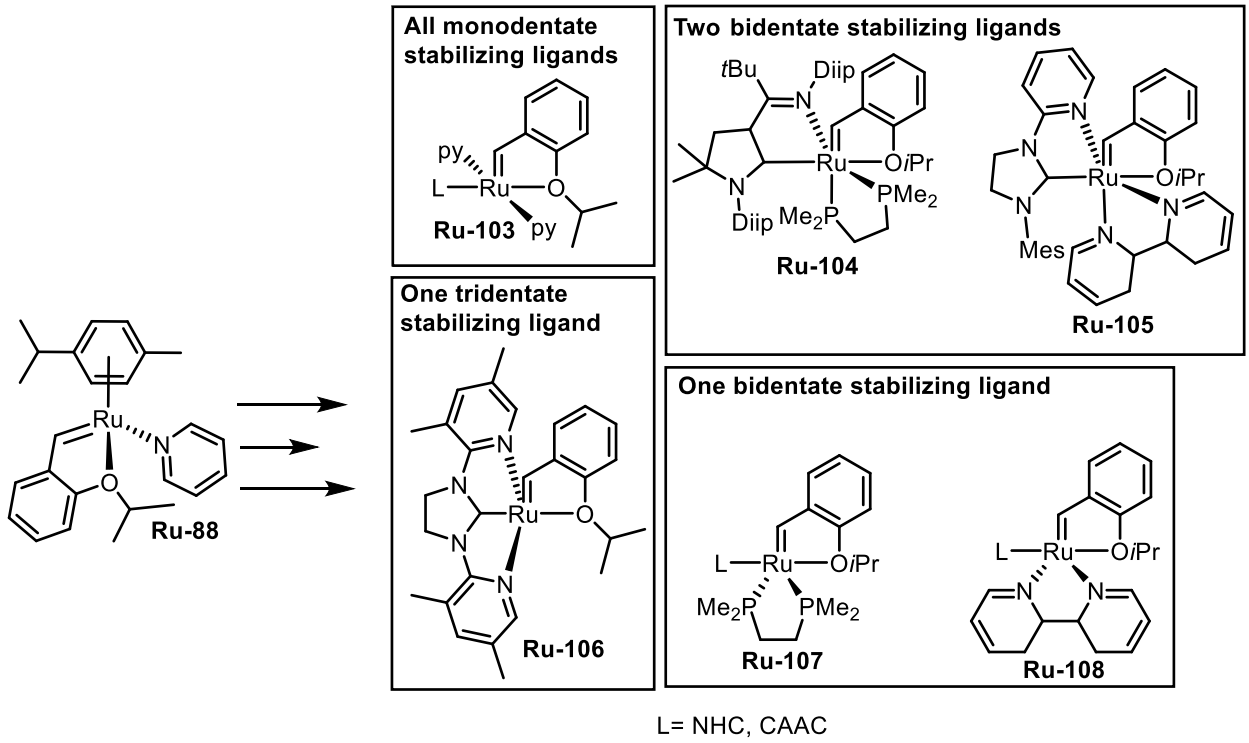

Once **Ru-88** or its p-cymene-free derivatives have been established as metathesis-active, their decomposition routes should be evaluated and compared to those established for high-valent metathesis catalysts. Of particular interest is the susceptibility of low-valent alkylidenes to nucleophilic attack, to which they are anticipated to be resistant. Even if low-valent alkylidenes prove to be poorly active or inactive in metathesis, evaluation of *why* they underperform known high-valent metathesis catalysts is anticipated to lead to structural and mechanistic insights that will guide the development of future catalysts.

5.6 Oxidation of Low-Valent Alkylidenes: Back-Door Access to High Valent Systems?

While reduction of known high-valent metathesis catalysts was not an effective route to low-valent alkylidenes, leading instead to rapid decomposition and loss of alkylidene, treatment of low-valent alkylidene **Ru-88** with a chlorinating agent may grant access to high-valent metathesis catalysts. If 1 equiv. PPh_3Cl_2 is used as the chlorinating agent, **Ru-39**, a highly useful precursor to second generation and CAAC-functionalized Hoveyda-type catalysts is the expected product (Scheme 5.14). Thus, even if low-valent alkylidenes turn out to be ineffective metathesis catalysts, they may enable a diazo-free, high yield route to high-valent benzylidenes. Particularly exciting is the potential to directly access nitro-Grela type catalysts by using a 2-(O*i*Pr)5-$(NO_2)C_6H_3CH_2$ ligand in place of *o*-(O*i*Pr)$C_6H_3CH_2$ (Scheme 5.15). Note that the nitro functionality is not compatible with highly basic Grignard reagents, but is generally tolerated by the milder alkylzinc analogues.

Therefore, initial installation of the nitro-variant of the benzyl ligand must be performed via salt metathesis with an alkylzinc rather than a Grignard type nucleophile.

Scheme 5.14: Proposed synthesis of known high-valent metathesis catalysts via oxidative chlorination of **Ru-88**

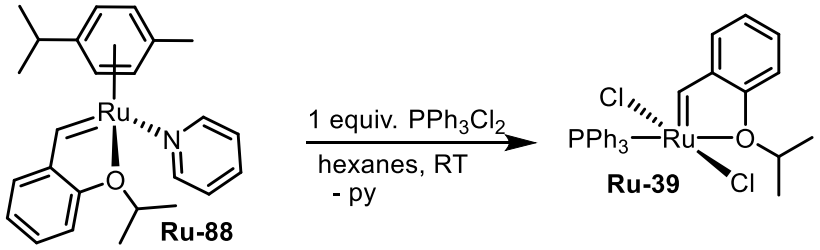

Scheme 5.15: Modification of the benzyl ligand in **Ru-88** to include a nitro group para to O*i*Pr should allow access to the Nitro-Grela type catalyst **nG-PPh$_3$**.

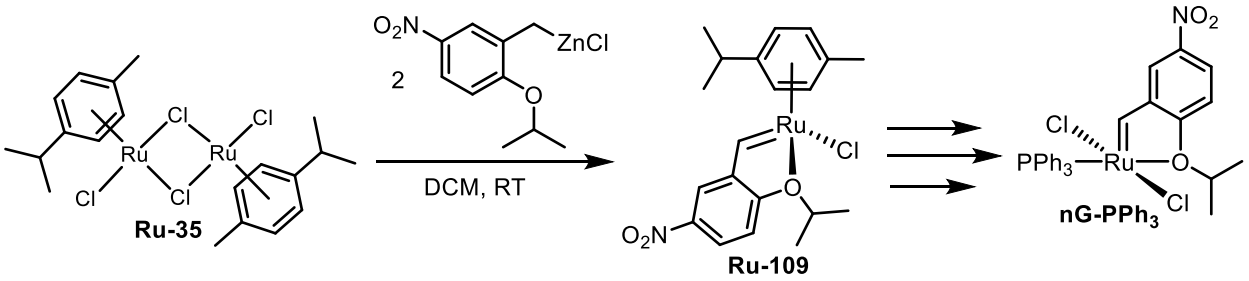

Additionally, the rather mild conditions and user-friendly procedure for the in-situ preparation of **Ru-88** suggest the possibility of a rapid and facile one-pot preparation of known high-valent alkylidenes starting from commercially available **Ru-35** (Scheme 5.16).

Scheme 5.16: Proposed one-pot synthesis of **Ru-39** starting from commercially available **Ru-35**. It is hoped that by carrying out the reaction in either C_6H_6 or hexanes, both $MgCl_2$ and [$C_6F_5O^-$][$^+NHEt_3$] will precipitate from solution and therefore not interfere with the final chlorination step. Otherwise a filtration step will need to be added to remove these salts prior to chlorination of **Ru-88**

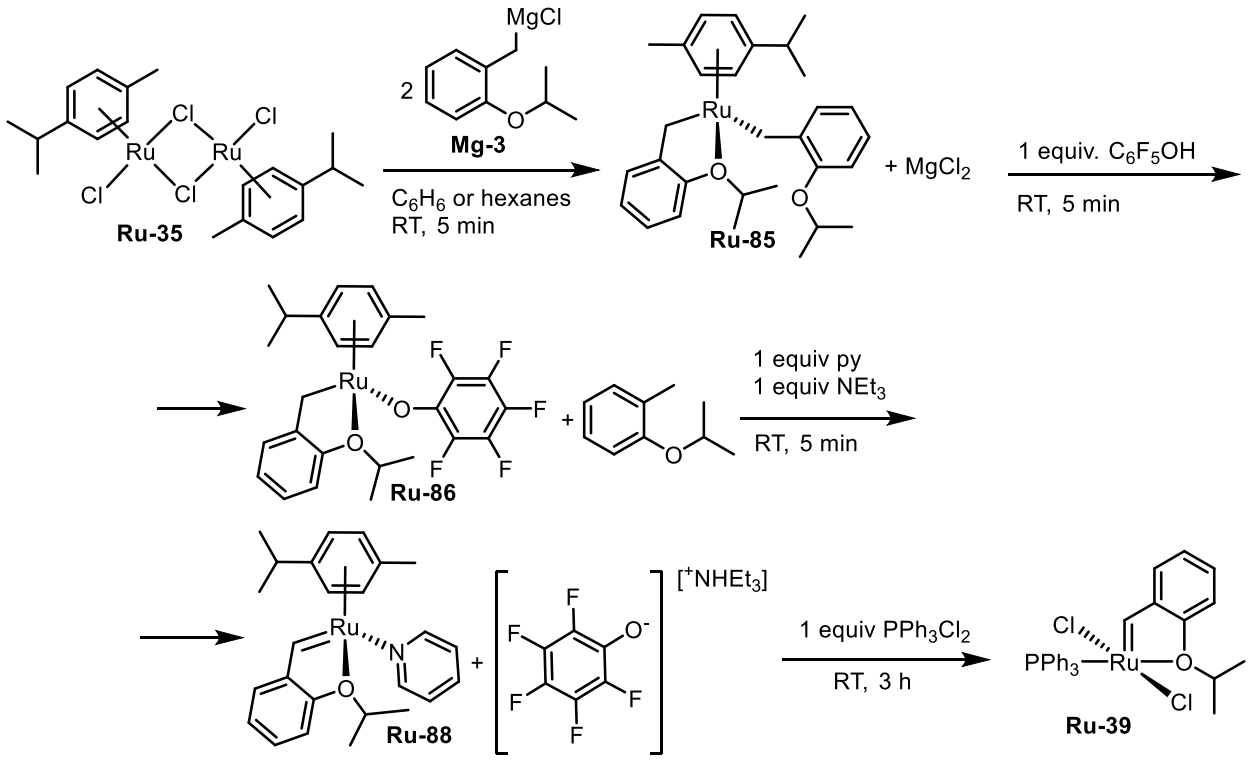

5.7 Leveraging Mg-3: An Empirical Measure of Catalyst Oxidation State

As touched upon in Chapter 4, the oxidation state of current generation metathesis catalysts is not obvious. The *o*-O*i*Pr benzyl ligand developed in this work (Scheme 5.17) represents an opportunity to use experimental rather than computational methodologies to get an empirical measure of electron density on ruthenium metathesis catalysts to assess oxidation state. X-ray Absorption Spectroscopy (XAS) provides information on the electronic structure around atomic nuclei and is routinely used to evaluate oxidation state,[12] including for transition metal complexes.[13-14] In order to evaluate the oxidation state of ruthenium metathesis catalysts via XAS, a complex of unambiguous oxidation state is required as a calibrant. As XAS spectra are highly dependent on the ligand environment, this calibrant should be as similar to a metathesis catalyst as possible: ideally, it should be identical except for the oxidatively ambiguous alkylidene ligand. Installing the *o*-O*i*Pr benzyl ligand on a Ru(III) trichloride substrate, such as $RuCl_3(py)_3$ (**Ru-110**) will produce an unambiguously Ru(III) alkyl analogue to Hoveyda-type alkylidene complexes (**Ru-111**, Scheme 5.18). The corresponding pyridine-functionalized Hoveyda-type alkylidene (**Ru-112**) should be accessible via a diazo reaction with **Ru-94** (Scheme 5.19).

Scheme 5.17: The *o*-O^{i}Pr benzyl ligand developed in this thesis, installed via **Mg-3**

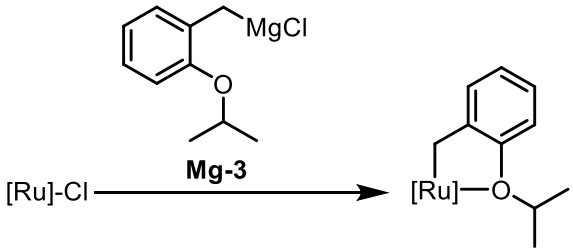

Scheme 5.18: Proposed synthesis of **Ru-111**

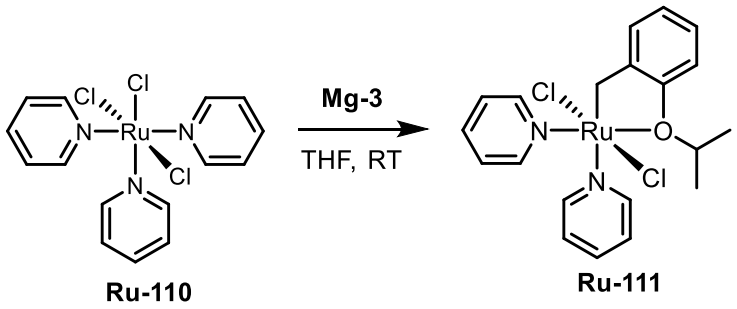

Scheme 5.19: Proposed synthesis of **Ru-112**

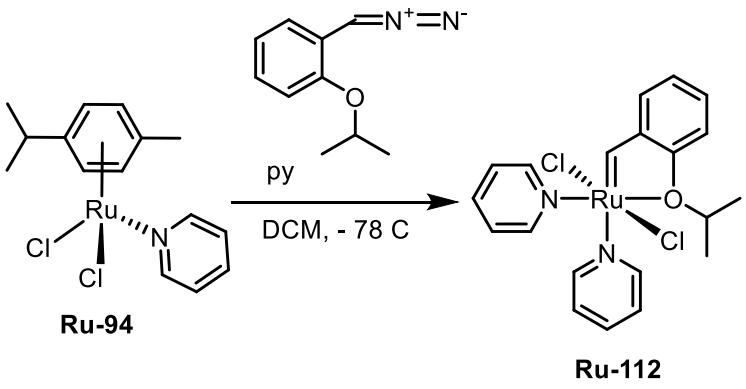

Comparison of the Ru-K edges of the XAS spectra for **Ru-111** and **Ru-112** will then allow assignment of oxidation state: if the Ru-K edge of **Ru-112** leads that of **Ru-111**, then the electron density is higher than the Ru(III) calibrant and the oxidation state of the alkylidene is +2. If the Ru-K edge trails that of **Ru-112**, then the electron density is lower than the Ru(III) calibrant and the oxidation state is +4. For practical reasons (e.g. to avoid bimolecular coupling of the alkylidene in **Ru-112**), it may be necessary to substitute pyridine for a less labile ligand. So long as the oxidation state is preserved, it is unimportant which ligand is chosen. 1,10-phenanthroline or 2,2'-bypyridine are operationally simple options that should be compatible with both the benzyl and benzylidene ligand. Bulky NHC or phosphine ligands should be avoided if possible, as this work has found the benzyl ligand to be incompatible with these ligand types on other substrates.

5.8 Alternative Use Case for Benzylruthenium Complexes Ru-84 and Ru-85—Ligand Installation Via Deprotonative Metalation

The route to **Ru-86** via deprotonative metalation discussed in Section 4.23 highlights an additional use case for stable, easily accessible benzylruthenium complexes as a potentially versatile and robust vector for anionic ligand installation on ruthenium. So long as the protonated form of the desired anionic ligand is sufficiently acidic, reaction with **Ru-84** or **Ru-85** should produce the mono- or bis- installation product respectively (Scheme 5.20). In the case of particularly bulky or poorly bridging ligands, where the dimeric structures **Ru-113** or **Ru-114** may be disfavoured, addition of an L-donor such as pyridine will prevent decomposition due to coordinative unsaturation (Scheme 5.21).

Scheme 5.20: Proposed synthesis of chloride-substituted derivatives of **Ru-35**. Addition of 1 or two equivalents of HX to **Ru-84** or **Ru-85** will respectively produce **Ru-113** or **Ru-114**.

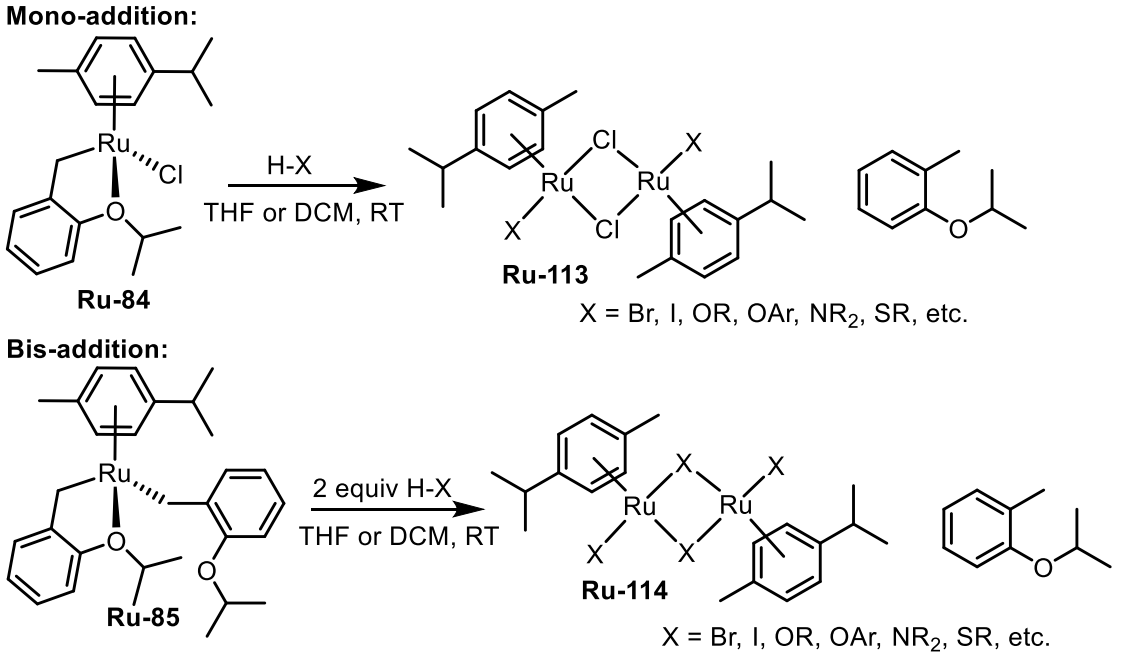

Scheme 5.21: Chloride-substituted dimers of type **Ru-114** may dissociate, producing coordinatively unsaturated monomers of type **Ru-115**. In such cases, the monomer may be trapped by adding an equivalent of pyridine.

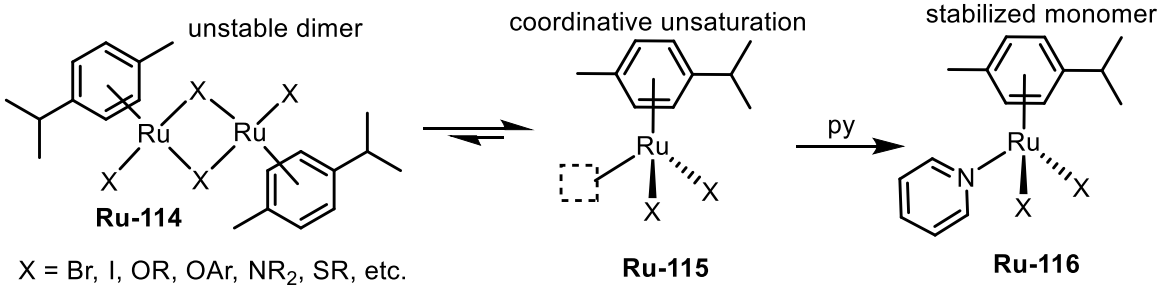

For metathesis applications, indenylidene or alkylidene may then be installed via conventional means, offering direct access to metathesis catalysts with tailored anionic ligands (Scheme 5.22). This approach is inherently less atom-economical than the Na-Zn methodology proposed in Section 3.4.2, but may be preferable for ligands bearing functional groups that are incompatible with Na bases (e.g. nitro, ester groups), or if unforeseen complications arise in the Na-Zn-transmetalation route.

Scheme 5.22: Sequential reaction of **Ru-117** with 1 equiv H_2IMes followed by treatment with the Hoveyda-type aryldiazomethane reagent is expected to produce pseudohalide-functionalized catalysts. Route to **Ru-58** pictured, but any pseudohalide is expected to be accessible, provided that the precursor **Ru-114** can be synthesized

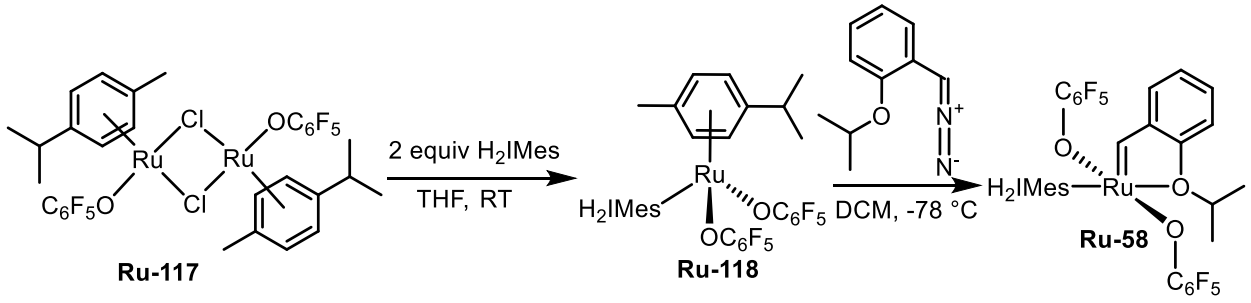

The applicability of ligand installation via deprotonative metalation need not be limited to anionic ligands, the protonated forms of neutral ligands offer the possibility of concomitant L and X ligand installation. For example, treatment of **Ru-84** with 1 equiv of the HCl adduct of H_2IMes should furnish known complex **Ru-33** (Scheme 5.23). While nominally less atom-economical than the most recently published synthesis of **Ru-33** (Scheme 5.24), this route offers several advantages. The current method requires large solvent volumes and very slow addition of reagents in order to avoid over-addition of free NHC to poorly soluble **Ru-35**.[15] The process of generating free H_2IMes is itself both time and solvent intensive,[16] further adding to the material and ecological costs of the route. The deprotonative metalation approach, by contrast, does not require isolation of the free carbene, eliminating the possibility of bis-addition of NHC. Rapid combination of the two reagents in a relatively small amount of solvent should be feasible, greatly reducing operational complexity and solvent use. Since NHC deprotonation and installation should in principle be concomitant, it may also be possible to use CH_2Cl_2 as the solvent system (typically avoided, as free NHC will react with CH_2Cl_2), both further reducing the volume of solvent required and accelerating the rate of reaction as the HCl adduct of H_2IMes is significantly more soluble in CH_2Cl_2 than THF.

Scheme 5.23: Proposed alternative synthesis of **Ru-33**. Treatment of **Ru-84** with 1 equiv H_2IMes·HCl at room temperature and in the absence of light is expected to produce **Ru-33** without the need for large volumes of solvent or the isolation of free carbene.

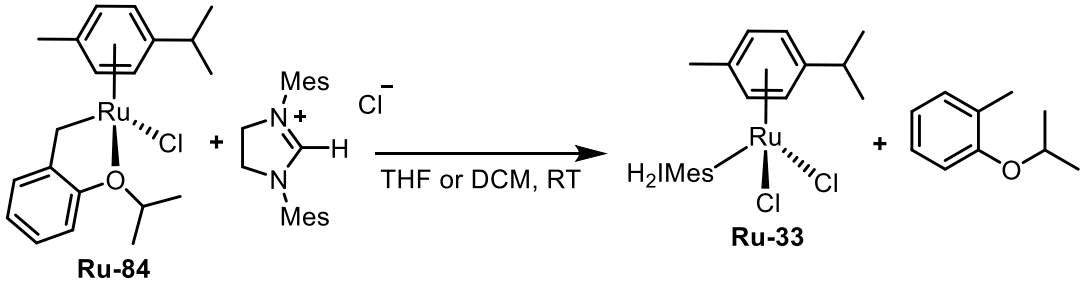

Ru-84 **Ru-33**

Scheme 5.24: Current state-of-the-art synthesis of **Ru-33**. Success of this reaction requires large volumes of THF, owing to the poor solubility of **Ru-35** in THF. H_2IMes must also be added slowly (over the course of ca. 1 hour) as a dilute solution in THF in order to prevent bis addition of the free carbene.

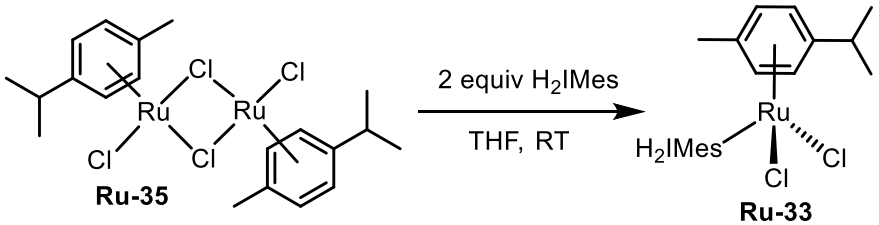

Ru-35 **Ru-33**

Performing the reaction at elevated temperature (e.g. 65 °C) and in the presence of at least 3 equiv. pyridine should also provide an improved one-pot synthesis of **Ru-50** (Scheme 5.25)

Scheme 5.25: Proposed alternative synthesis of **Ru-50**. Treatment of **Ru-84** with 1 equiv H_2IMes·HCl and at least 3 equiv pyridine at elevated temperature is expected to produce **Ru-50** via thermally labile **Ru-33.**

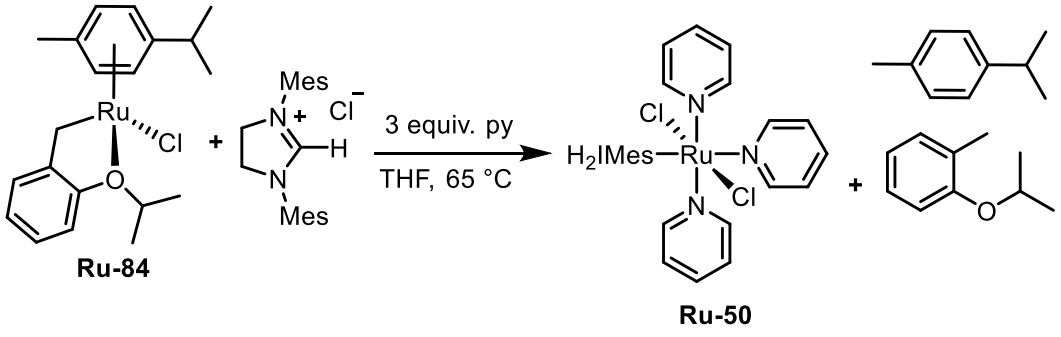

Ru-84 **Ru-50**

By tailoring the counterion of the protonated NHC, both NHC and pseudohalide installation may be accomplished in a single step, granting access to RuClX(NHC) (X ≠ Cl) platforms (Scheme 5.26). Starting instead from **Ru-85**, RuX_2(NHC) motifs may also be targeted (Scheme 5.26).

Scheme 5.26: Proposed synthesis of RuClX(η^6p-cymene)(H_2IMes) (X ≠ Cl) (**Ru-119**). Reaction of **Ru-84** with 1 equiv H_2IMes·HX is expected to produce **Ru-119.**

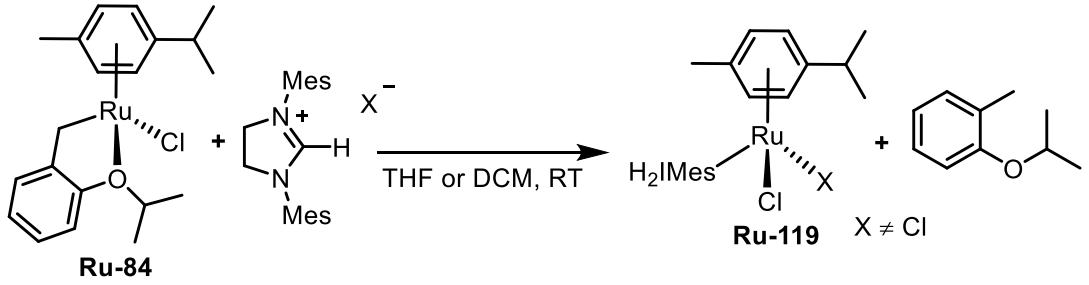

Scheme 5.27: Proposed synthesis of RuX_2(η^6p-cymene)(H_2IMes) (X ≠ Cl) (**Ru-120**) Sequential reaction of **Ru-85** with 1 equiv H-X followed by 1 equiv H_2IMes·HX is expected to produce **Ru-120**.

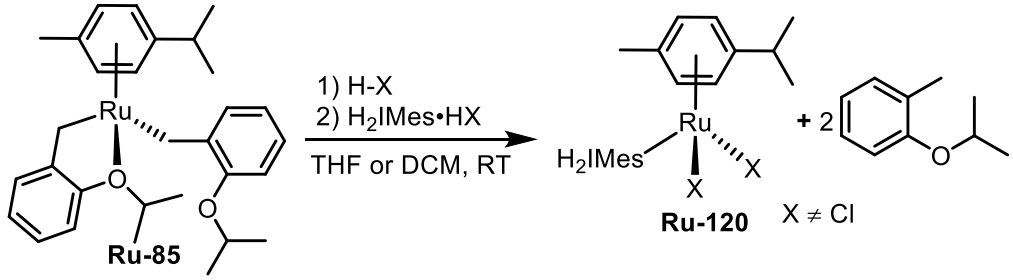

The deprotonative metalation approach also offers a potential solution to the problem of installing cyclic alkyl-amino carbene (CAAC) ligands on ruthenium. CAAC-bearing catalysts significantly outperform their NHC-functionalised predecessors, but CAAC installation remains challenging and low-yielding. The free carbenes for CAACs appear to be less stable than NHCs: they are not easily isolated, and are therefore typically generated in-situ and used without further purification. Attempts within the Fogg group to isolate **Ru-121**, a CAAC-analogue of **Ru-35** and potential entry point to the high-yield synthesis of CAAC-functionalized catalysts have been frustrated at least partly by the poor stability of free CAAC (a synthetic route that requires a prolonged, slow addition is not expected to be compatible with short-lived reagents). Deprotonative metalation eliminates the need to generate free CAAC in a separate step and may therefore allow unprecedented access to CAAC-derivatives of **Ru-35** (Scheme 5.28). Conventional alkylidene installation techniques should then provide CAAC-functionalized catalysts in high overall yield.

Scheme 5.28: Proposed installation of CAACs on ruthenium via deprotonative metalation of CAAC·HCl adduct by **Ru-84**.

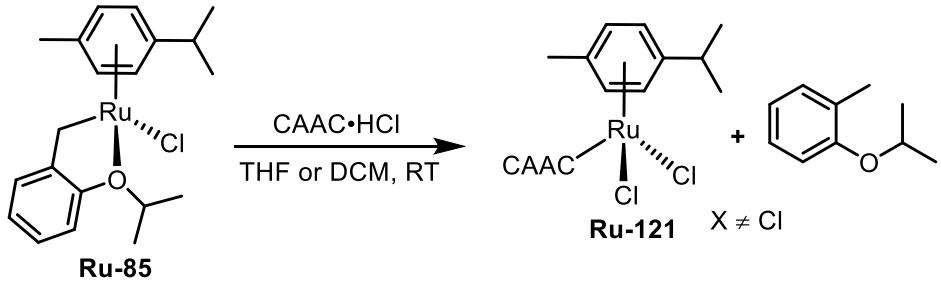

5.8 Full Characterization of New Ruthenium Complexes

Ru-56c requires a ^{13}C NMR spectrum and high-res mass spectrometry for complete characterization. **Ru-84** requires a ^{13}C NMR spectrum, high-res mass spectrometry, and X-ray or neutron diffraction crystallography is desirable to confirm and explain the unusual spectroscopic properties of the benzyl protons. **Ru-85**, **Ru-86**, and **Ru-88** each require ^{13}C NMR analysis, high-res mass spectrometry, and proper isolation to determine a yield. Isolation should be achieved by cooling a concentrated pentane solution of the crude products until crystallization occurs. **Ru-86** and **Ru-88** would benefit from ^{1}H-^{1}H COSY and ^{1}H-^{13}C HSQC experiments to aid in assigning ambiguous signals in their respective ^{1}H NMR spectra.

5.9 Concluding Statement

Although the field of olefin metathesis may be considered increasingly mature at this point, this thesis demonstrates that there are still significant and exciting developments to be made by exploring the fundamentals of organometallic synthesis. An α-hydrogen-abstraction-based route to low-valent ruthenium alkylidenes appears to have been achieved, and should lead to several fruitful advancements in the understanding of olefin metathesis.

5.10 References

(1) Simmons, H. E.; Smith, R. D., A New Synthesis of Cyclopropanes from Olefins. *J. Am. Chem. Soc.* **1958,** *80*, 5323-5324.
(2) Savos'kin, M. V.; Kapkan, L. M.; Vaiman, G. E.; Vdovichenko, A. N.; Gorkunenko, O. A.; Yaroshenko, A. P.; Popov, A. F.; Mashchenko, A. N.; Tkachev, V. A.; Voloshin, M. L.; Potapov, Y. F., New Approaches to the Development of High-Performance Hydrocarbon Propellants. *Russ. J. Appl. Chem.* **2007,** *80*, 31-37.
(3) Feringa, B. L., The Art of Building Small: From Molecular Switches to Motors (Nobel Lecture). *Angew. Chem., Int. Ed.* **2017,** *56*, 11060-11078.
(4) Yamada, K.; Goto, S.; Nagase, H.; Kyotani, Y.; Hirata, Y., Convenient Methods for Deoxygenation of Epoxides to Olefins. *J. Org. Chem.* **1978,** *43*, 2076-2077.
(5) Wills, V. S.; Zhou, X.; Allen, C.; Holstein, S. A.; Wiemer, D. F., Stereocontrolled Regeneration of Olefins from Epoxides. *Tetrahedron Lett.* **2016,** *57*, 1335-1337.
(6) Wu, F.-L.; Ross, B. P.; McGeary, R. P., New Methodology for the Conversion of Epoxides to Alkenes. *Eur. J. Org. Chem.* **2010,** *2010*, 1989-1998.
(7) Torres, J.; Carrión, M. C.; Leal, J.; Castañeda, G.; Manzano, B. R.; Jalón, F. A., Homoleptic Ruthenium Complexes with N-Heterocyclic Carbene Ligands as Photosensitizers in the Photocatalytic Generation of H2 from Water. *J. Organomet. Chem.* **2019,** *898*, 120880.
(8) Chen, C.; Lu, C.; Zheng, Q.; Ni, S.; Zhang, M.; Chen, W., Synthesis and Structures of Ruthenium–NHC Complexes and Their Catalysis in Hydrogen Transfer Reaction. *Beilstein J. Org. Chem.* **2015,** *11*, 1786-1795.
(9) Kaufhold, O.; Hahn, F. E.; Pape, T.; Hepp, A., Ruthenium(II) and Iron(II) Complexes of N-Pyridyl Substituted Imidazolin-2-Ylidenes. *J. Organomet. Chem.* **2008,** *693*, 3435-3440.
(10) Chu, J.; Munz, D.; Jazzar, R.; Melaimi, M.; Bertrand, G., Synthesis of Hemilabile Cyclic (Alkyl)(amino)carbenes (CAACs) and Applications in Organometallic Chemistry. *J. Am. Chem. Soc.* **2016,** *138*, 7884-7887.
(11) Higman, C. S.; Nascimento, D. L.; Ireland, B. J.; Audörsch, S.; Bailey, G. A.; McDonald, R.; Fogg, D. E., Chelate-Assisted Ring-Closing Metathesis: A Strategy for Accelerating Macrocyclization at Ambient Temperatures. *J. Am. Chem. Soc.* **2018,** *140*, 1604-1607.
(12) Newville, M., Fundamentals of XAFS. *Rev. Mineral Geochem.* **2014,** *78*, 33-74.
(13) Kubin, M.; Guo, M.; Kroll, T.; Löchel, H.; Källman, E.; Baker, M. L.; Mitzner, R.; Gul, S.; Kern, J.; Föhlisch, A.; Erko, A.; Bergmann, U.; Yachandra, V.; Yano, J.; Lundberg, M.; Wernet, P., Probing the Oxidation State of Transition Metal Complexes: a Case Study on how Charge and Spin Densities Determine Mn L-Edge X-ray Absorption Energies. *Chem. Sci.* **2018,** *9*, 6813-6829.
(14) Wilke, M.; Hahn, O.; Woodland, A. B.; Rickers, K., The Oxidation State of Iron Determined by Fe K-Edge XANES—Application to Iron Gall Ink in Historical Manuscripts. *J. Anal. At. Spectrom.* **2009,** *24*, 1364-1372.
(15) Day, C. S.; Fogg, D. E., High-Yield Synthesis of a Long-Sought, Labile Ru-NHC Complex and Its Application to the Concise Synthesis of Second-Generation Olefin Metathesis Catalysts. *Organometallics* **2018,** *37*, 4551-4555.
(16) Arduengo, A. J.; Krafczyk, R.; Schmutzler, R.; Craig, H. A.; Goerlich, J. R.; Marshall, W. J.; Unverzagt, M., Imidazolylidenes, Imidazolinylidenes and Imidazolidines. *Tetrahedron* **1999,** *55*, 14523-14534.

Appendix A: NMR and GC-MS data for new compounds and key experiments described in Chapter 3

Figure A1.1: ^{1}H NMR (300 MHz, $CDCl_3$) spectrum of *o*-(O*i*Pr)(C_6H_4)$CHCl_2$

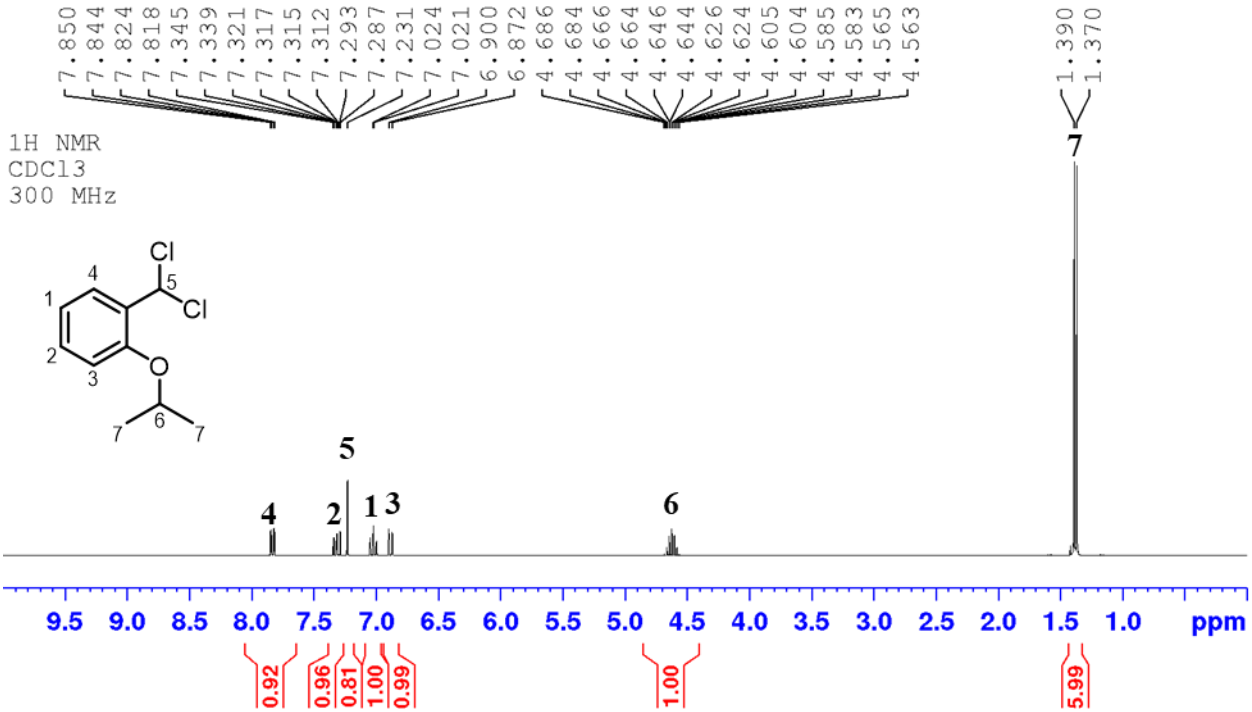

Figure A1.2: GC trace from GC-MS analysis of reaction between Mg-1 and *o*-(O*i*Pr)(C_6H_4)$CHCl_2$. Mass spectra of individual components can be found in Figures A1.3-5

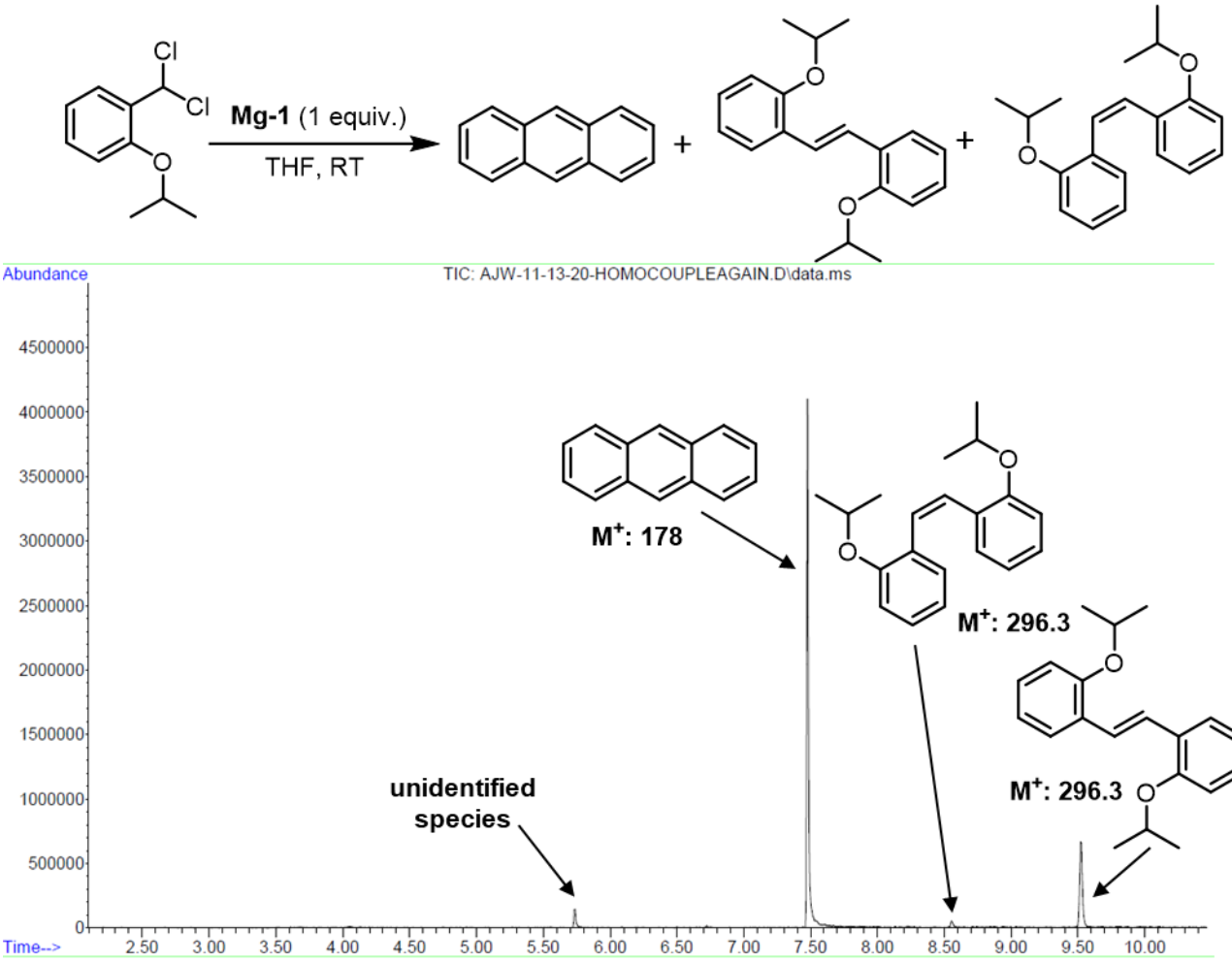

Figure A1.3: Mass spectrum of unidentified species eluting at 5.7 min. Believed to arise from an impurity in *o*-(O*i*Pr)(C_6H_4)$CHCl_2$

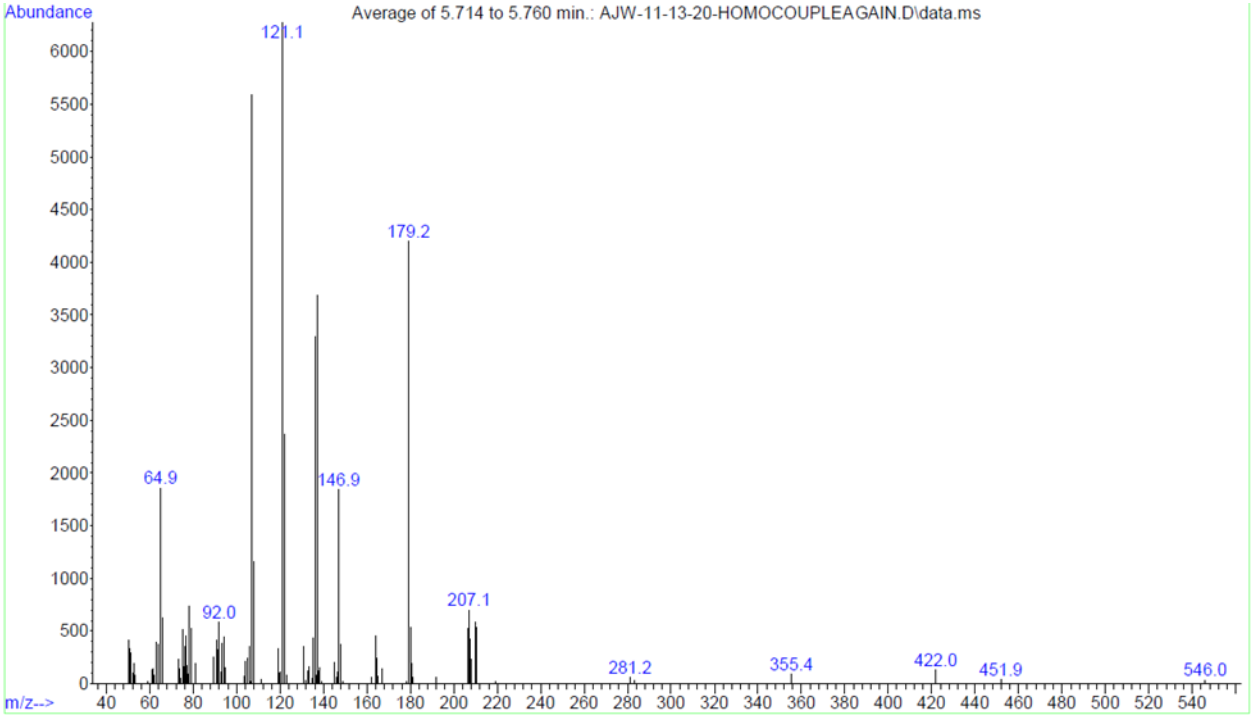

Figure A1.4: Mass spectrum of species eluting at 7.5 min. Identified as anthracene.

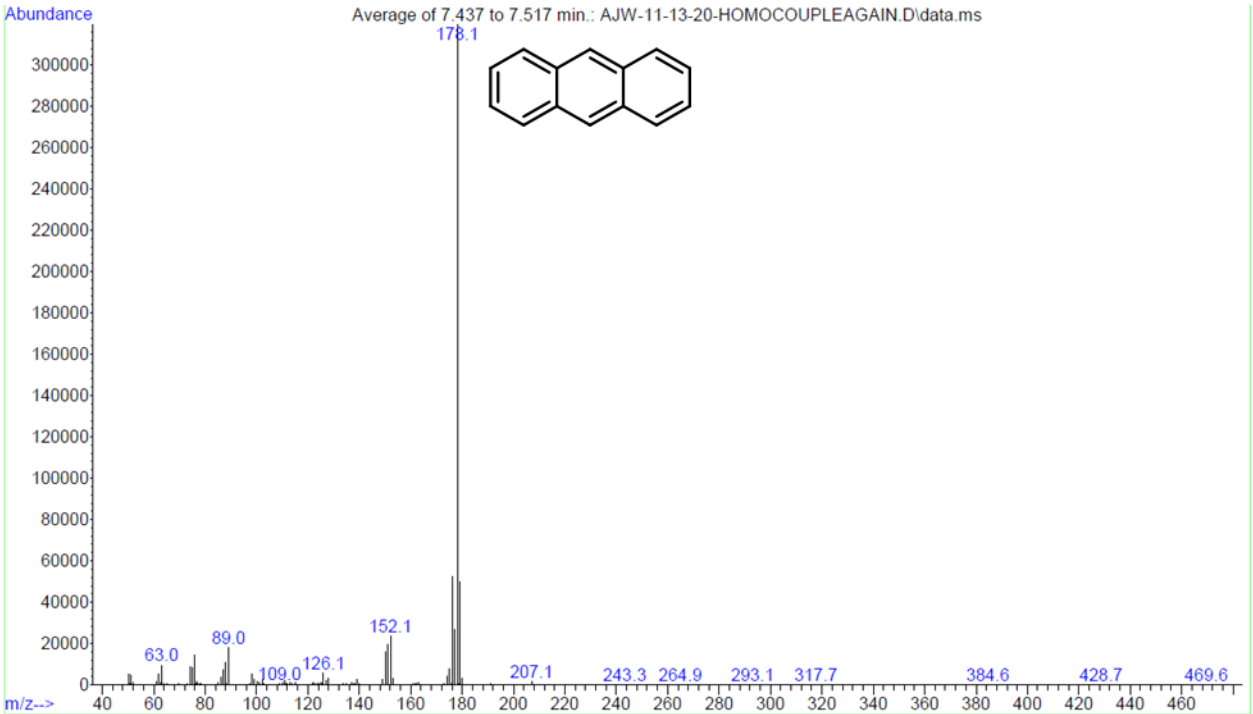

Figure A1.5: Mass spectrum of species eluting at 8.5 min. Identified as (Z)-[*o*-(O*i*Pr)(C_6H_4)]CH=CH[*o*-(O*i*Pr)(C_6H_4)]

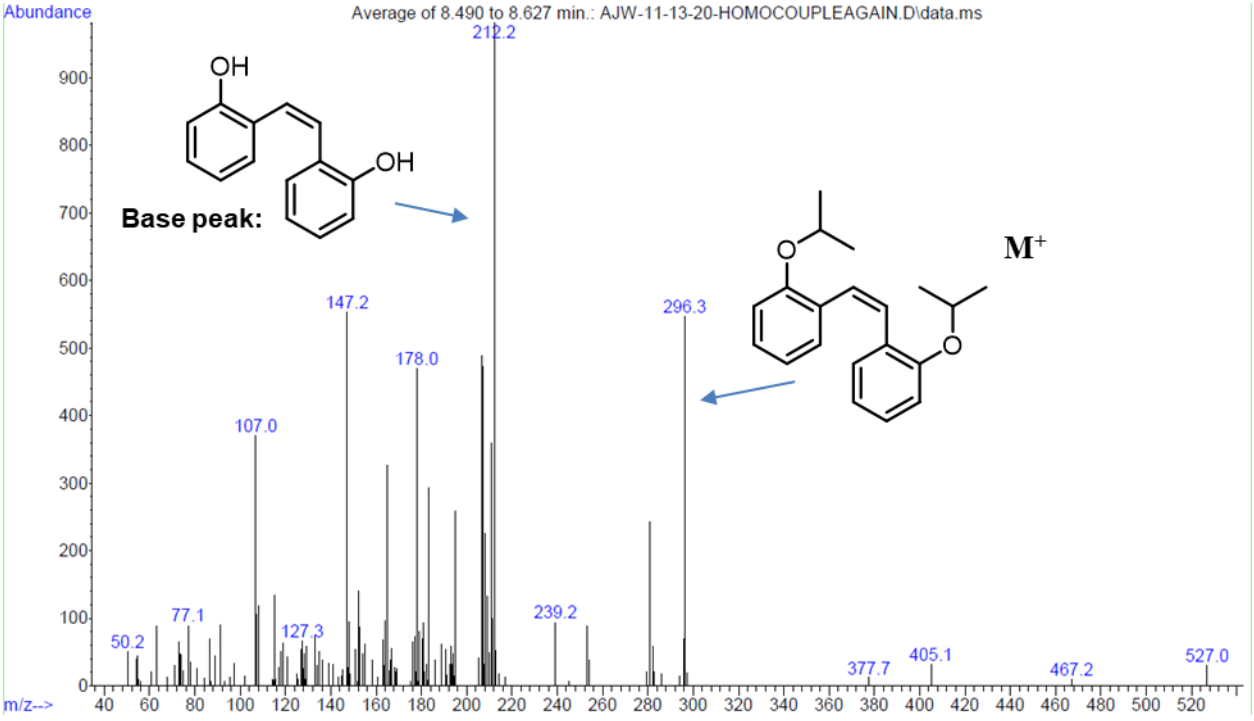

Figure A1.6: Mass spectrum of species eluting at 9.5 min. Identified as (E)-[*o*-(O*i*Pr)(C_6H_4)]CH=CH[*o*-(O*i*Pr)(C_6H_4)]

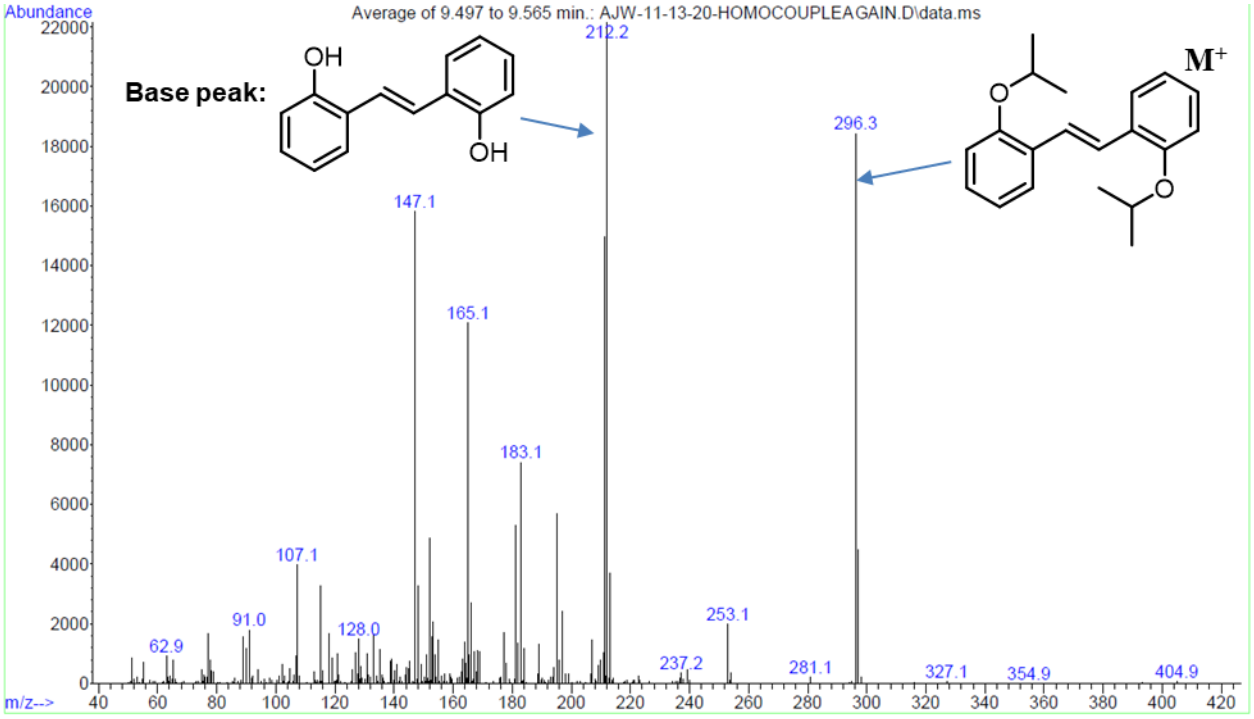

Figure A1.7: ^{1}H NMR (300 MHz, C_6D_6) spectrum of crude product mixture from attempted synthesis of **GI** via in-situ generated carbenoid PhCHClMgCl

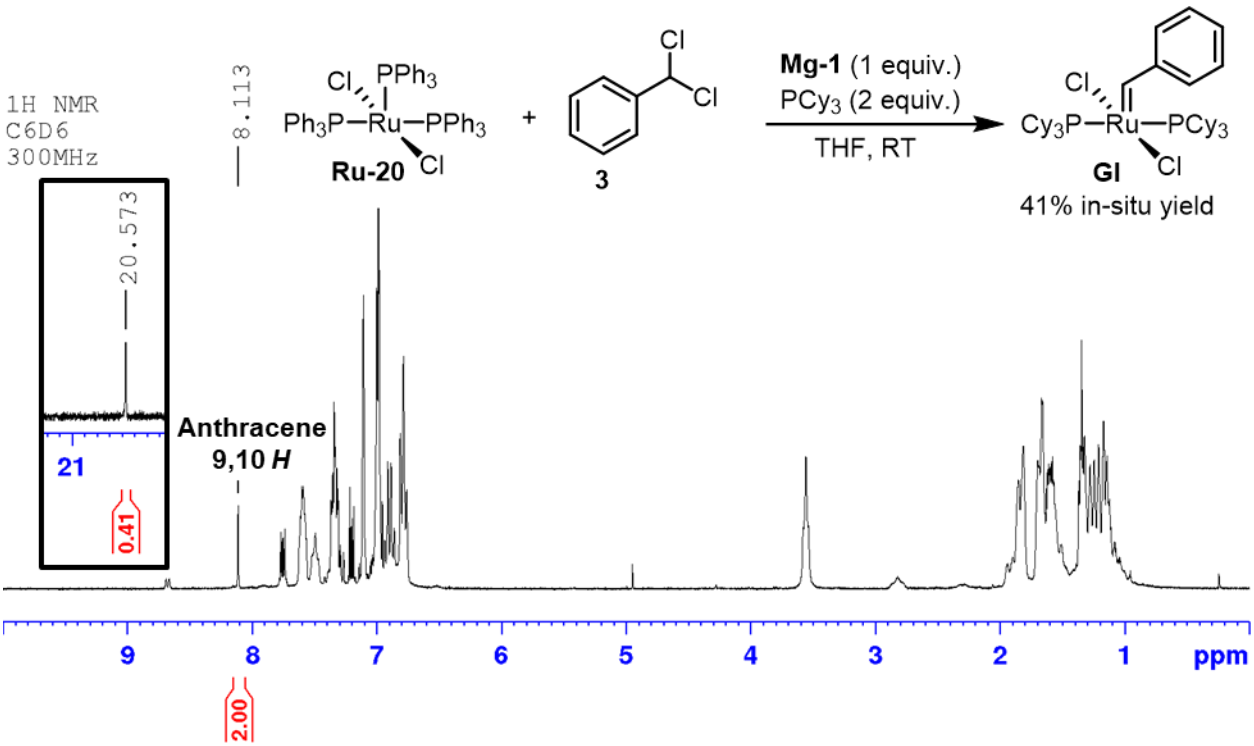

Figure A1.8: ^{1}H NMR (300 MHz, C_6D_6) spectrum of crude product mixture from attempted synthesis of **HII** via in-situ generated carbenoid **Mg-2**

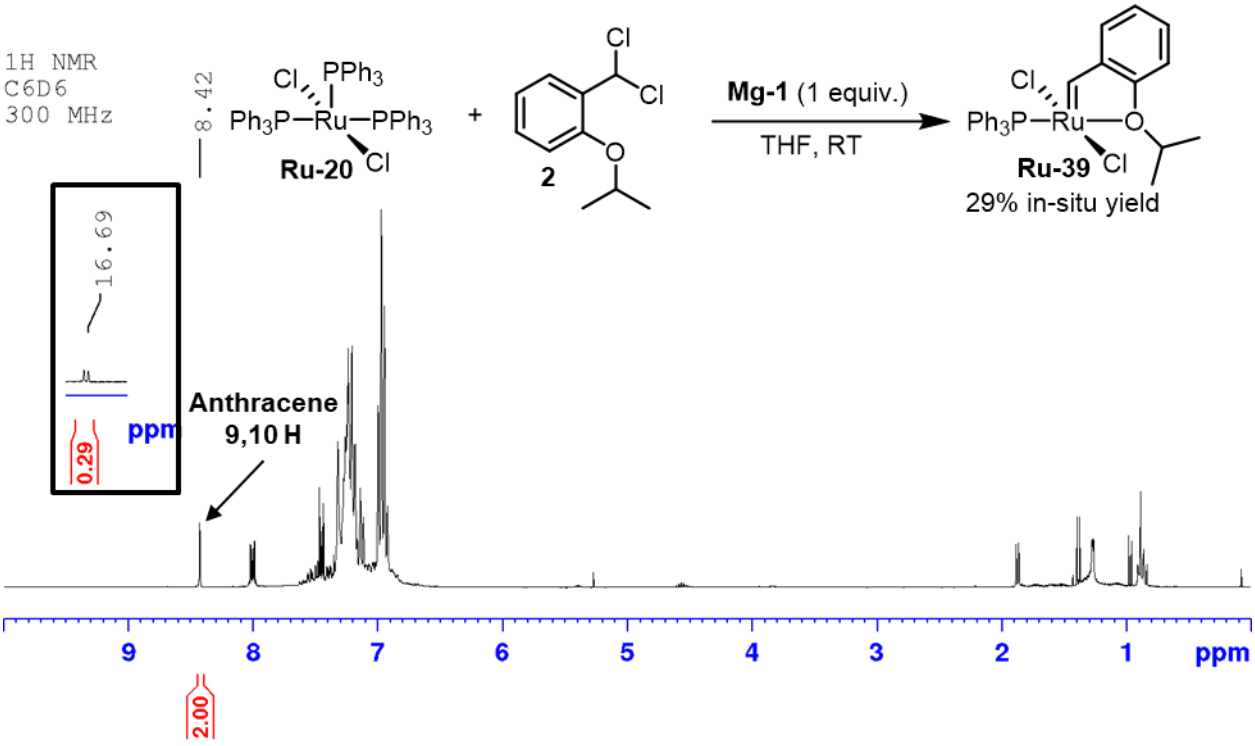

Figure A1.9: ^{1}H NMR (300 MHz, C_6D_6) spectrum of **Ru-50**

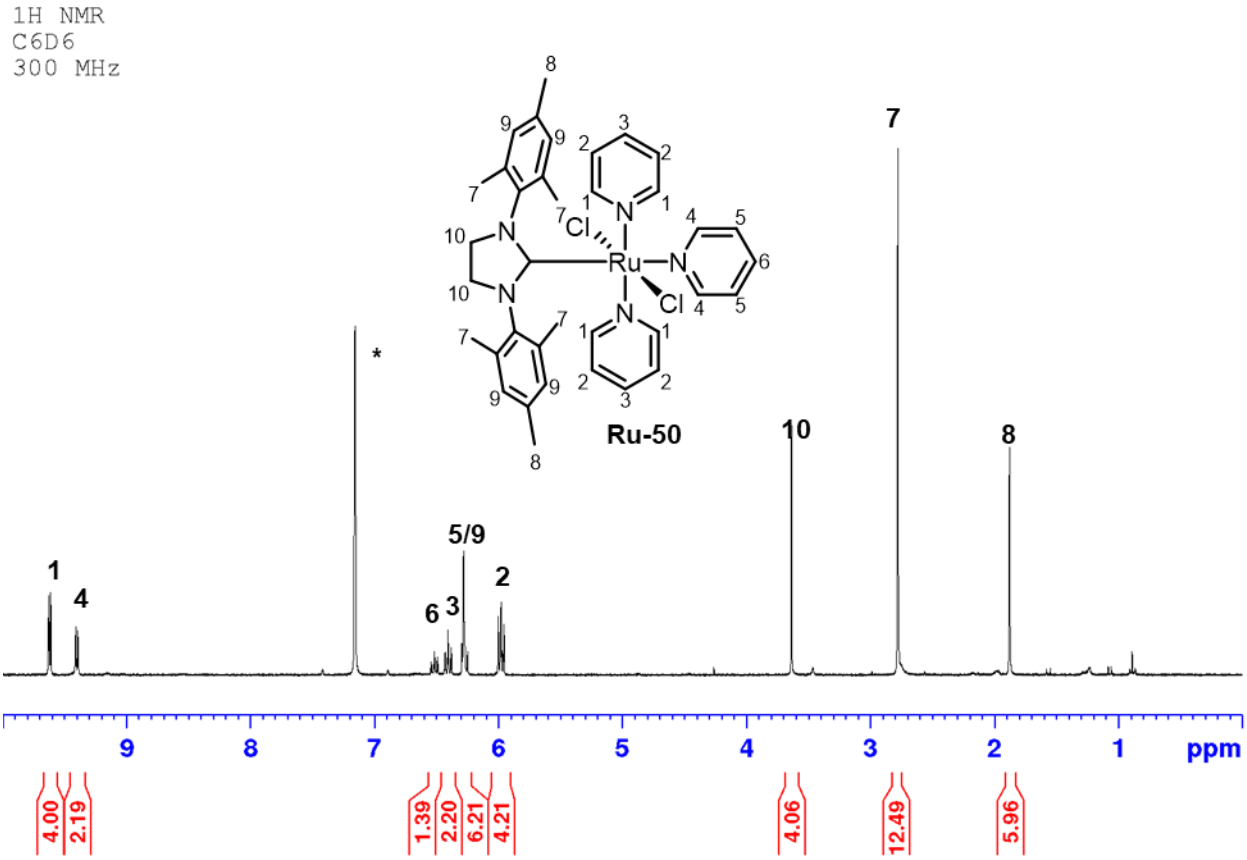

Figure A1.10: ^{1}H NMR (300 MHz, C_6D_6) showing results of NMR-tube scale ligand exchange experiment between **Ru-50** and MeCN

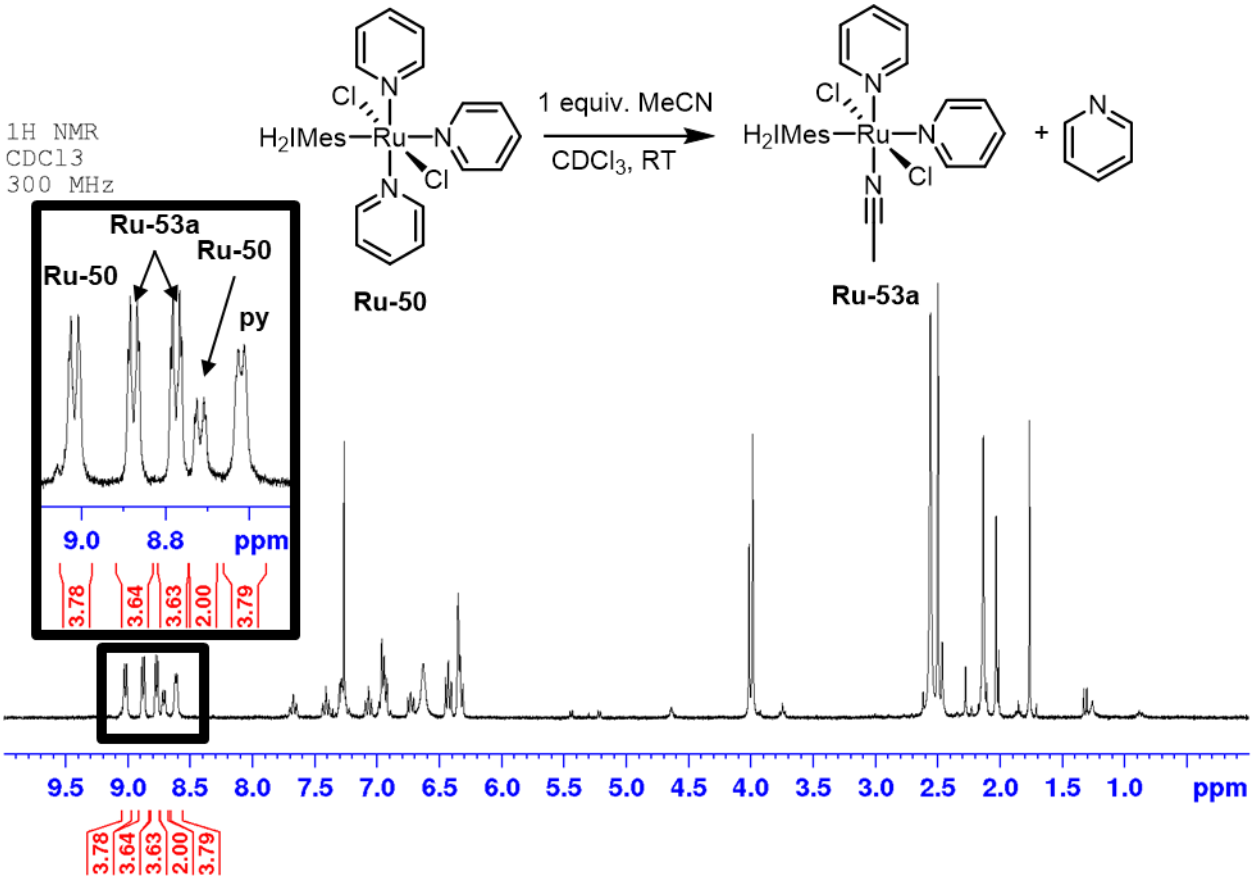

Figure A1.11: ^{1}H NMR (300 MHz, C_6D_6) showing results of NMR-tube scale ligand exchange experiment between **Ru-50** and NEt_3

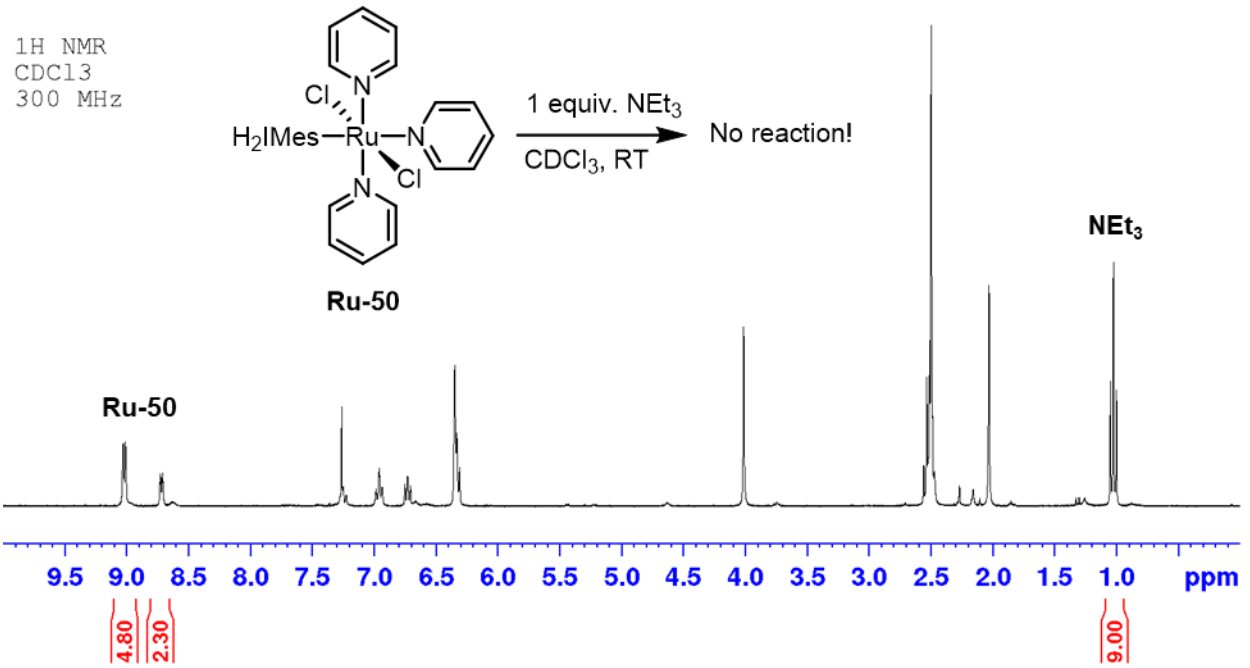

Figure A1.12: ^{1}H NMR (300 MHz, C_6D_6) showing results of NMR-tube scale ligand exchange experiment between **Ru-50** and PCy_3

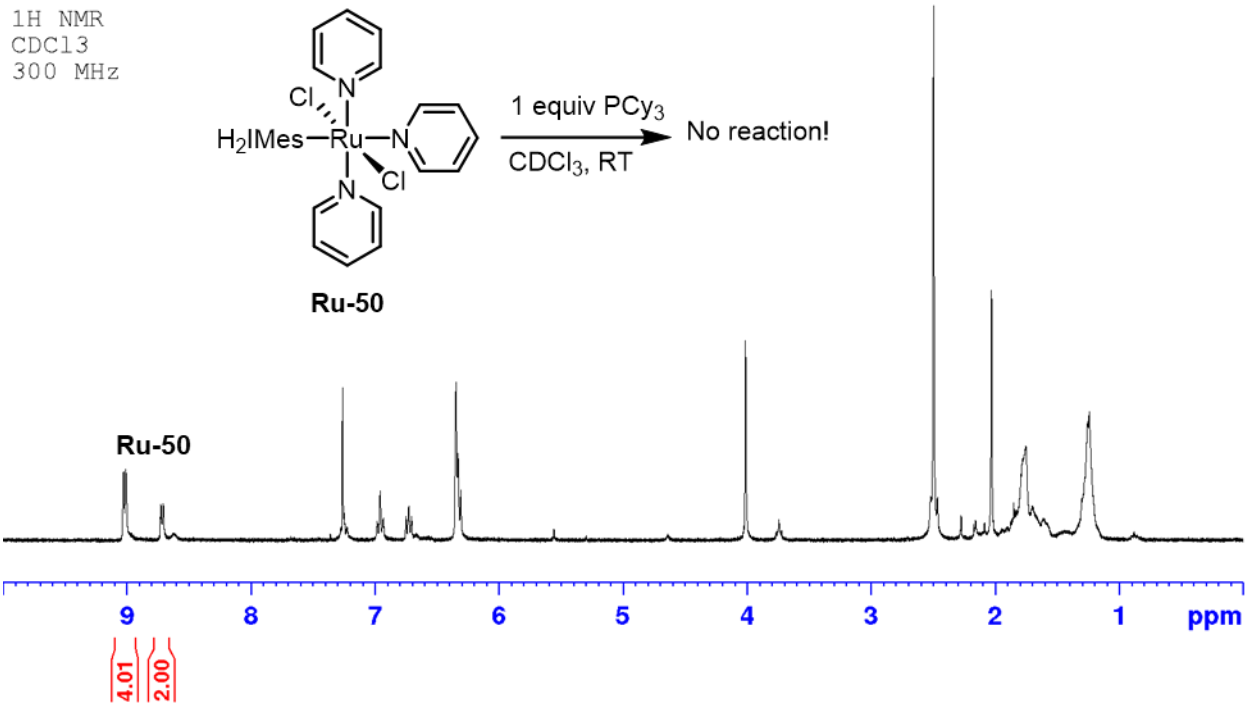

Figure A1.13: ^{1}H NMR (300 MHz, C_6D_6) showing results of NMR-tube scale ligand exchange experiment between **Ru-50** and PPh_3

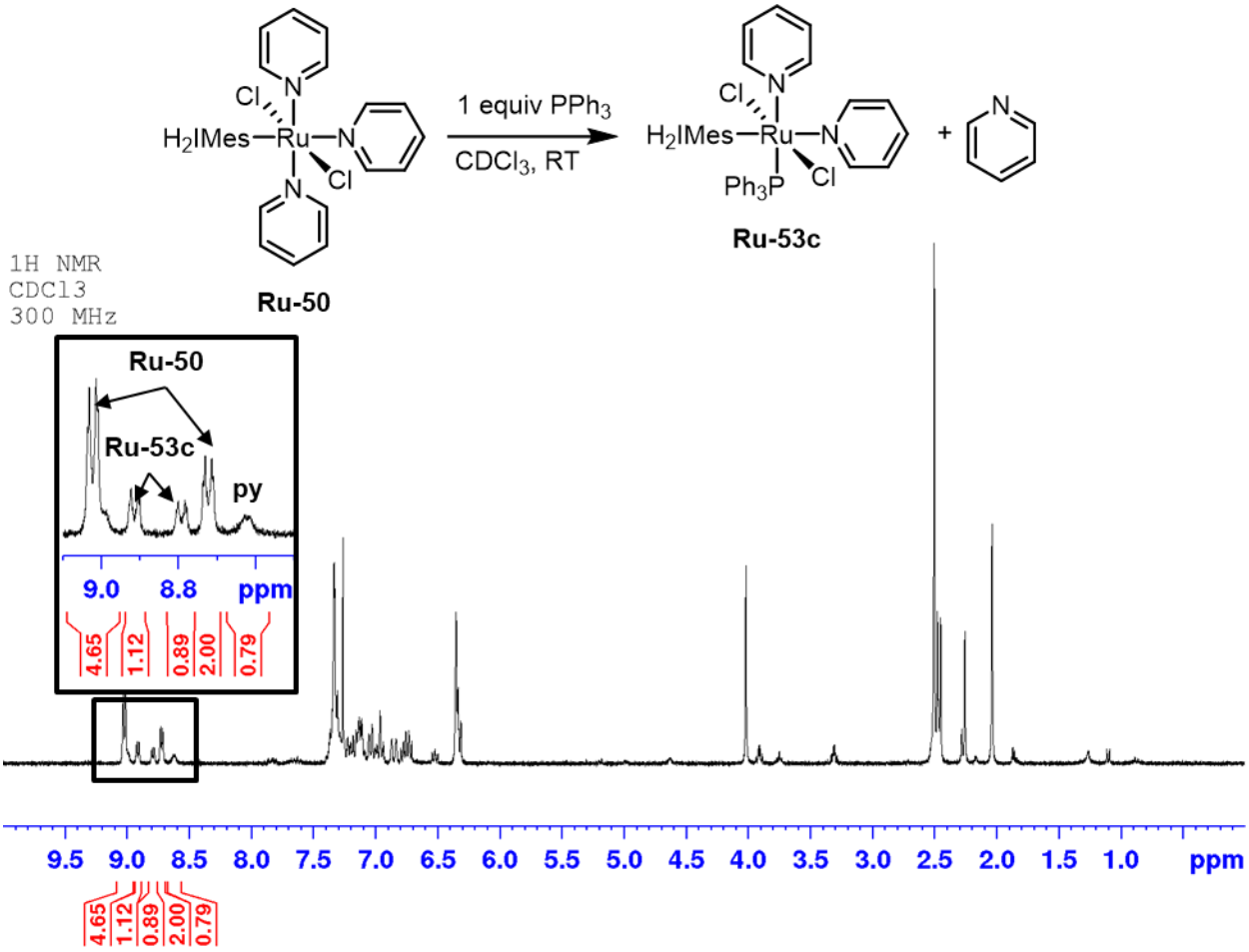

Figure A1.14: ^{1}H NMR (300 MHz, C_6D_6) showing results of attempted vinylidene installation on **Ru-50**. Spectrum shows mostly unreacted **Ru-50**, but presence of free pyridine suggests some decomposition.

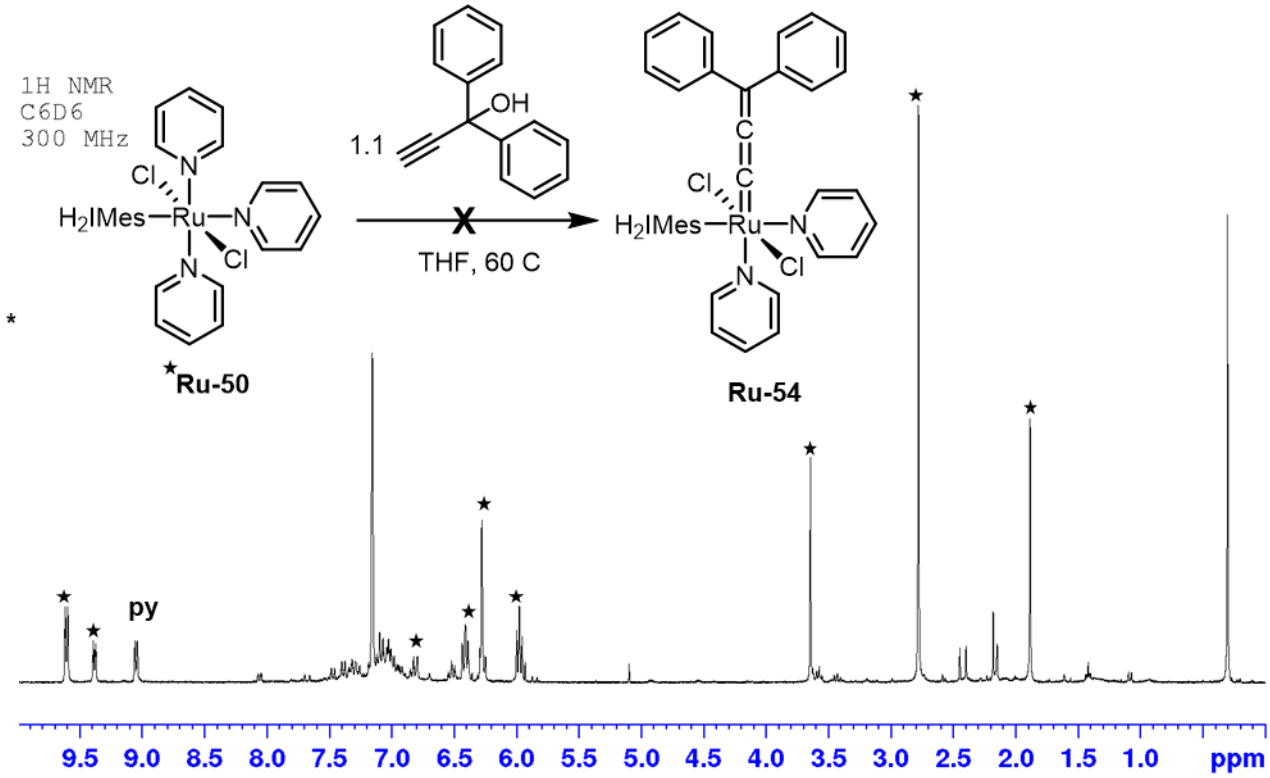

Figure A1.15: ^{1}H NMR (300 MHz, C_6D_6) showing results of attempted indenylidene installation on **Ru-50** in presence of CH_3COCl acting as an acid catalyst. Spectrum is dominated by residual THF and unreacted 1,1-diphenylpropargyl alcohol

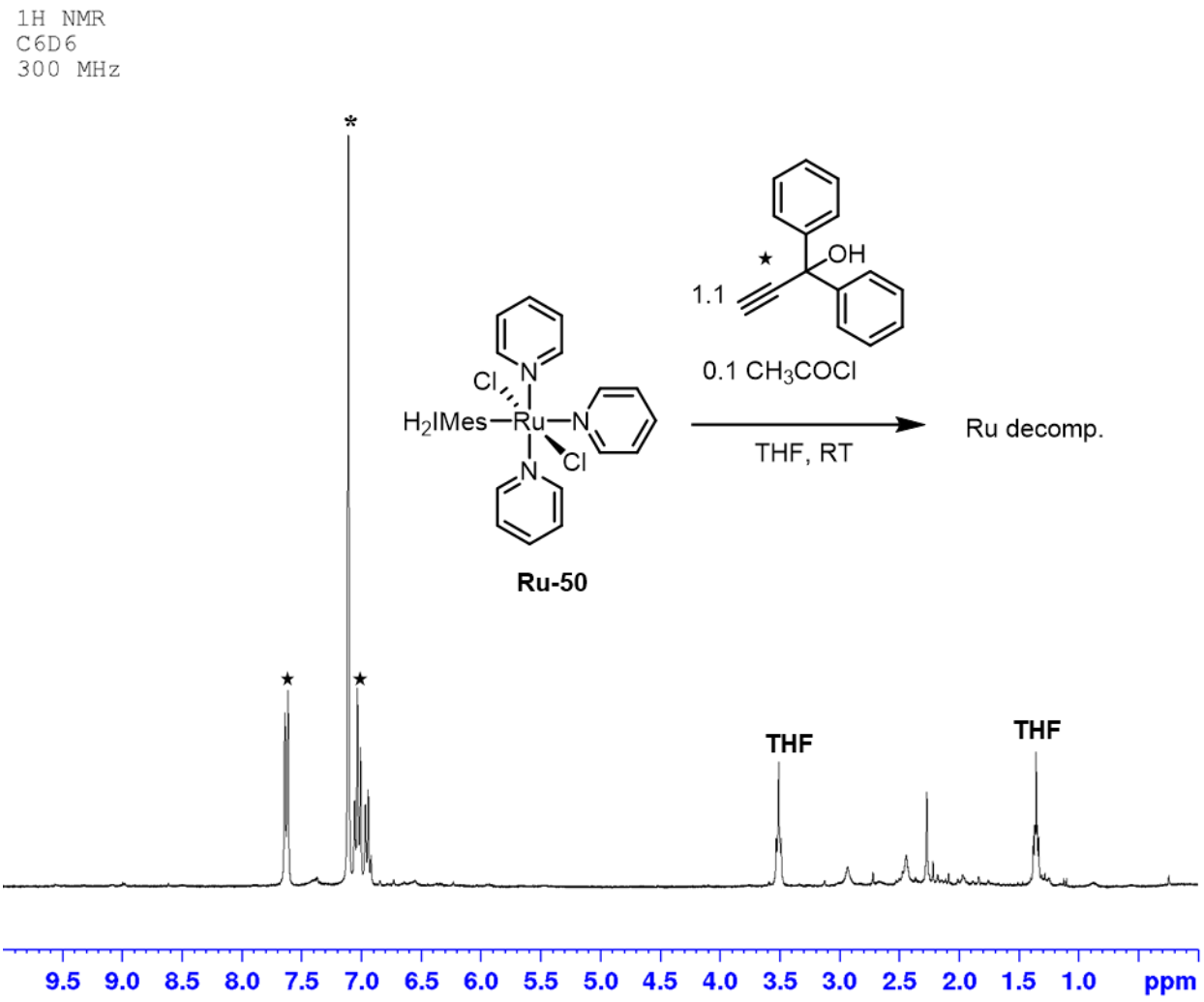

Figure A1.16: ^{1}H NMR (300 MHz, C_6D_6) of new complex **Ru-56c**

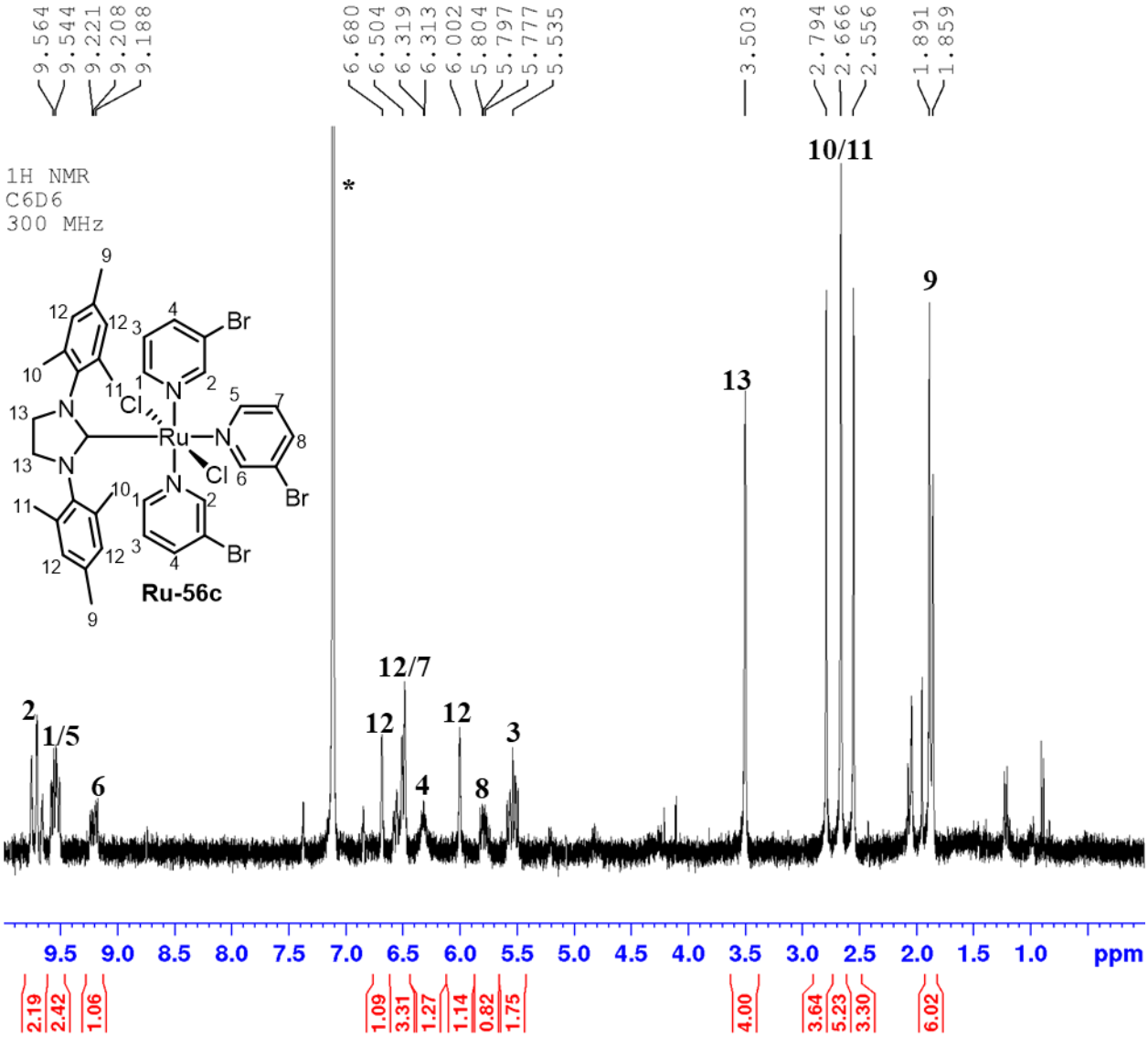

Figure A1.17: ^{1}H NMR (300 MHz, C_6D_6) showing result of attempted vinylidene installation on **Ru-56c**. Spectrum is dominated by starting materials, indicating lack of reactivity.

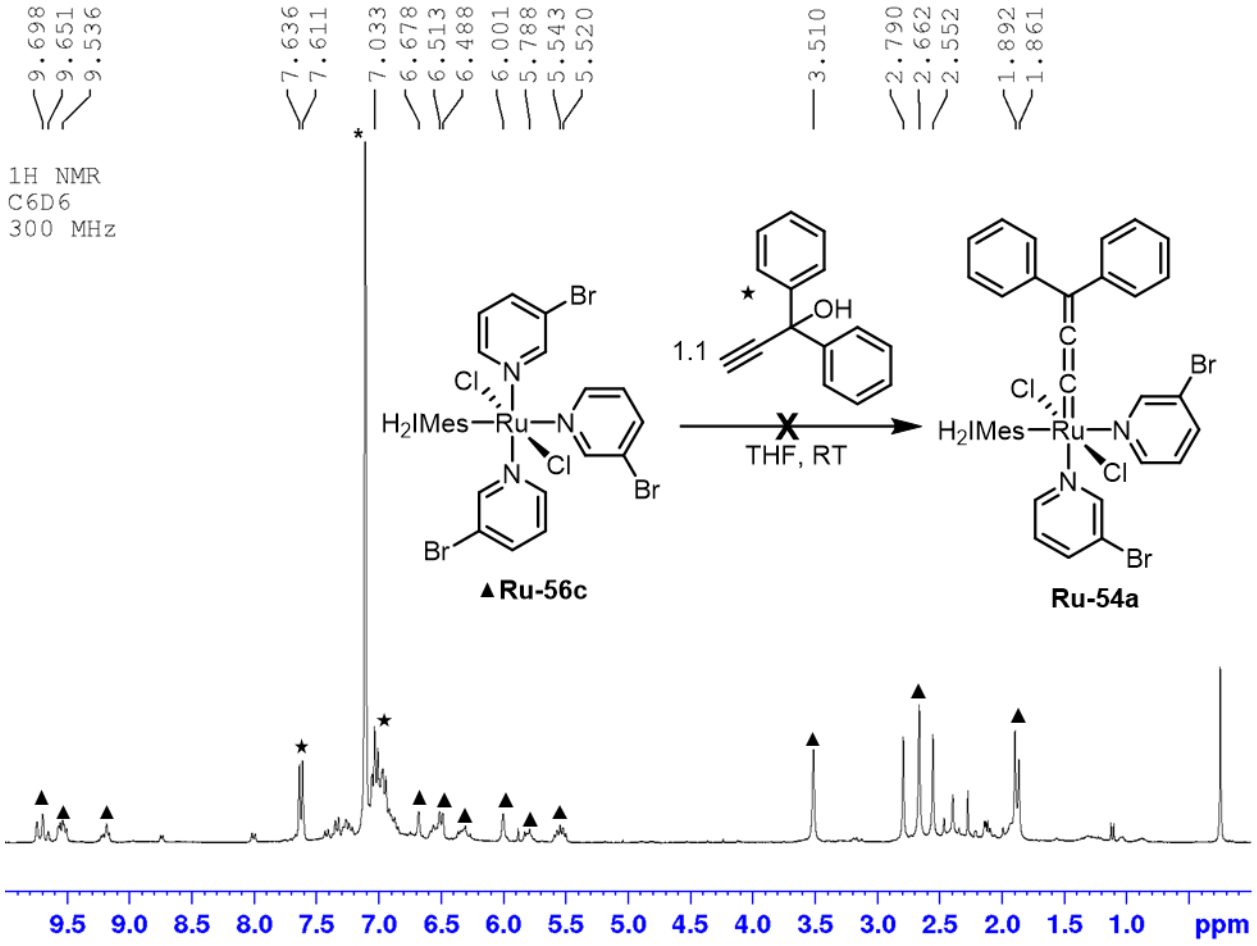

Figure A1.18: ^{1}H NMR (300 MHz, C_6D_6) showing result of attempted synthesis of **Ru-58** by treating **HII** with one equivalent of $Zn(OC_6F_5)_2$ in THF. Product ratio determined by comparing integration of diagnostic signals in the alkylidene region.

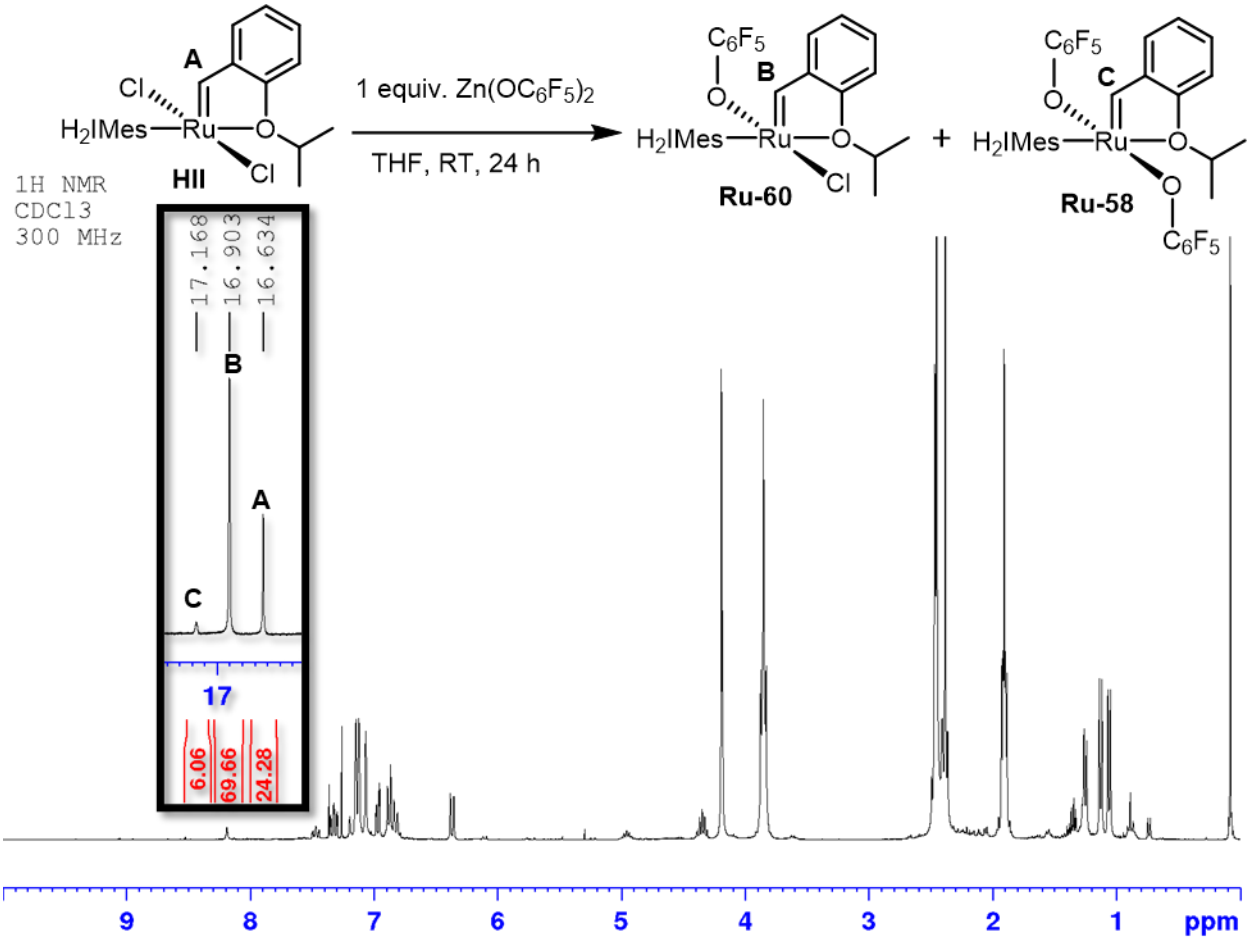

Appendix B: NMR data for new compounds and key experiments described in Chapter 4

Figure B2.1: ^{1}H NMR (300 MHz, C_6D_6) spectrum showing result of attempted reduction of **HII** with $K[CH(CH_3)CH_2CH_3]_3BH$. Sample is highly concentrated, yet residual solvent peak dominates, implying decomposition to spectroscopically unobservable products.

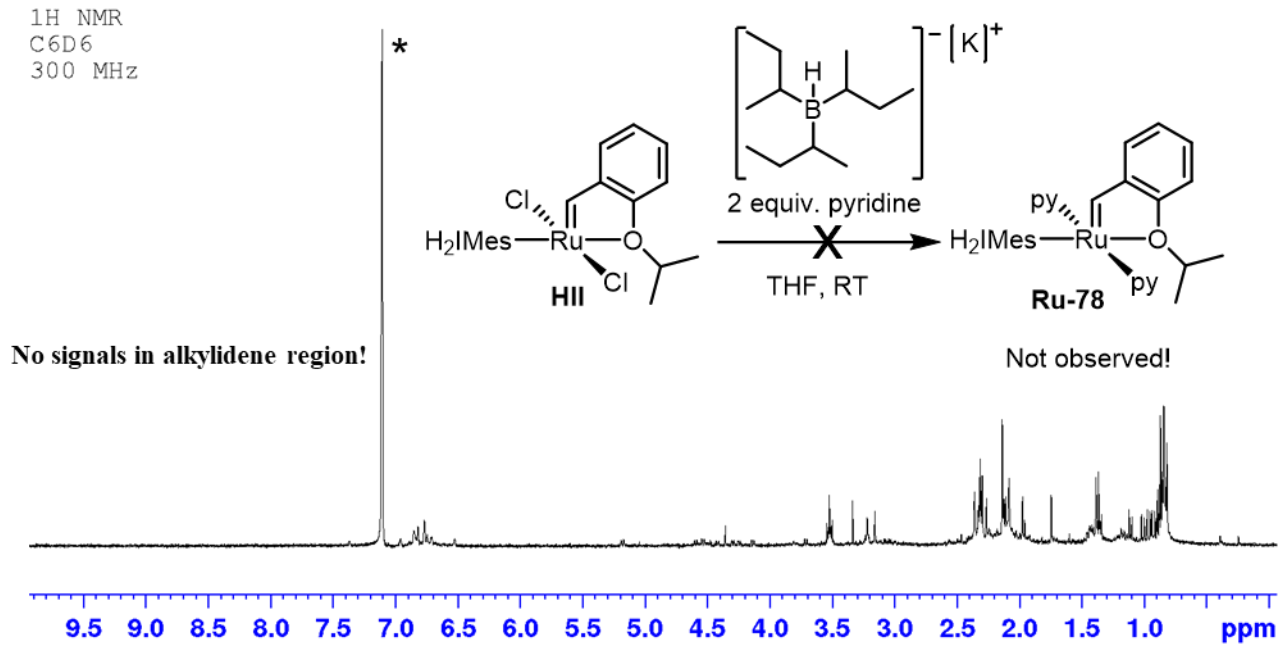

Figure B2.2: ^{1}H NMR (300 MHz, C_6D_6) spectrum of Grignard reagent Mg-3. A simplified representation of Schlenk equilibrium species **Mg-3** and **Mg-3'** (omitting $MgCl_2$ and coordinated THF) is depicted

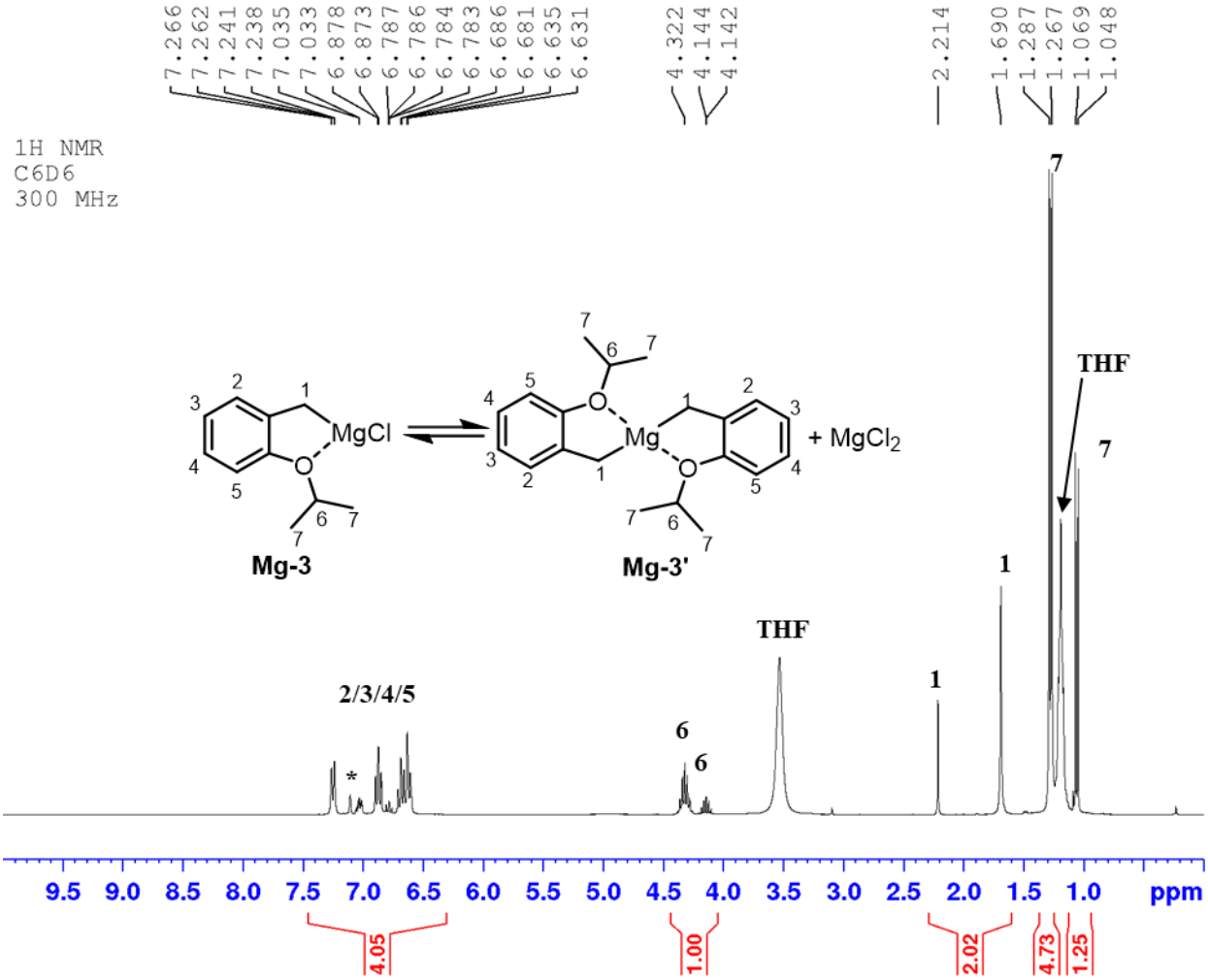

Figure B2.3: ^{1}H NMR (300 MHz, C_6D_6) spectrum showing the result of deliberate hydrolysis of Grignard reagent **Mg-3** with MeOH.

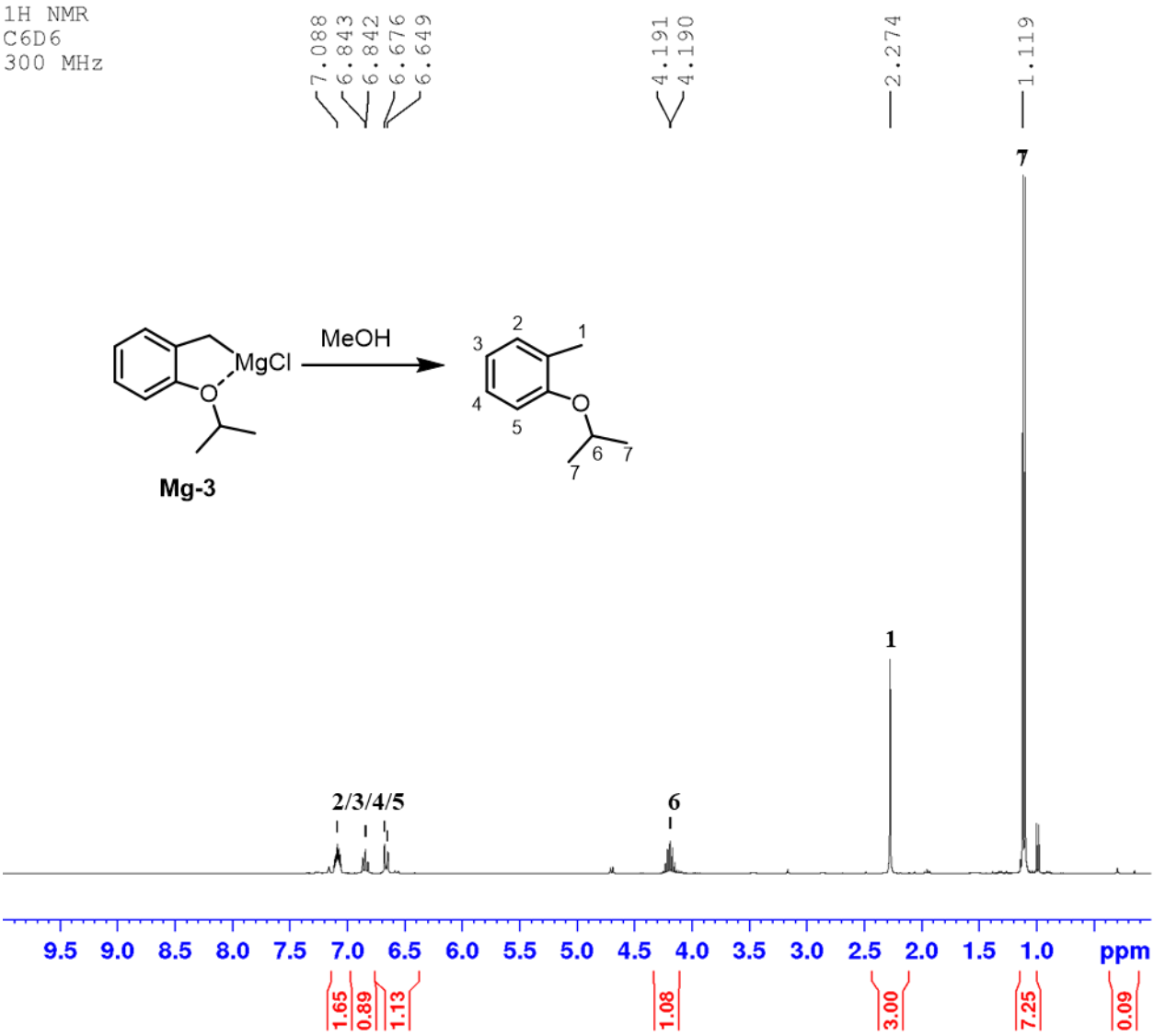

Figure B2.4: $^{31}P\{^{1}H\}$ NMR (121 MHz, C_6D_6) spectrum showing result of reaction of **Ru-80** with **Mg-3**

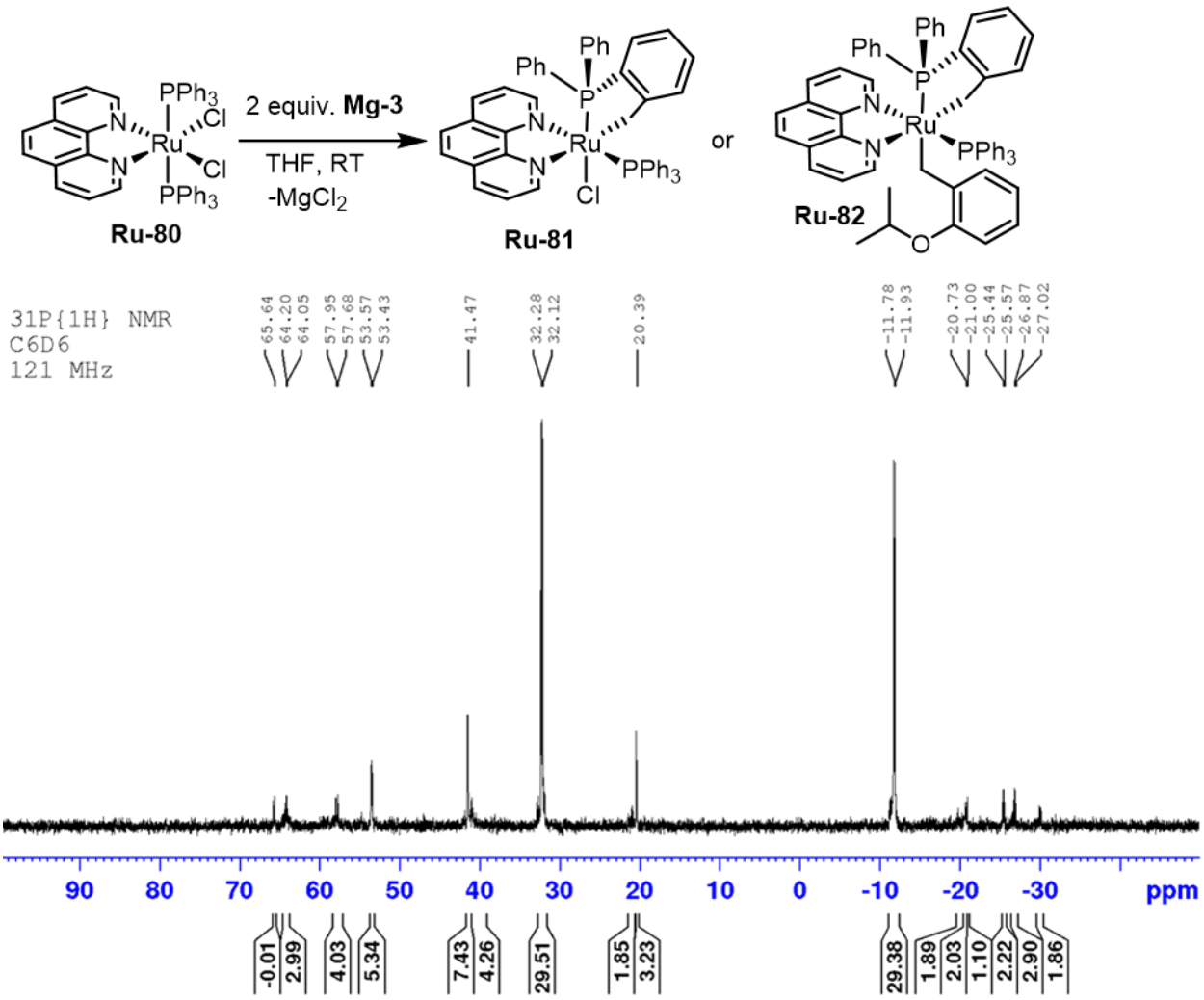

Figure B2.5: ^{1}H NMR (300 MHz, C_6D_6) spectrum showing result of reaction of **Ru-80** with **Mg-3**

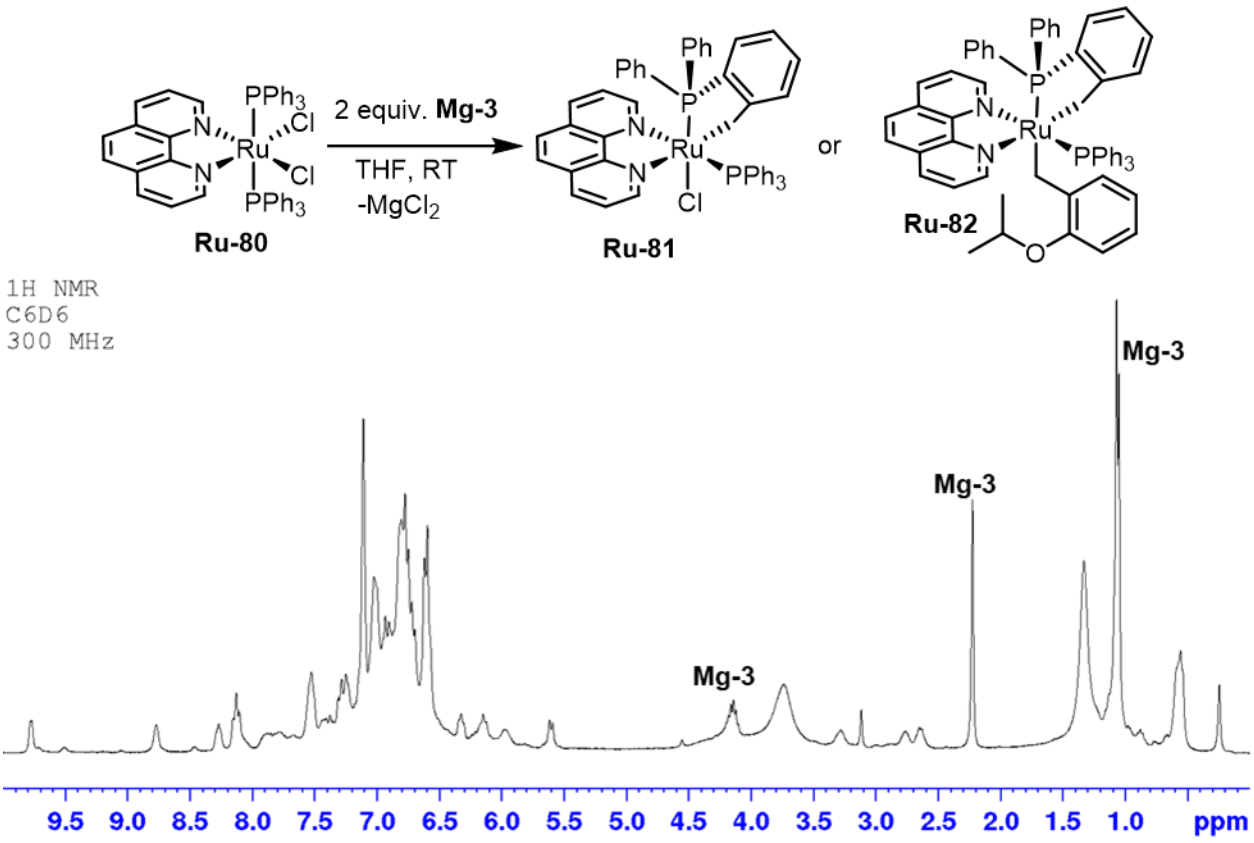

Figure B2.6: ^{1}H NMR (300 MHz, C_6D_6) spectrum of new complex **Ru-84**

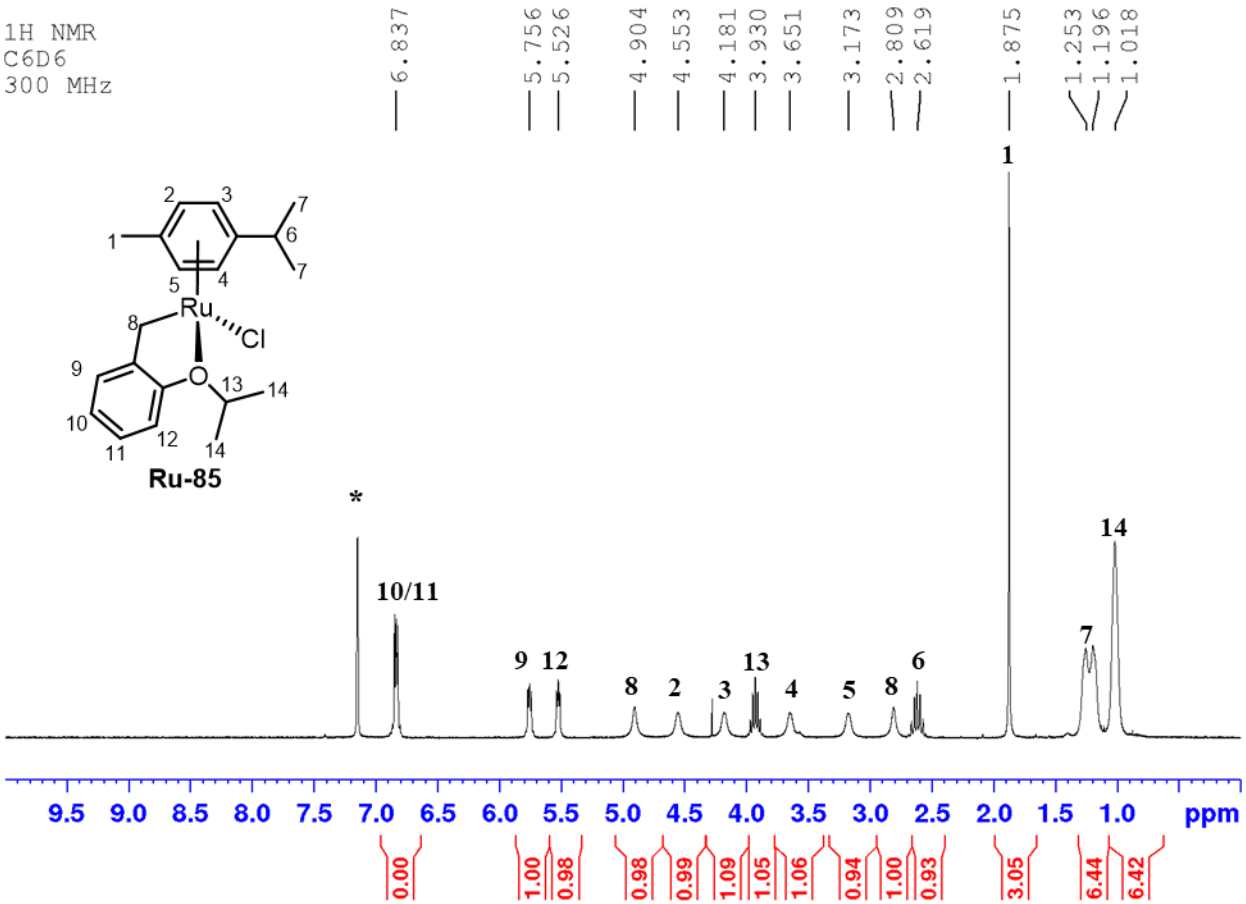

Figure B2.7: ^{1}H NMR (300 MHz, $CDCl_3$) spectrum of new compound **Ru-84**

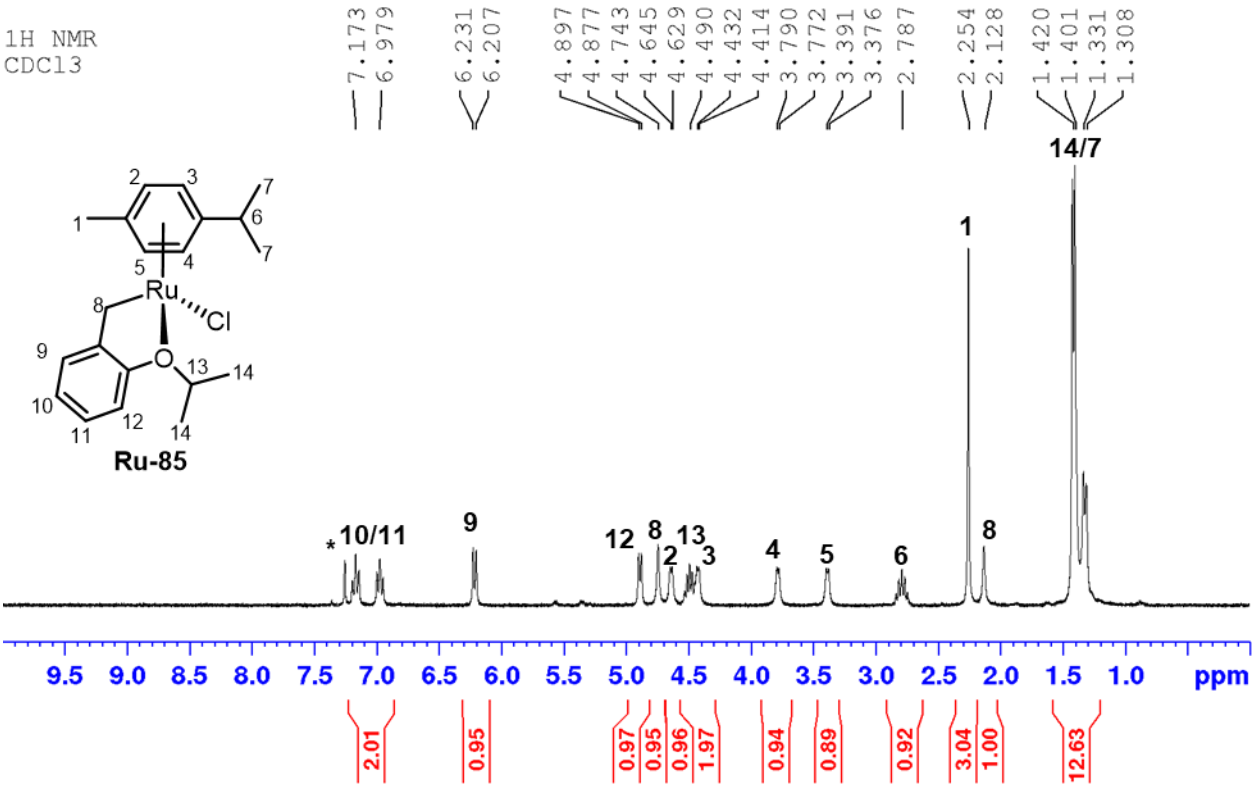

Figure B2.8: ^{1}H-^{13}C HMQC (300 MHz, C_6D_6) experiment on **Ru-84** for assistance in peak assignment in 2D spectrum Figure B2.7. Matching peaks confirm that the two singlets assigned as the benzyl CH_2 protons are bound to the same carbon.

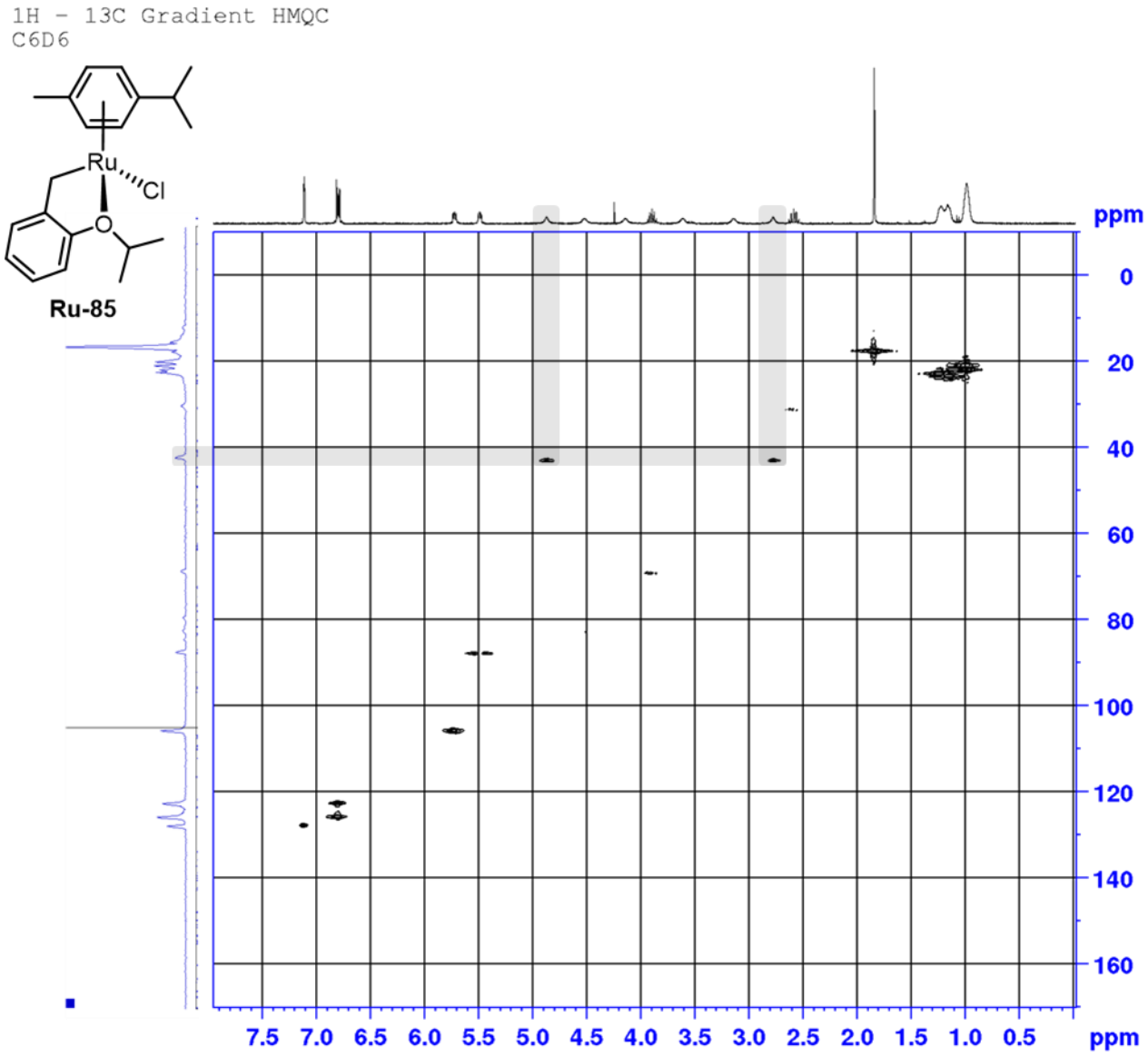

Figure B2.9: ^{1}H-^{1}H COSY (300 MHz, C_6D_6) experiment on **Ru-84** in for assistance in peak assignment in 2D spectrum Figure B2.7. No cross-peak is seen for the benzyl CH_2 protons.

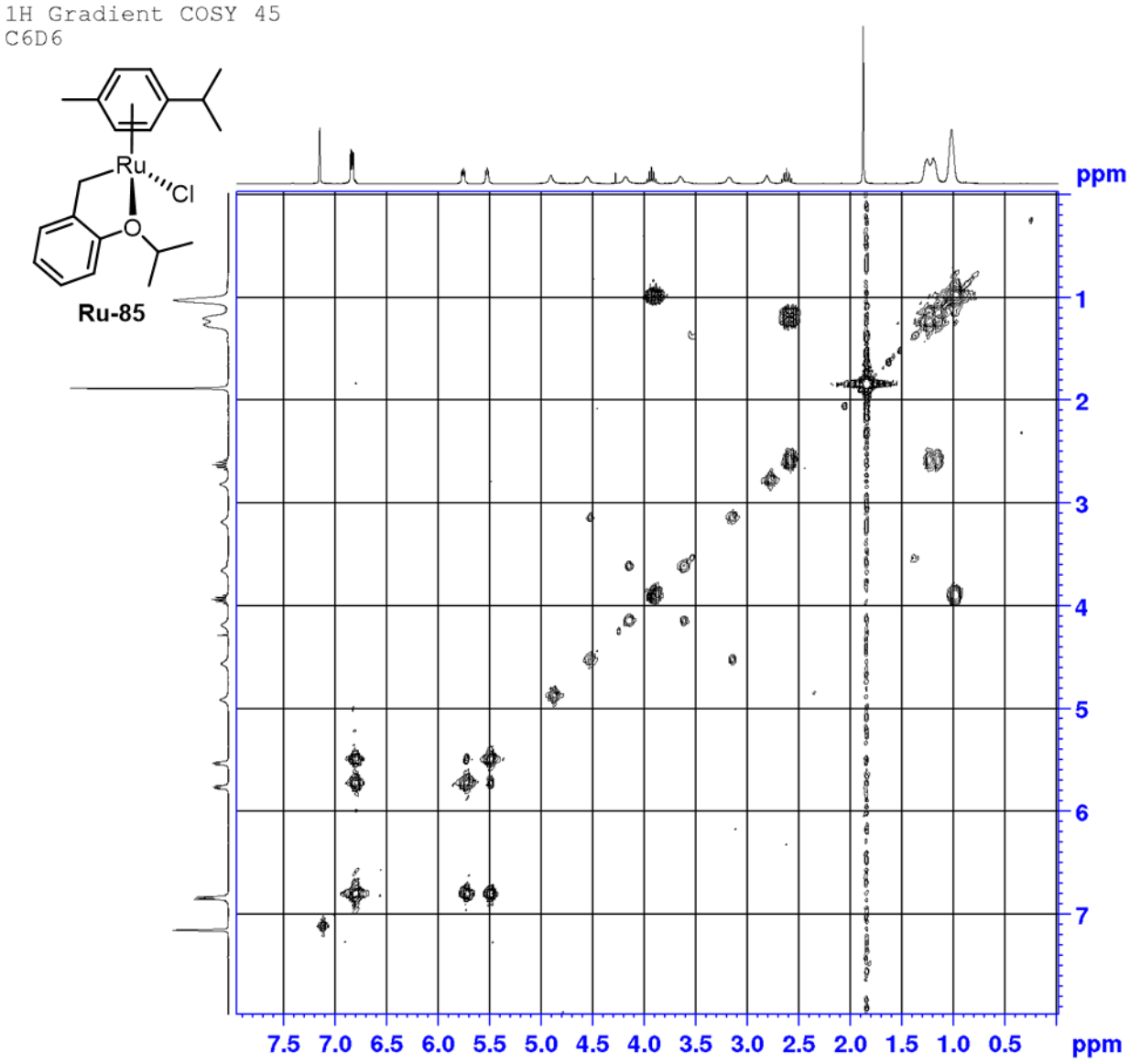

Figure B2.10: ^{1}H NMR (300 MHz, C_6D_6) spectrum of **Ru-84** on reaction with pyridine. Signals for free pyridine and **Ru-84** indicate an equilibrium. An AB doublets pattern (8) is seen for the benzyl CH_2 protons of **Ru-84-py**.

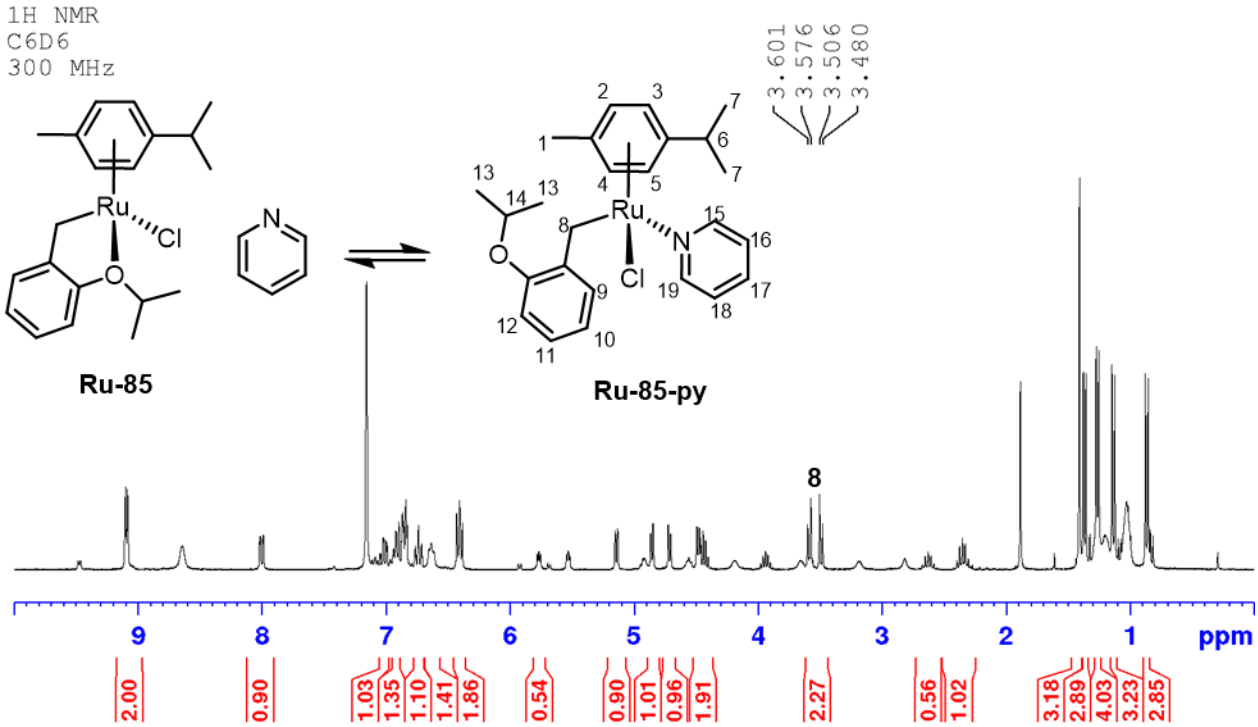

Figure B2.11: ^{1}H NMR (300 MHz, $CDCl_3$) spectrum of **Ru-84**. Aromatic p-cymene and benzyl H8-10 signals are not observed. Well-resolved p-cymene alkyl and benzyl H11-14 signals appear in the expected integration ratios. Very broad baseline signals are also present.

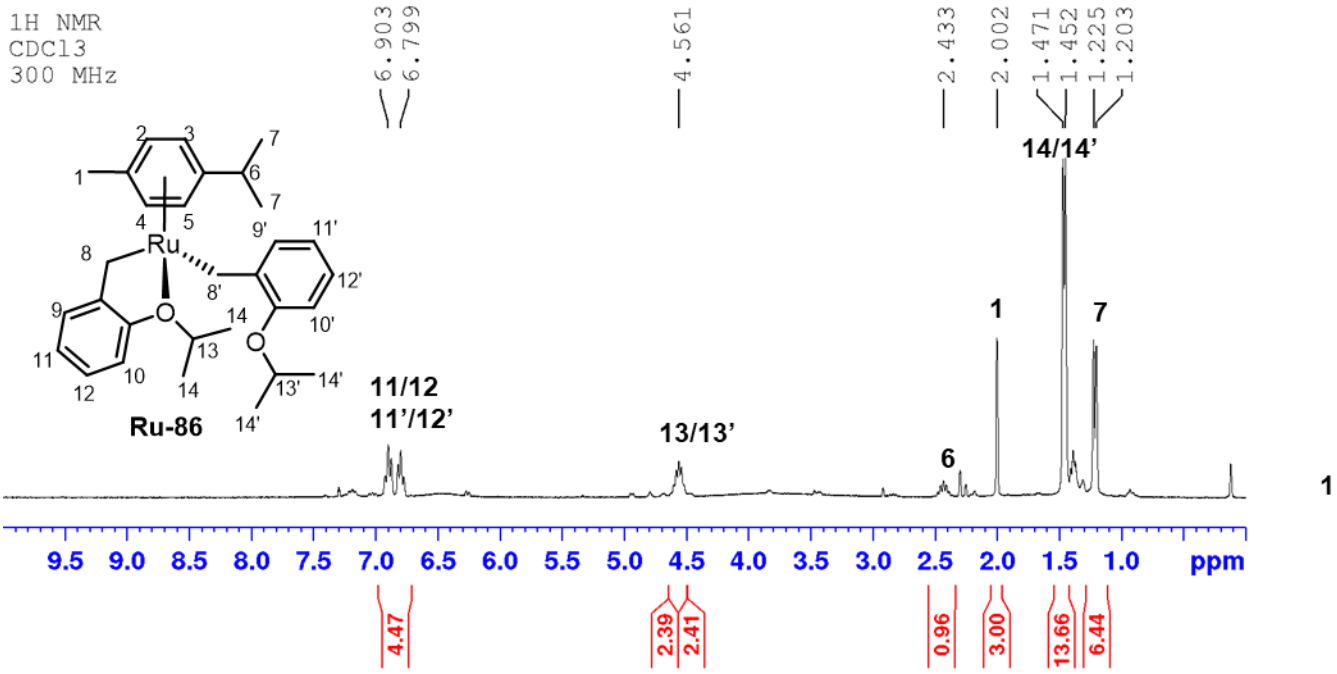

Figure B2.12: ^{1}H NMR (300 MHz, $CDCl_3$) spectrum of **Ru-84** at -20 °C. Broad signals observed at RT have resolved to sharp peaks and now all protons can be accounted for.`

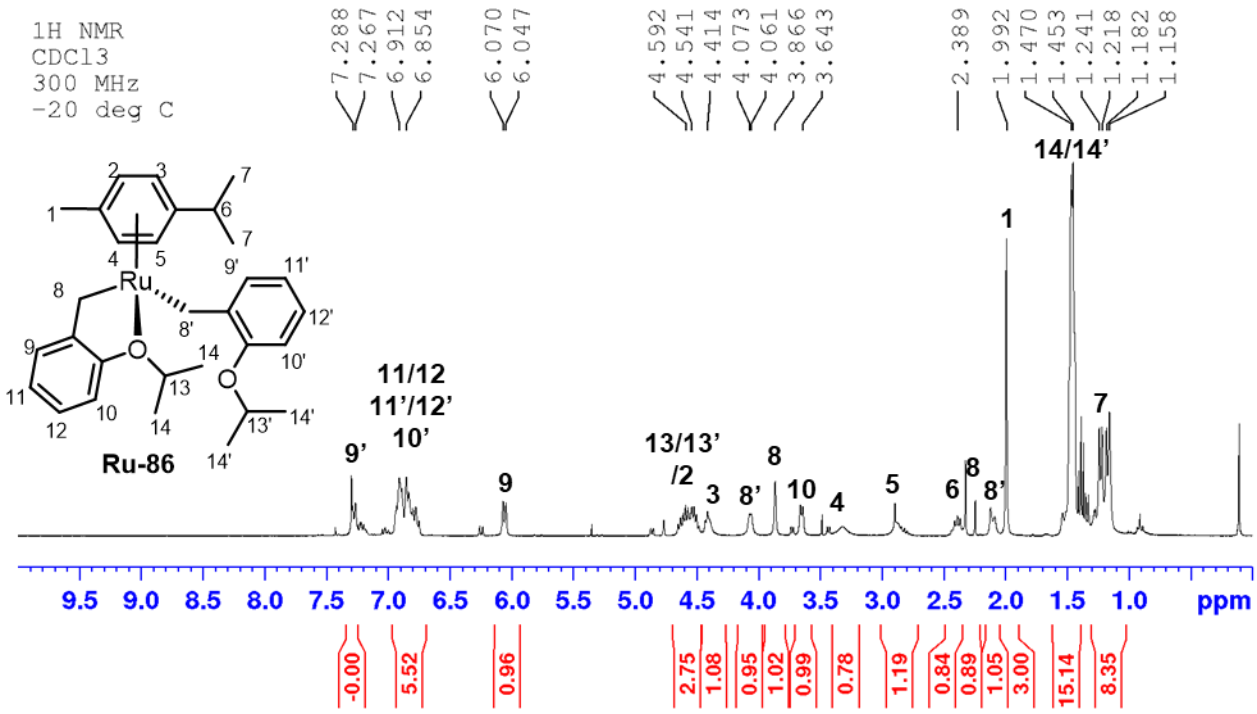

Figure B2.13: ^{1}H NMR (300 MHz, C_6D_6) spectrum of **Ru-86** (triangles) produced by reaction of **Ru-84** with in-situ generated $Zn(OC_6F_5)_2$ after attempted recrystallization from CH_2Cl_2-hexanes. Re-emergence of signals for **Ru-84** (squares) indicates rechlorination.

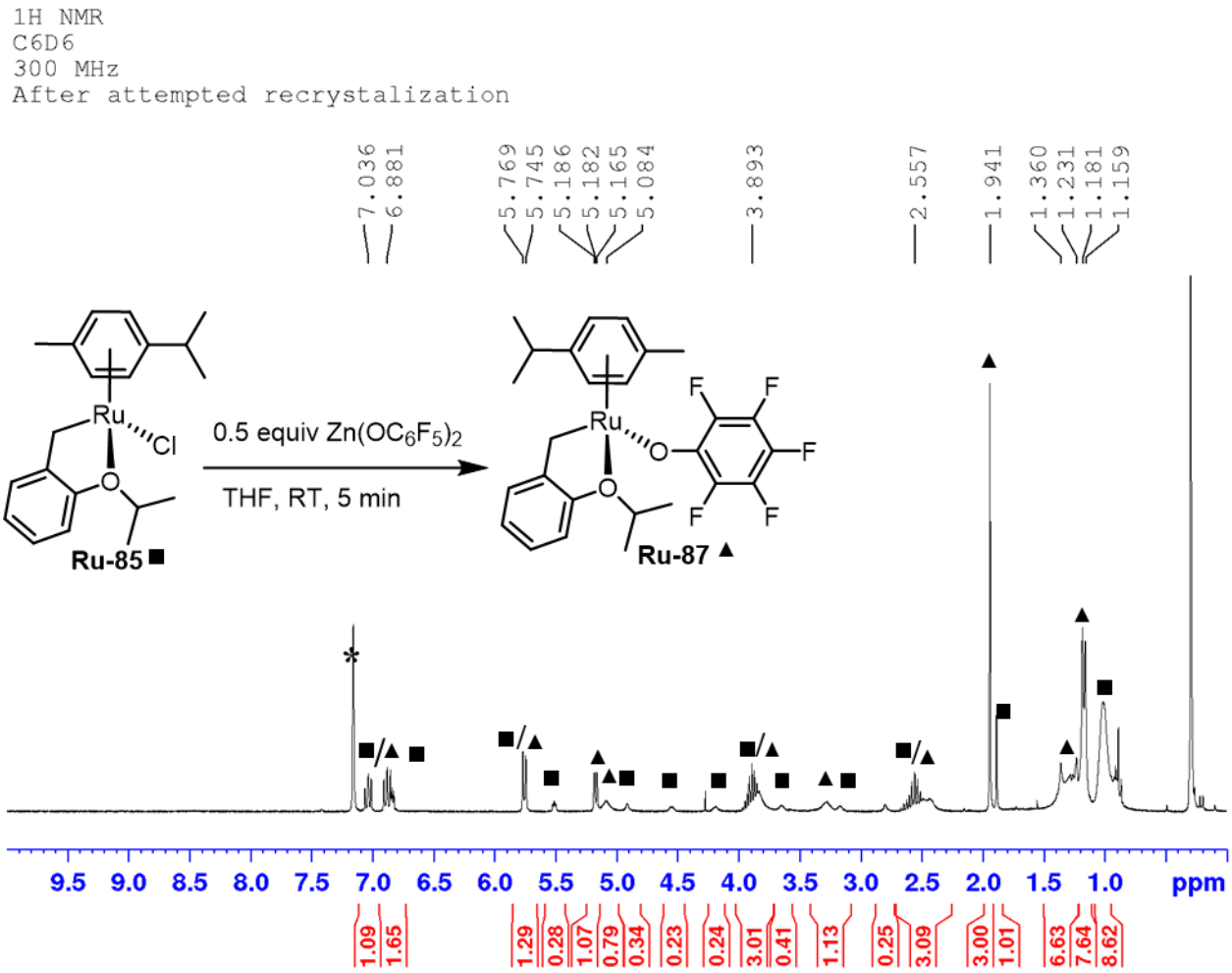

Figure B2.14: ^{1}H NMR (300 MHz, C_6D_6) spectrum of crude **Ru-86** produced by treating in situ generated **Ru-85** with 1 equiv C_6F_5OH. Also evident is *o*-(O*i*Pr)$C_6H_4CH_3$ (1 equiv). Signal assignment for Ru-86 is tentative, pending 2D experiments for confirmation.

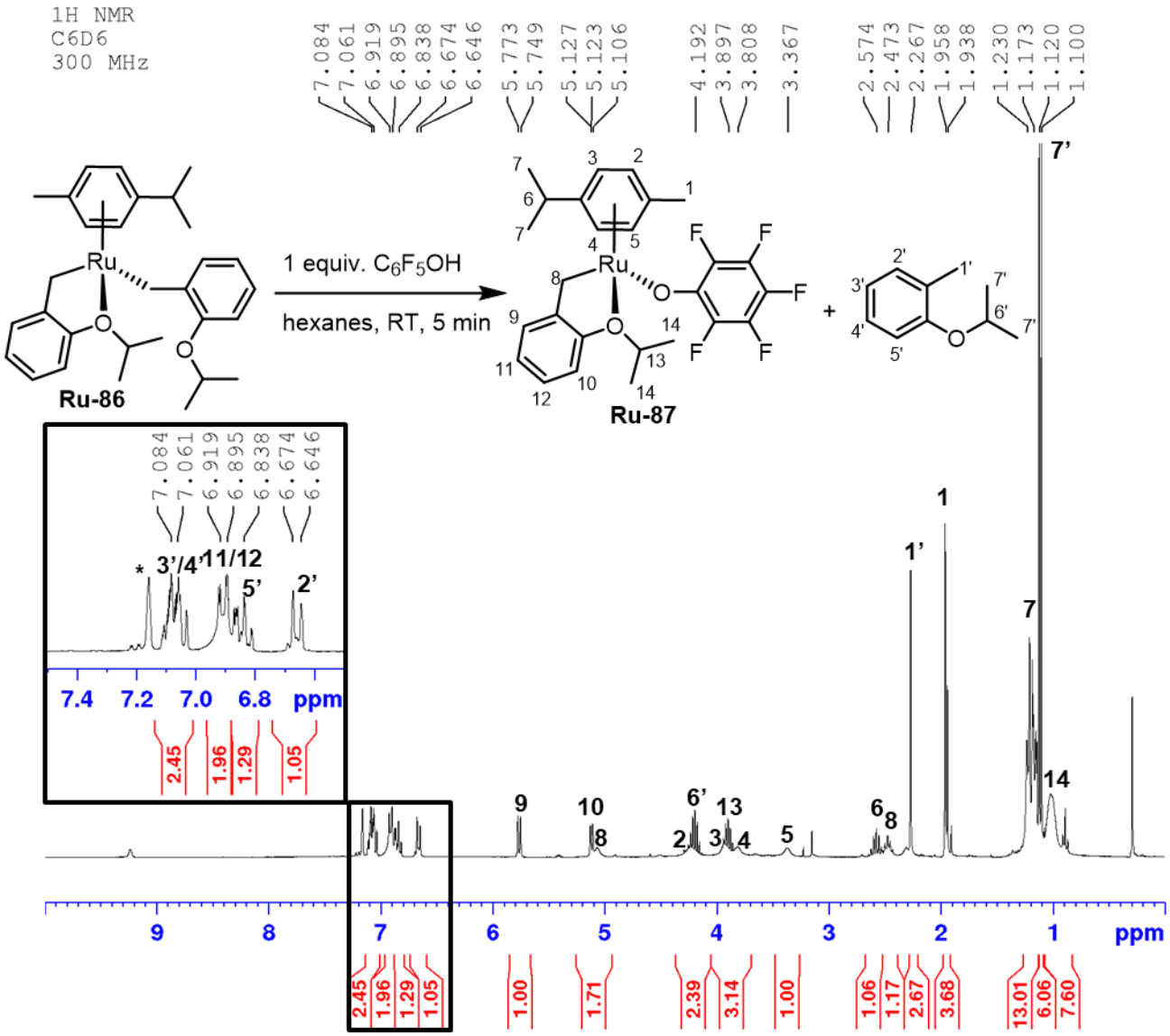

Figure B2.15: ^{1}H NMR (300 MHz, C_6D_6) spectrum of the attempted deprotonation of **Ru-86** by reaction with LiHMDS. Signals for starting **Ru-86** are shown as triangles: no other products evident.

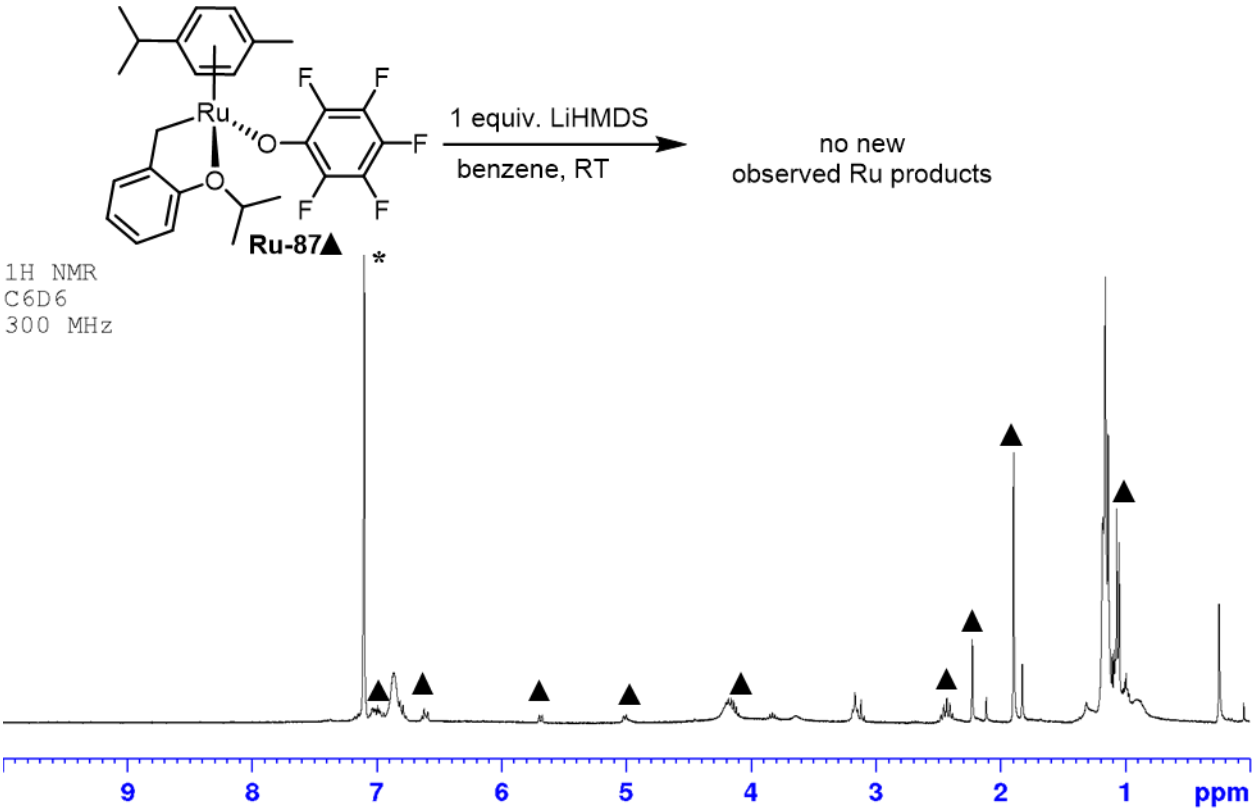

Figure B2.16: ^{1}H NMR (300 MHz, C_6D_6) spectrum for reaction of in situ generated **Ru-86** with pyridine. Signals for the ortho protons of Ru-bound pyridine appear at 8.76 and 8.38 ppm, and the signal for free pyridine at 8.5 ppm is absent, suggesting formation of a new Ru-py species. A broad signal in the alkylidene region (14.19 ppm) integrates to 0.9 H relative to the Ru-bound *o*-py protons, suggesting formation of **Ru-88**. Given the complexity of the spectrum, structure confirmation and signal assignment require further data.